frontiers | Research Topics

Technological innovations and pancreatic cancer

Edited by
Samir Pathak, Sanjay Pandanaboyana and Andrew Smith

Published in
Frontiers in Oncology

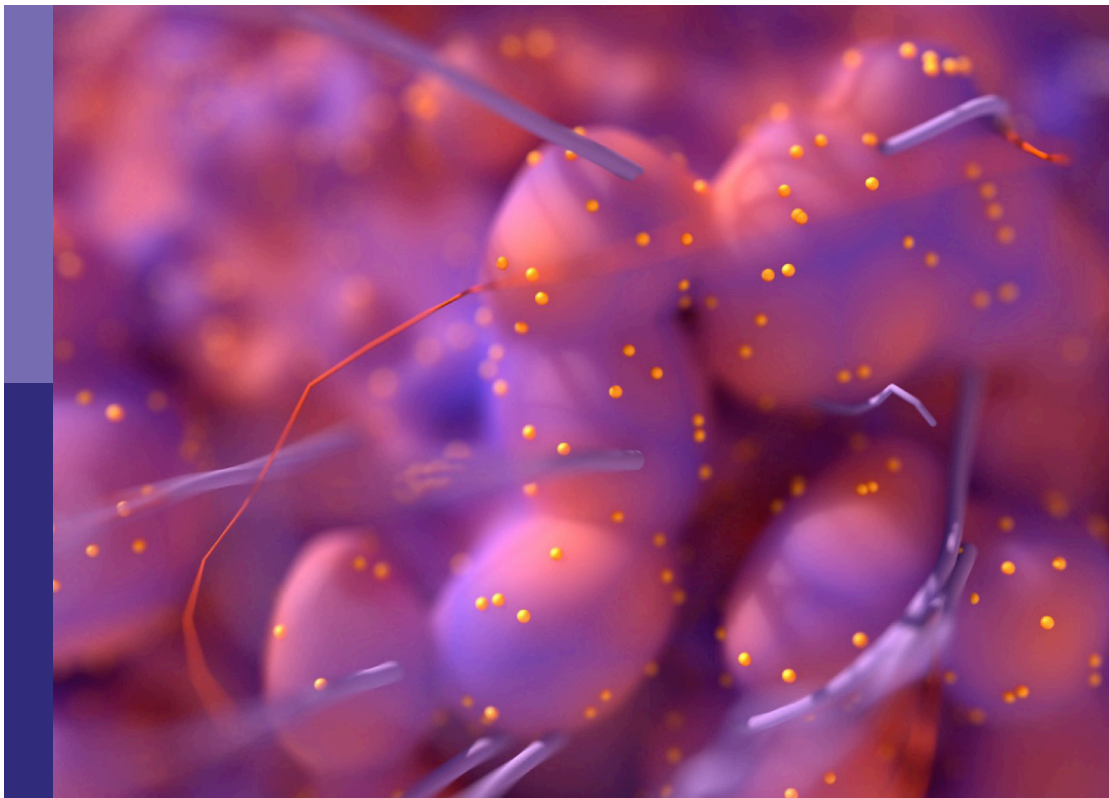

ISSN 1664-8714
ISBN 978-2-8325-5575-0
DOI 10.3389/978-2-8325-5575-0

About Frontiers

Frontiers is more than just an open access publisher of scholarly articles: it is a pioneering approach to the world of academia, radically improving the way scholarly research is managed. The grand vision of Frontiers is a world where all people have an equal opportunity to seek, share and generate knowledge. Frontiers provides immediate and permanent online open access to all its publications, but this alone is not enough to realize our grand goals.

Frontiers journal series

The Frontiers journal series is a multi-tier and interdisciplinary set of open-access, online journals, promising a paradigm shift from the current review, selection and dissemination processes in academic publishing. All Frontiers journals are driven by researchers for researchers; therefore, they constitute a service to the scholarly community. At the same time, the *Frontiers journal series* operates on a revolutionary invention, the tiered publishing system, initially addressing specific communities of scholars, and gradually climbing up to broader public understanding, thus serving the interests of the lay society, too.

Dedication to quality

Each Frontiers article is a landmark of the highest quality, thanks to genuinely collaborative interactions between authors and review editors, who include some of the world's best academicians. Research must be certified by peers before entering a stream of knowledge that may eventually reach the public - and shape society; therefore, Frontiers only applies the most rigorous and unbiased reviews. Frontiers revolutionizes research publishing by freely delivering the most outstanding research, evaluated with no bias from both the academic and social point of view. By applying the most advanced information technologies, Frontiers is catapulting scholarly publishing into a new generation.

What are Frontiers Research Topics?

Frontiers Research Topics are very popular trademarks of the *Frontiers journals series*: they are collections of at least ten articles, all centered on a particular subject. With their unique mix of varied contributions from Original Research to Review Articles, Frontiers Research Topics unify the most influential researchers, the latest key findings and historical advances in a hot research area.

Find out more on how to host your own Frontiers Research Topic or contribute to one as an author by contacting the Frontiers editorial office: frontiersin.org/about/contact

Technological innovations and pancreatic cancer

Topic editors

Samir Pathak — Bristol Royal Infirmary, United Kingdom

Sanjay Pandanaboyana — Freeman Hospital, United Kingdom

Andrew Smith — Leeds Cancer Centre, Leeds Teaching Hospitals NHS Trust, United Kingdom

Citation

Pathak, S., Pandanaboyana, S., Smith, A., eds. (2024). *Technological innovations and pancreatic cancer*. Lausanne: Frontiers Media SA. doi: 10.3389/978-2-8325-5575-0

Table of contents

frontiers | Frontiers in Oncology

TYPE Editorial
PUBLISHED 07 October 2024
DOI 10.3389/fonc.2024.1497367

OPEN ACCESS

EDITED AND REVIEWED BY
Liang Qiao,
The University of Sydney, Australia

*CORRESPONDENCE
Mikolaj Kowal
mikolajkowal@doctors.org.uk

RECEIVED 16 September 2024
ACCEPTED 17 September 2024
PUBLISHED 07 October 2024

CITATION
Kowal M, Smith A, Pandanaboyana S and Pathak S (2024) Editorial: Technological innovations and pancreatic cancer. *Front. Oncol.* 14:1497367. doi: 10.3389/fonc.2024.1497367

Editorial: Technological innovations and pancreatic cancer

Mikolaj Kowal[1,2]*, Andrew Smith[1,2], Sanjay Pandanaboyana[3] and Samir Pathak[1,2]

[1]The Department of Hepatobiliary Surgery, St. James's University Hospital, Leeds, United Kingdom, [2]Leeds Institute of Medical Research, Faculty of Medicine and Health, University of Leeds, Leeds, United Kingdom, [3]Hepato-Pancreato-Biliary and Transplant Unit, Freeman Hospital, Newcastle Upon Tyne, United Kingdom

KEYWORDS

pancreas - adenocarcinoma, pancreas, pancrea ticoduodenectomy, technology, innovation

Editorial on the Research Topic
Technological innovations and pancreatic cancer

Pancreatic ductal adenocarcinoma (PDAC) has poor survival outcomes. The main reasons include late presentation, resulting in only 20% of patients being eligible for surgery, and poor response to chemotherapy, secondary to the challenging tumour biology (1, 2). For patients undergoing surgery, the local anatomy and invasiveness of PDAC results in high operative risks, with morbidity and mortality estimated at 50-70% and 2-8%, respectively (3, 4). The incidence of PDAC is rising, making it the fourth leading cause of death in the United States (5). It is imperative to prioritise PDAC research. Technological advances may improve patient outcomes through early detection and optimisation of treatments. The editorial highlights the latest technological advances in PDAC and identifies areas for research (Figure 1).

Technological breakthroughs enabling early detection of PDAC were described in a review on liquid biopsy (6). This sampling method uses biomarkers such as circulating tumour DNA (ctDNA) and extracellular vesicles (EVs). Liquid biopsy is exciting due to its non-invasive, real-time and repeatable properties. Recent advances in methylation analysis, detecting epigenetic reprogramming in early tumorigenesis, have improved the detection of PDAC using ctDNA. A meta-analysis performed in 2019 showed sensitivity and specificity rates of 70% and 86% respectively. Another biomarker showing promise are EVs, with one study showing high sensitivity and specificity rates of 99% and 82% respectively. The current accuracy of liquid biopsy across all methods for PDAC was investigated in a meta-analysis (7). They concluded that liquid biopsy using biomarkers such as ctDNA was less accurate than CA19-9 for PDAC detection. However, ctDNA was associated with worse survival, making it a useful prognostication tool. Further research utilising multiple biomarkers may increase the accuracy in PDAC detection.

Advances in neoadjuvant chemotherapy regimens are enabling surgical treatment for patients with locally advanced PDAC. Zhang et al. documented the case of a patient with a locally advanced PDAC. Following six cycles of GEM-NabP chemotherapy the patient underwent surgery, with histology confirming near-complete response. Successes such as this are often attributed to favourable biology, but standardisation of neoadjuvant regimens may

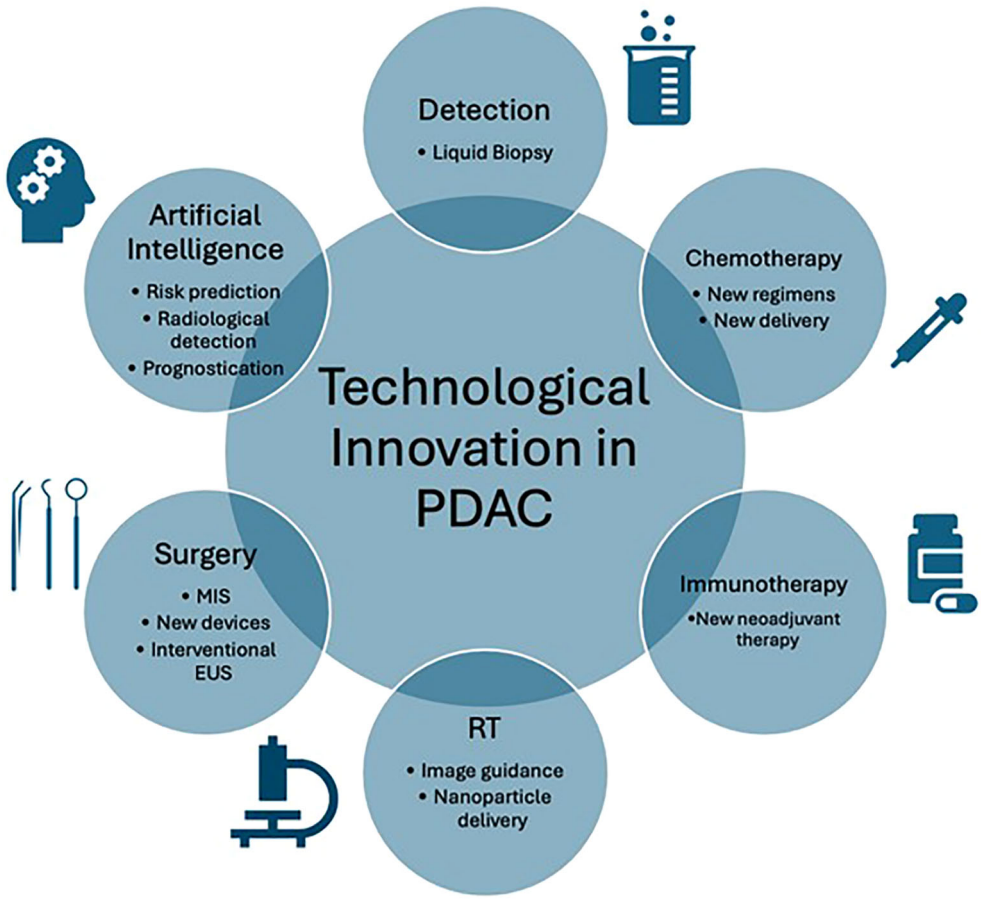

FIGURE 1
Graphical representation of technological innovation in pancreatic ductal adenocarcinoma (PDAC). EUS, Endoscopic ultrasound; MIS, Minimally invasive surgery; RT, Radiotherapy.

improve overall outcomes. Further improvements in neoadjuvant treatments are seen in combination with immunotherapy. Lu et al. published a case report of combined neoadjuvant treatment using a programmed cell death protein-1 inhibitor and chemoradiotherapy (8). Following neoadjuvant treatment for a locally advanced PDAC, the patient underwent a pylorus-preserving pancreaticoduodenectomy (PPPD) with histology showing a pathologic complete response. Further data is also showing the benefit of established adjuvant chemotherapy regimens. A retrospective cohort study by Choi et al. analysed outcomes for patients who received adjuvant chemotherapy for locally advanced PDAC. They showed that 5-fluorouracil-based regimens resulted in favourable survival. New advances have also been made in the delivery of chemotherapy. Cao et al. performed a meta-analysis of regional intra-arterial chemotherapy (RIAC) compared with systemic treatment. RIAC has been developed recently and trialled in PDAC due to its ability to deliver high concentrations locally, while maintaining low systemic drug levels. Their analysis concluded that patients who received RIAC had a higher rate of partial remission and fewer complications. The studies highlighted show progress within chemotherapy and immunotherapy. There is an urgent need for standardisation of regimens, combination therapy and drug delivery.

Technological advances in radiotherapy (RT) for PDAC were highlighted in a review article by Malla et al. (9). Despite the ability to convert borderline resectable cases to surgical resection, up to a third of patients can die during RT from disease progression. Advances in Stereotactic Body Radiation Therapy (SBRT) and hypofractionation enable the delivery of biologically effective doses with reduced toxicity to surrounding tissues. Specifically, innovation in magnetic resonance-guided on-table adaptive RT is enabling this. A recent phase two trial demonstrated reduced incidence of acute grade 3+ gastrointestinal toxicity at 90 days post treatment. New trials are also being conducted on nanoparticles to enhance RT delivery. Hafnium oxide nanoparticles NBTXR3 are activated by RT to improve radiation-induced abscopal effects. These technologies are likely to improve the effects of neoadjuvant RT for patients with PDAC. Healthcare professionals will have the tools to deliver highly effective doses of RT without the tissue toxicity that currently limits the treatment potential of this therapy.

For patients eligible for surgery, advances in surgical technology are improving outcomes. The uptake of minimally invasive surgery

(MIS) for PDAC was analysed by Yan et al. in their meta-analysis of laparoscopic versus open PPPD (10). The 39 studies demonstrated reduced morbidity, length of stay (LOS), blood loss, delayed gastric emptying as well as higher R0 rates in laparoscopic PPPD. The authors importantly highlight that only four randomised controlled studies (RCTs) were included. Two of these were multi-centre and all non-randomised trials were retrospective, showing a need for standardised high-quality surgical trials. The advances of MIS have since been taken further with the advent of robotic surgery. The recently published RCT concerning PDAC has demonstrated safety of the robotic approach for PPPD (11). Novel surgical devices are also prospects for improving patient outcomes. Sheen et al. compared the AEON™ endovascular stapler with traditional devices for laparoscopic distal pancreatectomy in 58 patients (12). Their analysis of using AEON™, characterised by uniform staple lengths and a multi-firing gear, showed a reduction in post-operative day three drain lipase and postoperative pancreatic fistula (POPF) from 65% to 20%. Similar advances have been made in endoscopic ultrasound (EUS). On et al. described the utility of EUS in PDAC in their review. Innovation in the field has enabled EUS-guided interventions such biliary drainage, gastrojejunostomy, coeliac plexus blocks and fiducial placements. Further uptake of interventional EUS is currently limited by a paucity of prospective RCTs. New technologies should be evaluated according to standardised frameworks, such as Idea, Development, Exploration, Assessment and Long-term follow-up, to develop evidence of clinical benefit for patients (13).

One technological area which could improve all aspects of PDAC treatment is Artificial Intelligence (AI). Zhao et al. reviewed the latest achievements of AI in PDAC. Recent advances include AI-based radiomics which can detect PDAC on imaging, and deep learning which can produce precision models for risk prediction and prognostication in PDAC. AI has been used to produce three-dimensional models of tumours, enabling thorough operative planning and improving outcomes such as operative time, blood loss and LOS. One study used artificial neural network models for PDAC prognostication, outperforming corresponding logistic regression models in predicting survival (14).

In summary, technological innovation is transforming the landscape of PDAC treatment. Healthcare professionals are empowered with new tools for detection, therapy delivery, surgery and data analysis in PDAC. Further translational research is needed in multi-biomarker liquid biopsy and RCTs on standardisation of neoadjuvant/adjuvant therapies. Surgical technologies should be evaluated in a robust framework with high quality trials to confer effective and safe treatments for patients with PDAC.

Author contributions

MK: Writing – original draft. AS: Writing – review & editing. SPan: Writing – review & editing. SPat: Writing – review & editing.

Conflict of interest

The authors declare that the research was conducted in the absence of any commercial or financial relationships that could be construed as a potential conflict of interest.

Publisher's note

References

1. Kanno A, Masamune A, Hanada K, Kikuyama M, Kitano M. Advances in early detection of pancreatic cancer. *Diagnostics (Basel)*. (2019) 9. doi: 10.20944/preprints201901.0133.v1

2. Santofimia-Castano P, Iovanna J. Combating pancreatic cancer chemoresistance by triggering multiple cell death pathways. *Pancreatology*. (2021) 21:522–9. doi: 10.1016/j.pan.2021.01.010

3. McGuigan A, Kelly P, Turkington RC, Jones C, Coleman HG, McCain RS. Pancreatic cancer: A review of clinical diagnosis, epidemiology, treatment and outcomes. *World J Gastroenterol*. (2018) 24:4846–61. doi: 10.3748/wjg.v24.i43.4846

4. Joliat GR. Latest advances and future challenges in pancreatic surgery. *J Clin Med*. (2023) 12. doi: 10.3390/jcm12010371

5. Bray F, Ferlay J, Soerjomataram I, Siegel RL, Torre LA, Jemal A. Global cancer statistics 2018: GLOBOCAN estimates of incidence and mortality worldwide for 36 cancers in 185 countries. *CA Cancer J Clin*. (2018) 68:394–424. doi: 10.3322/caac.21492

6. Chen X, Hu X, Liu T. Development of liquid biopsy in detection and screening of pancreatic cancer. *Front Oncol*. (2024) 14. doi: 10.3389/fonc.2024.1415260

7. Arayici ME, İnal A, Basbinar Y, Olgun N. Evaluation of the diagnostic and prognostic clinical values of circulating tumor DNA and cell-free DNA in pancreatic Malignancies: a comprehensive meta-analysis. *Front Oncol*. (2024) 14. doi: 10.3389/fonc.2024.1382369

8. Lu C, Zhu Y, Cheng H, Kong W, Zhu L, Wang L, et al. Case report: pathologic complete response to induction therapy in a patient with potentially resectable pancreatic cancer. *Front Oncol*. (2022) 12. doi: 10.3389/fonc.2022.898119

9. Malla M, Fekrmandi F, Malik N, Hatoum H, George S, Goldberg RM, et al. The evolving role of radiation in pancreatic cancer. *Front Oncol*. (2023) 12. doi: 10.3389/fonc.2022.1060885

10. Yan Y, Hua Y, Chang C, Zhu X, Sha Y, Wang B. Laparoscopic versus open pancreaticoduodenectomy for pancreatic and periampullary tumor: A meta-analysis of randomized controlled trials and non-randomized comparative studies. *Front Oncol*. (2023) 12. doi: 10.3389/fonc.2022.1093395

11. Klotz R, Mihaljevic AL, Kulu Y, Sander A, Klose C, Behnisch R, et al. Robotic versus open partial pancreatoduodenectomy (EUROPA): a randomised controlled stage 2b trial. *Lancet Reg Health Eur*. (2024) 39:100864. doi: 10.1016/j.lanepe.2024.100864

12. Sheen AJ, Bandyopadhyay S, Baltatzis M, Deshpande R, Jamdar S. Carino NdL. Preliminary experience in laparoscopic distal pancreatectomy using the AEON™ endovascular stapler. *Front Oncol*. (2023) 13. doi: 10.3389/fonc.2023.1146646

13. McCulloch P, Altman DG, Campbell WB, Flum DR, Glasziou P, Marshall JC, et al. No surgical innovation without evaluation: the IDEAL recommendations. *Lancet*. (2009) 374:1105–12. doi: 10.1016/S0140-6736(09)61116-8

14. Tong Z, Liu Y, Ma H, Zhang J, Lin B, Bao X, et al. Development, validation and comparison of artificial neural network models and logistic regression models predicting survival of unresectable pancreatic cancer. *Front Bioeng Biotechnol*. (2020) 8:196. doi: 10.3389/fbioe.2020.00196

frontiers | Frontiers in Oncology

TYPE Original Research
PUBLISHED 14 April 2023
DOI 10.3389/fonc.2023.1155555

OPEN ACCESS

EDITED BY
Samir Pathak,
Bristol Royal Infirmary, United Kingdom

REVIEWED BY
Sang Hyub Lee,
Seoul National University Hospital, Republic of Korea
Xiao Chen,
Affiliated Hospital of Nanjing University of Chinese Medicine, China

*CORRESPONDENCE
Xiaohong Ma
maxiaohong@cicams.ac.cn

†These authors have contributed equally to this work and share first authorship

SPECIALTY SECTION
This article was submitted to Gastrointestinal Cancers: Hepato Pancreatic Biliary Cancers, a section of the journal Frontiers in Oncology

RECEIVED 31 January 2023
ACCEPTED 27 March 2023
PUBLISHED 14 April 2023

CITATION
Cai W, Zhu Y, Teng Z, Li D, Feng Q, Jiang Z, Cong R, Chen Z, Liu S, Zhao X and Ma X (2023) Combined CT and serum CA19-9 for stratifying risk for progression in patients with locally advanced pancreatic cancer receiving intraoperative radiotherapy. *Front. Oncol.* 13:1155555. doi: 10.3389/fonc.2023.1155555

Combined CT and serum CA19-9 for stratifying risk for progression in patients with locally advanced pancreatic cancer receiving intraoperative radiotherapy

Wei Cai[1†], Yongjian Zhu[1†], Ze Teng[1], Dengfeng Li[1], Qinfu Feng[2], Zhichao Jiang[3], Rong Cong[1], Zhaowei Chen[1], Siyun Liu[4], Xinming Zhao[1] and Xiaohong Ma[1*]

[1]Department of Diagnostic Radiology, National Cancer Center/National Clinical Research Center for Cancer/Cancer Hospital, Chinese Academy of Medical Sciences and Peking Union Medical College, Beijing, China, [2]Department of Radiation Oncology, National Cancer Center/National Clinical Research Center for Cancer/Cancer Hospital, Chinese Academy of Medical Sciences and Peking Union Medical College, Beijing, China, [3]Department of Medical Oncology, National Cancer Center/National Clinical Research Center for Cancer/Cancer Hospital, Chinese Academy of Medical Sciences and Peking Union Medical College, Beijing, China, [4]Magnetic Resonance Imaging Research, General Electric Healthcare (China), Beijing, China

Background and purpose: The aim of this study was to evaluate the significance of baseline computed tomography (CT) imaging features and carbohydrate antigen 19-9 (CA19-9) in predicting prognosis of locally advanced pancreatic cancer (LAPC) receiving intraoperative radiotherapy (IORT) and to establish a progression risk nomogram that helps to identify the potential beneficiary of IORT.

Methods: A total of 88 LAPC patients with IORT as their initial treatment were enrolled retrospectively. Clinical data and CT imaging features were analyzed. Cox regression analyses were performed to identify the independent risk factors for progression-free survival (PFS) and to establish a nomogram. A risk-score was calculated by the coefficients of the regression model to stratify the risk of progression.

Results: Multivariate analyses revealed that relative enhanced value in portal-venous phase (REV-PVP), peripancreatic fat infiltration, necrosis, and CA19-9 were significantly associated with PFS (all $p < 0.05$). The nomogram was constructed according to the above variables and showed a good performance in predicting the risk of progression with a concordance index (C-index) of 0.779. Our nomogram stratified patients with LAPC into low- and high-risk groups with distinct differences in progression after IORT ($p < 0.001$).

Conclusion: The integrated nomogram would help clinicians to identify appropriate patients who might benefit from IORT before treatment and to adapt an individualized treatment strategy.

KEYWORDS

locally advanced pancreatic cancer, intraoperative radiotherapy, prognosis, progression, computed tomography, carbohydrate antigen 19-9

Introduction

Pancreatic ductal adenocarcinoma (PDAC) is a highly aggressive malignant tumor that results in many deaths as new cases (1, 2). Approximately 30-35% of patients were diagnosed with locally advanced pancreatic cancer (LAPC) based on the relationship between the primary tumor and the adjacent blood vessels (2, 3). Despite improvements in therapeutic approaches in recent years, the 5-year survival rate of PDAC is only approximately 10% (3).

With the improvement and optimization of chemotherapy regimens, the systemic conditions and distal metastases of LAPC could be controlled effectively. However, approximately 30% of LAPC patients died from local progression during the period of systemic therapy (4). Therefore, improved local control might provide more benefits to LAPC patients. Radiotherapy is proven to be an effective local treatment that can improve the local control rate and delay local progression, according to previous clinical studies (2, 5). Intraoperative radiotherapy (IORT), a more targeted form of radiotherapy, improves this effect by delivering high doses of irradiation to the target area, resulting in a higher rate of local control compared with conventional external radiation therapy. IORT has been proven to reduce complications, relieve pain, improve quality of life, and possibly prolong survival in LAPC (6–9). Experts' Consensus on IORT for PDAC established a standard protocol for IORT and identified LAPC as an indication for IORT (10). As well, the European Society for Radiotherapy and Oncology-Advisory Committee on Radiation Oncology Practice (ESTRO-ACROP) recommends IORT for unresectable locally progressive pancreatic cancer (11).

Nevertheless, the prognosis of LAPC patients after IORT varied significantly due to the heterogeneity and complexity of pancreatic cancer (12). Instead of benefiting, patients who are insensitive to IORT might progress rapidly after surgery and suffer a series of complications, toxicities, and financial losses (10). Therefore, it is of great clinical significance to accurately identify the appropriate individuals who could benefit from IORT before treatment.

Contrast-enhanced computed tomography (CECT), the most commonly used imaging technique for the depiction, staging, and assessment of the resectability of PDAC (2, 13, 14), could provide tumor biological and pathological information, including semantic features such as necrosis and peripancreatic tumor infiltration (15) and quantitative parameters such as tumor size and attenuation values (16, 17). Furthermore, CT imaging features have been reported as imaging markers of treatment efficiency and prognosis (15, 16). Serum tumor markers, such as carbohydrate antigen 19-9 (CA19-9), carcinoembryonic antigen (CEA), have been reported to be associated prognosis in PDAC (18, 19). Cai et al. found that the CT attenuation values of PDAC could help stratify the aggressiveness and prognosis (16). In addition, Marchegiani et al. reported that CT attenuation value changes could help identify the possibility of R0 resection after neoadjuvant therapy in locally advanced and borderline resectable pancreatic cancer (20). CA19-9 is a well-known serum biomarker for PDAC, and its level is correlated with tumor burden (21). A high preoperative CA19-9 level has been reported to be associated with severe tumor burden, low differentiation, and poor prognosis (18, 21). To date, there are only a few studies focused on the imaging evaluation of IORT response and prognosis of pancreatic cancer (22–24). To our knowledge, the value of CT combined with serum CA19-9 in predicting the prognosis of LAPC patients receiving IORT has not been fully clarified.

Therefore, the purpose of this study was to evaluate the significance of baseline CT imaging features and serum CA19-9 in predicting the risk of progression of LAPC receiving IORT and to establish an objective, simple, and clinically practical progression risk nomogram by integrating CT imaging features and CA19-9. This would assist clinicians to identify appropriate patients who would benefit from IORT before treatment and to adapt an individualized treatment strategy.

Abbreviations: AJCC, American Joint Committee on Cancer; ALB, albumin; AP, arterial phase; CA19-9, carbohydrate antigen; CA242, carbohydrate antigen 242; CEA, carcinoembryonic antigen; CECT, contrast-enhanced computed tomography; CI, confidence interval; C-index, concordance index; HR, hazard ratio; IORT, intraoperative radiotherapy; LAPC, locally advanced pancreatic cancer; N, non-enhanced; NPV, negative predictive value; PDAC, pancreatic ductal adenocarcinoma; PFS, progression-free survival; PPP, pancreatic parenchymal phase; PPV, positive predictive value; PVP, portal venous phase; RER, relative enhanced ratio; REV, relative enhanced value; ROI, regions of interest.

Materials and methods

Patients

The Institutional Review Board approved (IBR) this retrospective study, waiving the requirement for informed consent because of the retrospective study design (IBR number: 21/412-2608). Between June

2012 and April 2019, we retrospectively searched the medical record database in our institutional to collect the consecutive patients with pathologically confirmed PDAC based on imaging, with IORT as the initial treatment modality (n = 204). The definition of LAPC was in accordance with the NCCN guideline (2). The following inclusion criteria resulted in 148 participants: (a) underwent three-phase CECT examinations dedicated to the pancreas within 2 weeks before IORT; (b) regular follow-up after IORT. Among these patients, 60 were excluded for the following reasons: (a) no adjuvant therapy (chemotherapy or chemoradiotherapy) after IORT (n=24); (b) baseline serum CA19-9 was not available (n=12); (c) coexistence with other malignant tumors (n=6); (d) death due to other reasons (n=8); (e) follow-up time less than 1 month (n=10). The patient recruitment process and study design were depicted in Figure 1.

Clinical data collection

Clinical data were routinely collected, including age, sex, treatment type, jaundice, American Joint Committee on Cancer (AJCC^{8th}) TNM stage, CA19-9, CEA, carbohydrate antigen 242 (CA242), total and direct bilirubin, albumin (ALB), D-dimer, fibrinogen, glucose, and transferrin. Since serum CA19-9 level might be affected by jaundice (25). Endoscopic nasobiliary drainage (ENBD) was performed for biliary drainage on jaundiced patients. The cut-off value of laboratory tests is all based on the normal range at our hospital.

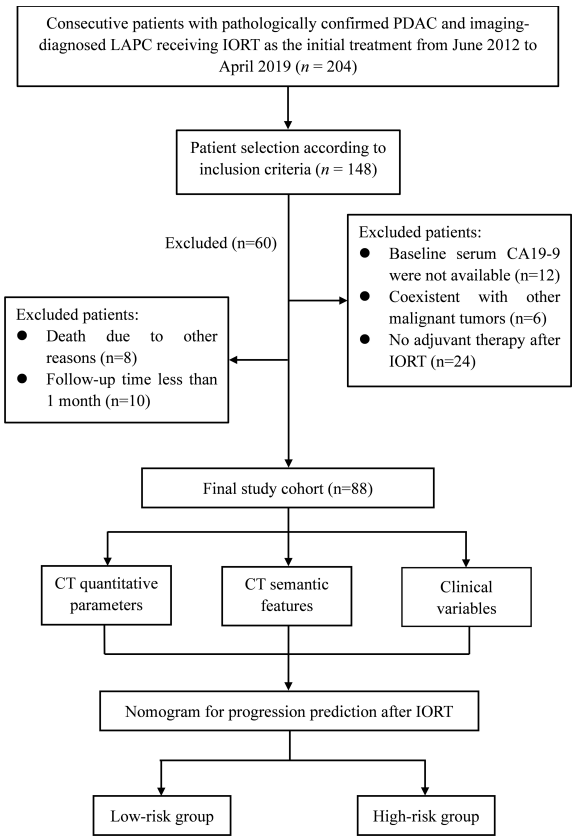

FIGURE 1
Flow chart of the patient enrollment process and illustration of this study. LAPC, locally advanced pancreatic cancer; IORT, intraoperative radiotherapy.

IORT and adjuvant therapy

The IORT procedure and sequential adjuvant therapy strategy were determined in accordance with a standardized protocol reported by experts' consensus (10) and established by the abdominal radiation oncology team at our institution. The illustration of the IORT procedure in LAPC was shown in Figure 2. Surgical bypass, including biliary bypass and gastrojejunostomy, might be performed before IORT depending on the tumor location and clinical symptoms. Details of the treatment plan can be seen in Supplementary Appendix S1 and Supplementary Table S1.

CT protocol

Multiphase CECT examinations consisting of non-enhanced (N), arterial phase (AP), pancreatic parenchymal phase (PPP), and portal venous phase (PVP), were performed on all patients. Impromide (Ultravist, Schering, Berlin, Germany) was administered to each patient at a rate of 4 mL/sec, with a weight-dependent dose of 1.5 mL/kg. AP, PPP, and PVP were defined as 25-30 sec, 40-50 sec, and 65-70 sec, respectively, after contrast injection. Images were

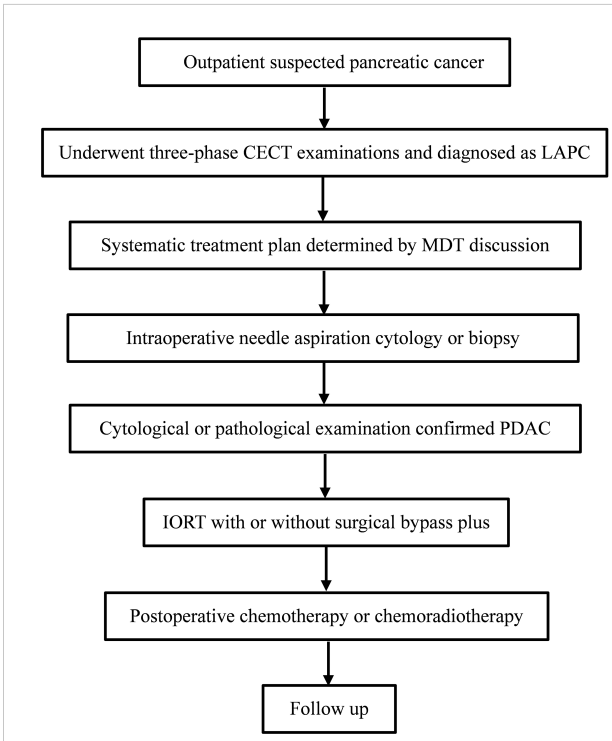

FIGURE 2
The illustration of IORT procedure in LAPC. IORT, intraoperative radiotherapy; LAPC, locally advanced pancreatic cancer; CECT, contrast-enhanced CT; MDT, multi-disciplinary team; PDAC, pancreatic ductal adenocarcinoma.

routinely generated at 5.0 mm thickness in the axial plane in all phases for radiographic evaluation. Given the time span of the study, the CT examinations were carried out on different instruments. Details of the CT scanner parameters are showed in Supplementary Table S2.

Imaging analysis

Two abdominal radiologists (with 10 and 6 years of experience, respectively) who were aware of the diagnosis of PDAC but blinded to the clinical details, independently reviewed the CT images. The following CT semantic features were evaluated: tumor attenuation in four phases, location, necrosis, rim-enhancement, peripancreatic fat infiltration, pancreatic duct dilatation, atrophic upstream pancreatic parenchyma, suspicious lymph nodes, according to the PDAC radiology reporting template proposed by the Society of Abdominal Radiology and previous studies (26–29). The definition of these features was summarized in Supplementary Table S3.

Quantitative CT parameters, including long and short diameters in PVP, relative enhanced value (REV), and relative enhanced ratio (RER) in the three phases, were measured and calculated as previous study reported (16). The specific definitions are detailed in Figure 3 and Supplementary Appendix S2.

Follow-up

After IORT, all patients were closely followed up through outpatient clinic visit. Physical examinations and laboratory tests were performed monthly. Imaging examinations, including CT or MRI, were performed every 3 months. Progression was defined as tumor local progression or distal metastasis confirmed by pathology or imaging, and any disease-

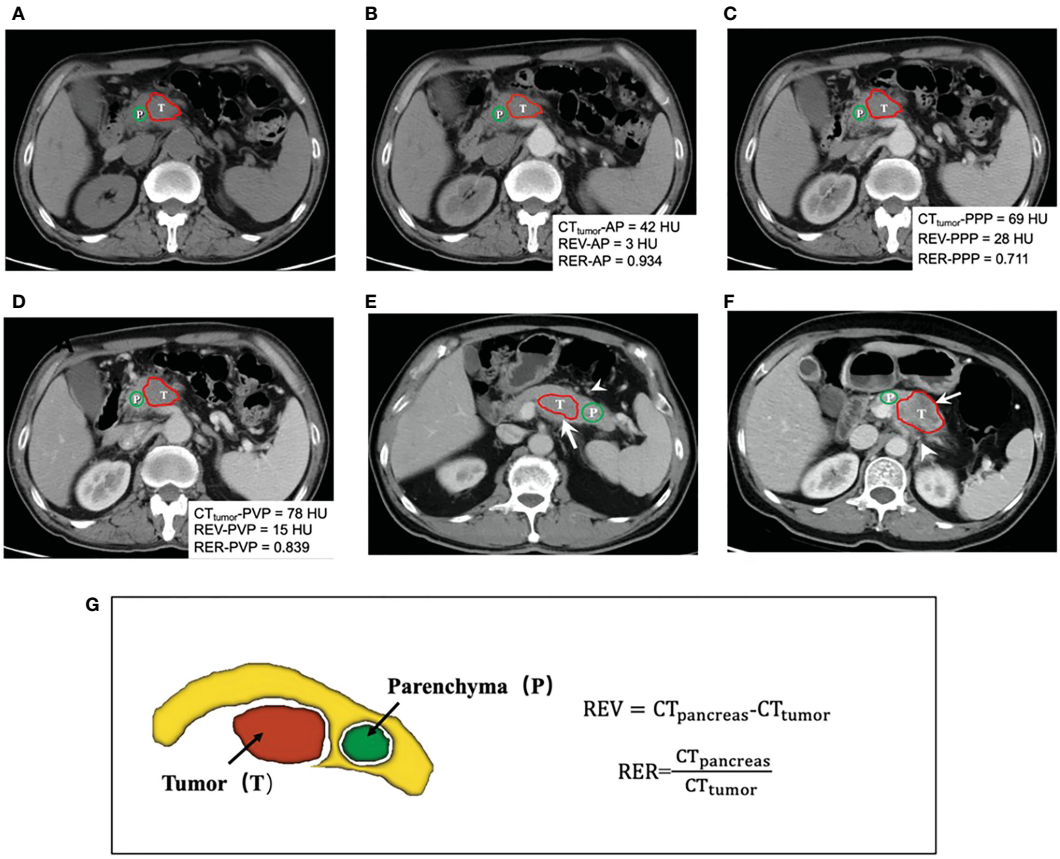

FIGURE 3
(A-D) shows a 58-year-old man with 4.5cm LAPC at uncinate of the pancreas in non-enhanced (N), arterial phase (AP), pancreatic parenchymal phase (PPP) and portal venous phase (PVP) before IORT. Quantification of CT attenuation values, relative enhanced value (REV) and relative enhanced ratio (RER) were calculated and displayed in the images. This patient was classified in the low-risk group. Finally, PFS time of this patients was 10.8 months after IORT and the final progression pattern was liver metastasis. CT images **(E)** in PVP in a 61-year-old man with a 4.2cm lesion appearing hypo-attenuation at the body of pancreas (arrow). The patient was at low risk of progression, without necrosis and peripancreatic fat infiltration (arrowhead). Subsequently, he was found local progression after 9.6 months of IORT. CT images **(F)** in PVP in a 64-year-old woman with 5.3cm LAPC at the body of pancreas. In this case, peripancreatic fat infiltration (arrowhead) and necrosis (arrow) could be observed. This patient was finally assessed as a high-risk group for progression. After 2.7 months of IORT, the patient was found to have peritoneal metastasis. Schematic diagram **(G)** demonstrated delineation of tumor (red), the surrounding normal pancreatic parenchyma (yellow), and delineation of normal pancreatic parenchyma (green). The formulas of CT quantitative parameters are displayed. Red and green lines show the delineation of tumor lesion and the normal peripancreatic parenchyma, respectively. T indicated the tumor and P represented surrounding normal peripancreatic parenchyma. REV, relative enhanced value; RER, relative enhanced ratio.

related death. Local progression was defined ≥ 20% increase in tumor size of tumor lesions or the appearance of new lesions according to RECIST v1.1 criteria (30). The progression-free survival (PFS) time was defined as the interval between IORT and the first day of confirmed progression or the last follow-up without progression. All patients were observed for progression until the final follow-up date of June 30, 2019.

Statistical analysis

Continuous variables were compared using the independent *t* test or Mann-Whitney *U* test, and categorical variables were analyzed using χ^2 or Fisher exact test as appropriate. Consistency between readers was evaluated using Cohen kappa statistics for CT semantic features and the intraclass correlation coefficient (ICC) for quantitative parameters.

Univariate Cox proportional hazards analysis was performed to evaluate the association between PFS and variables. Variables with $p < 0.10$ in univariate analysis, in which continuous variables were converted to a binary classification for clinical convenience, were entered into the multivariate analysis by using a forward stepwise method to identify significantly independent risk factors for PFS. A simple nomogram was established based on the multivariate Cox regression analysis to predict the individual probability of PFS. The Harrell's concordance index (C-index) and calibration curve were used to evaluate the nomogram's performance. Decision curve analysis was used to assess the clinical usefulness of the nomogram. We also evaluated the performance of this nomogram to predict the probability of the PFS, quantified by sensitivity, specificity, positive predictive value (PPV), and negative predictive value (NPV).

A risk-score was generated *via* the summing of the independent prognostic factors weighted by their respective coefficients. The patients were classified into the high-risk and low-risk groups according to the risk-score. The outcome-based optimal cut-off value for REV and RER were determined using the maximally selected rank statistics (Maxstat package) in R statistical software. Survival curve analysis was generated by the Kaplan-Meier method, and the log-rank test was used to compare between different risk groups. All statistical analyses were conducted using R (version 3.6.3, R Foundation for Statistical Computing, Vienna, Austria). $p < 0.05$ was considered statistical significance.

Results

Patient and follow-up

A total of 88 patients (mean age, 59 years ± 9 [SD]) including 50 men and 38 women were included. The baseline demographics and clinical characteristics are summarized in Table 1. No patients received radical surgery after IORT plus adjuvant therapy based on multidisciplinary discussion due to the poor performance status of the patients.

The median follow-up time was 5.14 months (range, 1.53–37.86 months). During follow-up, all patients developed disease progression after IORT. Distant metastases occurred in most patients (52/88, 59.1%), followed by local progression (19/88, 21.6%), and both in the remaining individuals (17/88, 19.3%). Detailed progression pattern

TABLE 1 Baseline clinical characteristics and univariate analysis for PFS.

Characteristic	N (%) or Mean ± SD*	Univariate analysis	
	(Total, n = 88)	HR (95% CI)	*p* Value**
Age (years)	59 ± 9	0.996 (0.973–1.018)	0.703
Sex			
Male	50 (56.8)	Reference	
Female	38 (43.2)	1.045 (0.632–1.484)	0.839
IORT Radiation dose	14.5 ± 0.73	0.78 (0.57-1.08)	0.201
Adjuvant Therapy			
Chemotherapy	56 (63.6)	Reference	
Chemoradiotherapy	32 (36.4)	0.981 (0.632–1.524)	0.932
AJCC 8th T stage			
T1-2	48 (54.5)	Reference	
T3-4	40 (45.5)	1.131 (0.967–1.532)	0.123
AJCC 8th N stage			
N0	54 (61.4)	Reference	0.725
N1	8 (9.1)	0.958 (0.414–1.905)	0.837

(Continued)

TABLE 1 Continued

Characteristic	N (%) or Mean ± SD*	Univariate analysis	
	(Total, n = 88)	HR (95% CI)	*p* Value**
N2	26 (29.5)	1.259 (0.831–1.927)	0.453
Jaundice			
Absent	52 (59.1)	Reference	
Present	36 (41.9)	1.322 (0.833–2.101)	0.236
BMI (kg/m^2)	25.7 (22.0–30.1)	1.038 (0.986–1.094)	0.153
CA 19-9 (U/ml)			
Normal (< 37 U/ml)	16 (18.2)	Reference	**<0.001**
Abnormal (≥ 37 U/ml)	72 (81.8)	3.073 (1.711-5.521)	
CEA (ng/ml)			
Normal (< 5 ng/ml)	57 (64.7)	Reference	0.322
Abnormal (≥ 5 ng/ml)	31 (35.3)	0.794 (0.504–1.253)	
CA 242 (U/ml)			
Normal (< 20 U/ml)	40 (45.5)	Reference	0.401
Abnormal (≥ 20 U/ml)	48 (54.5)	1.200 (0.784-1.837)	
Total bilirubin (μmol/L)			
Normal (< 26 μmol/L)	55 (62.5)	Reference	0.709
Abnormal (≥ 26 μmol/L)	33 (37.5)	1.088(0.698-1.698)	
Direct bilirubin(μmol/L)			
Normal (< 4 μmol/L)	17 (19.3)	Reference	0.456
Abormal (> 4 μmol/L)	71 (80.7)	1.224(0.719-2.084)	
D-dimer (mg/L)			
Normal (< 0.55 mg/L)	55 (62.5)	Reference	0.900
Abnormal (≥ 0.55 mg/L)	33 (37.5)	0.971(0.616-1.532)	
Fibrinogen (g/L)			
Normal (< 4.35 g/L)	72 (81.2)	Reference	0.911
Abnormal (≥ 4.35 g/L)	16 (18.2)	1.033(0.589-1.810)	
Glucose (mmol/L)			
Normal (< 6.1 mmol/L)	48 (54.5)	Reference	0.393
Abnormal (≥ 6.1 mmol/L)	40 (45.5)	0.831(0.544-1.270)	
Transferrin (mg/dl)			
Normal (< 400 mg/dl)	69 (78.4)	Reference	0.741
Abnormal (≥ 400 mg/dl)	19 (21.6)	1.090(0.653-1.820)	
Albumin (g/L)			
Normal (≥ 40 g/L)	63 (71.6)	Reference	**<0.001**
Abnormal (< 40 g/L)	25 (28.4)	3.418(2.019-5.785)	

Statistically significant results are marked in bold.
PFS, progression-free survival; CI, confidence interval; HR, hazard ratio; IORT, Intraoperative radiotherapy; AJCC, American Joint Committee on Cancer; BMI, body mass index; CA19-9, carbohydrate antigen 19-9; CEA, carcinoembryonic antigen; CA242, cancer antigen 242.
*Data are reported as mean ± standard deviation or median with interquartile range in parentheses for continuous variables, and number (%) of patients for category variables, as appropriate.
**p values were calculated via univariate cox proportional hazard analysis.

was shown in Supplementary Table S4. In the whole cohort, the median PFS time was 4.30 months (95% confidence interval [CI]: 2.89–5.71 months), while the PFS rates at 3 months, 6 months, and 1 year were 68.2%, 38.6%, and 15.9%, respectively.

Quantitative CT parameters and semantic feature

The quantitative CT parameters and semantic features are summarized in Table 2. The relationship between tumor and peripheral vascular was supplied in Supplementary Table S5. The κ values for the semantic features were 0.65–1.00 and the ICCs for the quantitative CT parameters were 0.79–0.87, both of which indicated moderate-to-excellent inter-reader agreement (Supplementary Table S6).

Identification of variables for progression prediction in LAPC receiving IORT

Univariate Cox proportional hazards analysis found that REV-PVP, RER-PVP, necrosis, peripancreatic fat infiltration, serum CA19-9 level, and ALB might be associated with PFS (Tables 1, 2).

The optimal cut-off values of REV-PVP and RER-PVP were 20 HU and 0.716, respectively. Ultimately, REV-PVP > 20 HU (hazard ratio [HR] = 3.315, 95% CI = 1.917–5.733, $p < 0.001$), peripancreatic fat infiltration (HR = 1.714, 95% CI = 1.055–2.783, $p = 0.009$), necrosis (HR = 1.938, 95% CI = 1.226–3.063, $p = 0.030$) and abnormal serum CA19-9 level (HR = 2.348, 95% CI = 1.270–4.341, $p = 0.007$) were independent risk factors for PFS through multivariate Cox analysis (Table 3 and Figure 4).

The results of Kaplan-Meier survival analysis based on the above four risk factors were shown in Table 4 and Figures 5A–D.

TABLE 2 Imaging features and univariate analysis for PFS.

Features	N (%) or Mean ± SD*	Univariate analysis	
	(Total, n = 88)	HR (95% CI)	*p* Value**
Quantitative parameters			
Long-axis			
2 cm–4 cm	53 (60.2)	Reference	
> 4 cm	35 (39.8)	1.497 (0.972–2.304)	0.108
Short-axis			0.307
≤ 2 cm	19 (21.6)	Reference	
2 cm–4 cm	61 (69.3)	1.459 (0.864–2.466)	0.158
> 4 cm	8 (9.1)	1.695 (0.728–3.943)	0.221
CT_{tumor} -AP (HU)	45.0 (41.25–51.0)	0.988 (0.959–1.018)	0.422
CT_{tumor} -PPP (HU)	61.0 (56.0–67.75)	0.981 (0.956–1.006)	0.129
CT_{tumor} -PVP (HU)	70.0 (64.0–79.0)	0.988 (0.972–1.004)	0.131
REV-AP (HU)	19.5 (12.0–33.0)	0.998 (0.989–1.007)	0.724
REV-PPP (HU)	36.1 ± 16.9	1.009 (0.996–1.022)	0.157
REV-PVP (HU)	23.0 (15.25–35.0)	1.054 (1.035–1.073)	**<0.001**
RER-AP	0.68 (0.57–0.79)	1.256 (0.416–3.792)	0.686
RER-PPP	0.61 ± 0.15	0.331 (0.078–1.408)	0.135
RER-PVP	0.63 (0.52–0.74)	0.169 (0.033–0.865)	**0.033**
Semantic features			
Tumor Location			
Head/uncinate	63 (71.6)	Reference	
Body/tail	25 (28.4)	0.821 (0.512–1.316)	0.412
N			
Iso-attenuating	68 (77.3)	Reference	
Hypo-attenuating	20 (22.7)	1.275 (0.768–2.118)	0.348

(Continued)

TABLE 2 Continued

Features	N (%) or Mean ± SD*	Univariate analysis	
	(Total, n = 88)	HR (95% CI)	*p* Value**
AP			
Iso-attenuating	26 (29.5)	Reference	
Hypo-attenuating	62 (70.5)	1.162 (0.731–1.847)	0.525
PPP			
Iso-attenuating	15 (17.0)	Reference	
Hypo-attenuating	73 (83.0)	1.051 (0601–1.837)	0.862
PVP			
Iso-attenuating	20 (22.7)	Reference	
Hypo-attenuating	68 (77.3)	1.356 (0.806–2.280)	0.251
Necrosis			
Absent	49 (55.7)	Reference	
Present	39 (44.3)	1.573 (1.019–2.428)	**0.041**
Rim-enhancement			
Absent	67 (76.1)	Reference	
Present	21 (23.9)	1.163 (0.710–1.904)	0.550
Peripancreatic fat infiltration			
Absent	49 (55.7)	Reference	
Present	39 (44.3)	2.672 (1.693–4.217)	**<0.001**
Suspicious lymph nodes			
Absent	54 (61.4)	Reference	
Present	34 (38.6)	1.130 (0.732–1.745)	0.580
Pancreatic duct dilatation			
Absent	49 (55.7)	Reference	
Present	39 (44.3)	1.020 (0.664–1.566)	0.928
Atrophic upstream pancreatic parenchyma			
Absent	42 (47.7)	Reference	
Present	46 (52.3)	1.149 (0.747–1.768)	0.527

Statistically significant results are marked in bold.
PFS, progression-free survival; CI, confidence interval; HR, hazard ratio; CT_{tumor}, the CT attenuation value of tumor; REV, relative enhanced value; RER, relative enhanced ratio; N, non-enhanced; AP, arterial phase; PPP, pancreatic parenchymal phase; PVP, portal venous phase.
*Data are reported as mean ± standard deviation or median with interquartile range in parentheses for continuous variables, and number (%) of patients for categoric variables, as appropriate.
**p values were calculated via univariate cox proportional hazard analysis.

LAPC patients with REV-PVP > 20 HU progressed significantly faster than those with REV-PVP ≤ 20 HU (median PFS: 10.4 months *vs.* 3.0 months, $p < 0.001$). The median PFS of patients with peripancreatic fat infiltration, necrosis, and abnormal serum CA19-9 level was significantly shorter than those without peripancreatic fat infiltration (3.0 months *vs.* 5.8 months), necrosis (2.9 months *vs.* 6.9 months), and normal CA19-9 level (3.5 months *vs.* 11.8 months) (all $p < 0.05$). The survival analysis of different chemotherapy regimens is shown in Supplementary Table S1 and Figure S1.

Nomogram development and evaluation

A nomogram integrating REV-PVP, peripancreatic fat infiltration, necrosis, and serum CA19-9 level, identified in multivariate Cox analysis, was constructed to predict 6-, 12-, and 24-month PFS for LAPC patients receiving IORT (Figure 6A). The prediction nomogram achieved a Harrell's C-index of 0.779 (95% CI = 0.736–0.822), indicating an acceptable predictive capability for PFS. The calibration curves of the nomogram showed good agreement between the nomogram-predicted risk probabilities

10.3389/fonc.2023.1155555

TABLE 3 Multivariate cox proportional hazard analysis for PFS of LAPC patients.

Variables	Multivariate analysis*	
	HR (95% CI)	*p* Value
CA19-9 (U/mL)		
Normal (≤ 37 U/mL)	Reference	0.007
Abnormal (> 37 U/mL)	2.348 (1.270–4.341)	
Albumin (g/L)		
Normal (≥35 g/L)	Reference	…
Abnormal (< 35 g/L)	…	
REV-PVP (HU)		
≤ 20 HU	Reference	
> 20 HU	3.315 (1.917–5.733)	<0.001
RER-PVP		
≤ 0.716	Reference	…
> 0.716	…	
Necrosis		
Absent	Reference	
Present	1.938 (1.226–3.063)	0.005
Peripancreatic fat infiltration		
Absent	Reference	
Present	1.714 (1.055–2.783)	0.030

Data in parentheses are 95% CIs. Ellipsis indicates p value is not significant and should be excluded from the multivariate Cox model.
PFS, progression-free survival; CI, confidence interval; HR, hazard ratio; CA19-9, carbohydrate antigen 19-9; REV, relative enhanced value; RER, relative enhanced ratio; PVP, portal venous phase.
*Variables with p < 0.05 in univariate analysis were applied to multivariate analysis using a stepwise Cox proportional hazards regression mode.

and the actual observed progression after IORT (Figure 6B). The clinical usefulness of the nomogram was evaluated *via* DCA, which indicated that when the threshold probability is between 25.0% and 93.4%, the prediction nomogram of 6-month will have a net benefit from IORT (Figure 6C).

Progression risk stratification based on the nomogram

A risk-scoring system was constructed with the independent risk factors and their regression coefficients in multivariate Cox analysis for predicting the progression of LAPC receiving IORT. The formula was as follows: Risk score = REV-PVP (>20 HU) × 1.199 + peripancreatic fat infiltration (present)× 0.539 + CA19-9 (>37 U/mL) × 0.853 + necrosis (present) × 0.661. The risk score ranged from 0 to 3.252, and the relationship between risk score and predicted PFS probability is shown in Figure 7.

The optimal cut-off value of the risk-score was 1.52, which stratifies the risk of progression into two groups: low-risk group (risk-score > 1.52; 34/88, 38.6%) and high-risk group (risk-score ≤ 1.52; 54/88, 61.4%). LAPC patients with high-risk progressed significantly faster than those with low-risk (median PFS: 3.0 months, 95% CI: 2.3–3.7 months *vs.* 10.6 months, 95% CI = 8.6–12.6 months, $p < 0.001$) (Table 4 and Figure 5E). The 3-month, 6-month, and 1-year PFS rates were 97.1%, 73.5%, and 41.2% in the

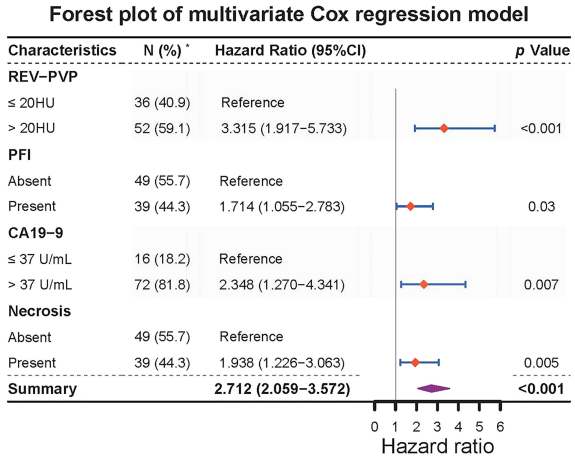

FIGURE 4
Forest plot of multivariate Cox regression model for progression-free survival in 88 LAPC patients. REV, relative enhanced value; PVP, portal venous phase. PFI, peripancreatic fat infiltration. PFS, progression-free survival; CI, confidence interval; REV, relative enhanced value; RER, relative enhanced ratio; PVP, portal venous phase; CA19-9, carbohydrate antigen 19-9.* The content in parentheses of parameter indicates the number and percentage of patients.

TABLE 4 Kaplan-Meier analysis for PFS stratified by risk factors.

Variables (n, %) *	Median PFS (months) (95% CI)	Log-Rank *p* Value
REV-PVP		
≤ 20 HU (n=21, 23.9)	10.4 (8.4–12.4)	<0.001
> 20 HU (n=67, 76.1)	3.0 (2.3–3.7)	
Peripancreatic fat infiltration		
Absent (n=49, 55.7)	5.8 (2.7–9.0)	0.001
Present (n=39, 44.3)	3.0 (2.0–4.0)	
Necrosis		
Absent (n=49, 55.7)	6.9 (4.9–8.0)	0.039
Present (n=39, 44.3)	2.9 (2.3–3.5)	
CA19-9 level		
Normal (n=16, 18.2)	11.8 (5.9–17.7)	<0.001
Abnormal (n=72, 81.8)	3.5 (2.9–4.2)	
Nomogram predicted risk		
Low-risk (n=34, 38.6)	10.6 (8.6–12.6)	<0.001
High-risk (n=54, 61.4)	3.0 (2.3–3.7)	

PFS, progression-free survival; CI, confidence interval; REV, relative enhanced value; RER, relative enhanced ratio; PVP, portal venous phase; CA19-9, carbohydrate antigen 19-9.
*The content in parentheses of parameter indicates the number and percentage of patients.

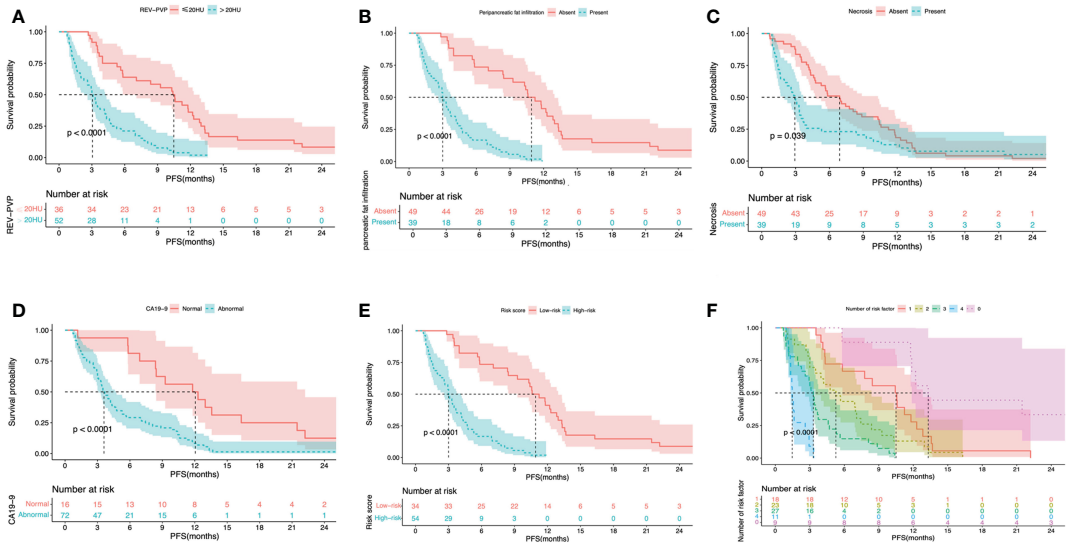

FIGURE 5
Kaplan-Meier survival curves shown PFS according to the REV-PVP (≤20 HU or >20 HU) **(A)**, peripancreatic fat infiltration (absent or present) **(B)**, necrosis (absent or present) **(C)**, serum CA19-9 level (normal or abnormal) **(D)**, nomogram-predicted high- or low-risk **(E)**, and the number of risk factor **(F)**. PFS, progression-free survival; REV, relative enhanced value; PVP, portal venous phase; CA19-9, carbohydrate antigen 19-9.

low-risk group, while 53.7%, 16.7%, and 0% in the high-risk group, respectively.

Predictive performance of risk factors and nomogram

Validation of any combination of the risk factors was performed and displayed in Table 5 and Figure 5F. Further stratified comparisons revealed that the difference in PFS among each other was also statistically significant (Supplementary Table S7). The results showed that patients with all four risk factors progressed most rapidly and had the worst median PFS (1.5 months, 95% CI = 1.2–1.7 months), with PFS rates at 3-month, 6-month, and 1-year of 11.1%, 0.0%, and 0.0%, respectively. In comparison, patients with none of the risk factors showed the longest median PFS (13.3 months, 95% CI = 10.1–16.5 months), with PFS rates at 3-month, 6-month, and 1-year of 100.0%, 88.9%, and 66.7%, respectively.

The predictive performance of PFS probabilities at different times calculated according to the nomogram is listed in Table 6. The accuracy of predictive PFS ranged from 64.8% to 79.5% at 6-months, from 78.4% to 87.5% at 1-years, and from 90.9% to 92.0% at 2-year, respectively. The nomogram exhibited the best performance when predicting PFS probability greater than 60% at 6-month, with the highest F1 score, accuracy, sensitivity, and specificity of 0.74, 79.5%, 73.5%, and 83.3%, respectively.

Discussion

In this study, we discovered that the baseline REV-PVP, peripancreatic fat infiltration, necrosis, and serum CA19-9 were independent risk factors for progression in LAPC patients after IORT. A risk prediction nomogram was constructed based on the above CT imaging features and CA19-9, with an excellent predictive performance for PFS (C-index of 0.779). This provides a potential noninvasive and simple approach to assist clinicians in identifying candidates who might benefit from IORT before treatment and achieving an individualized treatment.

The PFS time for the whole cohort in this study was 4.3 months, which was a little shorter than previous studies reported in a meta-analysis (4). The possible explanations might be due to no radical surgical resection performed after IORT, relatively late tumor stage and poor physical conditions of the patients. In a review of chemotherapy and radiotherapy for LAPC without surgery (31), the PFS times ranged from 2.1 to 7.6 months, which were partially in line with our result. Ogawa K et al. found IORT combined with chemotherapy obtained a survival benefit compared with that of IORT alone (9). Furthermore, IORT could improve local control rate and relieve pain substantially, so it is recommended to be performed in patients with LAPC (10).

Our results revealed that the simple CT quantitative parameter REV-PVP could be used as an objective imaging marker for progression prediction in LAPC after IORT, which was calculated based on the relative enhancement values between the primary tumor and pancreatic parenchyma. LAPC patients with high REV-PVP (>20HU), meaning a lower tumor attenuation compared with adjacent pancreatic parenchyma, progressed significantly more quickly than patients with lower REV-PVP (≤20HU). High REV-PVP implied the CT attenuation difference between pancreatic parenchyma and tumor was great, in other words, a relatively low CT attenuation of tumor itself. Previous studies found that a hypo-attenuated tumor on the CECT indicated poor differentiation of PDAC, in which cancer cells proliferated rapidly and probably lead to the insufficient blood supply and consequently more areas of necrosis (32, 33). In contrast, iso-attenuated lesions or lesions with

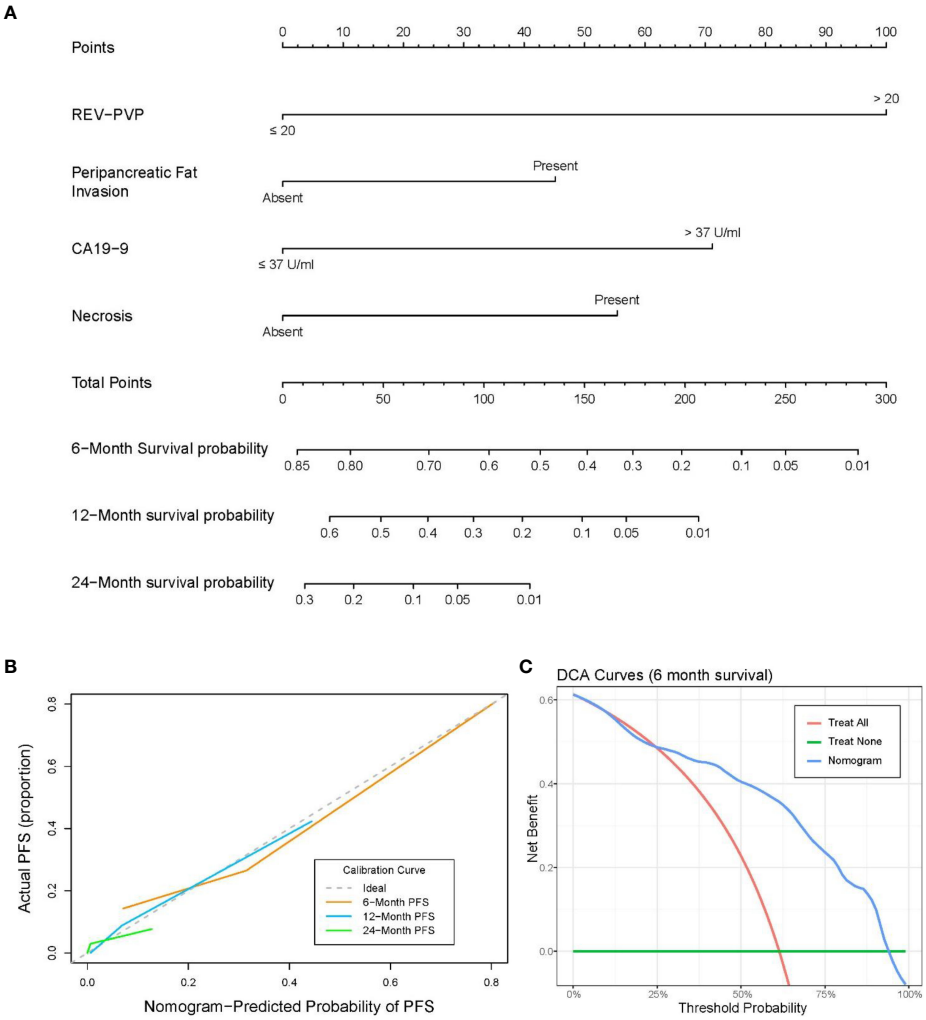

FIGURE 6
(A) Nomogram for predicting the 6-, 12-, and 24-month progression-free survival (PFS). **(B)** Calibration curve for PFS nomogram. **(C)** Decision-curve analysis (DCA) for the nomograms of 6-month PFS.

enhancement closer to surrounding pancreatic parenchyma are probably well- or moderately-differentiated, with more residual alveolar cells and closer to normal pancreatic tissue (33). Furthermore, PDAC appearing as hypo-attenuated may be associated with an extensive desmoplastic stromal reaction, resulting in decreased blood flow and insufficiency of blood supply (34). Moreover, dense fibrotic deposition also causes hypoxia, which is an important cause of resistance to radiotherapy (35, 36). Therefore, we speculated that low CT attenuation of tumor or high REV-PVP might indicate a more aggressive LAPC, less sensitivity to IORT, and a poorer prognosis. Shin et al. proposed PDAC with longer overall survival (OS) was associated with hyper-attenuation in resectable/borderline resectable/locally advanced pancreatic cancer (37), which is in line with our results. Our study just focused on patients with LAPC receiving IORT and utilized relative enhancement CT values between the tumor and the surrounding parenchyma instead of absolute values, avoiding the influence of hemodynamics and individual differences. Cai et al. also reported that high-delta-3 (differences in tumor and surrounding parenchymal attenuation coefficients at pancreatic phase) PDACs corresponded more often with aggressive histologic grade, larger tumor size, less extensive fibrous stromal fraction, and poor disease-free survival and OS (16). The advantage of our study was that we directly measured quantitative CT values at the maximum cross-section, which was more practical for clinical use.

Additionally, our research also supported the evidence that peripancreatic fat infiltration and necrosis, two semantic features of imaging, were indicators for poor prognosis, in accordance with previous studies (15, 38). Peripancreatic fat infiltration might reflect the extent of tumor invasion, not simple a desmoplastic reaction or edema (13, 15, 39). The presence of peripancreatic fat infiltration reduces the chance of R0 resection and leads to poor survival outcomes (13, 40). Necrosis correlates with a higher degree of malignancy in the tumor, which implies rapid proliferation of the tumor cells, leading to tissue ischemia and hypoxia (38). As known to all, hypoxia was a major cause of radiotherapy resistance (35, 36). Therefore, the presence of necrosis is considered as a poor prognostic imaging indicator in LAPC.

CA19-9 is the most important serological biomarker in PADC, which is also reported to be correlated with tumor burden and

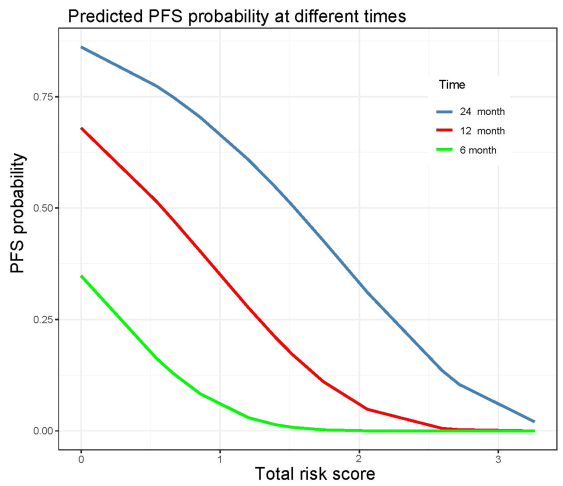

FIGURE 7
Probability of 6-, 12-, and 24-month progression-free survival according to the preoperative total risk score.

prognosis (15). In this study, we investigated the value of CA19-9 in prognosis prediction and demonstrated that high baseline serum CA19-9 levels could be used as an indicator of a short PFS time. So, we added CA19-9 to the nomogram to improve the prediction performance.

We constructed a combined nomogram that incorporates CT imaging features and CA19-9 for progression prediction in LAPC at the individual level. The results indicated that the nomogram showed satisfactory predictive accuracy, with a C-index of 0.779. Using this nomogram to predict no progression probability over 60% at 6-month, the F1 score, accuracy, sensitivity, and specificity could be achieved at 0.74, 79.5%, 73.5%, and 83.3%, respectively. This nomogram might show great clinical utility in predicting progression and identifying optimal candidates in LAPC prior to IORT using a simple and practical method. LAPC patients with a low risk of progression would be suitable for and benefit from IORT, whereas in the high-risk group, radiotherapy might be less effective and other treatment strategies might be considered to improve the patient's prognosis.

TABLE 5 Correlation of number of independently predictive factors with progression-free survival.

Number of Risk Factors * (n, %)	Cox proportional hazards regression analysis		PFS rate at different time			Median PFS (months) (95% CI)
	HR (95% CI)	*p* Value	3-month (%)	6-month (%)	1-year (%)	
0 (n=9, 10)	Reference		100	88.9	66.6	13.3 (10.1–16.5)
1 (n=18, 20)	3.1(1. 2, 8.0)	0.02	100	66.7	27.7	10.4 (6.0–14.7)
2 (n=23, 23)	6.0 (2.3, 15.6)	< 0.001	78.3	43.5	13.0	5.3 (3.0–7.6)
3 (n=27, 13)	14.7 (5.4, 39.8)	< 0.001	59.3	14.8	0.0	3.3 (2.7–3.9)
4 (n=11, 13)	57.9 (17.6, 191.4)	< 0.001	11.1	0.0	0.0	1.5 (1.2–1.7)

PFS, progression-free survival; HR, hazard ratio; CI, confidence interval.
*Risk factors include REV-PVP (> 20HU), peripancreatic fat infiltration, abnormal CA19-9 level, and necrosis. The content in parentheses of parameter indicates the number and percentage of patients.

TABLE 6 Prediction performance for PFS of nomogram.

Time	PFS probability	Accuracy (%)	Sensitivity (%)	Specificity (%)	PPV (%)	NPV (%)	F1 Score
6 months	≥ 90%	64.8 (53.9–74.7) [57/88]	14.7 (5.0–31.1) [5/34]	96.3 (87.3–99.5) [52/54]	71.4 (29.0–96.3) [5/7]	66.7 (55.3–76.8) [54/81]	0.24
	≥ 60%	79.5 (69.6–87.4) [70/88]	73.5 (55.6–87.1) [25/34]	83.3 (70.7–92.0) [45/54]	73.5 (55.6–87.1) [25/34]	83.3 (70.7–92.0) [45/54]	0.74
	≥ 30%	71.5 (70.0–80.7) [63/88]	88.2 (73.3–95.3) [30/34]	61.1 (46.9–74.0) [33/54]	58.8 (44.2–72.4) [30/51]	89.2 (74.6–97.0) [33/37]	0.71
1 year	≥ 60%	84.1 (74.8–91.0) [74/88]	21.4 (4.7–50.8) [3/14]	88.6 (95.9–99.2) [71/74]	50.0 (11.8–88.2) [3/6]	86.6 (77.2–93.1) [71/82]	0.30
	≥ 40%	87.5 (78.7–93.6) [77/88]	50.0 (23.0– 77.0) [7/14]	94.6 (86.7–98.5) [70/74]	63.6 (30.8–89.1) [7/11]	90.9 (82.2–96.3) [70/77]	0.56
	≥ 20%	78.4 (68.4–86.5) [69/88]	85.7 (57.2–98.2) [12/14]	77.0 (65.8–86.0) [57/74]	41.4 (23.5–61.1) [12/29]	96.6 (88.5–99.1) [57/59]	0.56
2 years	≥ 30%	92.0 (84.3–96.7) [81/88]	33.3 (0.8–90.6) [1/3]	94.1 (86.8–98.0) [80/85]	16.7 (4.2– 64.1) [1/6]	97.6 (91.5–99.7) [80/82]	0.22
	≥ 15%	90.9 (82.9–96.0) [80/88]	33.3 (0.8–90.6) [1/3]	92.9 (85.2–97.3) [79/85]	14.3(3.6–57.9) [1/7]	97.5 (91.4–99.7) [79/81]	0.20

Data are percentages with 95% CIs in parentheses and numbers of observations in brackets.
PFS, progression-free survival; CI, confidence interval; PPV, positive predictive value; NPV, negative predictive value.

We should note that our study has several limitations. First, in order to accurately find the most suitable patients for IORT, we only used the progression as the endpoint and did not include OS. The prediction ability of the nomogram for OS in LPAC patients receiving IORT needs to be further clarified in our future work. Second, the patients received different treatment modalities after IORT, which to some extent, may have introduced some bias. But it is consistent with the clinical fact that the treatment of LAPC is highly individual. Third, the recruited patients were from a single institution, and the sample size was small, so no validation of the nomogram was performed. A larger sample size from multicenter is needed to further validate our results. Fourth, the Lewis antigen status was not considered in this study. The nomogram could not be applied directly to Lewis antigen negative individuals. Further validation in an independent cohort of Lewis negative patients was needed. Finally, the CT scanners in this study were diverse. However, it might broaden the scope of application and compensate for the insufficiency of the single-center study to some extent.

Conclusion

In conclusion, CT imaging features and serum CA19-9 provide a tool for predicting progression in patients with LAPC receiving IORT. We constructed and proposed a simple and practical combined nomogram to stratify the risk of progression and identify suitable candidates for IORT before treatment in LAPC. Moreover, the nomogram that integrates baseline CT features and serum CA19-9 might serve as an effective tool in routine clinical practice to help clinicians identify patients who might benefit from IORT and make proper treatment decisions preoperatively and individually. A multicenter prospective study will be needed to further validate the p7otential predictive value of the nomogram in the future.

Data availability statement

The raw data supporting the conclusions of this article will be made available by the authors, without undue reservation.

Ethics statement

This retrospective study was approved by the Institutional Review Board of National Cancer Center/Cancer Hospital, Chinese Academy of Medical Sciences (No. 21/412-2608). The ethics committee waived the requirement of written informed consent for participation.

Author contributions

Conceptualization, WC, YZ, DL, XZ, and XM; Data curation, WC, YZ, ZT, DL, QF, ZJ, RC, and ZC; Formal analysis, WC, YZ, ZT, DL, XZ, and XM; Methodology, WC, YZ, QF, ZJ, RC, ZC, and SL; Software, WC, YZ, RC, ZC, and SL; Validation, ZT, DL, QF, ZJ, and SL; Writing—original draft, all authors; Writing—review and editing, all authors; Supervision, XZ and XM. All authors contributed to the article and approved the submitted version.

Acknowledgments

We would like to thank Siyun Liu form Magnetic Resonance Imaging Research, General Electric Healthcare (China), Beijing for her help in the statistical process.

Conflict of interest

The authors declare that the research was conducted in the absence of any commercial or financial relationships that could be construed as a potential conflict of interest.

Publisher's note

Supplementary material

The Supplementary Material for this article can be found online at: https://www.frontiersin.org/articles/10.3389/fonc.2023.1155555/full#supplementary-material

References

1. Cabasag CJ, Ferlay J, Laversanne M, Vignat J, Weber A, Soerjomataram I, et al. Pancreatic cancer: An increasing global public health concern. *Gut* (2022) 71(8):1686–87. doi: 10.1136/gutjnl-2021-326311

2. National Comprehensive Cancer Network. *NCCN Clinical Practice Guidelines in Oncology: Pancreatic adenocarcinoma, Version 2* (2022). https://www.nccn.org/professionals/physician_gls/pdf/pancreatic.pdf.

3. Park W, Chawla A, O'Reilly EM. Pancreatic cancer: A review. *JAMA* (2021) 326 (9):851–62. doi: 10.1001/jama.2021.13027

4. Suker M, Beumer BR, Sadot E, Marthey L, Faris JE, Mellon EA, et al. FOLFIRINOX for locally advanced pancreatic cancer: a systematic review and patient-level meta-analysis. *Lancet Oncol* (2016) 17(6):801–10. doi: 10.1016/s1470-2045(16)00172-8

5. Cuneo KC MM, Sahai V, Schipper MJ, Parsels LA, Parsels JD, Devasia T, et al. Dose escalation trial of the Wee1 inhibitor adavosertib (AZD1775) in combination with gemcitabine and radiation for patients with locally advanced pancreatic cancer. *J Clin Oncol* (2019) 37(29):2643–50. doi: 10.1200/JCO.19.00730

6. Harrison JM, Wo JY, Ferrone CR, Horick NK, Keane FK, Qadan M, et al. Intraoperative radiation therapy (IORT) for borderline resectable and locally advanced pancreatic ductal adenocarcinoma (BR/LA PDAC) in the era of modern neoadjuvant treatment: Short-term and long-term outcomes. *Ann Surg Oncol* (2020) 27(5):1400–06. doi: 10.1245/s10434-019-08084-2

7. Krempien R, Roeder F. Intraoperative radiation therapy (IORT) in pancreatic cancer. *Radiat Oncol* (2017) 12(1):8. doi: 10.1186/s13014-016-0753-0

8. Cai S, Hong TS, Goldberg SI, Fernandez-del Castillo C, Thayer SP, Ferrone CR, et al. Updated long-term outcomes and prognostic factors for patients with unresectable locally advanced pancreatic cancer treated with intraoperative radiotherapy at the Massachusetts general hospital, 1978 to 2010. *Cancer* (2013) 119 (23):4196–204. doi: 10.1002/cncr.28329

9. Ogawa K, Karasawa K, Ito Y, Ogawa Y, Jingu K, Onishi H, et al. Intraoperative radiotherapy for resected pancreatic cancer: a multi-institutional retrospective analysis of 210 patients. *Int J Radiat Oncol Biol Phys* (2010) 77(3):734–42. doi: 10.1016/j.ijrobp.2009.09.010

10. Li Y, Feng Q, Jin J, Shi S, Zhang Z, Che X, et al. Experts' consensus on intraoperative radiotherapy for pancreatic cancer. *Cancer Lett* (2019) 449:1–7. doi: 10.1016/j.canlet.2019.01.038

11. Calvo FA, Krengli M, Asencio JM, Serrano J, Poortmans P, Roeder F, et al. ESTRO IORT task Force/ACROP recommendations for intraoperative radiation therapy in unresected pancreatic cancer. *Radiother Oncol* (2020) 148:57–64. doi: 10.1016/j.radonc.2020.03.040

12. Hester CA, Perri G, Prakash LR, Maxwell JE, Ikoma N, Kim MP, et al. Radiographic and serologic response to first-line chemotherapy in unresected localized pancreatic cancer. *J Natl Compr Canc Netw* (2022) 20(8):887–97 e3. doi: 10.6004/jnccn.2022.7018

13. Safi SA, Haeberle L, Heuveldop S, Kroepil P, Fung S, Rehders A, et al. Pre-operative MDCT staging predicts mesopancreatic fat infiltration-a novel marker for neoadjuvant treatment? *Cancers (Basel)* (2021) 13(17):4361. doi: 10.3390/cancers13174361

14. Perri G, Prakash L, Wang H, Bhosale P, Varadhachary GR, Wolff R, et al. Radiographic and serologic predictors of pathologic major response to preoperative therapy for pancreatic cancer. *Ann Surg* (2021) 273(4):806–13. doi: 10.1097/sla.0000000000003442

15. Kim DW, Lee SS, Kim SO, Kim JH, Kim HJ, Byun JH, et al. Estimating recurrence after upfront surgery in patients with resectable pancreatic ductal adenocarcinoma by using pancreatic CT: Development and validation of a risk score. *Radiology* (2020) 296(3):541–51. doi: 10.1148/radiol.2020200281

16. Cai X, Gao F, Qi Y, Lan G, Zhang X, Ji R, et al. Pancreatic adenocarcinoma: quantitative CT features are correlated with fibrous stromal fraction and help predict outcome after resection. *Eur Radiol* (2020) 30(9):5158–69. doi: 10.1007/s00330-020-06853-2

17. Agarwal B CA, Ho L. Survival in pancreatic carcinoma based on tumor size. *Pancreas* (2008) 36(1):e15–20. doi: 10.1097/mpa.0b013e31814de421

18. Hess V, Glimelius B, Grawe P, Dietrich D, Bodoky G, Ruhstaller T, et al. CA 19-9 tumour-marker response to chemotherapy in patients with advanced pancreatic cancer enrolled in a randomised controlled trial. *Lancet Oncol* (2008) 9(2):132–38. doi: 10.1016/s1470-2045(08)70001-9

19. Kim SS, Lee S, Lee HS, Bang S, Han K, Park MS. Retrospective evaluation of treatment response in patients with nonmetastatic pancreatic cancer using CT and CA 19-9. *Radiology* (2022) 303(3):548–56. doi: 10.1148/radiol.212236

20. Marchegiani G, Todaro V, Boninsegna E, Negrelli R, Sureka B, Bonamini D, et al. Surgery after FOLFIRINOX treatment for locally advanced and borderline resectable pancreatic cancer: increase in tumour attenuation on CT correlates with R0 resection. *Eur Radiol* (2018) 28(10):4265–73. doi: 10.1007/s00330-018-5410-6

21. Ferrone CR, Finkelstein DM, Thayer SP, Muzikansky A, Fernandez-delCastillo C, Warshaw AL. Perioperative CA19-9 levels can predict stage and survival in patients with resectable pancreatic adenocarcinoma. *J Clin Oncol* (2006) 24(18):2897–902. doi: 10.1200/JCO.2005.05.3934

22. Kanamori S, Nishimura Y, Kokubo M, Sasai K, Hiraoka M, Shibamoto Y, et al. Tumor response and patterns of failure following intraoperative radiotherapy for unresectable pancreatic cancer. *Acta Oncol* (1999) 38(2):215–20. doi: 10.1080/028418699431645

23. Higashi T, Sakahara H, Torizuka T, Nakamoto Y, Kanamori S, Hiraoka M, et al. Evaluation of intraoperative radiation therapy for unresectable pancreatic cancer with FDG PET. *J Nucl Med 1999* (1999) 40(9):1424–33.

24. Kanamori YN S, Kokubo M, Hiraoka M, Abe M. CT changes following IORT for unresectable pancreatic cancer. *Front Radiat Ther Oncol* (1997) 31:189–92. doi: 10.1159/000061167

25. Luo G, Jin K, Deng S, Cheng H, Fan Z, Gong Y, et al. Roles of CA19-9 in pancreatic cancer: Biomarker, predictor and promoter. *Biochim Biophys Acta Rev Cancer* (2021) 1875(2):188409. doi: 10.1016/j.bbcan.2020.188409

26. Al-Hawary IRF MM, Chari ST, Fishman EK, Hough DM, Lu DS, Macari AJM M, et al. Pancreatic ductal adenocarcinoma radiology reporting template- consensus statement of the society of abdominal radiology and the American pancreatic association. *Radiology* (2014) 270(1):248–60. doi: 10.1148/radiol.13131184

27. Lee S, Kim SH, Park HK, Jang KT, Hwang JA, Kim S. Pancreatic ductal adenocarcinoma: Rim enhancement at MR imaging predicts prognosis after curative resection. *Radiology* (2018) 288(2):456–66. doi: 10.1148/radiol.2018172331

28. Toshima F, Inoue D, Yoshida K, Izumozaki A, Yoneda N, Minehiro K, et al. CT-diagnosed extra-pancreatic extension of pancreatic ductal adenocarcinoma is a more reliable prognostic factor for survival than pathology-diagnosed extension. *Eur Radiol* (2022) 32(1):22–33. doi: 10.1007/s00330-021-08180-6

29. Tseng DSJ, Pranger BK, van Leeuwen MS, Pennings JP, Brosens LA, Mohammad NH, et al. The role of CT in assessment of extraregional lymph node involvement in pancreatic and periampullary cancer: A diagnostic accuracy study. *Radiol Imaging Cancer* (2021) 3(2):e200014. doi: 10.1148/rycan.2021200014

30. Eisenhauer EA, Therasse P, Bogaerts J, Schwartz LH, Sargent D, Ford R, et al. New response evaluation criteria in solid tumours: revised RECIST guideline (version 1.1). *Eur J Cancer* (2009) 45(2):228–47. doi: 10.1016/j.ejca.2008.10.026

31. Chin V, Nagrial A, Sjoquist K, O'Connor CA, Chantrill L, Biankin AV, et al. Chemotherapy and radiotherapy for advanced pancreatic cancer. *Cochrane Database Syst Rev* (2018) 3(3):CD011044. doi: 10.1002/14651858.CD011044.pub2

32. Kim JH PS, Yu ES, Kim MH, Kim J, Byun JH, Lee SS, et al. Visually isoattenuating pancreatic adenocarcinoma at dynamic-enhanced CT: frequency, clinical and pathologic characteristics, and diagnosis at imaging examinations. *Radiology* (2010) 257(1):87–96. doi: 10.1148/radiol.10100015

33. Yoon SH LJ, Cho JY, Lee KB, Kim JE, Moon SK, Kim SJ, et al. Small (≤ 20 mm) pancreatic adenocarcinomas: analysis of enhancement patterns and secondary signs with multiphasic multidetector CT. *Radiology* (2011) 259:442–52. doi: 10.1148/radiol.11101133

34. Evan T, Wang VM, Behrens A. The roles of intratumour heterogeneity in the biology and treatment of pancreatic ductal adenocarcinoma. *Oncogene* (2022) 41 (42):4686–95. doi: 10.1038/s41388-022-02448-x

35. Tao J, Yang G, Zhou W, Qiu J, Chen G, Luo W, et al. Targeting hypoxic tumor microenvironment in pancreatic cancer. *J Hematol Oncol* (2021) 14(1):14. doi: 10.1186/s13045-020-01030-w

36. Buckley AM, Lynam-Lennon N, O'Neill H, O'Sullivan J. Targeting hallmarks of cancer to enhance radiosensitivity in gastrointestinal cancers. *Nat Rev Gastroenterol Hepatol* (2020) 17(5):298–313. doi: 10.1038/s41575-019-0247-2

37. Shin DW, Park J, Lee JC, Kim J, Kim YH, Hwang JH. Multi-phase, contrast-enhanced computed tomography-based radiomic prognostic marker of non-metastatic pancreatic ductal adenocarcinoma. *Cancers (Basel)* (2022) 14(10):2476. doi: 10.3390/cancers14102476

38. Kim H, Kim DH, Song IH, Youn SY, Kim B, Oh SN, et al. Identification of intratumoral fluid-containing area by magnetic resonance imaging to predict prognosis in patients with pancreatic ductal adenocarcinoma after curative resection. *Eur Radiol* (2022) 32(4):2518–28. doi: 10.1007/s00330-021-08328-4

39. Yoon SB, Jeon TY, Moon SH, Lee SM, Kim MH. Systematic review and meta-analysis of MRI features for differentiating autoimmune pancreatitis from pancreatic adenocarcinoma. *Eur Radiol* (2022) 32(10):6691–701. doi: 10.1007/s00330-022-08816-1

40. Safi SA, Haeberle L, Fluegen G, Lehwald-Tywuschik N, Krieg A, Keitel V, et al. Mesopancreatic excision for pancreatic ductal adenocarcinoma improves local disease control and survival. *Pancreatology* (2021) 21(4):787–95. doi: 10.1016/j.pan.2021.02.024

frontiers | Frontiers in Oncology

TYPE Case Report
PUBLISHED 25 May 2023
DOI 10.3389/fonc.2023.1155233

OPEN ACCESS

EDITED BY
Samir Pathak,
Bristol Royal Infirmary, United Kingdom

REVIEWED BY
Stefano Francesco Crinò,
University of Verona, Italy
Yazan Khaled,
University of Leeds, United Kingdom

*CORRESPONDENCE
Hongfeng Lin
dtonyl@hotmail.com

RECEIVED 31 January 2023
ACCEPTED 12 May 2023
PUBLISHED 25 May 2023

CITATION
Zhang Z, Lin H, Li H and Wang X (2023) A case report of surgical resection treatment for complete remission after chemotherapy for advanced pancreatic cancer. *Front. Oncol.* 13:1155233. doi: 10.3389/fonc.2023.1155233

A case report of surgical resection treatment for complete remission after chemotherapy for advanced pancreatic cancer

Zhongyan Zhang[1], Hongfeng Lin[1]*, Hehe Li[2] and Xin Wang[1]

[1]Department of Hepatobiliary Surgery, Weifang People's Hospital, Weifang, China, [2]Department of Geriatrics, Weifang People's Hospital, Weifang, China

Pancreatic cancer is a common type of cancer that is treated using surgery or chemotherapy. However, for patients who cannot have surgery, the treatment options are limited and have a low success rate. We report a case of a patient with locally advanced pancreatic cancer who was unable to have surgery due to a tumor that had invaded the coeliac axis and portal vein. However, after receiving chemotherapy with gemcitabine plus nab-paclitaxel(GEM-NabP), the patient achieved complete remission, and a PET-CT scan confirmed that the tumor had disappeared. Eventually, the patient underwent radical surgery with distal pancreatectomy with splenectomy, and the treatment was successful. This case is rare, and there are few reports of complete remission after chemotherapy for pancreatic cancer. This article reviews the relevant literature and guides future clinical practice

KEYWORDS

advanced pancreatic cancer, gemcitabine, chemotherapy, surgical resection, case report, nab-paclitaxel (nab-P)

Introduction

Pancreatic cancer is one of the most commonly seen malignant tumors in clinical practice, with a high mortality rate (1). Since the early clinical symptoms of pancreatic cancer are not obvious, most patients are already in the advanced stage when the diagnosis is confirmed. Due to the advanced stage of cancer, surgical outcomes are poor and the cancer is often declared inoperable. Currently, the main treatment methods for pancreatic cancer are surgical resection, chemotherapy, immunotherapy, radiation therapy, and local therapies such as radiofrequency ablation and irreversible electroporation (2). Surgical treatment is still recognized as the only potential cure for pancreatic cancer, with a 5-year survival rate of 10% to 25% for patients who undergo surgical resection. However, in patients with resectable pancreatic cancer, it is essential to ensure that the surgical margins

are negative (R0) to extend the patient's survival. For advanced pancreatic cancer patients, surgery is often palliative because it is difficult to achieve a curative (R0) resection effect (3). In recent years, with the widespread application of neoadjuvant chemotherapy for pancreatic cancer, patients in the advanced stage have had the opportunity for curative surgery (4). However, there is currently a lack of sufficient clinical research evidence. This article is based on a clinical case of a patient with locally advanced pancreatic cancer who achieved complete remission after conversion therapy and underwent curative surgery. It also reviews relevant literature in the hope of helping treatment options for locally advanced pancreatic cancer patients.

Case description

A 50-year-old male patient presented to the clinic in June 2022 with "upper abdominal pain for 1 week". Physical examination revealed upper abdominal tenderness, no rebound pain, no palpable abdominal masses, no jaundice on the skin and mucous membranes, and no obvious enlargement of the supraclavicular lymph nodes. Laboratory tests showed (on June 4, 2022) a significantly elevated CA19-9 level (394.4 U/mL, normal range 0-34 U/mL), while total bilirubin, CA125, AFP, and CEA were all within normal ranges. A chest and abdomen flat scan and contrast-enhanced CT (Figures 1A1, B1) on June 4, 2022, revealed a low-density area with unclear boundaries at the junction of the neck and body of the pancreas, mild enhancement on enhanced scans; dilation of the main pancreatic duct and involvement of the bile duct pancreatic segment, with thickening and obvious enhancement of the wall. The pancreatic neck and surrounding areas have been affected, including the bile duct system, pancreatic ducts, portal vein, splenic vein, and hepatic artery (AJCC T3N1M0). The whole body bone scan shows no obvious bone metastases. On June 9, 2022, a CT-guided pancreatic biopsy showed moderately differentiated pancreatic adenocarcinoma. Immunohistochemistry shows that tumor tissues are positive for CK7, CK19, and AAT, but negative for CK20, and CDX2. PD-1 is negative and PD-L1 expression is 15%. The Ki-67 index is about 65%. According to the WHO classification, our hospital's pathologists diagnosed it as a primary moderately differentiated pancreatic ductal adenocarcinoma(PDAC) (Figure 2A1–A9).

The patient is a 50-year-old male with pancreatic adenocarcinoma(AJCC T3N1M0) that invades the coeliac axis and portal vein. He underwent GEM-NabP chemotherapy for 6 cycles. After 6 cycles of chemotherapy, repeat abdominal CT showed progressive tumor shrinkage (Figures 1A1–B4), and tumor marker expression levels gradually decreased (Figure 3). On October 31, 2022, a PET/CT was performed. PET/CT scan showed a slightly low density in the pancreatic neck and body junction after pancreatic cancer treatment. No obvious increase in radioactive distribution was observed in the lymph nodes around the pancreas. The treatment effect was evaluated as complete remission.

After the last chemotherapy treatment, the patient's blood test, liver and kidney function showed no obvious abnormalities. The patient's HGB level was 74g/L, after a transfusion of 3.5U of packed red blood cells, the HGB level increased to 104g/L, correcting the anemia. On November 7, 2022, the patient underwent a pancreatic neck tumor and distal pancreatectomy with splenectomy. The surgery lasted for 395 minutes, with an estimated blood loss of 600ml, and a transfusion of 3.0U of packed red blood cells and 450ml of plasma. The surgery was successful (Figure 2B). The pathology report after the surgery (Figures 2C1–3) showed a small

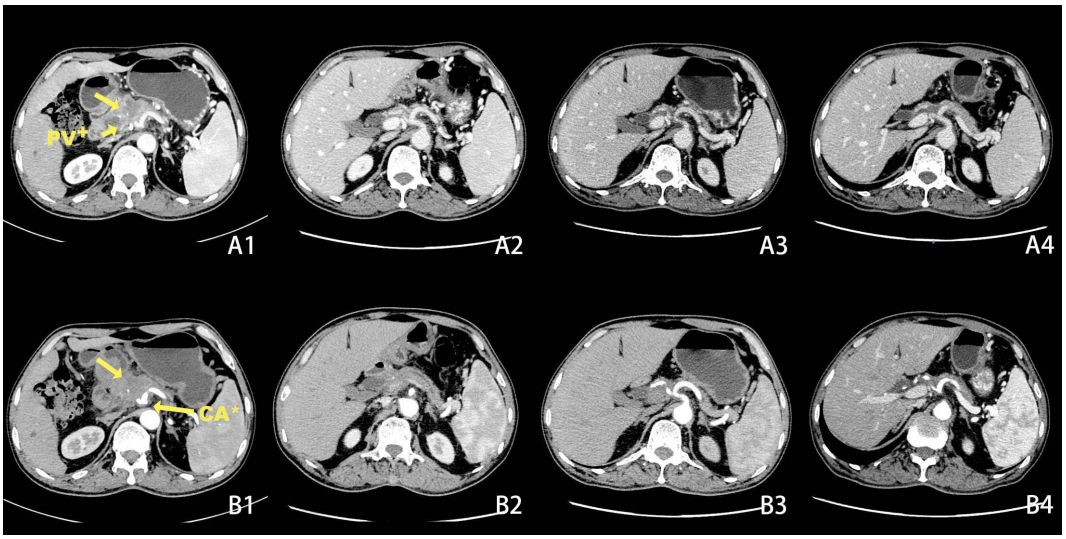

FIGURE 1
Changes in tumor size before and after chemotherapy on CT scans + Portal Vein, * Coeliac Axis. Before chemotherapy CT scan of the abdomen shows a lesion in the pancreatic neck with portal vein and coeliac axis invasion **(A1, B1)**. After 2 cycles of chemotherapy, the tumor had significantly decreased in size **(A2, B2)**. After 5 cycles of chemotherapy **(A3, B3)**. After 6 cycles of chemotherapy **(A4, B4)**.

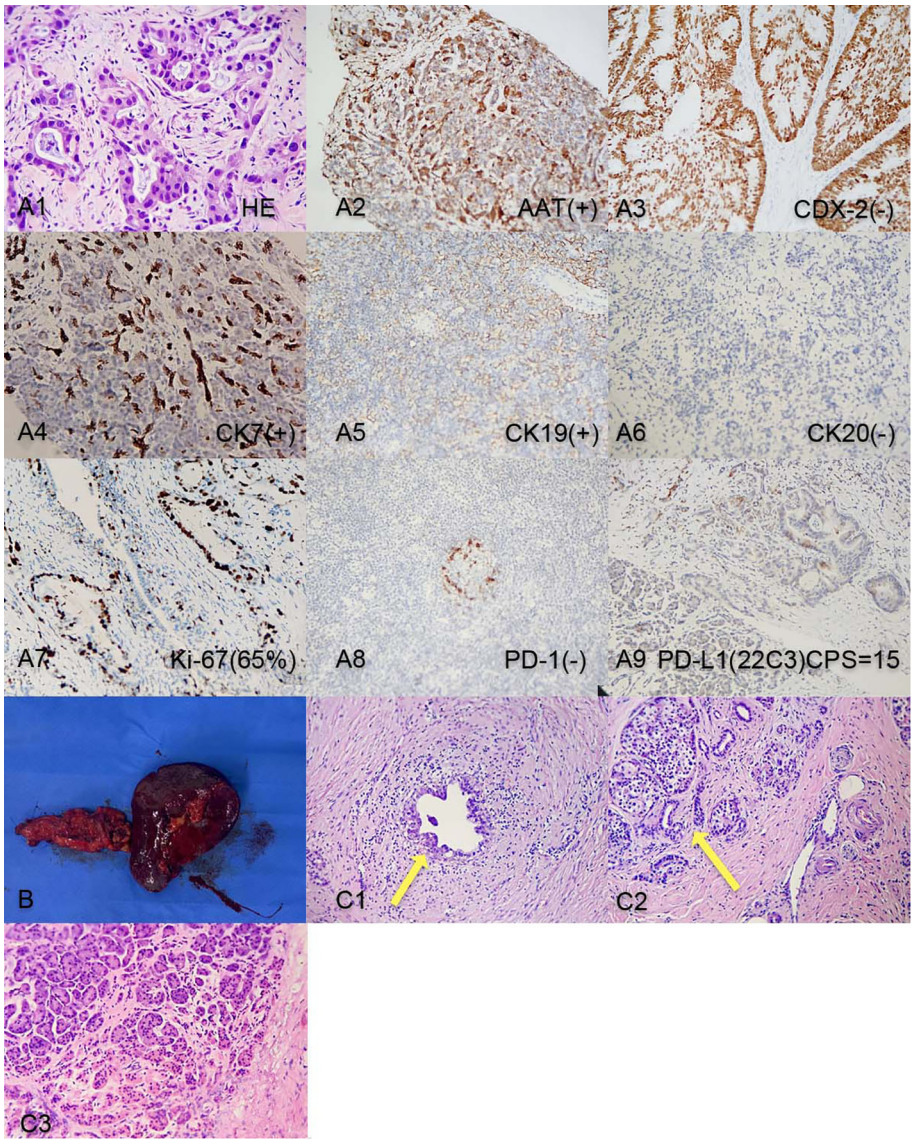

FIGURE 2
(A1-A9) Pancreatic tumor biopsy pathology results before chemotherapy. **(B)**. Post-surgery tissue of the tail of the pancreas and spleen; **(C1)** Post-surgery pathology: Residual pancreatic ductal adenocarcinoma cells; **(C2)** Post-surgery pathology: Pancreatic islet cell hyperplasia and ductal dilation; **(C3)** Intraoperative pathology result: no obvious malignant cells on the cut end of the pancreas.

amount of residual adenocarcinoma at the original tumor site with islet cell proliferation, ductal dilation, no obvious intratumoral thrombosis or nerve invasion, and no lymph node metastasis. According to the College of American Pathologists(CAP) grading system for tumor regression, this case belongs to grade 1(near-complete response with single cancer cells or rare small groups of cancer cells) (5).

Discussion

Pancreatic cancer is one of the worst prognoses of all cancers, 15% of pancreatic cancer patients have the resectable disease. 35% have locally advanced pancreatic cancer(LAPC) and 50% have metastatic disease (MPA). Unresectable pancreatic cancer includes LAPC and MPA. LAPC mainly refers to the primary tumor that cannot typically be removed safely because reconstruction of major vessels is seemingly not possible. MPA spreads to distant organs or non-regional lymph nodes (5). Currently, curative surgery (R0 resection) is still the only treatment that can potentially achieve a clinical cure for pancreatic cancer patients (6). However, due to the advanced stage of the disease when patients seek treatment, pancreatic cancer patients are very likely to invade surrounding organs and blood vessels, resulting in a low R0 resection rate (7).

For patients who have LAPC, chemotherapy is often used as a treatment option. Before chemotherapy, a pathological diagnosis is usually obtained. EUS-guided biopsy represents the gold standard

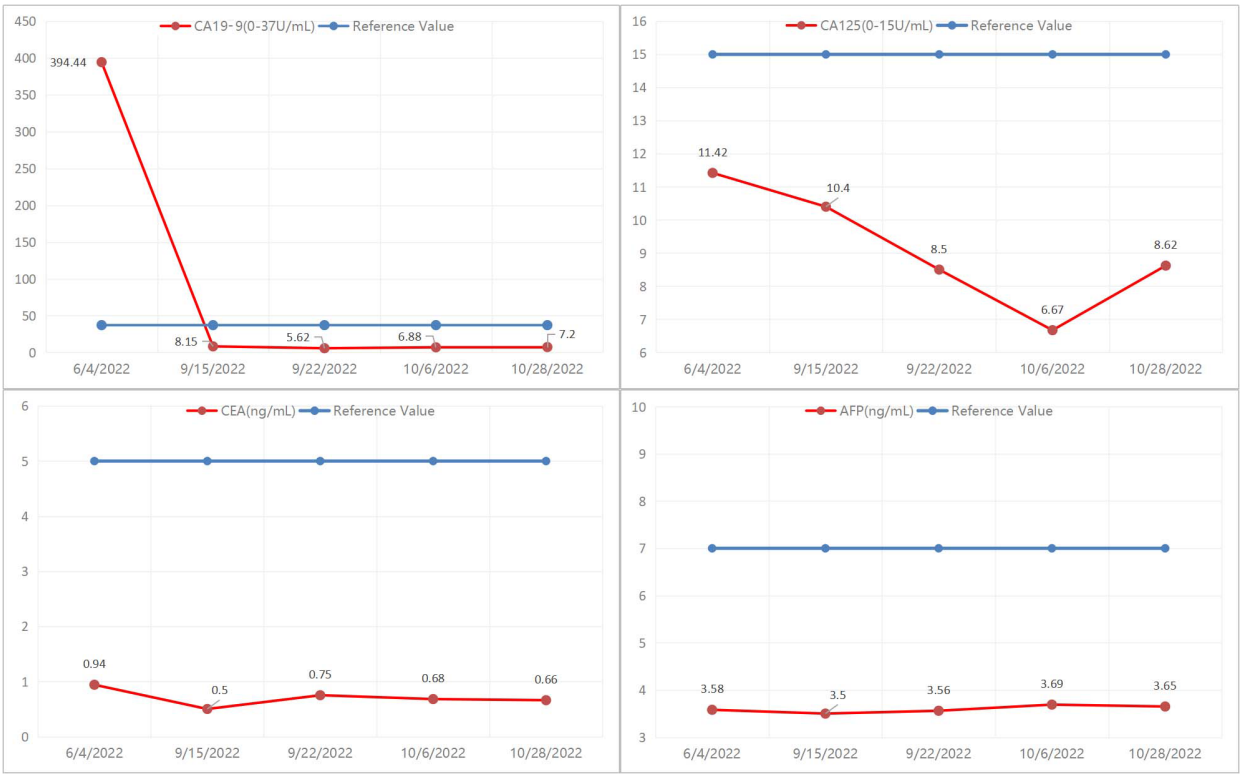

FIGURE 3
Trend of change in tumor marker expression level before and after chemotherapy.

for pathological diagnosis in pancreatic cancer patients. A multicenter, randomized, crossover trial comparing the wet-suction versus slow-pull technique for EUS-guided fine-needle biopsy showed that the wet-suction technique had a significantly higher diagnostic yield and fewer needle passes compared to the slow-pull technique (8). It is important to note that while CT-guided biopsy was used in this case, EUS-guided biopsy should be considered the preferred method for diagnosis in pancreatic cancer patients.

Evaluation of treatment response includes RECIST criteria and CA19-9 levels after chemotherapy (5). Studies have shown that the expression level of CA19-9 is inversely related to the prognosis of patients, the higher the expression level of CA19-9, the worse the prognosis of patients (9). Previous studies have shown that the decline of CA19-9 in LAPC patients after neoadjuvant therapy is more than 50%, which is closely related to a better prognosis. In this case, the patient's CA19-9 expression level was 394.4 U/mL before neoadjuvant therapy, and after 6 cycles of GEM-NabP chemotherapy, the CA19-9 expression level decreased to 7.2 U/mL. Our hospital's PET/CT showed that the tumor size decreased, the lesion metabolism decreased, and the CA19-9 decreased more than 50% of the initial value, considering the patient's disease remission after chemotherapy, and then underwent pancreatic cancer radical surgery. Although preoperative PET/CT showed no tumor activity, postoperative pathology confirmed that there were still small amounts of adenocarcinoma residues. Therefore, it can be suggested that PET/CT is not accurate when the tumor cell content is very low.

With the popularization of multidisciplinary treatment concepts, neoadjuvant therapy has gradually become prominent in the treatment of pancreatic cancer. Neoadjuvant therapy aims to downstaging the tumor and eliminate micrometastases, thereby improving the R0 resection rate and reducing recurrence and metastasis. Previous reports have shown that the R0 resection rate of pancreatic cancer patients after neoadjuvant chemotherapy can reach 81.8%. In our hospital, the patient, in this case achieved partial remission after 6 cycles of GEM-NabP chemotherapy and underwent radical surgery, achieving R0 resection. Therefore, late-stage pancreatic cancer patients are more likely to achieve R0 resection after neoadjuvant chemotherapy. Currently, the main neoadjuvant chemotherapy regimens for advanced pancreatic cancer are FOLFIRINOX (oxaliplatin + irinotecan + leucovorin + 5-fluorouracil) and GEM-NabP (10). Studies have shown that neoadjuvant chemotherapy can effectively improve the pathology of pancreatic cancer, reduce the invasion of lymphatic vessels in patients, increase R0 resection rates, and improve overall survival (Table 1, (11)). However, for the treatment regimens of LAPC, there is still a lack of a large number of clinical experimental studies to prove.

TABLE 1 Recent trials on neoadjuvant chemotherapy, resectability, and outcomes.

Study	Design	Local stage	Chemotherapy	n	Resectability	R0 rate	Median os (months)
McKenzie 2013	Phase 2 trial	Res	Gem/nP	25	80.0%	95%	NA
O'Reilly 2014	Phase 2 trial	Res	Gem/oxaliplatin	38	71.0%	74%	27.2
Sliesoraitis 2014	Phase 2 trial	Res/BR	Gem/nP VS surgery	32 (10 VS 22)	80% VS 100%	60% VS 77%	NA
lelpo 2016	Phase2 trial	Res/BR	Gem/nP	25	68.0%	100%	21
Katz 2016	Phase 1/2 trial	BR	mFOLFIRINOX	22	68.0%	93%	21.7
Okada 2017	Phase 1 trial	BR	Gem/nP	10	80.0%	70%	NA
Tsai 2018	Phase 2 trial	Res/BR	5-FU or gemcitabine-based chemotherapy,depending on molecular profiling	130	82.0%	81%	38
Reni 2018	Phase 2/3 trial	BR/LA	Gem/nP VS Gem/nP/cis/cap	54 (28 VS 26)	32% VS 31%		NA
Murphy 2018	Phase2 trial	BR	FOLFIRINOX+CRT	48	66.6%	97%	37.7
De Marsh 2018	Phase2 trial	Res	FOLFIRINOX	21	81.0%	94%	34
Wei 2019	Phase2 trial	Res	Gem/erlotinib	114	73.0%	81%	21.3
Barbour 2020	Phase2 trial	Res	Gem/nP	42	71.4%	86%	23.5
Sohal 2020	Phase2 trial	Res	FOLFIRINOX VS Gem/nP	55 VS 47	73%VS 70%	85%VS 85%	22.4 VS 23.6

Gem, gemcitabine; nP, nab-paclitaxel; CRT, chemoradiation therapy; OS, overall survival; Res, resectable; BR, borderline resectable.

Conclusion

In summary, for patients with locally advanced pancreatic cancer who have responded to chemotherapy further surgery is feasible. However, long-term follow-up is still necessary to evaluate the patient's long-term outcomes and survival. Large-scale trials are also needed to validate these conclusions.

Data availability statement

The raw data supporting the conclusions of this article will be made available by the authors, without undue reservation.

Ethics statement

Written informed consent was obtained from the individual(s) for the publication of any potentially identifiable images or data included in this article.

Author contributions

ZZ: guarantees the integrity of the entire case and edited the manuscript. HL and XW: performed the literature research, data analysis, and text proofreading. All authors contributed to the article and approved the submitted version.

Acknowledgments

I would like to express my gratitude to all those who helped me during the writing of this manuscript and their efforts in the management of this patient.

Conflict of interest

The authors declare that the research was conducted in the absence of any commercial or financial relationships that could be construed as a potential conflict of interest.

Publisher's note

References

1. He Yong-Gang HXLY. Efficacy and safety of laparoscopic radical resection following neoadjuvant therapy for pancreatic ductal adenocarcinoma: a retrospective study. *World J Gastrointest Oncol* (2022) 14(9):1785–97. doi: 10.4251/wjgo.v14.i9.1785

2. Paiella S, De Pastena M, D'Onofrio M, Crino SF, Pan TL, De Robertis R, et al. Palliative therapy in pancreatic cancer-interventional treatment with radiofrequency ablation/irreversible electroporation. *Transl Gastroenterol Hepatol* (2018) 3:80. doi: 10.21037/tgh.2018.10.05

3. Kawasaki Hiroshi HMKY. A locally advanced pancreatic body cancer presenting common bile duct invasion resected via distal pancreatectomy after gemcitabine plus nab-paclitaxel chemotherapy: a case report. *Int J Surg Case Rep* (2022) 92:106818. doi: 10.1016/j.ijscr.2022.106818

4. Ohmura Yoshiaki TYKY. A long-term survival case of locally advanced unresectable pancreatic adenocarcinoma after chemoradiotherapy and conversion surgery. *Gan To Kagaku Ryoho* (2021) 48(13):1999–2001.

5. Springfeld C, Ferrone CR, Katz M, Philip PA, Hong TS, Hackert T, et al. Neoadjuvant therapy for pancreatic cancer. *Nat Rev Clin Oncol* (2023) 20(5):318–37. doi: 10.1038/s41571-023-00746-1

6. Tamura Takashi IMAR. Covered self-expandable metal stents versus plastic stents for preoperative biliary drainage in patient receiving neo-adjuvant chemotherapy for borderline resectable pancreatic cancer: prospective randomized study. *Dig Endosc* (2021) 33(7):1170–8. doi: 10.1111/den.13926

7. Morimoto Osakuni ESHD. A case report of long survival in pancreatic cancer with superior mesenteric arterial invasion following multimodal therapy. *Gan To Kagaku Ryoho* (2019) 46(13):2342–44.

8. Crinò SF, Conti Bellocchi MC, Di Mitri R, Inzani F , Rimbaş M, Lisotti A, et al. Wet-suction versus slow-pull technique for endoscopic ultrasound-guided fine-needle biopsy: a multicenter, randomized, crossover trial. *Endoscopy* (2023) 55:225–34. doi: 10.1055/a-1915-1812

9. Schneitler Sophie KPRJ. Metastasized pancreatic carcinoma with neoadjuvant FOLFIRINOX therapy and R0 resection. *World J Gastroenterol* (2015) 21(20):6384–90. doi: 10.3748/wjg.v21.i20.6384

10. Tajima Hidehiro OTOM. Neoadjuvant chemotherapy with gemcitabine-based regimens improves the prognosis of node positive resectable pancreatic head cancer. *Mol Clin Oncol* (2019) 11(2):157–66. doi: 10.3892/mco.2019.1867

11. Kolbeinsson HM, Chandana S, Wright GP, Chung M. Pancreatic cancer: a review of current treatment and novel therapies. *J Invest Surg* (2023) 36:2129884. doi: 10.1080/08941939.2022.2129884

frontiers | Frontiers in Oncology

TYPE Review
PUBLISHED 03 July 2023
DOI 10.3389/fonc.2023.1210064

OPEN ACCESS

EDITED BY
Samir Pathak,
Bristol Royal Infirmary, United Kingdom

REVIEWED BY
Valeria Merz,
University of Verona, Italy
Satvinder Singh Mudan,
The London Clinic, United Kingdom

*CORRESPONDENCE
Xiangpan Li
rm001227@whu.edu.cn

†These authors have contributed equally to this work

RECEIVED 21 April 2023
ACCEPTED 20 June 2023
PUBLISHED 03 July 2023

CITATION
Zhao F, Yang D, Xu T, He J, Guo J and Li X (2023) New treatment insights into pancreatic acinar cell carcinoma: case report and literature review.
Front. Oncol. 13:1210064.
doi: 10.3389/fonc.2023.1210064

New treatment insights into pancreatic acinar cell carcinoma: case report and literature review

Fangrui Zhao[1†], Dashuai Yang[2†], Tangpeng Xu[1†], Jiahui He[1], Jin Guo[1] and Xiangpan Li[1*]

[1]Department of Oncology, Renmin Hospital of Wuhan University, Wuhan, Hubei, China, [2]Department of Hepatobiliary Surgery, Renmin Hospital of Wuhan University, Wuhan, Hubei, China

Pancreatic acinar cell carcinoma (PACC) is a rare pancreatic malignancy with unique clinical, molecular, and morphologic features. The long-term survival of patients with PACC is substantially better than that of patients with ductal adenocarcinoma of the pancreas. Surgical resection is considered the first choice for treatment; however, there is no standard treatment option for patients with inoperable disease. The patient with metastatic PACC reported herein survived for more than 5 years with various treatments including chemotherapy, radiotherapy, antiangiogenic therapy and combined immunotherapy.

KEYWORDS

pancreatic acinar cell carcinoma, chemotherapy, radiotherapy, antiangiogenic therapy, immunotherapy

Introduction

PACC is a rare malignancy, accounting for only 1-2% of all pancreatic malignancies. The main component is morphologically similar to alveolar cells and has the ability to synthesize exocrine enzymes. The primary site of PACC can be almost any part of the pancreas, but the head of the pancreas is the most common (1–3), with masses usually 10-11 cm in diameter (4–6).

Patients with PACC often come to the hospital with nonspecific symptoms, such as abdominal pain (60%), back pain (50%), weight loss (45%), nausea and vomiting (20%), black stools (12%), weakness, anorexia and diarrhea (8%) (7, 8). Unlike ductal adenocarcinoma, PACC rarely obstructs the bile ducts (9). Some patients may also present with lipase hypersecretion syndrome, which manifests as elevated lipase levels of more than 10,000 U or more than 10,000 U/dL (10, 11). Their levels of serum tumor markers, such as carbohydrate antigen 19-9 (CA 199) and carcinoembryonic antigen

(CEA), are not consistently elevated. However, the blood levels of alpha-fetoprotein (AFP) can be elevated in younger patients (1).

The prognosis of PACC is better than that of ductal carcinoma (12, 13). Previous studies have shown that the mean overall survival time is approximately 47 months for limited disease and 14 months for metastatic disease, with 5-year survival rates ranging from 36.2% to 72.8% for surgically resected individuals (12–14).

Masses are usually detected by computed tomography (CT) and magnetic resonance imaging (MRI) and are then confirmed by fine needle aspiration (FNA) biopsy. However, MRI is superior to CT in identifying tumor margins, intratumor hemorrhage, tissue infiltration, and ductal expansion (15).

There is no clear treatment option for PACC. Some studies have shown that surgical resection significantly improves the long-term survival of patients (12). However, surgery is for only limited disease. After surgical resection, there are no standard treatment guidelines, and adjuvant therapy is individualized for most patients, with individual differences. In fact, approximately 50% of patients have metastases at the time of diagnosis (16). Metastatic sites usually include the regional lymph nodes and liver, with lung, cervical lymph node and ovarian metastases being uncommon (17). Surgery is not possible for locally advanced and metastatic disease.

A growing number of studies have demonstrated the diversity of mutated genes in PACC, with APC mutations to inactivate WNT signaling and CTNNB1 mutations to activate WNT signaling found in approximately 20% of patients with PACC (18). Even mutations in genes involved in DNA repair, such as ATM, BRCA1, BRCA2, PALB2 and MSH2, have been found in a subset of patients (19, 20), mainly manifesting as genomic instability with microvolatility of 7%-14% (18, 20). In addition, there are studies reporting significant chromosomal gains and losses in PACC patients (18, 21, 22). Performing extensive molecular analysis to identify specific genetic alterations may help to improve new therapeutic ideas.

The patients with metastatic PACC reported herein survived for more than 5 years with multiple treatment modalities applied successively, suggesting that combination therapy may be a relatively promising strategy to control tumor progression.

Case presentation

A 44-year-old woman experienced intermittent back pain in October 2017. Positron emission tomography/computed tomography (PET/CT) demonstrated a primary tumor approximately 88*63 mm in size in the pancreatic corpus and tail; multiple lymph node metastases in the greater omentum, mesentery, hepato-renal space, and hepato-stomach space; and a metastase in the left lobe of the liver. The blood level of alpha-fetoprotein (AFP) was significantly increased, but those of carcinoembryonic antigen (CEA) and carbohydrate antigen (CA) 19-9 in this patient were normal. Ultrasound-guided biopsy of the pancreas was performed. The pathology diagnosis was pancreatic acinar cell carcinoma (PACC) (stage IV) (Figure 1). The results of pancreas biopsy and pathological diagnosis (November 9th, 2017) were PCK (+), EMA (partial +), CK19 (partial +), CK7 (scattered +), Syn (scattered +), and CgA (scattered +).

An adjuvant GS regimen (gemcitabine, 1000 mg/m2, Day 1 and Day 8; S-1, 40 mg/d 1–14, bid, Q21d) was initiated in December 2017. The GS regimen was stopped after two cycles because of progressive disease (PD). A chemotherapy regimen consisting of oxaliplatin plus irinotecan was used for 15 cycles from January 6th, 2018, to February 20th, 2019. The patient was reviewed periodically during treatment, and she achieved a partial response (PR) based on CT scan results until an abdominal CT scan in February showed that the numbers and sizes of primary tumor and local necrosis had increased. Therefore, treatment with single-agent albumin-bound paclitaxel was initiated. Chemotherapy was stopped after 2 cycles because of further progression of the primary tumor. Subsequently, the patient was treated with an antiangiogenic therapy, oral anlotinib (10 mg, once daily from Day 1 to 14, every 3 weeks). During anlotinib treatment, the patient underwent regular re-examination, which indicated that the patient's condition was stable and that the primary tumor gradually decreased in size. The progression-free survival (PFS) time was 23 months.

In March 2021, the patient presented with pelvic pain without an obvious cause. The serum AFP level was increased to 109.3

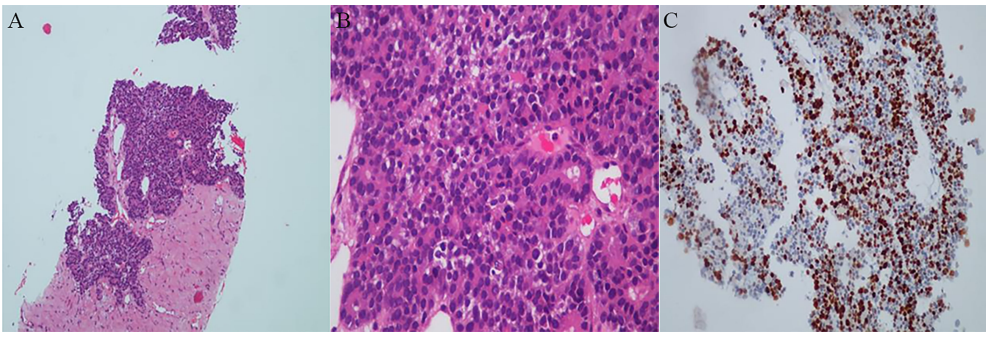

FIGURE 1
Histopathologic examinations of primary tumor. **(A)** Low magnification field of view. **(B)** High magnification field of view. A dense, nested or lamellar arrangement of tumor cells can be observed, some of which are in the form of vesicles or small glandular lumen structures. **(C)** Immunohistochemistry reaction. The results showed PCK (+), EMA (partial +), CK19 (partial +), CK7 (scattered +) Syn (scattered little +) and CgA (scattered little +).

mmol/L. PET/CT scan showed increased number of tumors at the primary site and detected a new pelvic metastase (Figure 2). Metastatic PACC was confirmed by biopsy of the pelvic metastase.

Immunohistochemical results were Ki-67 (+20%), CD10 (−), CD56 (−), CgA (−), P53(+), PCK (+), SYN (+), CK7(+), CK20(−), COX-2(+), Villin (+), CDX-2(+), P40(−), Pax-8(−), SSTR2(+), and PD-1 (−) (Figure 3). Then, the patient was treated with radiotherapy for the pelvic metastase (24 Gy in 3 fractions) and primary tumors (4 Gy in 2 fractions). Radiotherapy began on May 25th, 2021. Meanwhile, she was treated with a PD-1 inhibitor (sintilimab, 200 mg), and recombinant human granulocyte-macrophage (rhuGM-CSF) was injected subcutaneously at a dose of 200 mg per day for 2 weeks. However, the novel anticancer oral medication had a substantially high copay per month, despite insurance coverage, making the drug unaffordable for the patient. The drug anlotinib was made accessible to the patient at no charge through support provided by the CTTQ Patient Assistance Foundation. Subsequently, the patient received anti-PD-1 therapy and antiangiogenic therapy (oral anlotinib). There was a significant decrease in the AFP level and clinical improvement to a PR for the metastatic pelvic metastase. It is important to note that all the treatments were well tolerated, with only mild toxicities. However, in August 2022, CT examination indicated disease progression with multiple metastases to the liver and bone. Figure 4 showed the image changes of the same lesion site before and after treatment. Figure 5 showed the treatment flow chart.

Genetic tests were performed on samples from the pelvic metastase, and the heterozygous mutation c.182A > G (p. Gln61Arg) was detected in the NRAS gene, while no mutations were detected in the BRCA gene, BRAF gene, NTRK gene, EGFR gene or TP53 gene (wild-type).

Discussion

The prevalence of PACC has been estimated to be below 1% among all pancreatic malignancies. More than 50% of patients with PACC have metastatic disease at diagnosis. Although the reported prognosis of PACC is better than that of pancreatic ductal adenocarcinoma (23), the prognosis remains dismal. The OS time of patients with metastatic PACC is 19.6 months (24). Many studies point out surgical resection as the most effective therapeutic strategy. The survival benefit of systemic therapy is more controversial (12, 25, 26). The patient with metastatic PACC reported herein survived over 5 years through treatment with multiple therapies including radiation therapy, chemotherapy, antiangiogenic therapy, and combined immunotherapy.

PACC has unique characteristics in terms of biological behavior, imaging and prognosis relative to PDAC, such as the AFP level in some patients (27). In our case, the change in the AFP level during therapy was useful for evaluating the benefit of treatment. However, the levels of CA 19-9 and CEA, which are

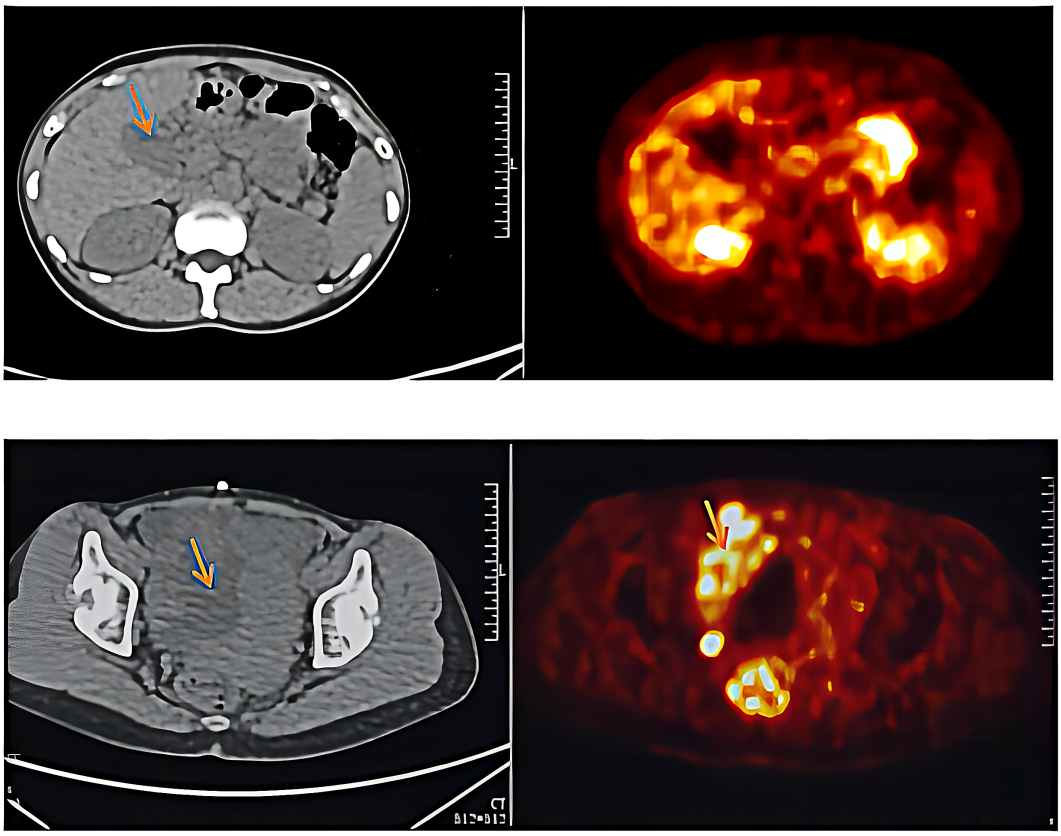

FIGURE 2
Results for PET-CT examination after chemotherapy and targeted therapy (March 10th, 2021).

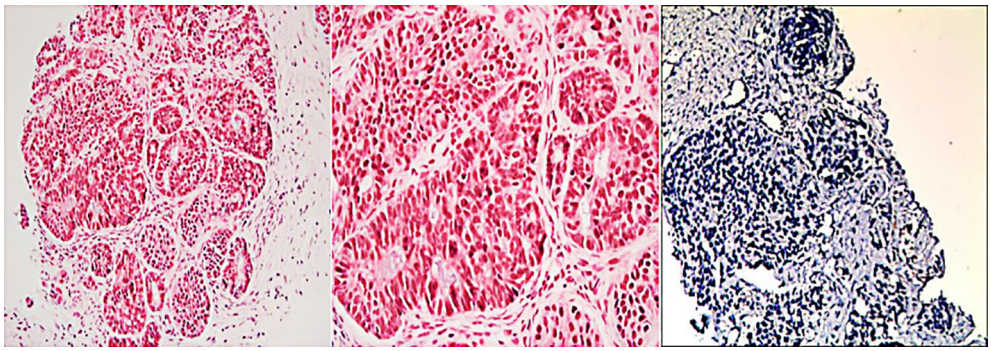

FIGURE 3
Histopathologic and immunohistochemical examinations of biopsy tissue from the pelvic metastase.

predictive markers for pancreatic cancer, remained normal in our case.

Surgical resection is the mainstay of treatment for PACC. It has been shown that the median survival of patients who underwent surgery was significantly better than those who did not (36 months vs 14 months) (7). Whether adjuvant therapy is recommended for patients after surgery is controversial, and most adjuvant therapy is individualised with variable and non-representative response rates. Due to the presence of genetic variants in the APC gene/β-catenin pathway in patients with PACC, chemotherapy regimens known to be active in PDAC or colorectal cancer are often used clinically (28). Combination chemotherapy regimens based on gemcitabine or fluoropyrimidine are commonly used (10, 29). No standard chemotherapy regimen has been established for patients with unresectable or recurrent PACC because PACC is a rare cancer of the pancreas, and no large-scale randomized controlled trials have yet been conducted for this disease. This group of patients usually receives neoadjuvant or palliative 5-FU chemotherapy (30, 31). Fluoropyrimidine-based combination chemotherapy can improve disease control rates (7, 10, 24, 29, 32, 33). Patients with good fitness status are treated with folinic acid/fluorouracil/oxaliplatin or folinic acid/fluorouracil/irinotecan. In contrast, patients in poor physical condition are usually treated with gemcitabine/protein-bound paclitaxel (34). Irinotecan-containing regimens are potentially beneficial regimens for unresectable or recurrent PACC (24, 26). Yoo et al. (35) confirmed that oxaliplatin-based chemotherapy had improved activity against pancreatic ACC compared to gemcitabine. Likewise, we found that the combination of oxaliplatin plus irinotecan was associated with a better response than the gemcitabine combination in our case. Compared with the benefit of gemcitabine in PDAC, the greater clinical benefit of systemic therapy observed in PACC may be explained by the greater use of combination chemotherapy regimens incorporating oxaliplatin and irinotecan over the last decade.

Myriad mutations known to have a role in tumorigenesis have been described in several PACC series (19, 20, 24, 36, 37). PACC has a genomic profile distinct from that of PDAC, with only rare mutations in TP53, KRAS, and p16, despite mutations in these genes being common in PDAC. Approximately 20% of patients with PACC have APC or CTNNB1 which could affect WNT signalling (18). Mutations in BRCA2, PALB2, ATM, BAP1, BRAF and JAK1 are likely to occur in more than a third of PACC patients (20). Genes that are involved in DNA repair, such as ATM, BRCA1, BRCA2, PALB2 and MSH2, can result in genomic instability when mutations occur (19, 20). Microsatellite instability ranges from 7% to 14% in patients with PACC (18, 20, 38). Recurrent rearrangements of BRAF and RAF1 are also present in approximately 23% of patients (37). Of these, RAF genomic alterations are observed to be mutually exclusive with altered inactivation of DNA repair genes in 45% of PACC patients (37). In addition, it has been reported that ALK mutations occur in PACC patient (39), which is quite rare, and in only 0.16% of PDAC patients (40).

There is currently no indication for tumor multigene testing for patients with advanced PACC. However, once a druggable molecular target is detected, it may improve patient survival and quality of life. Thus, a comprehensive molecular analysis was performed and the results indicated that only NRAS mutations were found, which was quite rare. The fact is that NRAS mutations occur predominantly in melanoma and the prognosis is dismal (41). Mutations in NRAS constitutively activate intracellular signaling through multiple pathways, most notably the Ras-Raf-MAPK and PI3K-Akt pathways. Activated signaling pathways can induce cell cycle dysregulation, prosurvival pathway activation, and cell proliferation (42). However, there are currently no drugs that target NRAS, but studying the signalling pathways downstream of NRAS and thus finding druggable targets has become a potential therapeutic approach (41).

Besides, inhibition of angiogenesis is an established therapeutic strategy for many solid tumors. The results of several preclinical and clinical trials have shown that antiangiogenic therapies do not improve the efficacy of pancreatic cancer treatment (43), but these trials did not involve PAAC. Anlotinib, a novel oral multitarget tyrosine kinase inhibitor, could inhibit VEGFR, PDGFR, FGFR, C-Kit, other kinases, and tumor angiogenesis- and proliferation-related signaling pathways (44). Although it has been reported in the treatment of PDAC (45), this is the first report on anlotinib treatment in advanced metastatic PACC achieving a long-term PFS time of 23 months after failure of multiline chemotherapy.

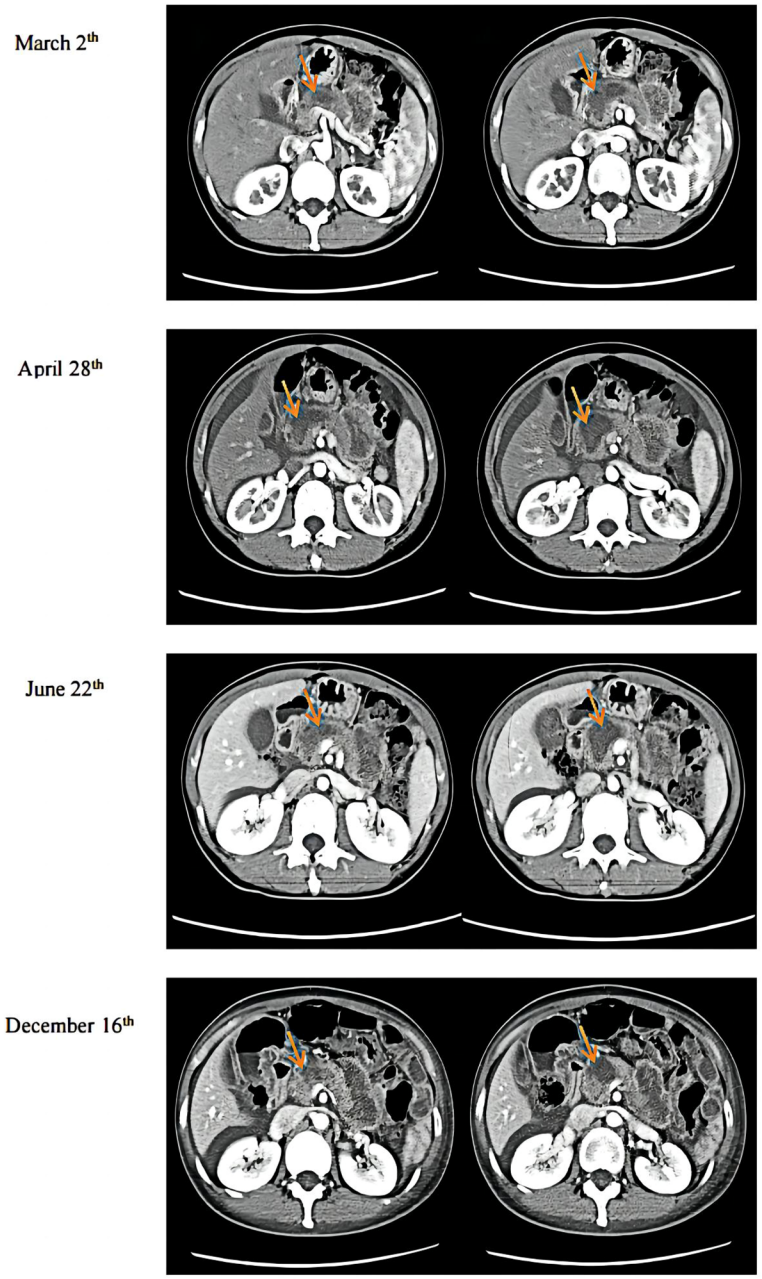

FIGURE 4
CT examination results. March 2nd was during anlotinib treatment. April 28th was before radiotherapy. June 22nd was after immunotherapy plus radiotherapy, and December 16th was during maintenance immunotherapy.

Radiotherapy (RT) is often used to "down-stage" or convert a tumor from borderline resectable to resectable and, in general, is provided as both conventional fractionation and hypofractionated stereotactic body radiotherapy (SBRT) (29). The goal of palliative RT is often to relieve pain and bleeding and/or ameliorate local obstructive symptoms in patients with nonmetastatic or metastatic disease. Besides, RT could improve survival in the metastatic disease context, which has been well established in SCLC. A systematic review revealed a modest response rate to radiotherapy in patients with localized acinar cell carcinoma of the pancreas. In several studies, a "major response" rate was observed in 25% to 35% of these patients (7, 10). However, if stable disease was included in the definition of response (i.e., the disease control rate), significantly higher response rates were seen in highly selected studies when radiotherapy was added (7, 10).

The improvement in condition of the patient after radiotherapy according to our developed protocol may be due to the following reasons. Firstly, radiotherapy can activate the immune system and trigger an antitumor immune response after cytotoxic death and immunostimulatory signal release, increasing T-cell transport to the tumor (46, 47). Although radiotherapy significantly upregulates PD-L1 expression (48), combined anti-PD-1/PD-L1 therapy counterbalances this negative effect. SBRT is more likely to induce immunogenic death in tumor cells, promote the release and

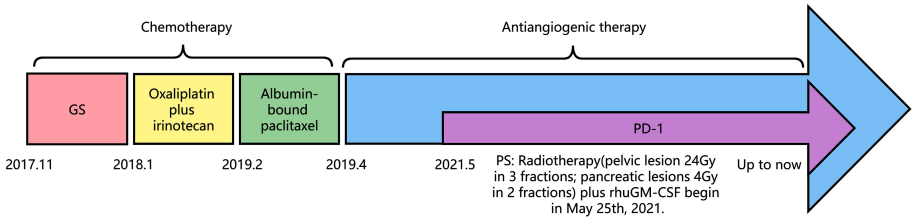

FIGURE 5
Flow chart of the treatment timeline.

presentation of tumor-associated antigens, and generate more potent systemic antitumor effects (49). Moreover, SBRT avoids lymphocytopenia, suggesting that SBRT is a better choice for combination therapy than is conventional stepwise radiotherapy.

Low-dose radiation cannot kill the tumor itself, but it is beneficial to T-cell recruitment, stromal microenvironmental regulation, and immune function promotion (50). Low-dose radiation can also improve the systemic response rates of metastatic disease treated with high-dose radiation and immunotherapy (51). In a study of a bilateral subcutaneous tumor mouse model, more than half of the mice recovered after triple treatment. This suggests that high/low-dose radiotherapy combined with anti-PD1 antibody therapy can produce a synergistic effect, and the additional low-dose radiotherapy is well tolerated by patients (52).

Immunotherapy is still at the experimental stage in the treatment of pancreatic cancer. Pembrolizumab was first included in the NCCN guidelines as a second-line treatment only for advanced solid tumors with high microsatellite instability (MSI-H) or DNA mismatch repair deficiency (dMMR). A total of 83% of pancreatic cancer patients responded to pembrolizumab treatment, with response durations ranging from 2.6 to 9.2 months (53). Tislelizumab is a humanized monoclonal antibody with high affinity and specificity for PD-1 that was specifically designed to minimize FcγR macrophage binding to eliminate antibody-dependent phagocytosis (54).

GM-CSF can enhance the effect of immunotherapy, which is closely related to its mechanism of promoting the proliferation of dendritic cells and M1-type macrophages and enhancing antigen presentation (55). Animal studies have shown that GM-CSF combined with immune checkpoint inhibitors can improve the effectiveness of PD-1/PD-L1 inhibitors by improving antigen presentation and attracting T cells to infiltrate the tumor microenvironment (56, 57). Similarly, combination therapies have been safe and effective in advanced metastatic melanoma clinical trials. In addition, some cytokines, including GM-CSF, synergize with radiotherapy (58). Abscopal responses are defined as systemic antitumor responses outside the primary radiation field. Interestingly, we found that GM-CSF combined with RT could improve the abscopal effect in preclinical data (59). A prospective study also showed that local radiotherapy combined with GM-CSF enhanced the abscopal effect (60). A phase II trial demonstrated the safety of the combination therapies. Additionally, similar clinical trials are ongoing, such as NCT04892498.

After combining high-dose radiotherapy with GM-CSF, this patient was treated with immunotherapy and achieved good disease control. Immunotherapy may benefit from combination with radiotherapy and GM-CSF due to systemic immune response activation. We should consider whether this triple therapy could provide a more diversified treatment strategy for advanced PACC and improve the poor prognosis of this disease.

Recent studies have shown that anlotinib can downregulate the expression of PD-L1 on vascular endothelial cells to alter the tumor immune microenvironment (61). NaZhou et al. (62) designed a phase IB trial to analyze the efficacy and safety of anlotinib in combination with a PD-1 inhibitor in advanced non-small cell lung cancer. The combination therapy showed favorable efficacy and manageable toxicity, especially in the 12 mg anlotinib cohort. However, the reason why anlotinib plays a vital role in treating PACC is still unclear.

Conclusion

The rarity of PACC has led to limited recognition of the disease. Surgical resection is considered the first choice of treatment; however, there is no standard regimen for inoperable individuals. Breakthroughs in precision medicine may assist clinicians in formulating tailor-made therapies for their patients. In addition, both subtype-specific therapy and combination therapy might represent relatively promising strategies to control tumor progression.

Author contributions

JH and JG collected data. FZ and TX wrote the manuscript. XL: Conception, organization, execution and review of manuscript. All authors contributed to the article and approved the submitted version.

Funding

This research was supported by Renmin Hospital of Wuhan University Cross-Innovation Talent Project (JCRCWL-2022-003).

Conflict of interest

The authors declare that the research was conducted in the absence of any commercial or financial relationships that could be construed as a potential conflict of interest.

Publisher's note

References

1. Klimstra DS. Nonductal neoplasms of the pancreas. *Mod Pathol* (2007) 20 Suppl 1:S94–112. doi: 10.1038/modpathol.3800686

2. Bechade D, Desjardin M, Salmon E, Desolneux G, Becouarn Y, Evrard S, et al. Pancreatic acinar cell carcinoma. *Case Rep Gastroenterol* (2016) 10(1):174–80. doi: 10.1159/000445867

3. Fontenot J, Spieler B, Hudson C, Boulmay B. Pancreatic acinar cell carcinoma–literature review and case report of a 56-year-old man presenting with abdominal pain. *Radiol Case Rep* (2020) 15(1):39–43. doi: 10.1016/j.radcr.2019.10.009

4. Raman SP, Hruban RH, Cameron JL, Wolfgang CL, Kawamoto S, Fishman EK. Acinar cell carcinoma of the pancreas: computed tomography features–a study of 15 patients. *Abdom Imaging* (2013) 38(1):137–43. doi: 10.1007/s00261-012-9868-4

5. Chiou YY, Chiang JH, Hwang JI, Yen CH, Tsay SH, Chang CY. Acinar cell carcinoma of the pancreas: clinical and computed tomography manifestations. *J Comput Assist Tomogr* (2004) 28(2):180–6. doi: 10.1097/00004728-200403000-00005

6. Thompson ED, Wood LD. Pancreatic neoplasms with acinar differentiation: a review of pathologic and molecular features. *Arch Pathol Lab Med* (2020) 144(7):808–15. doi: 10.5858/arpa.2019-0472-RA

7. Holen KD, Klimstra DS, Hummer A, Gonen M, Conlon K, Brennan M, et al. Clinical characteristics and outcomes from an institutional series of acinar cell carcinoma of the pancreas and related tumors. *J Clin Oncol* (2002) 20(24):4673–8. doi: 10.1200/JCO.2002.02.005

8. Sridharan V, Mino-Kenudson M, Cleary JM, Rahma OE, Perez K, Clark JW, et al. Pancreatic acinar cell carcinoma: a multi-center series on clinical characteristics and treatment outcomes. *Pancreatology* (2021), S1424-3903(21)00162-9. doi: 10.1016/j.pan.2021.05.011

9. Klimstra DS, Heffess CS, Oertel JE, Rosai J. Acinar cell carcinoma of the pancreas. a clinicopathologic study of 28 cases. *Am J Surg Pathol* (1992) 16(9):815–37. doi: 10.1097/00000478-199209000-00001

10. Seth AK, Argani P, Campbell KA, Cameron JL, Pawlik TM, Schulick RD, et al. Acinar cell carcinoma of the pancreas: an institutional series of resected patients and review of the current literature. *J Gastrointest Surg* (2008) 12(6):1061–7. doi: 10.1007/s11605-007-0338-1

11. Burns WA, Matthews MJ, Hamosh M, Weide GV, Blum R, Johnson FB. Lipase-secreting acinar cell carcinoma of the pancreas with polyarthropathy. a light and electron microscopic, histochemical, and biochemical study. *Cancer* (1974) 33(4):1002–9. doi: 10.1002/1097-0142(197404)33:4<1002::aid-cncr2820330415>3.0.co;2-r

12. Schmidt CM, Matos JM, Bentrem DJ, Talamonti MS, Lillemoe KD, Bilimoria KY. Acinar cell carcinoma of the pancreas in the united states: prognostic factors and comparison to ductal adenocarcinoma. *J Gastrointest Surg* (2008) 12(12):2078–86. doi: 10.1007/s11605-008-0705-6

13. Wisnoski NC, Townsend CMJr., Nealon WH, Freeman JL, Riall TS. 672 patients with acinar cell carcinoma of the pancreas: a population-based comparison to pancreatic adenocarcinoma. *Surgery* (2008) 144(2):141–8. doi: 10.1016/j.surg.2008.03.006

14. Kitagami H, Kondo S, Hirano S, Kawakami H, Egawa S, Tanaka M. Acinar cell carcinoma of the pancreas: clinical analysis of 115 patients from pancreatic cancer registry of Japan pancreas society. *Pancreas* (2007) 35(1):42–6. doi: 10.1097/mpa.0b013e31804bfbd3

15. Hsu MY, Pan KT, Chu SY, Hung CF, Wu RC, Tseng JH. CT and MRI features of acinar cell carcinoma of the pancreas with pathological correlations. *Clin Radiol* (2010) 65(3):223–9. doi: 10.1016/j.crad.2009.11.010

16. Kryklyva V, Haj Mohammad N, Morsink FHM, Ligtenberg MJL, Offerhaus GJA, Nagtegaal ID, et al. Pancreatic acinar cell carcinoma is associated with BRCA2 germline mutations: a case report and literature review. *Cancer Biol Ther* (2019) 20(7):949–55. doi: 10.1080/15384047.2019.1595274

17. Nasser F, Motta Leal Filho JM, Affonso BB, Galastri FL, Cavalcante RN, Martins DLN, et al. Liver metastases in pancreatic acinar cell carcinoma treated with selective internal radiation therapy with y-90 resin microspheres. *Case Rep Hepatol* (2017) 2017:1847428. doi: 10.1155/2017/1847428

18. Abraham SC, Wu TT, Hruban RH, Lee JH, Yeo CJ, Conlon K, et al. Genetic and immunohistochemical analysis of pancreatic acinar cell carcinoma: frequent allelic loss on chromosome 11p and alterations in the APC/beta-catenin pathway. *Am J Pathol* (2002) 160(3):953–62. doi: 10.1016/S0002-9440(10)64917-6

19. Furukawa T, Sakamoto H, Takeuchi S, Ameri M, Kuboki Y, Yamamoto T, et al. Whole exome sequencing reveals recurrent mutations in BRCA2 and FAT genes in acinar cell carcinomas of the pancreas. *Sci Rep* (2015) 5:8829. doi: 10.1038/srep08829

20. Jiao Y, Yonescu R, Offerhaus GJ, Klimstra DS, Maitra A, Eshleman JR, et al. Whole-exome sequencing of pancreatic neoplasms with acinar differentiation. *J Pathol* (2014) 232(4):428–35. doi: 10.1002/path.4310

21. Dewald GW, Smyrk TC, Thorland EC, McWilliams RR, Van Dyke DL, Keefe JG, et al. Fluorescence *in situ* hybridization to visualize genetic abnormalities in interphase cells of acinar cell carcinoma, ductal adenocarcinoma, and islet cell carcinoma of the pancreas. *Mayo Clin Proc* (2009) 84(9):801–10. doi: 10.4065/84.9.801

22. Taruscio D, Paradisi S, Zamboni G, Rigaud G, Falconi M, Scarpa A. Pancreatic acinar carcinoma shows a distinct pattern of chromosomal imbalances by comparative genomic hybridization. *Genes Chromosomes Cancer* (2000) 28(3):294–9. doi: 10.1002/1098-2264(200007)28:3<294::AID-GCC7>3.0.CO;2-N

23. Petrova E, Wellner J, Nording AK, Braun R, Honselmann KC, Bolm L, et al. Survival outcome and prognostic factors for pancreatic acinar cell carcinoma: retrospective analysis from the German cancer registry group. *Cancers (Basel)* (2021) 13(23):6121. doi: 10.3390/cancers13236121

24. Lowery MA, Klimstra DS, Shia J, Yu KH, Allen PJ, Brennan MF, et al. Acinar cell carcinoma of the pancreas: new genetic and treatment insights into a rare malignancy. *Oncologist* (2011) 16(12):1714–20. doi: 10.1634/theoncologist.2011-0231

25. Patel DJ, Lutfi W, Sweigert P, Eguia E, Abood G, Knab L, et al. Clinically resectable acinar cell carcinoma of the pancreas: is there a benefit to adjuvant systemic therapy? *Am J Surg* (2020) 219(3):522–6. doi: 10.1016/j.amjsurg.2019.10.013

26. Takahashi H, Ikeda M, Shiba S, Imaoka H, Todaka A, Shioji K, et al. Multicenter retrospective analysis of chemotherapy for advanced pancreatic acinar cell carcinoma: potential efficacy of platinum- and irinotecan-containing regimens. *Pancreas* (2021) 50(1):77–82. doi: 10.1097/MPA.0000000000001718

27. Nojima T, Kojima T, Kato H, Sato T, Koito K, Nagashima K. Alpha-fetoprotein-producing acinar cell carcinoma of the pancreas. *Hum Pathol* (1992) 23(7):828–30. doi: 10.1016/0046-8177(92)90354-6

28. Ordonez NG. Pancreatic acinar cell carcinoma. *Adv Anat Pathol* (2001) 8(3):144–59. doi: 10.1097/00125480-200105000-00003

29. Butturini G, Pisano M, Scarpa A, D'Onofrio M, Auriemma A, Bassi C. Aggressive approach to acinar cell carcinoma of the pancreas: a single-institution experience and a literature review. *Langenbecks Arch Surg* (2011) 396(3):363–9. doi: 10.1007/s00423-010-0706-2

30. Distler M, Ruckert F, Dittert DD, Stroszczynski C, Dobrowolski F, Kersting S, et al. Curative resection of a primarily unresectable acinar cell carcinoma of the pancreas after chemotherapy. *World J Surg Oncol* (2009) 7:22. doi: 10.1186/1477-7819-7-22

31. Antoine M, Khitrik-Palchuk M, Saif MW. Long-term survival in a patient with acinar cell carcinoma of pancreas. a case report and review of literature. *JOP* (2007) 8(6):783–9.

32. Matos JM, Schmidt CM, Turrini O, Agaram NP, Niedergethmann M, Saeger HD, et al. Pancreatic acinar cell carcinoma: a multi-institutional study. *J Gastrointest Surg* (2009) 13(8):1495–502. doi: 10.1007/s11605-009-0938-z

33. Seki Y, Okusaka T, Ikeda M, Morizane C, Ueno H. Four cases of pancreatic acinar cell carcinoma treated with gemcitabine or s-1 as a single agent. *Japanese J Clin Oncol* (2009) 39(11):751–5. doi: 10.1093/jjco/hyp085

34. Glazer ES, Neill KG, Frakes JM, Coppola D, Hodul PJ, Hoffe SE, et al. Systematic review and case series report of acinar cell carcinoma of the pancreas. *Cancer Control* (2016) 23(4):446–54. doi: 10.1177/107327481602300417

35. Yoo C, Kim BJ, Kim KP, Lee JL, Kim TW, Ryoo BY, et al. Efficacy of chemotherapy in patients with unresectable or metastatic pancreatic acinar cell carcinoma: potentially improved efficacy with oxaliplatin-containing regimen. *Cancer Res Treat* (2017) 49(3):759–65. doi: 10.4143/crt.2016.371

36. Bergmann F, Aulmann S, Sipos B, Kloor M, von Heydebreck A, Schweipert J, et al. Acinar cell carcinomas of the pancreas: a molecular analysis in a series of 57 cases. *Virchows Arch* (2014) 465(6):661–72. doi: 10.1007/s00428-014-1657-8

37. Chmielecki J, Hutchinson KE, Frampton GM, Chalmers ZR, Johnson A, Shi C, et al. Comprehensive genomic profiling of pancreatic acinar cell carcinomas identifies recurrent RAF fusions and frequent inactivation of DNA repair genes. *Cancer Discovery* (2014) 4(12):1398–405. doi: 10.1158/2159-8290.CD-14-0617

38. Liu K, Peng W, Zhou Z. The CT findings of pancreatic acinar cell carcinoma in five cases. *Clin Imaging* (2013) 37(2):302–7. doi: 10.1016/j.clinimag.2012.06.003

39. Gaule M, Pesoni C, Quinzii A, Zecchetto C, Casalino S, Merz V, et al. Exceptional clinical response to alectinib in pancreatic acinar cell carcinoma with a

novel ALK-KANK4 gene fusion. *JCO Precis Oncol* (2022) 6:e2100400. doi: 10.1200/PO.21.00400

40. Singhi AD, Ali SM, Lacy J, Hendifar A, Nguyen K, Koo J, et al. Identification of targetable ALK rearrangements in pancreatic ductal adenocarcinoma. *J Natl Compr Canc Netw* (2017) 15(5):555–62. doi: 10.6004/jnccn.2017.0058

41. Randic T, Kozar I, Margue C, Utikal J, Kreis S. NRAS mutant melanoma: towards better therapies. *Cancer Treat Rev* (2021) 99:102238. doi: 10.1016/j.ctrv.2021.102238

42. Hodis E, Watson IR, Kryukov GV, Arold ST, Imielinski M, Theurillat JP, et al. A landscape of driver mutations in melanoma. *Cell* (2012) 150(2):251–63. doi: 10.1016/j.cell.2012.06.024

43. Annese T, Tamma R, Ruggieri S, Ribatti D. Angiogenesis in pancreatic cancer: preclinical and clinical studies. *Cancers (Basel)* (2019) 11(3):381. doi: 10.3390/cancers11030381

44. Lin B, Song X, Yang D, Bai D, Yao Y, Lu N. Anlotinib inhibits angiogenesis *via* suppressing the activation of VEGFR2, PDGFRbeta and FGFR1. *Gene* (2018) 654:77–86. doi: 10.1016/j.gene.2018.02.026

45. Li S, Niu M, Deng W, Li N, Wei C, Luo S. Anlotinib is effective in the treatment of advanced pancreatic cancer: a case report. *Anticancer Drugs* (2022) 33(1):e558–e61. doi: 10.1097/CAD.0000000000001173

46. Burnette B, Weichselbaum RR. Radiation as an immune modulator. *Semin Radiat Oncol* (2013) 23(4):273–80. doi: 10.1016/j.semradonc.2013.05.009

47. Formenti SC, Demaria S. Combining radiotherapy and cancer immunotherapy: a paradigm shift. *J Natl Cancer Inst* (2013) 105(4):256–65. doi: 10.1093/jnci/djs629

48. Oweida A, Lennon S, Calame D, Korpela S, Bhatia S, Sharma J, et al. Ionizing radiation sensitizes tumors to PD-L1 immune checkpoint blockade in orthotopic murine head and neck squamous cell carcinoma. *Oncoimmunology* (2017) 6(10):e1356153. doi: 10.1080/2162402X.2017.1356153

49. Palma DA, Louie AV, Rodrigues GB. New strategies in stereotactic radiotherapy for oligometastases. *Clin Cancer Res* (2015) 21(23):5198–204. doi:10.1158/1078-0432.CCR-15-0822

50. Barsoumian HB, Ramapriyan R, Younes AI, Caetano MS, Menon H, Comeaux NI, et al. Low-dose radiation treatment enhances systemic antitumor immune responses by overcoming the inhibitory stroma. *J Immunother Cancer* (2020) 8(2):e000537. doi: 10.1136/jitc-2020-000537

51. Menon H, Chen D, Ramapriyan R, Verma V, Barsoumian HB, Cushman TR, et al. Influence of low-dose radiation on abscopal responses in patients receiving high-dose radiation and immunotherapy. *J Immunother Cancer* (2019) 7(1):237. doi: 10.1186/s40425-019-0718-6

52. Yin L, Xue J, Li R, Zhou L, Deng L, Chen L, et al. Effect of low-dose radiation therapy on abscopal responses to hypofractionated radiation therapy and anti-PD1 in mice and patients with non-small cell lung cancer. *Int J Radiat Oncol Biol Phys* (2020) 108(1):212–24. doi: 10.1016/j.ijrobp.2020.05.002

53. Lemery S, Keegan P, Pazdur R. First FDA approval agnostic of cancer site - when a biomarker defines the indication. *N Engl J Med* (2017) 377(15):1409–12. doi: 10.1056/NEJMp1709968

54. Dahan R, Sega E, Engelhardt J, Selby M, Korman AJ, Ravetch JV. FcgammaRs modulate the anti-tumor activity of antibodies targeting the PD-1/PD-L1 axis. *Cancer Cell* (2015) 28(3):285–95. doi: 10.1016/j.ccell.2015.08.004

55. van de Laar L, Coffer PJ, Woltman AM. Regulation of dendritic cell development by GM-CSF: molecular control and implications for immune homeostasis and therapy. *Blood* (2012) 119(15):3383–93. doi: 10.1182/blood-2011-11-370130

56. Everly JJ, Lonial S. Immunomodulatory effects of human recombinant granulocyte-macrophage colony-stimulating factor (rhuGM-CSF): evidence of antitumour activity. *Expert Opin Biol Ther* (2005) 5(3):293–311. doi: 10.1517/14712598.5.3.293

57. Gurbatri CR, Lia I, Vincent R, Coker C, Castro S, Treuting PM, et al. Engineered probiotics for local tumor delivery of checkpoint blockade nanobodies. *Sci Transl Med* (2020) 12(530):eaax0876. doi: 10.1126/scitranslmed.aax0876

58. Palata O, Hradilova Podzimkova N, Nedvedova E, Umprecht A, Sadilkova L, Palova Jelinkova L, et al. Radiotherapy in combination with cytokine treatment. *Front Oncol* (2019) 9:367. doi: 10.3389/fonc.2019.00367

59. Demaria S, Ng B, Devitt ML, Babb JS, Kawashima N, Liebes L, et al. Ionizing radiation inhibition of distant untreated tumors (abscopal effect) is immune mediated. *Int J Radiat Oncol Biol Phys* (2004) 58(3):862–70. doi: 10.1016/j.ijrobp.2003.09.012

60. Golden EB, Chhabra A, Chachoua A, Adams S, Donach M, Fenton-Kerimian M, et al. Local radiotherapy and granulocyte-macrophage colony-stimulating factor to generate abscopal responses in patients with metastatic solid tumours: a proof-of-principle trial. *Lancet Oncol* (2015) 16(7):795–803. doi: 10.1016/S1470-2045(15)00054-6

61. Liu S, Qin T, Liu Z, Wang J, Jia Y, Feng Y, et al. Anlotinib alters tumor immune microenvironment by downregulating PD-L1 expression on vascular endothelial cells. *Cell Death Dis* (2020) 11(5):309. doi: 10.1038/s41419-020-2511-3

62. Zhou N, Jiang M, Li T, Zhu J, Liu K, Hou H, et al. Anlotinib combined with anti-PD-1 antibody, camrelizumab for advanced NSCLCs after multiple lines treatment: an open-label, dose escalation and expansion study. *Lung Cancer* (2021) 160:111–7. doi: 10.1016/j.lungcan.2021.08.006

frontiers | Frontiers in Oncology

TYPE Systematic Review
PUBLISHED 27 July 2023
DOI 10.3389/fonc.2023.1191008

OPEN ACCESS

EDITED BY
Samir Pathak,
Bristol Royal Infirmary, United Kingdom

REVIEWED BY
Yao Lu,
Sun Yat-sen University, China
Stefano Francesco Crinò,
University of Verona, Italy

*CORRESPONDENCE
Yanting Shi
yantingshi@hotmail.com

RECEIVED 21 March 2023
ACCEPTED 13 July 2023
PUBLISHED 27 July 2023

CITATION
Lv B, Wang K, Wei N, Yu F, Tao T and Shi Y (2023) Diagnostic value of deep learning-assisted endoscopic ultrasound for pancreatic tumors: a systematic review and meta-analysis. *Front. Oncol.* 13:1191008. doi: 10.3389/fonc.2023.1191008

Diagnostic value of deep learning-assisted endoscopic ultrasound for pancreatic tumors: a systematic review and meta-analysis

Bing Lv[1], Kunhong Wang[2], Ning Wei[2], Feng Yu[2], Tao Tao[2] and Yanting Shi[2]*

[1]School of Computer Science and Technology, Shandong University of Technology, Zibo, Shandong, China, [2]Department of Gastroenterology, Zibo Central Hospital, Zibo, Shandong, China

Background and aims: Endoscopic ultrasonography (EUS) is commonly utilized in the diagnosis of pancreatic tumors, although as this modality relies primarily on the practitioner's visual judgment, it is prone to result in a missed diagnosis or misdiagnosis due to inexperience, fatigue, or distraction. Deep learning (DL) techniques, which can be used to automatically extract detailed imaging features from images, have been increasingly beneficial in the field of medical image-based assisted diagnosis. The present systematic review included a meta-analysis aimed at evaluating the accuracy of DL-assisted EUS for the diagnosis of pancreatic tumors diagnosis.

Methods: We performed a comprehensive search for all studies relevant to EUS and DL in the following four databases, from their inception through February 2023: PubMed, Embase, Web of Science, and the Cochrane Library. Target studies were strictly screened based on specific inclusion and exclusion criteria, after which we performed a meta-analysis using Stata 16.0 to assess the diagnostic ability of DL and compare it with that of EUS practitioners. Any sources of heterogeneity were explored using subgroup and meta-regression analyses.

Results: A total of 10 studies, involving 3,529 patients and 34,773 training images, were included in the present meta-analysis. The pooled sensitivity was 93% (95% confidence interval [CI], 87–96%), the pooled specificity was 95% (95% CI, 89–98%), and the area under the summary receiver operating characteristic curve (AUC) was 0.98 (95% CI, 0.96–0.99).

Conclusion: DL-assisted EUS has a high accuracy and clinical applicability for diagnosing pancreatic tumors.

Systematic review registration: https://www.crd.york.ac.uk/prospero/display_record.php?ID=CRD42023391853, identifier CRD42023391853.

KEYWORDS

pancreatic tumor, artificial intelligence, deep learning, endoscopic ultrasound, meta-analysis, systemic review

1 Introduction

Pancreatic tumors (PTs) are relatively common tumors of the digestive tract. Benign PTs include serous cystadenomas, mucinous cystadenomas, and intraductal papillary mucinous neoplasms (IPMNs), while malignant tumors include pancreatic ductal adenocarcinomas (PDACs), pancreatic neuroendocrine tumors (PNETs), and pancreatic adenosquamous carcinomas (PASCs). Overall, PDAC, which has a high degree of malignancy, is the most common type of pancreatic cancer (PC), and owing to a lack of obvious symptoms in the early stages along with rapid progression, it is often detected at a late stage (1). Studies have shown that the five-year survival rate for PDAC is only 8–10% (2). Different degrees of malignancy in PT, however, result in significantly different prognoses. PNET, for example, has a 5-year survival rate of > 60% when diagnosed as pathological grade 1 or 2, which are low-grade malignancies, whereas those diagnosed as grade 3, or a high-grade malignancy, have a 5-year survival rate of < 30% (3–5). The accurate and timely identification and staging of PT can help determine patient prognosis and the appropriate course of treatment.

Currently, computed tomography (CT), magnetic resonance imaging (MRI), and endoscopic ultrasound (EUS) are the primary modalities utilized for the diagnosis of PT. MRI and CT, however, are less sensitive for monitoring smaller pancreatic lesions, and also for differentiating between benign and malignant tumors (6, 7). By combining endoscopy with ultrasound, EUS provides a more accurate and complete display of the pancreatic structure and visualization of space-occupying lesions (8), and previous studies have shown that EUS performs well in the diagnosis of a variety of pancreatic masses, with higher accuracy than many other clinical diagnostic techniques (9, 10). Additionally, EUS-guided fine-needle aspiration/biopsy (EUS-FNA/EUS-FNB) allows for the quick and easy sampling of pathological tissue, further improving the accuracy of PT diagnoses (11). The primary method for the imaging-based diagnosis of PT in clinical practice still relies heavily on the visual judgment of the individual operating the endoscope, which is overly dependent on their experience, and can lead to missed diagnoses or misdiagnosed cases as the result of insufficient experience, fatigue, or distraction. Computer-aided diagnosis/detection (CAD) analyses medical image data and other data using computer technology to assist practitioners in more objectively, quickly, and accurately completing diagnostic work. Many studies have verified the feasibility of utilizing CAD in the process of image-based diagnosis (12–14).

In recent years, artificial intelligence (AI) technology has been increasingly utilized in various fields of medicine, such as image analysis, diagnostic recommendations, and clinical risk prediction, which has reduced medical errors, to a certain extent, and improved diagnostic efficiency (15). Sunwoo et al. (16), for example, used AI technology to analyze the diagnosis of brain metastases from MRI scans, and the sensitivity increased from 77.6% to 81.9%, while the reading time decreased from 114.4 seconds to 72.1 seconds. There are two primary methods for utilizing AI in the analysis of medical images for assisted diagnosis: diagnosis based on traditional machine learning methods and diagnosis based on deep learning (DL) methods.

As a branch of AI, traditional machine learning-based methods primarily involve the manual extraction of features and the selection of suitable classifiers for statistical analysis. DL, in turn, is a subset of machine learning. At the 2012 ImageNet Large Scale Visual Recognition Challenge (17), Krizhevsky et al. (18) proposed AlexNet, a deep convolutional neural network, that overwhelmingly won the competition and triggered a wave of DL in various fields. Compared to traditional machine learning, DL automates feature extraction in a data-driven manner, and is capable of learning deeper and more abstract features from the target data (19, 20). DL significantly improves accuracy in areas such as image classification, object detection, and semantic segmentation, and its performance exceeds that of traditional machine learning techniques (19, 21).

A previous meta-analysis showed that practitioners using EUS for the diagnosis of PT had a sensitivity of 85% (95% confidence interval [CI], 69–94%), specificity of 58% (95% CI, 40–74%), and accuracy of 75% (95% CI, 67–82%) (6). Dumitrescu et al. (22) conducted a meta-analysis of AI-assisted EUS for PC diagnosis, which included 10 studies; three used traditional machine learning techniques, and seven used DL techniques. The pooled sensitivity for the AI diagnoses was 92% (95% CI, 89–95%), and the pooled specificity was 90% (95% CI, 83–94%). We are hopeful that the results of these studies can be compared with the results of our meta-analysis as a way to evaluate the advantages of DL-assisted EUS for the diagnosis of PC.

In the present study, the accuracy of DL-assisted EUS in the diagnosis of PT was quantified through a meta-analysis, which aimed to provide comprehensive and objective evidence for its utilization in clinical practice. The primary outcome of the present study was the overall performance of DL in diagnosing PT, while the secondary outcome was the ability to compare DL and practitioners performing traditional EUS.

Abbreviations: AI, artificial intelligence; AUC, area under the curve; CAD, computer-aided diagnosis/detection; CEUS, contrast-enhanced endoscopic ultrasound; CI, confidence interval; CP, chronic pancreatitis; CT, computed tomography; DL, deep learning; DOR, diagnostic odds ratio; EUS, endoscopic ultrasound; EUS-FNA, EUS-guided fine-needle aspiration; EUS-FNB, EUS-guided fine-needle biopsy; FN, false negative; FP, false positive; IPMN, intraductal papillary mucinous neoplasms; MI, Mechanical index; MRI, magnetic resonance imaging; NLR, negative likelihood ratio; NP, normal pancreas; NPC, non-pancreatic cancer; PASC, pancreatic adenosquamous carcinoma; PC, pancreatic cancer; PDAC, pancreatic ductal adenocarcinoma; PLR, positive likelihood ratio; PNET, pancreatic neuroendocrine tumors; PT, pancreatic tumor; SROC, summary receiver operating characteristic.

2 Methods

The present study followed the Preferred Reporting Items for Systematic Review and Meta-Analysis of Diagnostic Test Accuracy Studies (PRISMA-DTA) guidelines (23), the checklist for which is presented in Supplementary Table S1. Prior to its onset, the present study was registered with the International Prospective Register of

Systematic Reviews (PROSPERO) (24) on January 25, 2023 (ID: CRD42023391853), and because all of the data analyzed were collected from the included literature, ethical approval was not required.

2.1 Search strategy

We performed searches for the present meta-analysis in four commonly used databases: PubMed, Embase, Web of Science, and the Cochrane Library database. The final search was conducted on February 21, 2023, and included all articles from the four databases, beginning at the time of their creation and ending at the time of the final search. The keywords which were searched relating to DL included "deep learning", "artificial intelligence", "machine learning", "computer-aided", "natural networks", "image classification", "object detection", and "semantic segmentation"; those relating to EUS included "ultrasonography", "ultrasound", and "EUS"; and those relating to PT included "pancreas" and "pancreatic". The detailed search strategy is presented in Supplementary Table S2.

2.2 Study selection

The inclusion criteria for the present study were as follows (1): studies using DL to detect PT; (2) detection based on EUS images or videos; (3) use of pathological findings or expert labeling as diagnostic criteria; (4) detailed description of the source and composition of the training and test sets; and (5) true positive (TP), false positive (FP), true negative (TN), and false negative (FN) values were obtained directly or indirectly. For studies with missing data, the corresponding author was contacted via email in order to fill in the blanks.

The exclusion criteria were as follows: (1) articles without raw data, such as reviews, comments, or letters; (2) not full-text articles; (3) TP, FP, TN, and FN data not included, or no response received from the corresponding author via email when attempting to gather the missing data.

The initial articles returned from the searches were screened for inclusion by KW and NW, based on the aforementioned criteria, and any disagreements were resolved through discussions with BL.

2.3 Data extraction

KW and TT independently extracted data from the included studies, and resolved any disagreements through discussion. The following information was collected from each included study: first author, year of publication, country or region, diagnostic criteria, number of patients, data source, number of training sets, DL algorithms, sensitivity, and specificity. For studies with multiple test results, we extracted the resulting data in the following order: prospective test set, external test set, and test set with the largest sample size. We also extracted diagnostic data regarding the EUS practitioners for comparison with the DL models.

2.4 Quality assessment

We utilized the Quality Assessment of Diagnostic Accuracy Studies version 2 (QUADAS-2) to assess the quality of the included studies, although to more accurately assess the DL models, we supplemented the patient selection section with the following questions: (1) "Was the composition of the training and test sets described?"; and (2) "Were imaging modalities and image/video quality described in detail?". We also added the following questions to the index test section: (1) "Was the algorithm development and training processes described?"; and (2) "Does the model be evaluated using an independent test set?".

2.5 Statistical analysis

We conducted our meta-analysis using a bivariate random-effects model to evaluate the performance of DL in the diagnosis of PT. We plotted a summary receiver operating characteristic (SROC) curve, and calculated the pooled sensitivity, specificity, positive likelihood ratio (PLR), negative likelihood ratio (NLR), diagnostic odds ratio (DOR), area under the SROC curve (AUC), and 95% CIs. High sensitivity and PLR indicated that the DL model was suitable for confirming the diagnosis of PT; high specificity and low NLR indicated that the DL model was good at excluding patients who did not have the disease; and DOR and AUC are overall measures of diagnostic accuracy, with a high DOR and AUC indicating that the DL model was good at confirming and excluding PT.

Statistical heterogeneity was determined by the I^2 statistic as follows: < 30% indicated low heterogeneity; 30–60% indicated moderate heterogeneity; and > 60% indicated high heterogeneity. Publication bias was analyzed using Deeks' funnel plot asymmetry test, for which $P < 0.05$ indicated publication bias. We utilized subgroup analysis and meta-regression to identify sources of heterogeneity, and also to explore the diagnostic performance of the different subgroups, and we used Fagan plots to assess the clinical applicability of DL for the diagnosis of PT.

The quality of the included studies was assessed using Review Manager 5.4 (Cochrane Collaboration, Oxford, UK), while other statistics and charts were obtained using Stata/SE 16.0 (Stata, College Station, TX, USA).

3 Results

3.1 Included studies and quality assessment

Our initial search yielded 2,233 relevant articles, of which 322 duplicates were automatically removed by the software and 1,872 that were not relevant were manually excluded after reading the titles and abstracts. After reading the full-text, a total of ten articles were included in the present meta-analysis (25–34). The data extraction process is shown in Figure 1, and the details of the included studies are listed in Table 1.

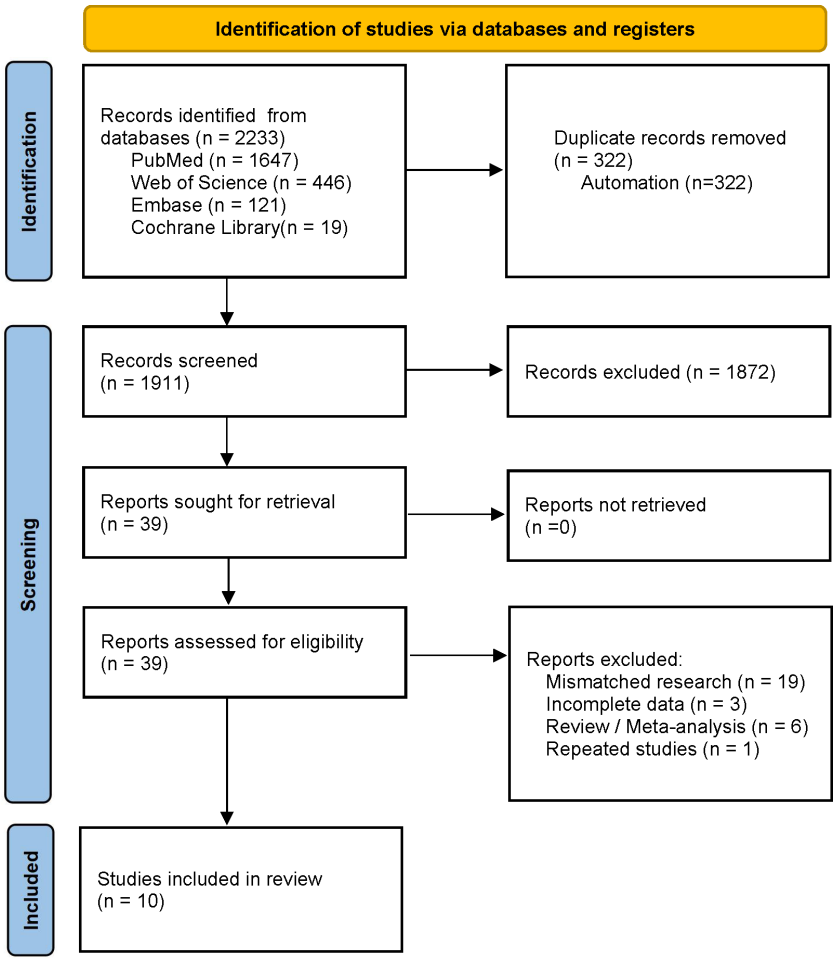

FIGURE 1
Preferred Reporting Items for Systematic Review and Meta-Analysis of Diagnostic Test Accuracy Studies (PRISMA) flow diagram for study selection.

The QUADAS-2 tool was used to assess the quality of the included studies, one of which (26) used data-enhanced images for testing, and was deemed to have a high risk of bias in the index test section, while two (26, 27) failed to describe their patient selection processes and were considered, therefore, to have an unknown risk of bias in the patient selection section. The overall assessment results are shown in Figure 2.

The 10 included studies encompassed 3,529 patients, with nine of the studies being retrospective while one was prospective (34). All of the studies used pathological findings as the diagnostic criteria, and seven studies were single-center (25, 26, 28–30, 32, 33) while three were multicenter (27, 31, 34); eight were from East Asia (25, 27–31, 33, 34) and two were from Europe (26, 32); six used plain EUS images (25, 27, 29, 30, 32, 34) while three used contrast-enhanced EUS (CEUS) images (28, 31, 33) and one used grey-scale, low-mechanical index (MI) contrast enhancement, high-MI color Doppler, and real-time elastography multiple imaging techniques (26); six studies used image classification algorithms (25, 26, 28, 30–32), one (30) used object detection algorithms, and three (27, 33, 34) used semantic segmentation algorithms; and six studies (25–27, 31–33) tested the model on an image basis, while four (28–30, 34) tested the model on a patient or video basis. The study aims, participant characteristics, types of lesions, and funding sources of the included studies are listed in Supplementary Table S3.

3.2 Study characteristics and data extraction

Tonozuka et al. (25) constructed a DL model using convolutional neural networks to identify patients with a normal pancreas (NP) versus those with chronic pancreatitis (CP) and PDAC. A total of 139 patients were included in their study – 76 with PDAC, 34 with CP, and 29 with NP, for whom the sensitivity and specificity were 92.4% and 84.1%, respectively.

Udriștoiu et al. (26) developed a convolutional neural network-based CAD system with long short-term memory neural networks to identify cases of chronic pseudotumoral pancreatitis (CPP), PNET, and PDAC. A total of 65 patients were included in their study – 30 with PDAC, 20 with CPP, and 15 with PNETs. The overall accuracy of their model was 98.26%. In the meta-analysis, we combined the sensitivity and specificity of these models for the diagnosis of PNET and PDAC.

TABLE 1 Details of the included studies.

Study	Country/ Region	Study Center	Study design	Imaging type	Algorithm	Standard Reference	Patients (n)	Train set images(n)	Test set	Tester	Sensitivity	Specificity
Tonozuka 2021 (25)	Japan	Single	Retrospective	EUS	Customized CNN	Pathology	139	920	Internal Image	DL	0.924	0.841
Udriștoiu 2021 (26)	Romania	Single	Retrospective	Gray-Scale CHI CDI RTE	Customized CNN	Pathology	65	2688	Internal Image	DL	0.9821	0.9955
Oh 2021 (27)	Korea	Multi	Retrospective	EUS	Attention U-Net	Pathology	111	43	External Image	DL	0.723	0.989
Huang 2022 (28)	China	Single	Retrospective	CEUS	SE-ResNeXt	Pathology	104	2480	Internal Patient	DL	0.75	0.83
Kuwahara 2022 (29)	Japan	Single	Retrospective	EUS	EfficientNetV2	Pathology	933	18318	Internal Video	DL	0.94	0.82
Tian 2022 (30)	China	Single	Retrospective	EUS	YoloV5	Pathology	157	807	Internal Patient	DL	0.95	0.75
										practitioner	0.8	0.875
Tong 2022 (31)	China	Multi	Retrospective	CEUS	ResNet	Pathology	558	351	External Image	DL	0.922	0.8571
										practitioner	0.857	0.81
VilasBoas 2022 (32)	Portugal	Single	Retrospective	EUS	Xception	Pathology	28	4404	Internal Image	DL	0.983	0.989
Seo 2022 (33)	Korea	Single	Retrospective	EUS	DAF-Net	Pathology	150	330	Internal Image	DL	0.84	0.981
Tang 2023 (34)	China	Multi	Prospective	CEUS	UNet++	Pathology	1,284	4432	Internal Video	DL	0.923	0.923
										practitioner	0.885	0.846

CDI, High-MI color Doppler; CEUS, Contrast-enhanced endoscopic ultrasound; CHI, Low-MI contrast-enhancement; MI, Mechanical index; RTE, Real-time elastography.

10.3389/fonc.2023.1191008

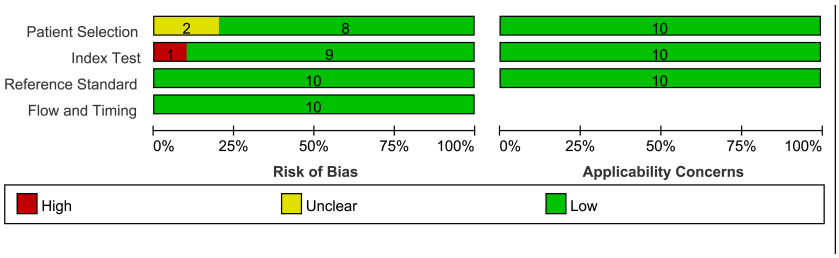

FIGURE 2
Summary of risk of bias and applicability of concerns graph.

Oh et al. (27) used DL techniques to automatically segment PT on EUS, and their study included 111 patients from 2 hospitals. Their model was tested using internal and external test sets, and the test results were extracted from the external test set for inclusion in the present meta-analysis.

Huang et al. (28) combined DL with traditional machine learning techniques to predict the preoperative invasiveness of PNETs. A total of 104 patients were included in their study, and the AUC of the DL model was 0.81 (95% CI, 0.62–1.00). We only extracted the test results from the DL model for the present meta-analysis.

Kuwahara et al. (29) created a DL model to distinguish between pancreatic and non-pancreatic cancer (NPC) cases, and their study included 933 patients with 9 pancreatic masses, including PDACs, PNETs, and CP. The test results were extracted from the video test set, and the accuracy and AUC of the DL model were 91% (95% CI, 85–95%) and 0.90 (95% CI, 0.84–0.97), respectively.

Tian et al. (30) performed a real-time diagnosis of PC or NPC based on an object detection algorithm compared with the results of EUS practitioners. Their study included 157 patients, 102 with PC and 55 with NPC. The sensitivity and specificity of their model were 95% and 75%, respectively, while those for the EUS practitioners were 80% and 87.5%, respectively.

Tong et al. (31) created a DL model for differentiating between PDAC and CP. In their study, 558 patients were recruited from 3 hospitals, including 414 patients with PADCs and 144 with CP. Data from one hospital were used for model training and internal testing, while those from the other two were used as the two external test cohorts. We combined the test results of the two external test cohorts for the present meta-analysis.

Vilas-Boas et al. (32) constructed a DL model for the identification of mucinous and non-mucinous pancreatic cystic lesions (PCLs), in which they included a total of 28 patients – 17 with mucinous PCLs and 11 with non-mucinous PCLs. The overall accuracy of their model was 98.5%.

Seo et al. (33) proposed a DL method for PC segmentation. A total of 150 patients with PC were included in this study. The sensitivity and specificity of this model were 89.0% and 98.1%, respectively.

Tang et al. (34) developed a DL-based CAD system to distinguish PC from benign pancreatic masses, for which they retrospectively collected the EUS images of 1,245 patients from multiple centers for training and testing, and also recruited 39 patients for prospective testing. The CAD system achieved an accuracy, sensitivity, and specificity of 93.8%, 90.9%, and 100%, respectively.

We performed a meta-analysis of the aforementioned studies, the results of which were the primary outcomes of the present study. Of the 10 studies included in the present meta-analysis, three (30, 31, 34) compared the diagnostic abilities of the DL model with those of the EUS practitioners. We extracted the data from these three groups and performed a comparative analysis, which was the secondary outcome of the present study.

3.3 Performance of DL

The pooled sensitivity of DL for diagnosing PT was 93% (95% CI, 87–96%; I^2 = 96.08%), and the pooled specificity was 95% (95% CI, 89–98%; I^2 = 98.09%) (Figure 3). The PLR was 18.2 (95% CI, 7.91–41.86), the NLR was 0.08 (95% CI, 0.04–0.15), and the DOR was 238.04 (95% CI, 76.3–742.61) (Supplementary Figures S1, S2). A PLR > 10 indicates that DL can accurately diagnose PT, while an NLR < 0.1 indicates that DL can effectively exclude PT and a DOR significantly > 1 indicates that DL has good discriminatory ability for PT. We plotted SROC curves to provide a more comprehensive assessment of the performance of the DL model (Figure 4), which showed an AUC of 0.98 (95% CI, 0.96–0.99). The AUC value was very close to 1, indicating that DL accurately diagnosed PT.

We evaluated the clinical application of DL in the diagnosis of PT using Fagan plots (Figure 5). When the pre-test probability was set at 50%, the probability of positive patients being diagnosed with PT was 95%, while the probability of negative patients being diagnosed with PT was 7%. These results indicate that DL has a high accuracy, and is an important clinical tool for the diagnosis of PT.

3.4 Subgroup analysis and meta-regression

Although the pooled sensitivity, specificity, and DOR showed excellent diagnostic performance for DL, the I^2 showed high heterogeneity; therefore, we performed a subgroup analysis with meta-regression to analyze the potential sources of heterogeneity. The grouping conditions were as follows: (1) imaging type – normal EUS images vs. other images, such as CEUS; (2) number of training set images – regardless of whether or not the training set had > 1,000 images, using 1,000 divided the 10 studies equally into two

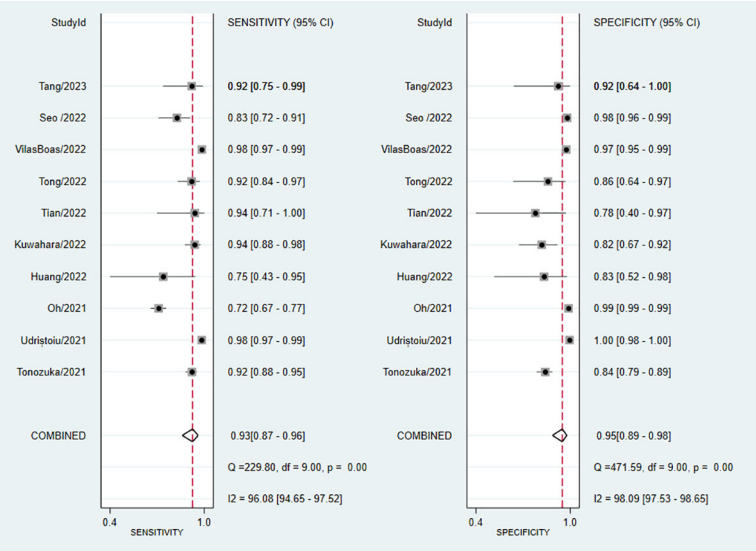

FIGURE 3
Forest plot of sensitivity and specificity of deep learning (DL) in identifying pancreatic tumors.

parts; (3) test set data type – whether the test data were images, videos, or patients; (4) DL algorithm types – classification vs. other algorithms; and (5) lesion type – solid vs. cystic lesions, the detailed classification is shown in Supplementary Table S3. The results of the subgroup analyses showed no statistically significant differences between the subgroups (Table 2), indicating that the heterogeneity in the meta-analysis was not due to these factors.

3.5 Sensitivity analysis and publication bias

We further analyzed the sources of heterogeneity in the included studies by performing a sensitivity analysis. After removing each study individually, we examined whether sensitivity, specificity, and the corresponding I^2 values changed significantly after each change. After removing the study by Oh et al. (27), the sensitivity changed

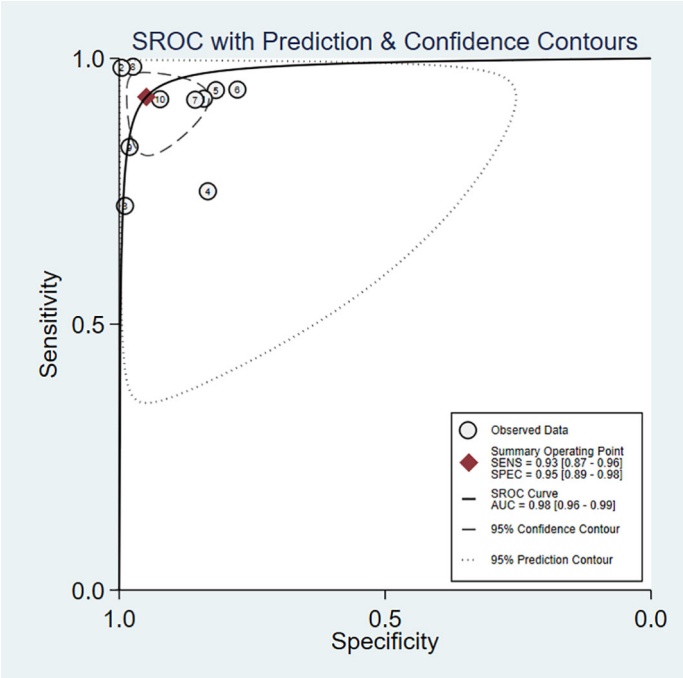

FIGURE 4
Summary receiver operating characteristic (SROC) curves for the diagnosis of pancreatic tumors using DL. Each circle indicates an individual study, red diamond represents summary sensitivity and specificity.

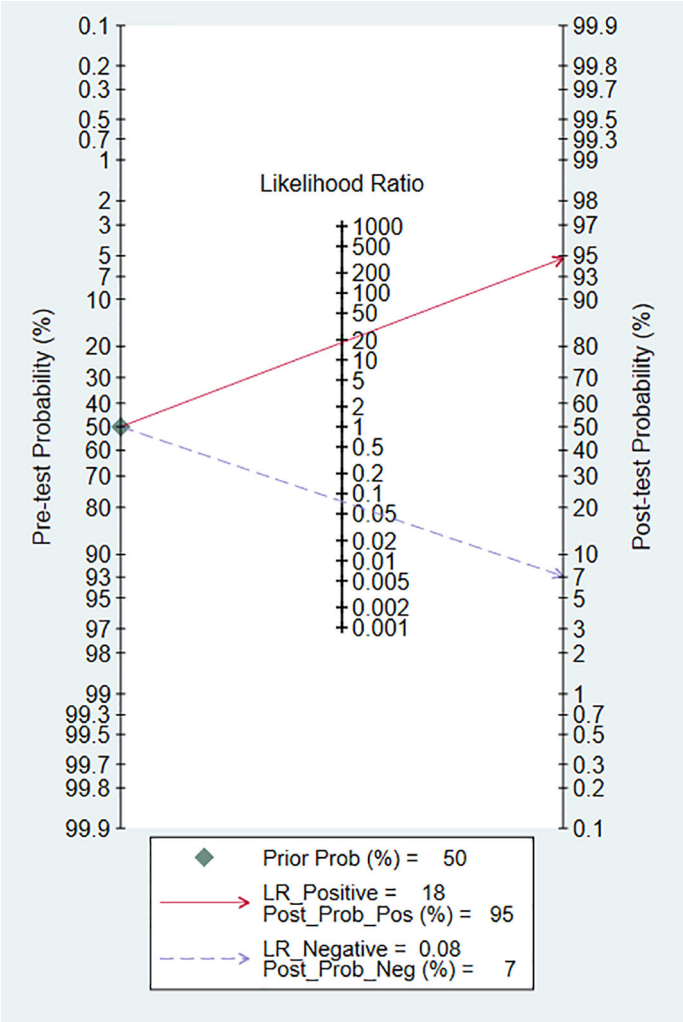

FIGURE 5
Fagan nomogram of the accuracy of DL in the diagnosis of pancreatic tumors.

TABLE 2 Subgroup analyses and meta-regression results.

Parameter	Category	Studies(n)	Sensitivity(95%CI)	P	Specificity(95%CI)	P
imaging type	normal EUS	6	0.92(0.86-0.98)	0.18	0.95(0.89-1.00)	0.75
	others	4	0.94(0.87-1.00)		0.95(0.89-1.00)	
training images number	>1000	5	0.96(0.93-0.99)	0.77	0.95(0.90-1.00)	0.90
	<1000	5	0.88(0.80-0.96)		0.94(0.88-1.00)	
test data type	image	6	0.93(0.88-0.98)	0.54	0.97(0.95-0.99)	0.26
	video/patient	4	0.92(0.83-1.00)		0.86(0.71-1.00)	
DL algorithm	classification algorithm	6	0.95(0.92-0.98)	0.94	0.93(0.86-0.99)	0.12
	others	4	0.83(0.71-0.95)		0.98(0.94-1.00)	
lesion type	solid lesions	7	0.93(0.87-0.98)	0.40	0.94(0.88-0.99)	0.25
	contains cystic lesions	3	0.93(0.85-1.00)		0.97(0.93-1.00)	

from 93% (95% CI, 87–96%; I^2 = 96.08%) to 94% (95% CI, 89–97%; I^2 = 87.1%), with the most significant change in I^2, although the results still suggested high heterogeneity. Given these results, no source of heterogeneity was identified in the sensitivity analysis, and the overall results of the meta-analysis were considered relatively stable.

Publication bias was evaluated using Deeks' funnel plot (Figure 6), which showed P = 0.39 (P >0.05), indicating that there was no publication bias. Although Deeks' test was performed, a high publication bias could not definitively be excluded, due to the small number of included studies.

3.6 DL vs. EUS practitioners

Of the 10 studies 3 (30, 31, 34) compared DL models with the performance of EUS practitioners (Table 1). We performed a subgroup analysis of these three data sets, with a resulting combined sensitivity of 92% (95% CI, 88–97%) vs. 86% (95% CI, 80–92%; P = 0.1), and specificity of 86% (95% CI, 76–96%) vs. 84% (95% CI, 73–95%; P = 0.37), respectively. Although the DL model performed better than the practitioners, the difference was not statistically significant. As the data from only three groups were included in the comparison, the reliability of the results requires further validation.

4 Discussion

DL techniques are being used more and more in clinical practice to significantly improve diagnostic accuracy, stability, and efficiency. In the present study, we performed a meta-analysis to comprehensively evaluate the accuracy of DL-assisted EUS for the diagnosis of PT. A total of 10 studies, encompassing 3,529 patients and 34,773 training images, were included in the present study. The combined sensitivity was 93% (95% CI, 87–96%), specificity was 95% (95% CI, 89–98%), and AUC was 0.98 (95% CI, 0.96–0.99), indicating that the DL-assisted diagnosis of PT is highly accurate. Additionally, we found that the DL model had a better diagnostic ability than that of EUS practitioners, although the difference was not statistically significant.

In the present study, we observed high heterogeneity among the 10 included studies; however, even though subgroup and sensitivity analyses were performed, no sources of heterogeneity were identified. In addition, smaller sample sizes, various DL algorithms, parameter settings, image quality, and EUS devices are possible sources of heterogeneity but need further investigation.

In addition to the high heterogeneity among the included studies, the present meta-analysis had the following limitations (1): most of the included studies were retrospective, while only one was prospective – the clinical applicability of DL, therefore, needs to be validated through more prospective studies; (2) most of the included studies were single-center studies, with only three involving multiple centers – due to differences in equipment and practitioner operating habits, using data from a variety of centers may result in differences in imaging, meaning the generalisability of the single-center trained model requires further validation; (3) most of the included studies involved populations from East Asian, with only two involving European populations, meaning the results of these studies were representative of only a certain population; and (4) some of the included studies involved only a small number of patients, such as one study (30) which included only 28 patients for training and testing, meaning the small sample size may have led to sample bias.

Although we have initially validated the effectiveness of DL models in the diagnosis of PT, these models are still in the clinical exploration stage, and some aspects still need to be improved. One such aspect is the availability of public datasets. Most medical institutions are reluctant to share EUS imaging data for legal purposes, the protection of patient privacy, or for information security, making it difficult for researchers to conduct studies using data from multiple centers. Therefore, there is an urgent need to

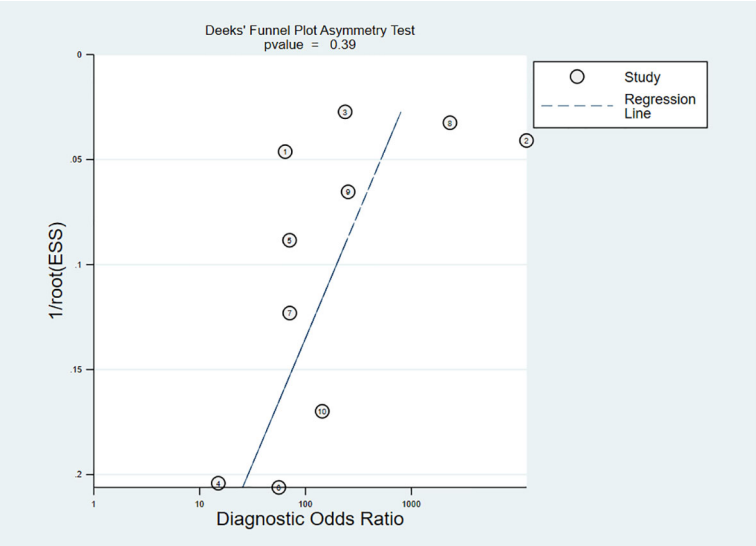

FIGURE 6
Deeks' funnel plot asymmetry test for publication.

establish a standard public EUS image database for future research. Another such aspect is open source code. Although most studies used public algorithms, using different parameter settings can affect the results. The availability of open source code, however, could help replicate research and promote the development of this field.

In recent years, emerging EUS-based techniques have shown good performance in the diagnosis of pancreatic lesions (35–37), with one study showing that the accuracy for diagnosing solid pancreatic lesions using wet suction EUS-FNB is 90.4% (35), and a meta-analysis showing that the sensitivity and specificity for detecting malignant pancreatic cystic lesions using EUS-guided through-the-needle biopsy (EUS-TTNB) were 97% and 95%, respectively (36). These techniques, however, require physicians with enhanced expertise and skills to be utilized effectively. As such, one of the included studies constructed a DL-based real-time assisted diagnostic system to guide EUS-FNA and improve the accuracy and efficiency of diagnosing pancreatic masses (34). Combining these new technologies with DL techniques is an important direction for future technological development, and further research is required to improve the efficiency and accuracy of the clinical diagnosis of PT.

The present systematic review provides a comprehensive introduction and quantitative analysis of current research on DL-assisted EUS for the diagnosis of PT. The results of our meta-analysis showed that DL has an excellent diagnostic capability, and can be used as an effective diagnostic aid in clinical practice.

Data availability statement

The original contributions presented in the study are included in the article/Supplementary Material. Further inquiries can be directed to the corresponding author.

Ethics statement

All of the data for the present study were collected from the referenced literature; therefore, ethical approval was not required.

Author contributions

YS and BL conceived the idea for the present meta-analysis. BL analyzed the data and wrote the manuscript with the support of the other authors. KW, NW, and TT screened the data. YS and FY provided suggestions for the project and revised the manuscript accordingly. All of the authors discussed the project, and read and approved the final manuscript.

Acknowledgments

We thank Jian Yang from Zibo Central Hospital for proofreading the manuscript for language.

Conflict of interest

The authors declare that the research was conducted in the absence of any commercial or financial relationships that could be construed as a potential conflict of interest.

Publisher's note

Supplementary material

The Supplementary Material for this article can be found online at: https://www.frontiersin.org/articles/10.3389/fonc.2023.1191008/full#supplementary-material

References

1. Goral V. Pancreatic cancer: pathogenesis and diagnosis. *Asian Pac J Cancer Prev* (2015) 16:5619–24. doi: 10.7314/apjcp.2015.16.14.5619

2. Siegel RL, Miller KD, Fuchs HE, Jemal A. Cancer statistics, 2022. *CA Cancer J Clin* (2022) 72:7–33. doi: 10.3322/caac.21708

3. Shah MH, Goldner WS, Halfdanarson TR, Bergsland E, Berlin JD, Halperin D, et al. NCCN guidelines insights: neuroendocrine and adrenal tumors, version 2.2018. *J Natl Compr Canc Netw* (2018) 16:693–702. doi: 10.6004/jnccn.2018.0056

4. Plöckinger U, Rindi G, Arnold R, Eriksson B, Krenning EP, de Herder WW, et al. Guidelines for the diagnosis and treatment of neuroendocrine gastrointestinal tumours. A consensus statement on behalf of the European Neuroendocrine Tumour Society (ENETS). *Neuroendocrinology* (2004) 80:394–424. doi: 10.1159/000085237

5. Scarpa A, Mantovani W, Capelli P, Beghelli S, Boninsegna L, Bettini R, et al. Pancreatic endocrine tumors: improved TNM staging and histopathological grading permit a clinically efficient prognostic stratification of patients. *Mod Pathol* (2010) 23:824–33. doi: 10.1038/modpathol.2010.58

6. Krishna SG, Rao BB, Ugbarugba E, Shah ZK, Blaszczak A, Hinton A, et al. Diagnostic performance of endoscopic ultrasound for detection of pancreatic malignancy following an indeterminate multidetector CT scan: a systemic review and meta-analysis. *Surg Endosc* (2017) 31:4558–67. doi: 10.1007/s00464-017-5516-y

7. Kartalis N, Manikis GC, Loizou L, Albiin N, Zöllner FG, Del Chiaro M, et al. Diffusion-weighted MR imaging of pancreatic cancer: A comparison of mono-exponential, bi-exponential and non-Gaussian kurtosis models. *Eur J Radiol Open* (2016) 3:79–85. doi: 10.1016/j.ejro.2016.04.002

8. Wang AY, Yachimski PS. Endoscopic management of pancreatobiliary neoplasms. *Gastroenterology* (2018) 154:1947–63. doi: 10.1053/j.gastro.2017.11.295

9. Udare A, Agarwal M, Alabousi M, McInnes M, Rubino JG, Marcaccio M, et al. Diagnostic accuracy of MRI for differentiation of benign and malignant cystic lesions compared to CT and endoscopic ultrasound: systematic review and meta-analysis. *J Magn Reson Imaging* (2021) 54:1126–37. doi: 10.1002/jmri.27606

10. Bhutani MS, Gupta V, Guha S, Gheonea DI, Săftoiu A. Pancreatic cyst fluid analysis – A review. *J Gastrointestinal Liver Dis* (2011) 20:175–80.

11. Kim E, Telford JJ. Endoscopic ultrasound advances, part 1: diagnosis. *Can J Gastroenterol* (2009) 23:594–601. doi: 10.1155/2009/876057

12. Ahmad OF, Soares AS, Mazomenos E, Brandao P, Vega R, Seward E, et al. Artificial intelligence and computer-aided diagnosis in colonoscopy: current evidence and future directions. *Lancet Gastroenterol Hepatol* (2019) 4:71–80. doi: 10.1016/S2468-1253(18)30282-6

13. Zheng H, Xiao Z, Luo S, Wu S, Huang C, Hong T, et al. Improve follicular thyroid carcinoma diagnosis using computer aided diagnosis system on ultrasound images. *Front Oncol* (2022) 12:939418. doi: 10.3389/fonc.2022.939418

14. Jiang Y, Yang G, Liang Y, Shi Q, Cui B, Chang X, et al. Computer-aided system application value for assessing hip development. *Front Physiol* (2020) 11:587161. doi: 10.3389/fphys.2020.587161

15. Jiang F, Jiang Y, Zhi H, Dong Y, Li H, Ma S, et al. Artificial intelligence in healthcare: past, present and future. *Stroke Vasc Neurol* (2017) 2:230–43. doi: 10.1136/svn-2017-000101

16. Sunwoo L, Kim YJ, Choi SH, Kim K-G, Kang JH, Kang Y, et al. Computer-aided detection of brain metastasis on 3D MR imaging: Observer performance study. *PloS One* (2017) 12:e0178265. doi: 10.1371/journal.pone.0178265

17. Russakovsky O, Deng J, Su H, Krause J, Satheesh S, Ma S, et al. ImageNet large scale visual recognition challenge. *Int J Comput Vis* (2015) 115:211–52. doi: 10.1007/s11263-015-0816-y

18. Krizhevsky A, Sutskever I, Hinton GE. ImageNet classification with deep convolutional neural networks. *Commun ACM* (2017) 60:84–90. doi: 10.1145/3065386

19. LeCun Y, Bengio Y, Hinton G. Deep learning. *Nature* (2015) 521:436–44. doi: 10.1038/nature14539

20. Rusk N. Deep learning. *Nat Methods* (2016) 13:35–5. doi: 10.1038/nmeth.3707

21. Litjens G, Kooi T, Bejnordi BE, Setio AAA, Ciompi F, Ghafoorian M, van der Laak JAWM, van Ginneken B, Sánchez CI. A survey on deep learning in medical image analysis. *Medical Image Analysis*. Singapore: Springer (2017). 42:60–88. doi: 10.1016/j.media.2017.07.005

22. Dumitrescu EA, Ungureanu BS, Cazacu IM, Florescu LM, Streba L, Croitoru VM, et al. Diagnostic value of artificial intelligence-assisted endoscopic ultrasound for pancreatic cancer: A systematic review and meta-analysis. *Diagnostics* (2022) 12:309. doi: 10.3390/diagnostics12020309

23. Salameh J-P, Bossuyt PM, McGrath TA, Thombs BD, Hyde CJ, Macaskill P, et al. Preferred reporting items for systematic review and meta-analysis of diagnostic test accuracy studies (PRISMA-DTA): explanation, elaboration, and checklist. *BMJ* (2020) 370:m2632. doi: 10.1136/bmj.m2632

24. Booth A, Clarke M, Ghersi D, Moher D, Petticrew M, Stewart L. An international registry of systematic-review protocols. *Lancet* (2011) 377:108–9. doi: 10.1016/S0140-6736(10)60903-8

25. Tonozuka R, Itoi T, Nagata N, Kojima H, Sofuni A, Tsuchiya T, et al. Deep learning analysis for the detection of pancreatic cancer on endosonographic images: a pilot study. *J Hepatobiliary Pancreat Sci* (2021) 28:95–104. doi: 10.1002/jhbp.825

26. Udriştoiu AL, Cazacu IM, Gruionu LG, Gruionu G, Iacob AV, Burtea DE, et al. Real-time computer-aided diagnosis of focal pancreatic masses from endoscopic ultrasound imaging based on a hybrid convolutional and long short-term memory neural network model. *PLoS One* (2021) 16:e0251701. doi: 10.1371/journal.pone.0251701

27. Oh S, Kim Y-J, Park Y-T, Kim K-G. Automatic pancreatic cyst lesion segmentation on EUS images using a deep-learning approach. *Sensors (Basel)* (2021) 22:245. doi: 10.3390/s22010245

28. Huang J, Xie X, Wu H, Zhang X, Zheng Y, Xie X, et al. Development and validation of a combined nomogram model based on deep learning contrast-enhanced ultrasound and clinical factors to predict preoperative aggressiveness in pancreatic neuroendocrine neoplasms. *Eur Radiol* (2022) 32:7965–75. doi: 10.1007/s00330-022-08703-9

29. Kuwahara T, Hara K, Mizuno N, Haba S, Okuno N, Kuraishi Y, et al. Artificial intelligence using deep learning analysis of endoscopic ultrasonography images for the differential diagnosis of pancreatic masses. *Endoscopy* (2022) 55:140–9. doi: 10.1055/a-1873-7920

30. Tian G, Xu D, He Y, Chai W, Deng Z, Cheng C, et al. Deep learning for real-time auxiliary diagnosis of pancreatic cancer in endoscopic ultrasonography. *Front Oncol* (2022) 12:973652. doi: 10.3389/fonc.2022.973652

31. Tong T, Gu J, Xu D, Song L, Zhao Q, Cheng F, et al. Deep learning radiomics based on contrast-enhanced ultrasound images for assisted diagnosis of pancreatic ductal adenocarcinoma and chronic pancreatitis. *BMC Med* (2022) 20:74. doi: 10.1186/s12916-022-02258-8

32. Vilas-Boas F, Ribeiro T, Afonso J, Cardoso H, Lopes S, Moutinho-Ribeiro P, et al. Deep learning for automatic differentiation of mucinous versus non-mucinous pancreatic cystic lesions: A pilot study. *Diagnost (Basel)* (2022) 12:2041. doi: 10.3390/diagnostics12092041

33. Tang A, Tian L, Gao K, Liu R, Hu S, Liu J, et al. Contrast-enhanced harmonic endoscopic ultrasound (CH-EUS) MASTER: A novel deep learning-based system in pancreatic mass diagnosis. *Cancer Med* (2023) cam4:5578. doi: 10.1002/cam4.5578

34. Seo K, Lim J-H, Seo J, Nguon LS, Yoon H, Park J-S, et al. Semantic segmentation of pancreatic cancer in endoscopic ultrasound images using deepd learning approach. *Cancers (Basel)* (2022) 14:5111. doi: 10.3390/cancers14205111

35. Crinò SF, Conti Bellocchi MC, Di Mitri R, Inzani F, Rimbaş M, Lisotti A, et al. Wet-suction versus slow-pull technique for endoscopic ultrasound-guided fine-needle biopsy: a multicenter, randomized, crossover trial. *Endoscopy* (2023) 55:225–34. doi: 10.1055/a-1915-1812

36. Li S-Y, Wang Z-J, Pan C-Y, Wu C, Li Z-S, Jin Z-D, et al. Comparative performance of endoscopic ultrasound-based techniques in patients with pancreatic cystic lesions: A network meta-analysis. *Am J Gastroenterol* (2023) 118:243–55. doi: 10.14309/ajg.0000000000002088

37. Facciorusso A, Kovacevic B, Yang D, Vilas-Boas F, Martínez-Moreno B, Stigliano S, et al. Predictors of adverse events after endoscopic ultrasound-guided through-the-needle biopsy of pancreatic cysts: a recursive partitioning analysis. *Endoscopy* (2022) 54:1158–68. doi: 10.1055/a-1831-5385

frontiers | Frontiers in Oncology

TYPE Original Research
PUBLISHED 01 September 2023
DOI 10.3389/fonc.2023.1206565

OPEN ACCESS

EDITED BY
Samir Pathak,
Bristol Royal Infirmary, United Kingdom

REVIEWED BY
Yazan S. Khaled,
University of Leeds, United Kingdom
Sang Hyub Lee,
Seoul National University Hospital,
Republic of Korea

*CORRESPONDENCE
Hee Seung Lee
LHS6865@yuhs.ac

RECEIVED 15 April 2023
ACCEPTED 14 August 2023
PUBLISHED 01 September 2023

CITATION
Lee HS, Jung EH, Shin H, Park CS, Park SB, Jung DE, Leem G, Kim SJ, Jo JH, Chung MJ, Park JY, Bang S, Park SW and Song SY (2023) Phenotypic characteristics of circulating tumor cells and predictive impact for efficacy of chemotherapy in patients with pancreatic cancer: a prospective study.
Front. Oncol. 13:1206565.
doi: 10.3389/fonc.2023.1206565

Phenotypic characteristics of circulating tumor cells and predictive impact for efficacy of chemotherapy in patients with pancreatic cancer: a prospective study

Hee Seung Lee[1,2]*, Eun Hye Jung[1], Hyejung Shin[3], Chan Su Park[1], Soo Been Park[1], Dawoon E. Jung[2], Galam Leem[1], So Jung Kim[1], Jung Hyun Jo[1,2], Moon Jae Chung[1,2], Jeong Youp Park[1,2], Seungmin Bang[1,2], Seung Woo Park[1,2] and Si Young Song[1,2]

[1]Division of Gastroenterology, Department of Internal Medicine, Yonsei University College of Medicine, Seoul, Republic of Korea, [2]Institute of Gastroenterology, Yonsei University College of Medicine, Seoul, Republic of Korea, [3]Biostatistics Collaboration Unit, Medical Research Center, Yonsei University College of Medicine, Seoul, Republic of Korea

Objective: Early chemoresistance and tumor mass progression are associated with poor prognosis in pancreatic ductal adenocarcinoma (PDAC). Circulating tumor cells (CTCs) have been studied as potential predictors of treatment response and prognosis in PDAC; however, this approach has yet to be applied in clinical practice. The aim of our study was to investigate the phenotypic characteristics of CTCs and determine their predictive value for PDAC progression.

Methods: We prospectively enrolled 40 patients who were pathologically diagnosed with PDAC and collected blood samples at diagnosis, 2 months after diagnosis, and during disease progression or recurrence. We used a microfabricated filter-based enrichment system to retrieve and analyze CTCs, which were classified using immunofluorescence staining (CD45, EpCAM, and vimentin).

Results: Our study included 20 women and 20 men (median age, 66 years). Overall, 45% of the patients (18/40) had disseminated disease, and 77.5% (31/40) received chemotherapy. Multivariate analysis revealed that the total CTC count and carbohydrate antigen 19-9 level at 2 months after diagnosis were associated with disease progression ($P<0.05$). Linear mixed model analysis revealed that the total CTC count and vimentin-positive CTCs were significantly correlated with treatment response during chemotherapy ($P=0.024$ and 0.017, respectively). Kaplan–Meier analysis showed that total CTC positivity at 2 months was significantly associated with poor progression-free survival ($P=0.038$).

Conclusion: Our study's findings suggest that CTCs can serve as predictive biomarkers of clinical outcomes in patients with PDAC receiving palliative chemotherapy. In particular, the total CTC count and vimentin-positive CTCs showed changes associated with the chemotherapy response.

KEYWORDS

pancreatic ductal adenocarcinoma, circulating tumor cells, prospective study, biomarker, outcome

Introduction

Pancreatic ductal adenocarcinoma (PDAC) is a well-known solid tumor with a poor prognosis. Despite technical advancements in early diagnosis, treatment, and cancer management, the 5-year survival rate remains low (1–3). Typically, patients with unresectable PDAC receive chemotherapy, such as FOLFIRINOX (fluorouracil, leucovorin, irinotecan, and oxaliplatin) or gemcitabine/nab-paclitaxel, and the tumor response is evaluated using imaging modalities or tumor markers, such as carbohydrate antigen 19-9 (CA 19-9) and carcinoembryonic antigen (4–6). These blood tumor markers are commonly used to diagnose and monitor the treatment response of patients with PDAC; however, recent studies have shown that circulating tumor cells (CTCs) may offer more valuable insights (7, 8).

CTCs are an uncommon subpopulation of tumor cells found in the peripheral blood of patients with cancer and are induced by tumor angiogenesis. Therefore, CTCs are expected to be involved in tumor invasion and metastasis (9, 10). Previous studies have shown that CTC levels can change during several weeks of treatment and can be used to investigate the effectiveness or resistance of treatments (7, 11, 12). Javed et al. Reported that persistent circulating tumor cells after oncologic resection predict early recurrence in PDAC, with a median time to recurrence of 3.9 months compared to 27.1 months in those without such cells (13). Okubo et al. studied the number of CTCs in patients with advanced PDAC before and after treatment (7). They found that patients with progressive disease had a significantly higher rate of positive CTCs (45.4%) compared to those with stable disease or partial response (24.1%). This suggests that changes in CTCs are linked to the tumor's response to treatment.

However, prospectively designed sequential blood sampling studies are rare, and the clinical role of CTCs subtypes in PDAC has not yet been established. Therefore, in this study, we aimed to investigate the phenotypic characteristics of CTCs and verify the relationship between the chemotherapy response of PDAC and CTCs by analyzing the count and change in CTC levels, sequentially.

Materials and methods

Ethics statement

This study was conducted in accordance with the ethical guidelines of the 1975 Declaration of Helsinki, and all patients provided written informed consent for the use of their blood. This study was also approved by the Institutional Review Board of Yonsei University (IRB approval number: 4-2017-1161) and registered with ClinicalTrials.gov (Identifier: NCT05745415).

Study design and patients

We prospectively investigated the predictive function of CTCs in patients with PDAC. The study's inclusion criteria are as follows: (1) Men and women over 20 years of age with a histological diagnosis of PDAC. (2) Eastern Cooperative Oncology Group (ECOG) performance status of 0-1. (3) Life expectancy of greater than 90 days, as assessed by the investigator. (4) Ability to provide informed consent. (5) Presence of measurable disease according to RECIST 1.1 criteria. The exclusion criteria are as follows: (1) Patients who have received prior systemic anti-cancer therapy or are currently receiving anti-cancer therapy. (2) Patients considered unsafe for inclusion in the study by the investigator for any medical or non-medical reason.

Data collection and definitions

Information on age, sex, tumor location, tumor size, tumor stage, treatment, tumor response, and CA 19-9 levels was collected from electronic medical records. Tumor response was assessed using computed tomography every 2 months. The RECIST (Response Evaluation Criteria in Solid Tumors) criteria define three tumor response categories: Partial Response (PR) indicates a significant decrease in tumor size (typically ≥30%), with no new lesions or tumor progression elsewhere. Stable Disease (SD) refers to no significant change in tumor size, and any changes are within a limited range. Disease Progression (PD) is characterized by a significant increase in tumor size (typically ≥20%), appearance of new lesions, or worsening of existing lesions. Patients with PDAC were divided into two groups based on their response to chemotherapy. Responders were defined as patients whose best response was partial response (PR) or stable disease (SD) after chemotherapy. Non-responders were defined as patients whose best response was progressive disease (PD) after chemotherapy.

Overall survival (OS) was defined as the interval from the date of diagnosis to the date of death due to any cause or the last follow-

up. Progression-free survival (PFS) was defined as the time interval from the date of diagnosis to the date of disease progression or death.

CTC acquisition and detection

Patient's blood samples were obtained at the initial diagnosis before treatment to standardize the time of sampling. For sequential blood sampling, we collected samples immediately prior to the next chemotherapy session to reduce the effect of previous chemotherapy on CTCs. Samples were collected three times: at the initial diagnosis (V1), 2 months later (V2), and at the time of tumor progression based on the RECIST criteria (V3) (Figures 1A, B). A total of 7.5 mL of blood was obtained and analyzed according to a previous protocol (14). CTCs were isolated using the SMART BIOPSY SYSTEM Isolation kit (cat no. CIKW10; Cytogen, Inc., Seoul, Korea) (15). Briefly, blood samples were incubated with 20 μg/μL of a specifically developed antibody cocktail from the kit, which targets white blood cells (CD45) and red blood cells (globin). Then, the samples were mixed with a pre-activation buffer, followed by density gradient centrifugation at 400 g for 30 minutes at room temperature. Cell suspensions containing CTCs were collected and gradually diluted with a dilution buffer (Cytogen, Inc.). Next, the diluted cell suspensions were filtered through an HDM chip (Cytogen, Inc.), as previously described (Supplementary Figure 1A) (14). Cells on the HDM chip were collected and transferred to microtubes.

For immunofluorescence staining, isolated cells were fixed on slides in 4% paraformaldehyde for 5 minutes at room temperature and then stored at 4°C until further processing. Cells on the slides were permeabilized with 0.2% Triton X-100 in phosphate-buffered saline (PBS) for 10 minutes at room temperature. Then, they were blocked with 1% bovine serum albumin in PBS for 60 minutes and incubated with primary antibodies for 60 minutes, followed by incubation with secondary antibodies under the same conditions. The following primary antibodies were used: mouse anti-EpCAM (Cell Signaling Technology, Danvers, MA), mouse anti-cytokeratin (Sigma-Aldrich, St. Louis, MO), rabbit anti-vimentin (Thermo Fisher Scientific, Waltham, MA), and rabbit anti-CD45 (Cell Signaling Technology). The secondary antibodies used were goat anti-rabbit Alexa Fluor 647 (Thermo Fisher Scientific) and goat anti-mouse Alexa Fluor 488 (Thermo Fisher Scientific). The slides were mounted using the Fluoroshield Mounting Medium with DAPI (ImmunoBioScience Corp.), stained cells were observed, and images were captured using a fluorescence microscope (Eclipse Ti; Nikon Corporation, Tokyo, Japan) with a 400× objective. We defined the total CTC-positive cells as more than 2 CTCs in the patient's blood.

Statistical analyses

Descriptive statistics are presented as medians (first quartile, third quartile) or numbers (percentages). The Mann–Whitney U

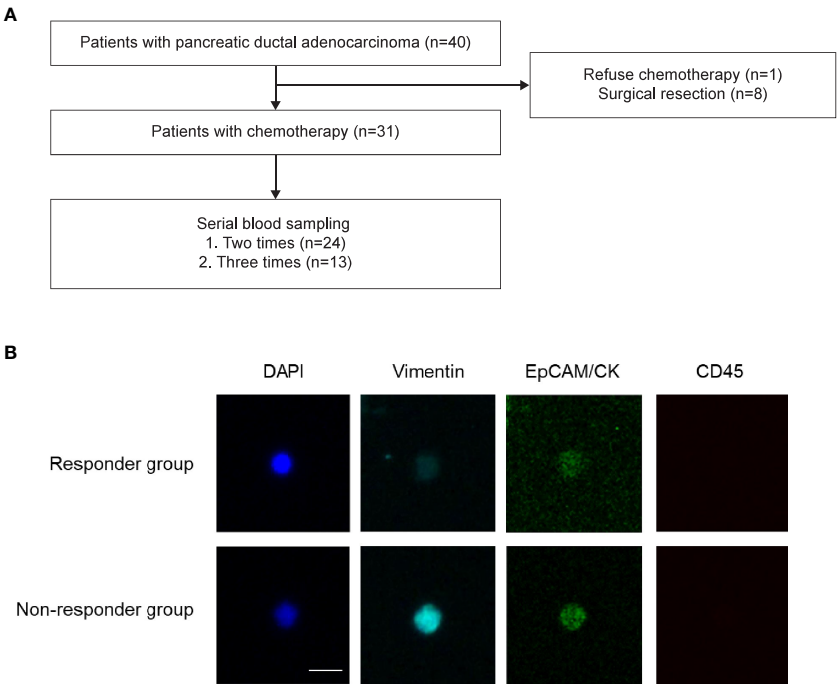

FIGURE 1
Study flow. **(A)** Patient enrollment flow. Forty patients with pancreatic ductal adenocarcinoma were prospectively enrolled in the present study. **(B)** Representative images of circulating tumor cells. Responder Responders were defined as patients whose best response was partial response or stable disease after chemotherapy. Non-responders were defined as patients whose best response was progressive disease after chemotherapy.

test was performed to test group differences in continuous variables. Various types of continuous CTC variables and the CA19-9 level were measured twice. These outcomes were analyzed using the linear mixed model method to assess the interaction effect between group and time. A compound symmetry covariance structure was assumed to address the within-subject effect. The association between survival outcomes and the explanatory variables of the CTC variable at each time point and baseline characteristic variables was evaluated using Cox regression analysis. Variables with *P*-values <0.05 in the univariate analysis were examined by multivariate analysis. The survival rate was estimated using the Kaplan–Meier method and compared between groups using the log-rank test.

Statistical analyses were conducted using SAS, version 9.4 (SAS Institute, Cary, NC) and R package software (version 4.0.4, http://www.r-project.org/). Statistical significance was set at $P<0.05$.

Results

Patient characteristics

We analyzed 78 blood samples from 40 patients (Figure 1). Baseline characteristics of the patients are presented in Table 1. Our study included 20 women and 20 men (median age, 66 years). Among the 40 patients, 9 (22.5%) were resectable and underwent surgical treatment. Overall, 45% of the patients (18/40) had disseminated disease, and 77.5% (31/40) received chemotherapy as the initial treatment. Among the 13 patients who were treated with the gem-based regimen, 12 patients received gemcitabine plus nab-paclitaxel, and 1 patient received gemcitabine plus erlotinib.

TABLE 1 Patients' demographics.

Variable	N=40
Age, y	66 (61, 75)
Male sex	20 (50.0%)
Location	
Head	22
Body	10
Tail	8
Tumor size, mm	33
Stage	
I	9 (22.5%)
II	7 (17.5%)
III	6 (15.0%)
IV	18 (45.0%)
Chemotherapy	
FOLFIRINOX	18
Gemcitabine-based chemotherapy	13
Tumor response after 2 months of chemotherapy	
Progression	6 (19.4%)
Stable disease	15 (48.4%)
Partial response	5 (16.1%)
CA 19-9 level, IU	426 (68.3, 2894)

Variables are expressed as n (%) and median (first quartile, third quartile).
Resectability was assessed according to the National Comprehensive Cancer Network guideline.
FOLFIRINOX (fluorouracil, leucovorin, irinotecan, and oxaliplatin)
CA 19-9, carbohydrate antigen 19-9.

Disease progression-related risk factors during chemotherapy

Among 31 patients who received chemotherapy, 19 (61.3%) showed disease progression. Risk factors for disease progression were analyzed using univariate and multivariate Cox regression analyses of data obtained from patients undergoing chemotherapy. Univariate analysis indicated statistical significance in metastasis at diagnosis, V2 CTCs, and V2 CA 19-9 (all, $P<0.05$). Multivariate analysis indicated the statistical significance of V2 CA 19-9 ($P=0.047$) and near statistical significance of metastasis at diagnosis ($P=0.066$) and V2 CTCs ($P=0.056$) (Table 2).

Correlation between the number of CTCs and treatment response

The changing patterns of total CTCs and vimentin-positive CTCs (vCTCs) over time revealed a difference between the responder and non-responder groups. As shown in Figure 2A, the slopes of the lines were significantly higher in the non-responder group than in the responder group (total CTCs, $P=0.024$; vCTCs, $P=0.017$). The tumor marker CA 19-9 level also increased in the non-responder group and decreased in the responder group from visit 1 to visit 2 ($P=0.027$). However, the EpCAM-positive CTC (eCTC) did not show an association between change in the number of CTCs and treatment response ($P=0.822$). We also compared the number of CTCs between the V2 partial response group and disease progression group. The total number of CTCs and vCTCs was significantly higher in the disease progression group than in the partial response group (median number 7 vs. 1, $P=0.015$) (Figure 2B).

Overall survival and progression-free survival according to CTC positivity

The OS and PFS according to the total CTC status at three different time points (V1, V2, and V3) are shown in Figure 3 and Supplementary Figure 2. PFS was significantly longer in patients with a negative total CTC after 2 months of chemotherapy than in those with positive total CTCs (median PFS, 447 vs. 240 days, $P=0.038$). Regarding OS, V2 total CTC positivity did not show a survival difference (median OS, not reached vs. 336 days, $P=0.065$). One-year survival rates of patients with negative and positive total CTCs were 86% and 42%, respectively.

TABLE 2 Results of univariate and multivariate analyses according to disease progression-related risk factors in patients who underwent chemotherapy.

	Univariate analysis			Multivariate analysis	
	HR (95% CI)	*P*-value	C-index (95% CI)	HR (95% CI)	*P*-value
Age	1.007 (0.959, 1.058)	0.774	0.518 (0.348, 0.688)		
Women vs. men	1.182 (0.475, 2.942)	0.719	0.525 (0.400, 0.650)		
Metastasis at diagnosis	3.751 (1.258, 11.184)	0.017	0.627 (0.509, 0.746)	3.440 (0.920, 12.867)	0.066
Distant node (+)	2.352 (0.760, 7.278)	0.138	0.561 (0.466, 0.656)		
V1 total CTCs, yes vs. no	0.889 (0.325, 2.434)	0.819	0.502 (0.373, 0.631)		
V1 tumor size, mm	1.007 (0.976, 1.039)	0.668	0.529 (0.387, 0.671)		
V1 CA 19-9 level, U/mL	1.004 (0.998, 1.011)	0.219	0.604 (0.455, 0.753)		
V2 total CTCs, yes vs. no	3.122 (1.009, 9.658)	0.048	0.658 (0.556, 0.761)	3.250 (0.970, 10.896)	0.056
V2 tumor size, mm	1.018 (0.991, 1.045)	0.198	0.628 (0.482, 0.774)		
V2 CA 19-9 level, U/mL	1.016 (1.006, 1.025)	0.001	0.683 (0.533, 0.833)	1.012 (1.000, 1.025)	0.047
Gemcitabine-based chemotherapy vs. FFX	1.552 (0.591, 4.073)	0.372	0.545 (0.413, 0.677)		

HR, hazard ratio; CI, confidence interval; vs., versus; CTCs, circulating tumor cells; CA 19-9, carbohydrate antigen 19-9; V1, at the initial diagnosis; V2, 2 months later; FFX, FOLFIRINOX.

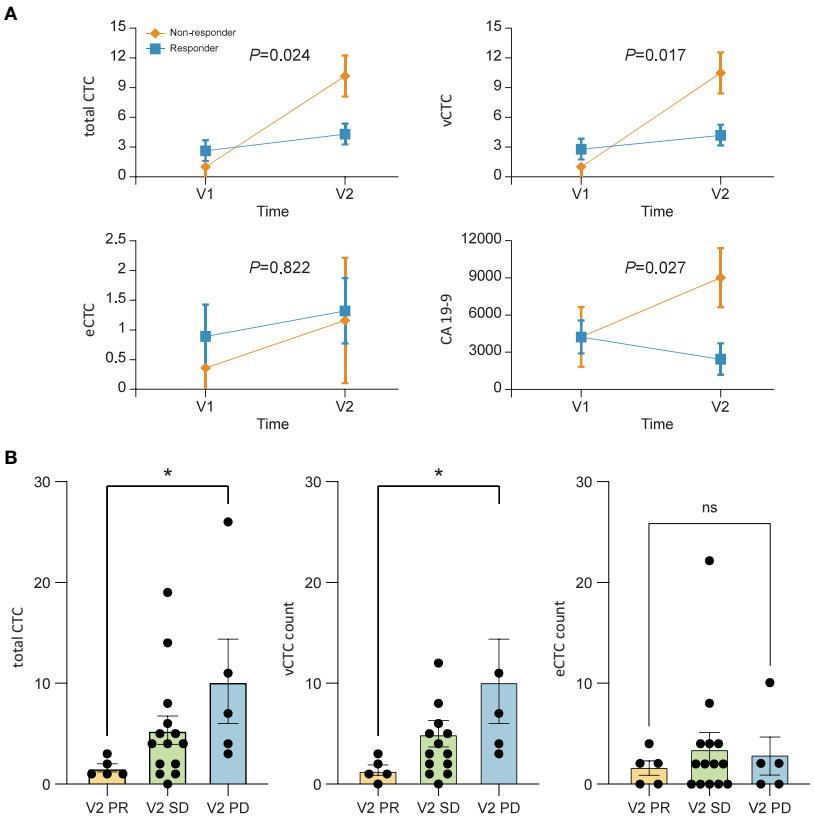

FIGURE 2
(A) Mean profile plot. Linear mixed model to find the correlation between treatment response and circulating tumor cell (CTC) counts. The changing pattern of CTCs over time according to the tumor response. The levels of total CTCs (*P*=0.024), vimentin-positive CTCs (vCTCs) (*P*=0.017), and carbohydrate antigen 19-9 (*P*=0.027) are significantly correlated with patient prognosis. **(B)** The numbers of total CTCs and vCTCs after 2 months of chemotherapy are significantly higher in patients who showed tumor progression than in those with a partial response. Values represent the estimated means with standard error from linear mixed models.

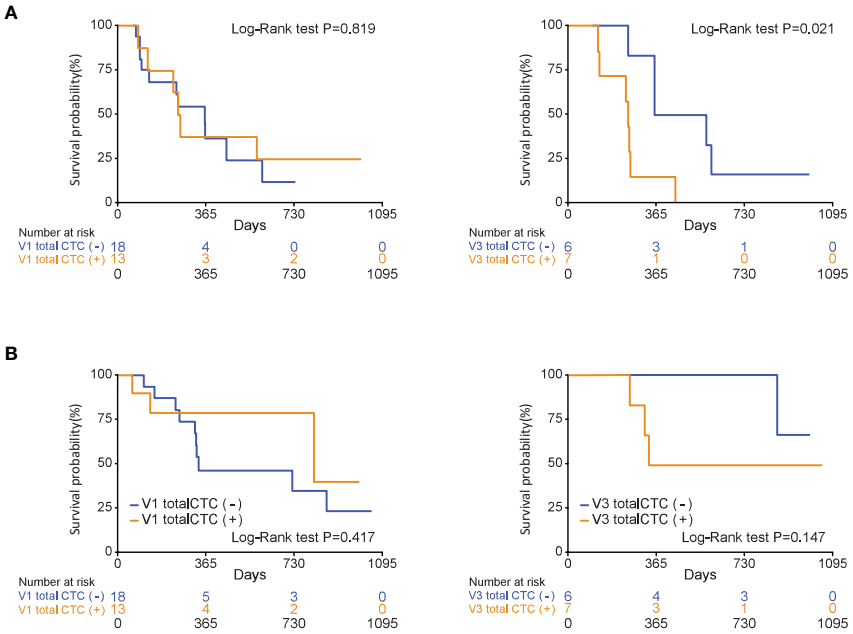

FIGURE 3
During chemotherapy, total circulating tumor cell (CTC) positivity is associated with progression-free survival in patients who were diagnosed with pancreatic ductal adenocarcinoma (V3 total CTCs (+), P=0.021). **(A)** Progression-free survival, **(B)** overall survival.

Association between the total CTC count and clinical tumor status

As shown in the representative patient example in Figures 4A–C, we analyzed the trend of changes in the number of CTCs in patients before chemotherapy, 2 months after chemotherapy, and after disease progression. In representative cases, the total number of CTCs reflected the treatment response in patients with PDAC receiving chemotherapy.

Discussion

Our study was designed to investigate the association between the number of CTCs in the blood of patients with pancreatic cancer and their response to chemotherapy and prognosis. Blood samples were collected from 40 patients at three time points: diagnosis, 2 months after diagnosis and treatment, and at the time of progression. Therefore, it was confirmed that there was a significant difference in the total number of CTCs between those who progressed 2 months after diagnosis and those who did not. Additionally, when the three time points were viewed serially, the tendency of CA 19-9 and CTC values to increase over time differed between the progression group and non-progression groups. The presence of CTC was associated with PFS, but not with OS. Subsequent chemotherapies may significantly influence the final survival duration in pancreatic cancer. Additionally, it is essential to consider that the prognosis of pancreatic cancer is fatal, and unlike PFS numerous factors can contribute to patient outcomes, such as tumor size, age, sex, and tumor characteristics. Therefore, it is challenging to attribute the patients' survival solely to the presence of circulating tumor cells. In previous study, median OS was significantly correlated with the percentage of patients who received subsequent chemotherapy after first line chemotherapy of their disease (16). Another study also reported that the positivity of CTCs was not predictive of decreased OS but was associated with tumor recurrence (17).

Considering the fatal prognosis of pancreatic cancer due to unnoticeable early metastasis, CTCs are considered good candidates for detecting distant invasion and metastasis (18). According to a meta-analysis, CTC-positive patients had shorter OS and PFS than CTC-negative patients (19). Pilot studies have demonstrated that CTCs can also be detected in the premalignant stages of pancreatic cancer; however, larger confirmatory studies are required (20). These data suggest that CTCs may serve as predictive biomarkers for pancreatic cancer before treatment (19). However, the relationship between the prognosis of pancreatic cancer and CTCs remains controversial, with inconsistent results in other studies. Recent studies have also focused on the heterogeneity of CTCs to classify and analyze their characteristics (21–23). For the last three decades, technological advancements in the detection and characterization of CTCs have allowed us to understand their function in metastatic processes (24). To characterize cell populations, mesenchymal markers, such as vimentin and N-cadherin, and markers related to stemness, such as CD133, CD44, and ALDH, have been used (25). Our study also analyzed CTCs by dividing not only total CTCs, but also vimentin-positive CTCs and EpCAM-positive CTCs. Additionally, reliable results were obtained by analyzing CA19-9, which is widely used for prognostic analyses in clinical practice.

Cancer cells often lose their epithelial characteristics and acquire features of a more mesenchymal phenotype, a process

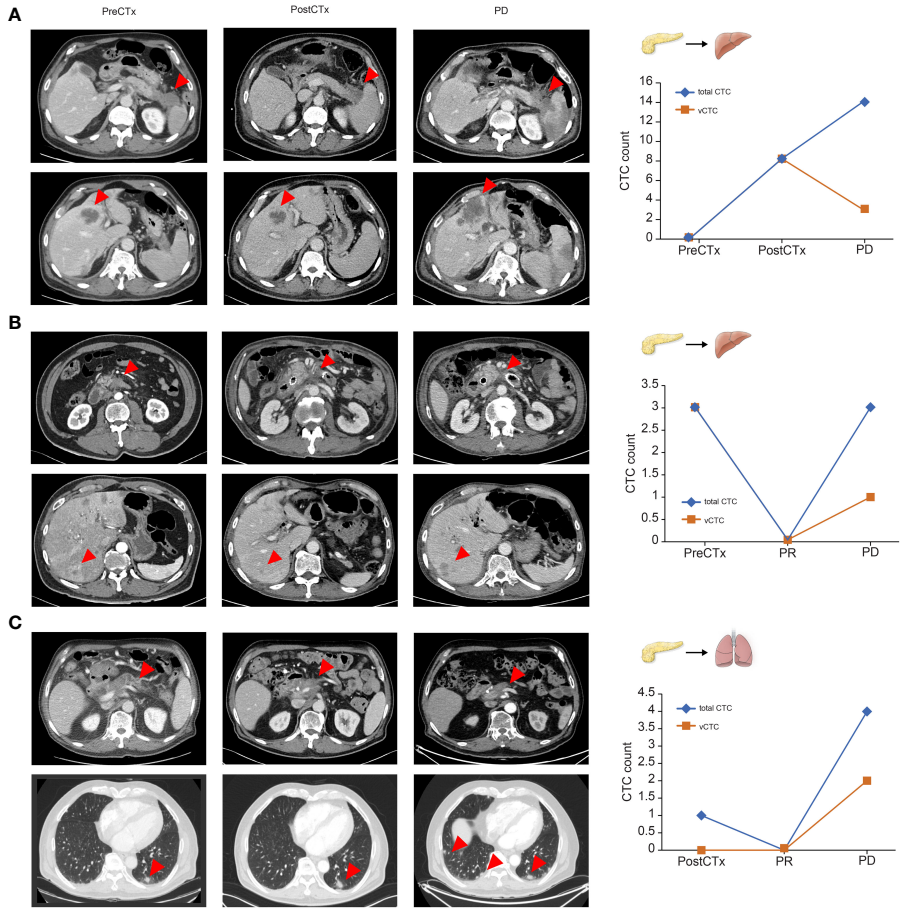

FIGURE 4
Representative cases of circulating tumor cell dynamics and correlation with treatment response **(A–C)**. Arrows represent primary pancreatic tumors and metastatic lesions.

referred to as epithelial-to-mesenchymal transition (EMT) (26). Some CTCs undergo EMT, resulting in the down-regulation of cytokeratin expression (27). In our study, the significant association of vimentin-positive CTCs with prognosis highlights the potential importance of mesenchymal-type CTCs in pancreatic cancer management. Mesenchymal-type CTCs are known to possess unique characteristics that may contribute to cancer progression, metastasis, and treatment resistance (25). Understanding the biological features of these CTCs can provide valuable insights into the disease's aggressive behavior and guide treatment decisions, particularly given the highly active EMT process in PDAC. The presence and significance of vimentin-type CTCs in the bloodstream hold particular importance in this context. However, it is also important to acknowledge the limitations associated with the detection and analysis of mesenchymal-type CTCs. Their relative rarity and dynamic nature in circulation can present challenges in their reliable identification and quantification. Additionally, the clinical implications of mesenchymal-type CTCs should be interpreted in the context of other prognostic factors and tumor characteristics.

In addition to CTCs, circulating tumor DNA (ctDNA) has been widely investigated in the prognostic studies of pancreatic cancer. According to a recent systematic review, increased detection of ctDNA showed a tendency toward more aggressive tumor behavior and decreased OS and PFS (28). However, they have not yet entered clinical routine owing to their inaccessibility and lack of standardized methods for detection. Among the metastatic subgroups, no correlation was found between the number of *KRAS* mutations and PFS or OS (29). Despite the high prevalence of *KRAS* mutations in pancreatic cancer, the ctDNA detection rates are 50–75% in metastatic patients with pancreatic cancer, which is lower than that in patients with breast or lung cancers, whose detection rate is usually less than 70–80% (30). The use of ctDNA in advanced-stage disease is also less appealing because of the low rate of targetable mutations associated with Food and Drug Administration (FDA)-approved medications (31).

Contrary to expectations, there was no significant difference between the stages, and the number of CTCs did not show a tendency to be higher in chemotherapeutic patients than in surgical patients. This may be problematic because of the small sample size and enrollment of patients at only one institution. As the characteristics of cancer differ among patients, it is difficult to simply compare the numbers. Comparisons within same patients may be more important than CTCs number comparisons between patients. Even if the difference between patients is small, it is meaningful because the number of CTCs tends to increase in

cases of metastasis, recurrence, or progression within a patient. CTC identification rates of approximately 5–40% in several studies using the FDA-approved CellSearch® technology were fairly underwhelming for patients with PDAC (32–34). In our study, the detection rate of CTCs was not very high; therefore, there was a limitation in the statistical analysis. The cut-off number of CTCs was different for each study, and there is no unified standard yet. Usually, the cut-off number of CTCs dividing CTC positivity/negativity is ≥3 CTCs/4 mL (12, 35) or ≥2 CTCs/4 mL (36). In our study, a cut-off of ≥3 CTCs/7.5 mL had meaningful results when comparing the progression and non-progression groups. And, validation through flow cytometry is necessary to confirm the presence of circulating tumor cells. Large-scale prospective studies are needed to clarify the issue of CTCs counts and its impact on chemo-response prediction in the future.

Despite these limitations, our study obtained significant results by comparing and analyzing the number of CTCs in patients with pancreatic cancer by dividing the patients into those with and without progression at a single time point. Moreover, it is meaningful in that it was possible to see the change in the CTC count of each patient by serially tracking 40 patients and collecting the CTC count at different time points. Through this, a comparison of the number of CTCs within each patient was meaningful. In our study, not only the number of CTCs but also the CA19-9 levels of the patients were measured, confirming a similar trend. Similar to other studies, this approach has the advantage of obtaining more accurate results when predicting the prognosis of patients with pancreatic cancer by combining the CA19-9 level and CTCs (19, 21).

In conclusion, we confirmed the significant correlation between the number of CTCs and advanced pancreatic cancer. In addition, it was confirmed that the ratio of the number of CTCs increased over time in the group with poor prognosis compared to the group with a good response to treatment. Thus, it is expected that CTCs can help predict the prognosis of patients with pancreatic cancer.

Data availability statement

The data generated in this study are available upon request from the corresponding author.

Ethics statement

The studies involving humans were approved by Institutional Review Board of Yonsei University (IRB approval number: 4-2017-1161). The studies were conducted in accordance with the local legislation and institutional requirements. The participants provided their written informed consent to participate in this study.

Author contributions

HL, SS: study conception and design; EJ, HS, GL, SK, JJ, MC, JP, SB, SWP, SS, HL: data acquisition, and data analysis and interpretation; EJ, HS, HL: manuscript writing and data analysis; All authors: final review; GL, SK, JJ, MC, JP, SB, SWP, SS, HL: patients enrollment and data review; EJ, HS: Statistical analysis; SBP, DJ: Sample preparation and Experimental analysis.

Funding

This work was supported by the National Research Foundation of Korea (NRF) grant funded by the Korea government (NRF-2017R1C1B2012956, 2021R1A2C1008898). This work was supported by the National Research Foundation of Korea (NRF) grant funded by the Korea government (2021R1A2C1006234). This work was supported by the Technology Innovation program (20008829) funded by the Ministry of Trade, Industry & Energy (MOTIE, Korea). This research was supported by a grant of the Korea Health Technology R&D Project through the Korea Health Industry Development Institute (KHIDI), funded by the Ministry of Health & Welfare, Republic of Korea (grant number : HI14C1324).

Acknowledgments

We would like to thank Editage (www.editage.co.kr) for English language editing. We are grateful to Dong-Su Jang (Medical Illustrator, Medical Research Support Section, Yonsei University College of Medicine, Seoul, Republic of Korea) for his help with the figures.

Conflict of interest

The authors declare that the research was conducted in the absence of any commercial or financial relationships that could be construed as a potential conflict of interest.

Publisher's note

Supplementary material

The Supplementary Material for this article can be found online at: https://www.frontiersin.org/articles/10.3389/fonc.2023.1206565/full#supplementary-material

References

1. Henley SJ, Ward EM, Scott S, Ma J, Anderson RN, Firth AU, et al. Annual report to the nation on the status of cancer, part I: National cancer statistics. *Cancer* (2020) 126(10):2225–49. doi: 10.1002/cncr.32802

2. Ryan DP, Hong TS, Bardeesy N. Pancreatic adenocarcinoma. *N Engl J Med* (2014) 371(11):1039–49. doi: 10.1056/NEJMra1404198

3. Neoptolemos JP, Springfeld C, Hackert T. A review of pancreatic cancer. *JAMA* (2021) 326(23):2436. doi: 10.1001/jama.2021.20065

4. Von Hoff DD, Ervin T, Arena FP, Chiorean EG, Infante J, Moore M, et al. Increased survival in pancreatic cancer with nab-paclitaxel plus gemcitabine. *N Engl J Med* (2013) 369(18):1691–703. doi: 10.1056/NEJMoa1304369

5. Conroy T, Desseigne F, Ychou M, Bouché O, Guimbaud R, Bécouarn Y, et al. FOLFIRINOX versus gemcitabine for metastatic pancreatic cancer. *N Engl J Med* (2011) 364(19):1817–25. doi: 10.1056/NEJMoa1011923

6. Lee KJ, Yi SW, Chung MJ, Park SW, Song SY, Chung JB, et al. Serum CA 19-9 and CEA levels as a prognostic factor in pancreatic adenocarcinoma. *Yonsei Med J* (2013) 54 (3):643–9. doi: 10.3349/ymj.2013.54.3.643

7. Okubo K, Uenosono Y, Arigami T, Mataki Y, Matsushita D, Yanagita S, et al. Clinical impact of circulating tumor cells and therapy response in pancreatic cancer. *Eur J Surg Oncol* (2017) 43(6):1050–5. doi: 10.1016/j.ejso.2017.01.241

8. Wang Y, Yu X, Hartmann D, Zhou J. Circulating tumor cells in peripheral blood of pancreatic cancer patients and their prognostic role: a systematic review and meta-analysis. *HPB (Oxford)* (2020) 22(5):660–9. doi: 10.1016/j.hpb.2019.11.003

9. Yang J, Xu R, Wang C, Qiu J, Ren B, You L. Early screening and diagnosis strategies of pancreatic cancer: a comprehensive review. *Cancer Commun (Lond)* (2021) 41(12):1257–74. doi: 10.1002/cac2.12204

10. Park HS, Han HJ, Lee S, Kim GM, Park S, Choi YA, et al. Detection of circulating tumor cells in breast cancer patients using cytokeratin-19 real-time RT-PCR. *Yonsei Med J* (2017) 58(1):19–26. doi: 10.3349/ymj.2017.58.1.19

11. Sparano J, O'Neill A, Alpaugh K, Wolff AC, Northfelt DW, Dang CT, et al. Association of circulating tumor cells with late recurrence of estrogen receptor-positive breast cancer: A secondary analysis of a randomized clinical trial. *JAMA Oncol* (2018) 4 (12):1700–6. doi: 10.1001/jamaoncol.2018.2574

12. Court CM, Ankeny JS, Sho S, Winograd P, Hou S, Song M, et al. Circulating tumor cells predict occult metastatic disease and prognosis in pancreatic cancer. *Ann Surg Oncol* (2018) 25(4):1000–8. doi: 10.1245/s10434-017-6290-8

13. Javed AA, Ding D, Hasanain A, van Oosten F, Yu J, Cameron JL, et al. Persistent Circulating Tumor Cells at One Year after Oncologic Resection Predict Late Recurrence in Pancreatic Cancer. *Ann Surg* (2022) 277(6):859–865. doi: 10.1097/SLA.0000000000005708

14. Gwark S, Kim J, Kwon NJ, Kim KY, Kim Y, Lee CH, et al. Analysis of the serial circulating tumor cell count during neoadjuvant chemotherapy in breast cancer patients. *Sci Rep* (2020) 10(1):17466. doi: 10.1038/s41598-020-74577-w

15. Kim EH, Lee JK, Kim BC, Rhim SH, Kim JW, Kim KH, et al. Enrichment of cancer cells from whole blood using a microfabricated porous filter. *Anal Biochem* (2013) 440(1):114–6. doi: 10.1016/j.ab.2013.05.016

16. Sakai D, Kudo T, Kato A, Sueda T, Takahashi H, Haraguchi N, et al. Effect of subsequent chemotherapy on overall survival in first-line chemotherapy with targeted agents for patients with metastatic colorectal cancer: Systematic review and meta-analysis of randomized control trials. *J Clin Oncol* (2017) 35(4_suppl):782–. doi: 10.1200/JCO.2017.35.4_suppl.782

17. Poruk KE, Valero V 3rd, Saunders T, Blackford AL, Griffin JF, Poling J, et al. Circulating tumor cell phenotype predicts recurrence and survival in pancreatic adenocarcinoma. *Ann Surg* (2016) 264(6):1073–81. doi: 10.1097/SLA.0000000000001600

18. Makohon-Moore A, Iacobuzio-Donahue CA. Pancreatic cancer biology and genetics from an evolutionary perspective. *Nat Rev Cancer* (2016) 16(9):553–65. doi: 10.1038/nrc.2016.66

19. Chen J, Wang H, Zhou L, Liu Z, Tan X. A combination of circulating tumor cells and CA199 improves the diagnosis of pancreatic cancer. *J Clin Lab Anal* (2022) 36(5): e24341. doi: 10.1002/jcla.24341

20. Franses JW, Basar O, Kadayifci A, Yuksel O, Choz M, Kulkarni AS, et al. Improved detection of circulating epithelial cells in patients with intraductal papillary mucinous neoplasms. *Oncologist* (2018) 23(10):1260. doi: 10.1634/theoncologist.2017-0234erratum

21. Wei T, Zhang X, Zhang Q, Yang J, Chen Q, Wang J, et al. Vimentin-positive circulating tumor cells as a biomarker for diagnosis and treatment monitoring in patients with pancreatic cancer. *Cancer Lett* (2019) 452:237–43. doi: 10.1016/j.canlet.2019.03.009

22. Dimitrov-Markov S, Perales-Paton J, Bockorny B, Dopazo A, Munoz M, Banos N, et al. Discovery of new targets to control metastasis in pancreatic cancer by single-cell transcriptomics analysis of circulating tumor cells. *Mol Cancer Ther* (2020) 19 (8):1751–60. doi: 10.1158/1535-7163.MCT-19-1166

23. Yu J, Gemenetzis G, Kinny-Koster B, Habib JR, Groot VP, Teinor J, et al. Pancreatic circulating tumor cell detection by targeted single-cell next-generation sequencing. *Cancer Lett* (2020) 493:245–53. doi: 10.1016/j.canlet.2020.08.043

24. Lin D, Shen L, Luo M, Zhang K, Li J, Yang Q, et al. Circulating tumor cells: biology and clinical significance. *Signal Transduct Target Ther* (2021) 6(1):404. doi: 10.1038/s41392-021-00817-8

25. Barriere G, Fici P, Gallerani G, Fabbri F, Zoli W, Rigaud M. Circulating tumor cells and epithelial, mesenchymal and stemness markers: characterization of cell subpopulations. *Ann Transl Med* (2014) 2(11):109. doi: 10.3978/j.issn.2305-5839.2014.10.04

26. Dong X, Ma Y, Zhao X, Tian X, Sun Y, Yang Y, et al. Spatial heterogeneity in epithelial to mesenchymal transition properties of circulating tumor cells associated with distant recurrence in pancreatic cancer patients. *Ann Transl Med* (2020) 8 (11):676. doi: 10.21037/atm-20-782

27. Zhao XH, Wang ZR, Chen CL, Di L, Bi ZF, Li ZH, et al. Molecular detection of epithelial-mesenchymal transition markers in circulating tumor cells from pancreatic cancer patients: Potential role in clinical practice. *World J Gastroenterol* (2019) 25 (1):138–50. doi: 10.3748/wjg.v25.i1.138

28. Bunduc S, Gede N, Váncsa S, Lillik V, Kiss S, Dembrovszky F, et al. Prognostic role of cell-free DNA biomarkers in pancreatic adenocarcinoma: A systematic review and meta-analysis. *Crit Rev Oncol Hematol* (2022) 169:103548. doi: 10.1016/j.critrevonc.2021.103548

29. Kim MK, Woo SM, Park B, Yoon KA, Kim YH, Joo J, et al. Prognostic implications of multiplex detection of KRAS mutations in cell-free DNA from patients with pancreatic ductal adenocarcinoma. *Clin Chem* (2018) 64(4):726–34. doi: 10.1373/clinchem.2017.283721

30. Riva F, Dronov OI, Khomenko DI, Huguet F, Louvet C, Mariani P, et al. Clinical applications of circulating tumor DNA and circulating tumor cells in pancreatic cancer. *Mol Oncol* (2016) 10(3):481–93. doi: 10.1016/j.molonc.2016.01.006

31. Leroux C, Konstantinidou G. Targeted therapies for pancreatic cancer: overview of current treatments and new opportunities for personalized oncology. *Cancers (Basel)* (2021) 13(4):799–799. doi: 10.3390/cancers13040799

32. Bidard FC, Huguet F, Louvet C, Mineur L, Bouche O, Chibaudel B, et al. Circulating tumor cells in locally advanced pancreatic adenocarcinoma: the ancillary CirCe 07 study to the LAP 07 trial. *Ann Oncol* (2013) 24(8):2057–61. doi: 10.1093/annonc/mdt176

33. de Albuquerque A, Kubisch I, Breier G, Stamminger G, Fersis N, Eichler A, et al. Multimarker gene analysis of circulating tumor cells in pancreatic cancer patients: a feasibility study. *Oncology* (2012) 82(1):3–10. doi: 10.1159/000335479

34. Kurihara T, Itoi T, Sofuni A, Itokawa F, Tsuchiya T, Tsuji S, et al. Detection of circulating tumor cells in patients with pancreatic cancer: a preliminary result. *J Hepatobiliary Pancreat Surg* (2008) 15(2):189–95. doi: 10.1007/s00534-007-1250-5

35. Kulemann B, Rosch S, Seifert S, Timme S, Bronsert P, Seifert G, et al. Pancreatic cancer: Circulating Tumor Cells and Primary Tumors show Heterogeneous KRAS Mutations. *Sci Rep* (2017) 7(1):4510. doi: 10.1038/s41598-017-04601-z

36. Konno N, Suzuki R, Takagi T, Sugimoto M, Asama H, Sato Y, et al. Clinical utility of a newly developed microfluidic device for detecting circulating tumor cells in the blood of patients with pancreatico-biliary Malignancies. *J Hepatobiliary Pancreat Sci* (2021) 28(1):115–24. doi: 10.1002/jhbp.850

frontiers | Frontiers in Oncology

TYPE Review
PUBLISHED 15 September 2023
DOI 10.3389/fonc.2023.1252824

OPEN ACCESS

EDITED BY
Sanjay Pandanaboyana,
Freeman Hospital, United Kingdom

REVIEWED BY
Stefano Francesco Crinò,
University of Verona, Italy
Satvinder Singh Mudan,
The London Clinic, United Kingdom
Yazan S. Khaled,
University of Leeds, United Kingdom

*CORRESPONDENCE
Wei On
aaron.on@nhs.net;
aaron.on@nhs.net

RECEIVED 04 July 2023
ACCEPTED 30 August 2023
PUBLISHED 15 September 2023

CITATION
On W, Ahmed W, Everett S, Huggett M and Paranandi B (2023) Utility of interventional endoscopic ultrasound in pancreatic cancer. *Front. Oncol.* 13:1252824. doi: 10.3389/fonc.2023.1252824

Utility of interventional endoscopic ultrasound in pancreatic cancer

Wei On*, Wafaa Ahmed, Simon Everett, Matthew Huggett and Bharat Paranandi

Department of Gastroenterology, Leeds Teaching Hospitals NHS Trust, Leeds, United Kingdom

Endoscopic ultrasound (EUS) has an important role in the management algorithm of patients with pancreatic ductal adenocarcinoma (PDAC), typically for its diagnostic utilities. The past two decades have seen a rapid expansion of the therapeutic capabilities of EUS. Interventional EUS is now one of the more exciting developments within the field of endoscopy. The local effects of PDAC tend to be in anatomical areas which are difficult to target and endoscopy has cemented itself as a key role in managing the clinical sequelae of PDAC. Interventional EUS is increasingly utilized in situations whereby conventional endoscopy is either impossible to perform or unsuccessful. It also adds a different dimension to the host of oncological and surgical treatments for patients with PDAC. In this review, we aim to summarize the various ways in which interventional EUS could benefit patients with PDAC and aim to provide a balanced commentary on the current evidence of interventional EUS in the literature.

KEYWORDS

pancreatic cancer, pancreatic ductal adenocarcinoma, endoscopic ultrasound, interventional endoscopy, pancreatobiliary endoscopy

1 Introduction

Pancreatic ductal adenocarcinoma (PDAC) is a disease with a poor prognosis and an estimated 5-year survival rate of <10% (1). Survival trends have remained static over time in comparison with other forms of cancer (2). The recent Bratislava Statement highlights PDAC as part of a group of 'neglected cancers' due to the lack of effective treatments and visible research efforts in the understanding and treatment of the disease (3). This has galvanized position papers and statements in eminent publications to place PDAC in the spotlight as a disease in need of concentrated research in a bid to improve outcomes (4, 5). Undoubtedly, PDAC is a disease that requires a multi-faceted approach including surgeons, oncologists and endoscopists amongst other highly valued professionals. Therefore, there are multiple avenues for research and innovation in PDAC that will require coordinated involvement of separate disciplines.

Endoscopic ultrasound (EUS) was developed in the 1980s. It permits sonographic visualization of the linings of the digestive tract and the solid organs beyond it. Evaluation of the entire pancreatobiliary system from the upper digestive tract is possible. Since its inception, EUS has established itself as an invaluable and complementary tool in the diagnosis (including tissue acquisition) and staging of PDAC, alongside other imaging modalities (6, 7). Locoregional staging information obtained via EUS is often used in conjunction with other modalities to finalize decision making regarding suitability of resection.

Over the past decade, innovation and technological advances have led to endoscopists pushing the boundaries of EUS, unlocking its potential to establish it as an interventional tool for various clinical indications (8). EUS has the unique ability of accessing difficult to reach areas within the body in a minimally invasive fashion. This is particularly advantageous in treating and managing sequelae of PDAC given the deep location of the pancreas.

In this review, we aim to provide a balanced overview of interventional EUS, and highlight areas of potential future research.

2 EUS-guided interventions in pancreatic cancer

2.1 EUS-guided biliary drainage

Over the past decade, there has been widespread, international adoption of therapeutic EUS. With regards to biliary drainage, EUS allows the operator to sonographically identify and visualize the entire biliary tract. As such, this opens up an avenue for which the biliary tract can be accessed for purposes of intervention and decompression in patients with biliary obstruction. The first reported case of endoscopic ultrasound guided biliary drainage (EUS-BD) was by Giovannini, et al. in 2001 (9). They described the use of directly accessing the biliary tract from the duodenum with the use of a needle-knife (an accessory that applies diathermy to cut through tissue) under EUS guidance, with subsequent placement of a plastic stent into bile duct, effectively creating a choledocho-duodenal tract.

Since then, EUS-BD has evolved significantly and has become more sophisticated in terms of expanding the possible routes of access into the biliary tract via the development of dedicated accessories. Nowadays, EUS-BD is an umbrella term for various techniques which be broadly classified into two main routes: transmural drainage via creation of an extra-anatomical tract with a stent or via the transpapillary route with a rendezvous technique or an antegrade approach (10, 11). The in-depth technical descriptions of each approach is outside the scope of this review but it is important to be aware of the different options in EUS-BD which are available (12).

2.1.1 EUS guided biliary drainage in patients with pancreatic cancer

Obstructive jaundice is a common presentation throughout the course of the disease length in patients with PDAC. Biliary decompression via endoscopic retrograde cholangiopancreatography (ERCP) is considered the first line treatment in these patients (13). However, ERCP may be unsuccessful in up to 15% of patients for a variety of reasons, which include failure to cannulate the biliary tract, surgically altered anatomy, duodenal stenosis and malignant infiltration of the papilla (14, 15). Historically, percutaneous transhepatic biliary drainage (PTBD) or surgical bypass were alternative approaches following unsuccessful ERCP. PTBD is more likely to be utilized as a rescue procedure, however, there is a high likelihood of morbidity relating to adverse events, pain, multiple re-interventions and a detrimental impact on quality of life (QOL) (16–18). A recent network meta-analysis comparing rescue procedures after ERCP failure in patients with malignant distal biliary obstruction (MDBO) demonstrated similar technical and clinical successes between EUS-BD, surgical bypass and PTBD; although there was a trend towards higher adverse events in the PTBD group (19).

Both transmural and transpapillary routes of drainage are viable options for biliary decompression in jaundiced patients with PDAC. However, the transpapillary route requires the operator to negotiate a guidewire across the malignant stenosis which can prove challenging and time-consuming. Furthermore, transpapillary drainage via the rendezvous route would be impossible in certain patients such as those with concomitant malignant duodenal stenosis. As such, the transmural route is preferred in these cases.

There are two main options for transmural drainage via EUS-BD: placement of a plastic or metal stent after forming a conduit between the extrahepatic bile duct and the duodenum (Figure 1. choledochoduodenostomy, or CDD), or a conduit between the intrahepatic left sided bile ducts and the stomach (Figure 2. hepaticogastrostomy, or HGS). In patients with PDAC, EUS-CDD is preferable. This is because the level of malignant obstruction is in the distal biliary tree, therefore the close proximity of the proximally dilated extrahepatic bile duct to the duodenal wall with its relatively fixed position in the retroperitoneum renders access more straightforward (20). However, there may be some patients in whom EUS-CDD is not technically feasible; for example a lack of endoscopic duodenal access, an inadequately dilated bile duct or with paraduodenal varices precluding a safe window for access into the bile duct. In these situations, EUS-HG may be preferable as long as there is no disease affecting the plane between the left lobe of the liver and the stomach. Nevertheless, both options are viable in their respective individual circumstances, and in expert hands, are similar in terms of safety and success (21).

These techniques require multiple steps and accessory exchanges which can be time consuming, potentially increasing the risk of adverse events such as bile leakage and pneumoperitoneum (22, 23). Lumen apposing metal stents (LAMS) have gained popularity in recent times due to their versatility in various innovative applications within the digestive tract, and also particularly the relative ease and speed of deployment as a single step device. LAMS was initially developed for drainage of pancreatic fluid collections (24) but has rapidly cemented its position as the device of choice for EUS-BD in patients with MDBO. The saddle-shaped, biflanged design of the stent permits apposition between the bile duct and the duodenum as an anti-migratory measure whilst the mesh of the stent is covered to prevent

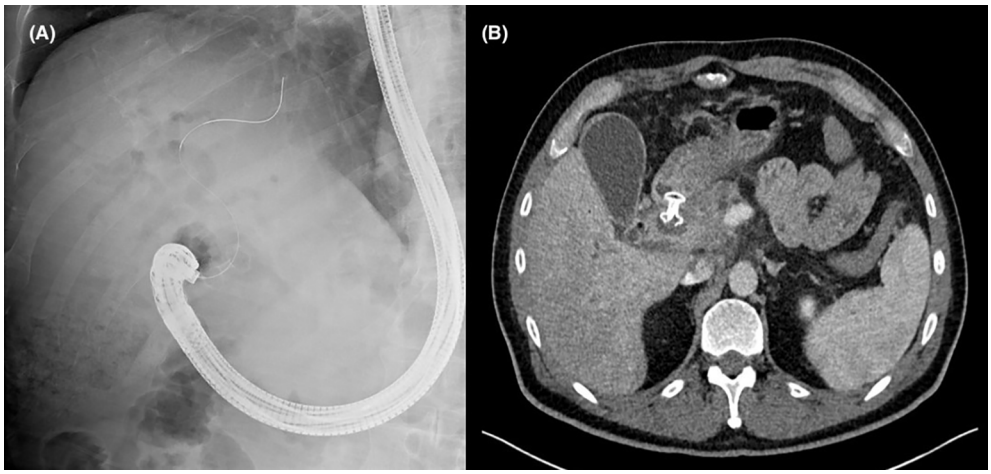

FIGURE 1
(A) Fluoroscopic image demonstrating successful creation of a choledochoduodenostomy with a lumen apposing metal stent. **(B)** Axial computed tomography image of the same patient showing the position of an appropriately placed choledochoduodenostomy stent.

bile leakage. Due to its unique design, it can only be deployed via the CDD route. The popularity of EUS-CDD with a LAMS has led to an influx of large case series in the literature from various geographical regions across the world and this route of biliary drainage has become the first choice in patients with MDBO (25–33).

A recent meta-analysis evaluating the outcomes of EUS-CDD with LAMS of 284 patients (of which the majority were patients with MDBO) across 7 studies demonstrated a pooled technical success rate of 95.7% (95% CI 93.2-98.1), clinical success rate of 95.9% (95% CI 92.8-98.9) and post procedure adverse event rate of 5.2% (95% CI 2.6-7.9).

Lastly, biliary decompression via drainage of the gallbladder in patients with a patent cystic duct could be considered if other forms of EUS-BD were not possible. This can be achieved by placement of a LAMS under EUS guidance draining the gallbladder into the duodenum or the stomach. Two recent studies of this technique in patients with MDBO have reported high technical and clinical success rates (34, 35).

2.1.2 Safety of EUS-BD

Just like with any novel intervention, it would be expected that the safety and adverse event profile associated with EUS-BD evolves over time as more experience with the procedure is accrued and best practice is shared via collaborative work. Wang, et al. reported a systematic review of the safety of EUS -BD, comprising of 1192 patients over 42 studies (36). They demonstrated a cumulative adverse event rate of 23.32% which included events such as bleeding (4.03%), bile leaks (4.03%), pneumoperitoneum (3.02%), stent migration (2.68%), cholangitis (2.43%), abdominal pain (1.51%), and peritonitis (1.26%). The rate of pancreatitis was 0.5%, which

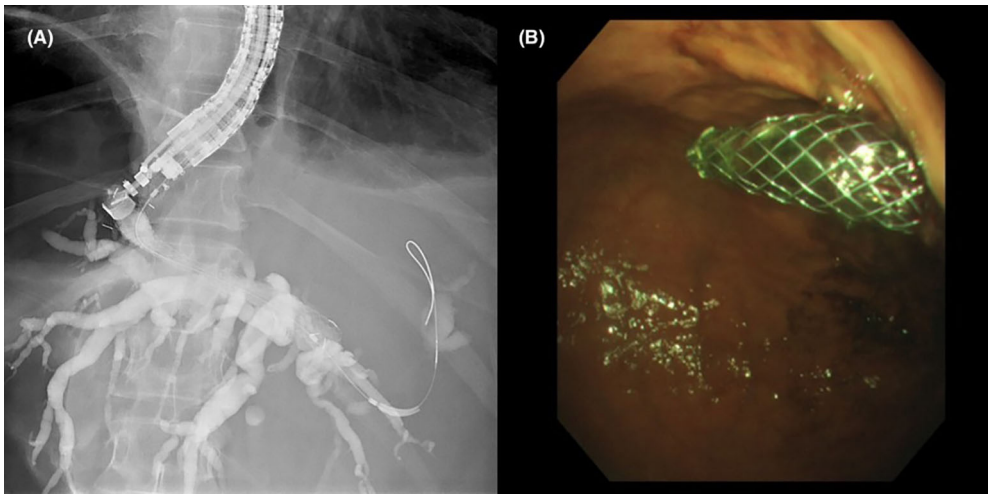

FIGURE 2
(A) Fluoroscopic image of contrast opacifying the left sided intrahepatic ducts with placement of a hepaticogastrostomy stent. **(B)** Gastric end of the stent protruding from the cardia into the gastric lumen.

represents a much lower rate than is expected from ERCP. Although uncommon, pancreatitis after EUS-BD could still occur if there was an immediate prior attempt at ERCP or if techniques which involve instrumental manipulation in the vicinity of the major papilla and pancreatic duct orifice were attempted.

One of the major limitations of the systematic review by Wang, et al. was the heterogenous study population due to their inclusion of the different EUS-BD techniques. A meta-analysis specifically evaluating the use of LAMS for EUS-CDD demonstrated a pooled adverse event rate of 5.6% amongst 284 patients from 7 studies, with the following occurrence of adverse events: bleeding (2.5%), perforation (1.5%), cholangitis (1.5%), bile leaks (1.2%) and abdominal pain (1.2%) (37). Crucially, they also demonstrated that the pooled rate of recurrent jaundice was 8.7% over the follow-up period with 90% of cases being due to obstruction of the lumen of the LAMS and the rest due to migration of the LAMS.

The duration of stent patency, recurrent jaundice and repeated cholangitis after LAMS insertion at EUS-CDD in patients with MDBO have been increasingly recognized to be a potential hinderance in causing delays in the patients' pathway with interruptions to oncological treatment, repeated hospitalizations and compromise to their physiological reserves. It is hypothesized that stent dysfunction relating to reflux of enteric contents leads to blockage of the lumen of the LAMS. The risk of this is particularly amplified by the presence of gastric outlet obstruction from duodenal stenosis due to the increased volume of stagnant enteric contents (38). Vanella, et al. evaluated the risk of development of stent dysfunction of LAMS in 93 patients with MDBO and demonstrated a stent dysfunction rate of 31.8% after a mean follow-up period of 166 days (39). They also devised a unique classification of stent dysfunction demonstrating the various mechanisms in which patency of the LAMS could be compromised, and detailing the different endoscopic rescue strategies which was successful in the majority of patients.

2.1.3 Comparison of EUS guided biliary drainage versus percutaneous biliary drainage

Since the inception of EUS-BD, it has challenged PTBD as the salvage procedure of choice in patients with MDBO after an unsuccessful ERCP. In 2012, Artifon, et al. performed the first randomized controlled trial (RCT) comparing both procedures (EUS-BD, n=13; PTBD, n=12) after unsuccessful ERCP with patients with MDBO (40). They demonstrated a 100% technical and clinical success rates in both groups, with a similar safety profile and cost effectiveness. Further RCTs have demonstrated there were a lower risk of adverse events and re-intervention rates in patients undergoing EUS-BD compared to PTBD (41, 42). These results are backed up by a number of meta-analyses reporting EUS-BD to be of similar efficacy to PTBD (43–45).

One of the major deficits in the literature relates to the relative dearth of comparator studies evaluating the QOL after both modalities. In the RCT by Lee, et al, they demonstrated no difference in QOL between both groups, despite a lower rate of adverse events and re-intervention rates in the PTBD group (41). A prospective, multi-centre trial designed as a non-inferiority trial to assess PTBD against EUS-BD in patients with MDBO after unsuccessful ERCP is underway, although interestingly the authors have not included QOL as an outcome measure in their trial design (46).

The other limiting factor in widespread uptake of EUS-BD is the fact that these procedures tend to only be available in tertiary hospitals and performed by expert endoscopists whereas PTBD is within the repertoire of most interventional radiologists. Local and regional networks play a part in determining which procedure a patient should be offered after a failed ERCP. Nevertheless, EUS-BD is widely recognized and recommended to be the salvage procedure of choice as long as it is feasible and there is available expertise (47).

2.1.4 Comparison of EUS guided biliary drainage versus ERCP

ERCP remains the first-line modality for biliary decompression but can be unsuccessful in up to 15% of cases (14, 15). There are also associated risks of adverse events, particularly post-ERCP pancreatitis, with an incidence of up to 14% depending on underlying risk factors (48). The theoretical advantage of avoiding pancreatitis in patients undergoing EUS-BD as opposed to ERCP is also attractive.

Several studies have explored primary EUS-BD versus ERCP in patients with inoperable MDBO. Two RCTs by Bang, et al. and Paik, et al. demonstrated similar technical and clinical successes following EUS-BD and ERCP (49, 50). In both studies, EUS-BD was performed via a CDD route with the 'traditional' approach; entailing a multi-step procedure and subsequent placement of a tubular metal stent draining the bile duct into the duodenum. Similar results were demonstrated by another RCT by Paik, et al. who evaluated EUS-BD done via two different routes ('traditional' EUS-CDD with tubular metal stents and EUS-HG) (51). A meta-analysis of these RCTs (and including a fourth study, which was a retrospective cohort study) demonstrated similar efficacy and safety between both groups, but EUS-BD was associated with increased stent patency compared to ERCP (52).

It is crucial to point out that the above studies included only patients who had a 'traditional' EUS-CDD with tubular metal stents. Due to the increasing popularity and convenience of LAMS, most institutions have adopted this technique as the one of choice for EUS-CDD. The DRA-MBO RCT was recently published by Teoh, et al, being the seminal paper in the literature evaluating primary EUS-CDD with LAMS against ERCP in patients with inoperable MDBO. They demonstrated similar outcomes in clinical success, 30 day mortality, adverse events and 1 year stent patency rates between both groups (53). There was a stark difference between the technical success rates as EUS-CDD demonstrated a significant advantage over ERCP (96.2% vs 76.3%, $p< 0.001$). Even by exclusion of those patients who had an inaccessible papilla, there was still a 15% technical failure rate of ERCP, which illustrates the challenges of an ERCP in patients with MDBO and potentially strengthens the argument for primary EUS-CDD in patients with MDBO. However, generalized applicability of EUS-CDD could be hindered by anatomical factors. In the DRA-MBO study, an instance of technical failure occurred due to the presence of

paraduodenal varices. An inadequately dilated bile duct could also be a relative contraindication with a diameter of 15mm typically suggested as a cut-off value (30). In essence, individualized decision making taking into account the patient's anatomy as evaluated by pre-procedural cross sectional imaging is key. Table 1 summarizes the key results of the current evidence base for RCTs evaluating EUS-BD versus ERCP.

2.1.5 EUS guided biliary drainage in patients with operable disease

Up to 15-20% of patients with PDAC have disease that is operable at the time of diagnosis (54) and there is a rationale for pre-operative biliary decompression to restore the homeostatic mechanisms that is otherwise hampered by obstructive cholestasis. This includes, but is not limited to, the role of bile and bile acids in coagulation, immunoregulation and nutritional absorption (55, 56). The hypothetical benefit of improved surgical outcomes and overall survival after pre-operative biliary drainage remains debated with some evidence that avoiding pre-operative drainage may be more beneficial (57, 58). However, this may be influenced by the growing evidence of neo-adjuvant treatment, and the need for biliary drainage to facilitate this treatment, in patients with both borderline operable and operable disease (59). In the real world, there is no dogmatic approach towards pre-operative drainage and there is variation in practice, taking into account each individual patient's condition, logistical scheduling and institutional preferences.

Real world data on pre-operative outcomes of ERCP was encapsulated by the Dutch Pancreatic Cancer audit. Latenstein, et al. demonstrated that 575 out of 1056 patients with resected pancreatic head or periampullary tumours underwent pre-operative endoscopic drainage, with an overall endoscopic related complication rate of 18.6% (pancreatitis in 8.2% and cholangitis in 7.5%) (60). The development of post-ERCP pancreatitis in particular could preclude successful surgical resection in patients who may have been deemed operable at the time of presentation due to deconditioning from the episode of pancreatitis, malignant progression of the disease whilst undergoing a period of convalescence, or creating a hostile surgical field at the point of operation rendering the resection technically impossible. As such, the benefit of EUS-BD over ERCP in these situations is the avoidance of pancreatitis (which would be the case if attempted ERCP was not performed beforehand). This would of course, have to be balanced with the other adverse events associated with EUS-BD, particularly bile leaks and biliary peritonitis (61), which is not associated with ERCP but may be circumvented by the usage of a LAMS due to its unique design.

There remains reticence regarding the applicability of EUS-BD in patients with operable disease and understandable concerns regarding subsequent surgical resection. There is increasing evidence that EUS-BD does not hinder subsequent pancreaticoduodenectomy, although this only applies to EUS-CDD as the choledochoduodenostomy tract and stent lies within the surgical resection field. This has been demonstrated by several studies (30, 32, 49, 62, 63).. Janet, et al. also included a comparator cohort group of patients who underwent ERCP and demonstrated a lower rate of post-operative complications in patients who had EUS-CDD (77.3% vs 93.7%, p=0.01) but no differences in the R0 resection rates, overall survival and progression free survival rates between both groups (63). With the caveat that this was a retrospective study, it adds to the body of evidence supporting EUS-CDD as a viable modality of biliary drainage in patients with operable disease, and instill the confidence in developing future RCTs comparing EUS-CDD against ERCP as a primary modality of biliary decompression in patients with resectable disease.

2.1.6 Conclusion

The increasing body of evidence supporting the use of EUS-BD has led to it superseding PTBD as the salvage procedure of choice after unsuccessful ERCP in the European Society of Gastrointestinal Endoscopy (ESGE) guidelines (47) and Asia-Pacific expert consensus guidelines (64). Compared to EUS-BD, PTBD tends to

TABLE 1 Key results of available randomized controlled trials in the literature evaluating endoscopic ultrasound guided biliary drainage versus endoscopic retrograde cholangiopancreatography for malignant distal biliary obstruction.

Authors	Year	Groups	Technical success	Clinical success	Adverse Events	Re-interventions
Bang, *et al*	2018	EUS-BD (n=33) ERCP (n=34)	90.9% 94.1% p=0.67	97% 91.2% p=0.61	21.2% 14.7% p=0.49	3.0% 2.9% p=0.99
Park, *et al*	2018	EUS-BD (n=15) ERCP (n=15)	93% 100% p=1.00	100% 93% p=1.00	0% 0%	*Not reported*
Paik, et al	2018	EUS-BD (n=64) ERCP (n=61)	93.8% 90.2% *Non-inferiority for EUS-BD reported*	90% 94.5% p=0.49	6.3% 19.7% p=0.03	15.6% 42.6% p=0.001
Teoh, et al	2023	EUS-BD (n=79) ERCP (n=76)	96.2% 76.3% p=<0.001	93.7% 90.8% p=0.559	16.5% 17.1% p=1.00	10.5% 12.1% p=0.48

be more readily available and not necessarily limited to tertiary instititutions, which is the case in the United Kingdom, although neither will be able to be provided out of hours at all times. Therefore, it is recommended that a tertiary institution creates arrangements within a regional network to provide an EUS-BD service for neighbouring ERCP providers. It must be said that there will still be a role for PTBD in patients with MDBO, for example in an acutely cholangitic or severely jaundiced patient where access to EUS BD is not available or if the procedure is not technically feasible.

The status quo of ERCP as the modality of choice for biliary decompression in patients with MDBO is also being challenged. This makes sense if the capabilities of EUS are maximally utilized in patients with MDBO; being able to obtain tissue, stage the disease and drain the biliary tract in one seating. The major limitation in affirming EUS-BD as the standard of care would be the fact that expertise is confined to tertiary institutions. Further studies are also required to identify specific cohorts of patients who would benefit most from primary EUS-BD.

2.2 EUS guided gastrojejunostomy

EUS guided gastrojejunostomy (EUS-GJ) was first reported by Binmoeller and Shah in 2012 (65). Although various techniques exist, the core premise is the endosonographic identification of a jejunal limb from the stomach and creation of a conduit between the stomach and the jejunum with the placement of a LAMS, thereby creating a preferential passage of food through this artificial conduit (66, 67). The key steps of EUS-GJ are summarized in Figure 3. Therefore, EUS-GJ confers a minimally invasive approach whilst placement of the stent at a distance away from the site obstruction, obviating the risk of tumour ingrowth into the stent, thereby reduces the chances of stent dysfunction and re-intervention rates.

2.2.1 Gastric outlet obstruction

Gastric outlet obstruction (GOO) in patients with PDAC is characterized by localized tumoral infiltration of the distal stomach or duodenum, causing mechanical obstruction. Symptoms of GOO comprise early satiety, abdominal pain, nausea, vomiting, weight loss and failure to thrive (68). GOO may manifest at all stages of the disease course in PDAC and, if left untreated, will be a detriment to patients' QOL and nutrition status, potentially rendering them unsuitable for surgical or oncological therapies (69). It should be noted that the majority of studies evaluating malignant GOO have a heterogenous study population by inclusion of patients with other malignancies in addition to those with PDAC, for example gastric cancer, duodenal cancer, and metastatic disease from other primaries.

Prior to the advent of interventional EUS, the mainstay of treatment in patients with malignant GOO was either endoscopic enteral stenting (ES) or a surgical gastrojejunostomy (S-GJ), via an open or laparoscopic approach (70, 71). ES has the benefit of being minimally invasive but its efficacy diminishes over time as GOO recurs when there is tumor ingrowth through the mesh of the stent or stent dysfunction occurs. On the contrary, S-GJ provides longer lasting patency to enable oral intake but is invasive and requires the patient to have a physiological and nutritional threshold to withstand an operative procedure (69).

Despite the relatively common incidence of malignant GOO, only three small RCTs exist with 27, 18 and 39 patients respectively. All three studies evaluated (72–74) ES against S-GJ, demonstrating shorter procedural time, quicker restoration of oral diet and shorter length of stay (LOS) in the ES group. However, the SUSTENT study demonstrated lower rates of re-intervention and longer lasting relief of GOO in the S-GJ group (74).

Since then, a large number of retrospective comparator studies have sought to compare various outcomes between ES and S-GJ. A recently published comprehensive meta-analysis compared 3,128 ES patients and 2,116 S-GJ patients across 39 studies (75). The authors demonstrated that the ES group had a shorter LOS, quicker restoration of oral diet and less surgical site infections. However, there was a greater risk of re-intervention (risk ratio 2.60, 95% Cl 1.87 to 3.63, $p < 0.001$), less likely to undergo adjuvant palliative chemotherapy (risk ratio 0.81, 95% Cl 0.70 to 0.93, $p = 0.004$) and a shorter survival time (mean difference -24.77 days, 95% Cl − 45.11 to − 4.43, $p = 0.02$) in the ES group compared to the S-GJ group. The difference in survival time and commencement of palliative chemotherapy may be explained by the selection bias in patients undergoing ES, with these patients being more likely to have a poorer prognosis compared to patients in the S-GJ group. This point was succinctly expressed in an editorial by Adler (76) and it remains a limitation in drawing definite conclusions from retrospective studies, although it is clear that both ES and S-GJ remain viable options depending on the individual patient's circumstances. S-GJ could be considered ahead of ES in patients with a good performance status and a life expectancy of over 3-6 months (77). It has to be noted that oncological advances have led to improved life expectancy in such patients. In patients who underwent ES successfully with sustained improvements in their nutritional status and are able to withstand a subsequent chemotherapy regimen, their prognosis is likely to exceed the initial expectations and it is this cohort of patients who may encounter stent dysfunction as time passes. Therefore, ES should be considered in patients who clearly have a prognosis which can be measured in weeks or short months.

2.2.2 Safety of EUS guided gastrojejunostomy

EUS-GJ is firmly placed in the highest echelons of an interventional endoscopist's skillset, and there is evidence that even an expert endoscopist has to scale a learning curve before achieving proficiency (78). It involves multiple steps, with little margin for error and requires significant technical and cognitive expertise to rectify errors, should they occur. Two meta-analyses have demonstrated the overall adverse event rate of 10-12%, including events such as bleeding, peritonitis, abdominal pain and stent misdeployments (79, 80).

A large retrospective review of 467 procedures from 12 tertiary institutions demonstrated a stent misdeployment rate of 9.85% (81). Although most were classed as mild to moderate, which could be managed endoscopically, there was a surgical intervention required in approximately 11% of cases. Therefore, if rescue surgery is required, this is likely to be of high risk due to the fact that these

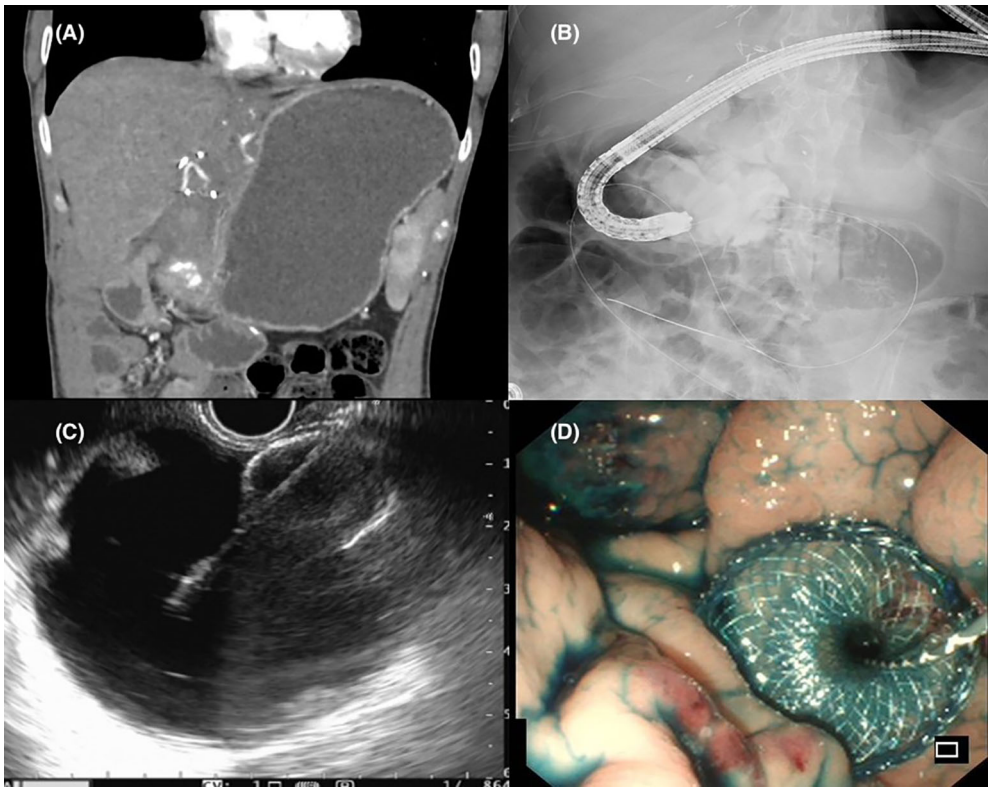

FIGURE 3
(A) Radiological evidence of gastric outlet obstruction. **(B)** Fluoroscopic capture of the stenosis being bypassed with a wire passed down an endoscope with contrast infused into the jejunum to identify a suitable limb for gastrojejunostomy formation. **(C)** Endosonographic views of a distended jejunal bowel loop and successful placement of a lumen apposing metal stent. **(D)** Endoscopic view following successful EUS guided gastrojejunostomy with reflux of methylene blue stained contrast solution into the stomach.

patients have an impaired physiological reserve resulting from their underlying disease state and a degree of malnutrition.

2.2.3 EUS guided gastrojejunostomy vs endoscopic enteral stenting and surgical gastrojejunostomy

To date, there has not been any prospective RCT evaluating EUS-GJ against ES although there are a plethora of retrospective studies comparing both modalities (82–87). In all studies, the technical success of EUS-GJ was comparable to ES. In terms of clinical success, the results are less clear cut with some evidence to suggest that EUS-GJ is advantageous over ES (84, 85, 87). Of note, the reporting of clinical success and adverse events was variable across the studies with a mixture of definitions used in the literature. The study by Jaruvongvanich, et al. reported a significantly higher rate of adverse events in the ES group (38.9% vs 8.6%) although the majority of these events were related to stent obstruction or tumour ingrowth rather than procedural related adverse events (85). As would be expected, re-intervention rates were lower in patients who had an EUS-GJ (83–85, 87).

With regards to S-GJ in comparison with EUS-GJ, all studies are retrospective (82, 85, 88–93). In general, both technical and clinical success were similar between the groups. The inclusion of both open and laparoscopic approaches for S-GJ added additional heterogeneity, which may also account for higher adverse events in some studies, including bleeding, infection, anastomotic breakdown and ileus (85, 88, 89, 92). Crucially, the studies by Kouanda, et al. and Abbas, et al. demonstrated a shorter time to starting oncological treatment in the EUS-GJ group (88, 91). The study by Pawa, et al. showed that patients who underwent EUS-GJ had a shorter length of stay (4.3 vs. 8.2 days, $p = 0.0009$) and resumed oral diet quicker (1.0 vs. 5.8 days, $p < 0.0001$) compared to those who had a S-GJ via a robotic approach.

A meta-analysis concluded that clinical efficacy was of equal parity between all three modalities with similar safety profiles. Procedure related bleeding was least common but re-intervention rate was most common in the ES group (94). Although EUS-GJ has become increasingly popular, until the results of prospective studies are carried out, it is difficult to draw any firm comparisons. The American Society of Gastrointestinal Endoscopy (ASGE) guidelines for management of GOO published in 2021 acknowledges EUS-GJ within the evidence base but has not made any recommendations for its application (95). The ESGE guidelines for interventional EUS published in 2022 recommend EUS-GE as an alternative to ES or S-GJ but stop short of making specific criteria for choosing one over the other (47).

2.2.4 Conclusion

The advent of interventional EUS and EUS-GJ has expanded the repertoire of procedures that are available for treating GOO. Although EUS-GJ is a promising technique, both ES and S-GJ are ‘tried and tested’ over the passage of time and both remain valid options for treating patients with GOO. It is likely that EUS-GJ and S-GJ would be

on par in terms of providing symptomatic benefit for patients in the longer term with EUS-GJ having the advantage of being minimally invasive with a shorter recovery period. However, the practice of EUS-GJ is confined to specialist centres and performed by expert endoscopists. Ultimately, each modality has its merits and the decision making has to be individualized to the specific patient's clinical condition, with life expectancy and physiological state taken into account of. The importance of multi-discplinary team (MDT) decision making is key.

2.3 EUS guided coeliac plexus intervention

Abdominal pain in patients with PDAC can range from mild to severe and debilitating, leading to a significant detrimental impact on QOL. It is highly prevalent, especially in patients with a primary tumor site in the body or tail of pancreas (96). More severe pain in patients with PDAC appears to be associated with worse performance status scores, when measured with the Eastern Cooperative Oncology Group (ECOG) and Karnofsky performance status scores (97). Interestingly, the pre-operative pain score also appears to be related to survival after resectional surgery. An observational study categorized 139 patients into three pain groups (none, mild, moderate-severe) based on a composite score evaluating pain severity, intensity and frequency. The median survival time after resection was 21.8 months, 15.0 months and 10.0 months (p=0.0015) in patients with no pain, mild pain and moderate-severe pain respectively (98). It is hypothesized that severity of pain may reflect a more advanced stage of disease at a microscopic level of neural invasion and likely also has collateral impact on patient related factors such as nutritional status and ability to tolerate oncological treatment (99).

2.3.1 Pathophysiology of pain in PDAC

Pain in patients with PDAC share similar characteristics and mechanisms of action in patients with chronic pancreatitis and it is vital to commit research into the pathophysiology of pain in both groups of patients. The key concept is the neuroanatomy, which is characterized by the bidirectional pathways between the pancreas and the cerebral cortex, with the gland itself innervated by both sympathetic and parasympathetic nerve fibers of the autonomic nervous system (100). The coeliac plexus is one of the key gateways in this neural highway as it receives impulses via afferent neurons from the pancreas.

There are two main proposed mechanisms leading to the development of pain in patients with PDAC. The first mechanism relates to obstruction of the main pancreatic duct, impairing secretion of digestive enzymes into the duodenum and results in ductal and interstitial hypertension. This then impedes parenchymal blood flow and generates a pain of ischaemic aetiology, akin to a form of compartment syndrome (101). The second mechanism relates to development of a neuropathy due to a combination of factors including local activation of an inflammatory cascade from malignant cells that are present, direct malignant invasion of the perineurium, expression of cations involved in nociception such as the transient receptor potential cation channel and lastly, secretion of molecules that stimulate the nociceptive pathway (98, 99, 102, 103).

2.3.2 Strategies to manage pain in PDAC

The optimum approach to improve pain in patients with PDAC often requires multiple modalities and also the involvement of the multi-disciplinary team. The initial method, and most convenient, of choice is with oral analgesics, which include the use of non-steroidal anti-inflammatories, opioids and neuroanalgesics. Strategies to escalate and individualize oral analgesics in the specific context of patients with PDAC are described by the National Comprehensive Cancer Network (NCCN) (104).

Chemotherapy itself could also have a beneficial effect on pain in patients with advanced PDAC. Kristensen, et al. conducted a systematic review of 30 studies investigating the impact of chemotherapy on QOL and performed a sub-analysis on 24 studies, which included pain scores as an outcome measure (105). They demonstrated that there was an improvement in pain with the delivery of chemotherapy, particularly with gemcitabine. There are of course, other systemic side effects relating to the use of chemotherapy and whilst it would not be expected that chemotherapy is commenced for the purposes of pain control, it may provide an additive analgesic benefit when given for oncological purposes. In addition, stereotactic body radiotherapy is another facet of oncological treatment which could improve pain control in patients with PDAC (106).

Finally, direct intervention to the coeliac plexus to manage pain can also be performed via an endoscopic or percutaneous route. It is important to recognize that the aforementioned different strategies to manage pain can be complementary and all avenues should be explored to achieve the best possible outcome for these patients.

2.3.3 EUS guided coeliac plexus intervention

Directed EUS guided therapy to the coeliac plexus (Figure 4) can be broadly divided into coeliac plexus neurolysis (CPN) or coeliac plexus block (CPB), depending on the injectable agent used. In CPN, typically ethanol or phenol is used whereas in CPB, combined steroids and local analgesia (such as triamcinolone and bupivacaine) are administered (107). CPB tends to be favoured in patients with pain from benign pancreatic disease as the use of ethanol in CPN leads to a localized inflammatory process, with subsequent fibrosis, which may hinder surgery if it were to be contemplated in these patients (108). Pain relief in these patients (either from CPN or CPB) tends not to last beyond 2-3 months. It is hypothesized that this is because the solvent flows away from its injected site due to its fluidity (109).

In 1996, Wieserma and Wieserma first reported the use of EUS CPN in a series of 30 patients with intraabdominal malignancies of whom 25 had underlying PDAC (110). They demonstrated that up to 88% of patients had an improvement in their pain scores at 12 weeks. Since then, several variations of EUS-CPN have been described (111, 112). The injection solvent can be injected either directly above the root of the coeliac artery (central injection) or either side of it (bilateral injections). The site of injection may also vary – coeliac ganglia neurolysis (CGN), which involves directly targeting the coeliac plexus

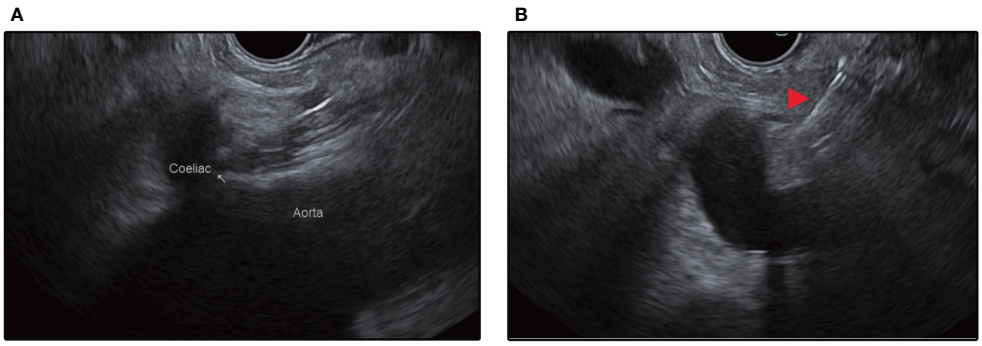

FIGURE 4
(A) Endosonographic identification of the aorta and the coeliac trunk take-off from the stomach. **(B)** Red arrow depicts injection needle targeting the space above the coeliac trunk for central injection.

ganglia or broad plexus neurolysis (BPN), which involves targeting the superior mesenteric ganglia.

2.3.4 Efficacy and safety of EUS guided coeliac plexus intervention

Overall, studies have reported moderate to high efficacy of EUS guided coeliac plexus interventions in improving pain control in patients with PDAC. Multiple meta-analyses have reported improvement in pain scores after EUS-CPN in 70-80% of patients with PDAC (113–115). In their meta-analysis, Lu, et al. reported that patients with PDAC had similar improvements in short term pain relief after EUS-CPN regardless of whether a central or bilateral injection technique was performed although the bilateral technique led to a significant reduction in post-procedural analgesic use [RR = 0.66, 95% CI (0.47, 0.94), p = 0.02] (116).

Although EUS-CPN/B is considered a minimally invasive intervention, patients and clinicians have to remain vigilant of potential adverse events. Alvarez-Sánchez, et al. performed an analysis of 20 studies comprising 1,142 patients who underwent EUS-CPN/B, demonstrating that complications occurred in 7% of patients who had EUS-CPB (n=481) and 21% of patients who had EUS-CPN (n=661) (117). The majority of adverse events in both groups related to the injected solvent's antagonistic impact on the sympathetic activity of the coeliac plexus and resultant unopposed parasympathetic activity, leading to diarrhoea and/or hypotension. Transient increase in pain post-procedurally can also be expected and is usually managed conservatively. Major complications occurred in 0.6% of patients after EUS-CPB (two patients developed abscesses and one developed a gastric haematoma) and 0.2% of patients after EUS-CPN (one patient developed retroperitoneal bleeding). There are also a handful of individual case reports describing the development of ischaemic multi-visceral injuries and development of paraplegia after EUS-CPN (117).

2.3.5 Comparison with other modalities

To date, there have not been any RCTs evaluating EUS-CPN against percutaneous CPN in patients with PDAC although this has been studied in patients with chronic pancreatitis. The only published RCT was conducted by Wyse, et al. (118) They sought to evaluate the early use of EUS-CPN in patients who require an EUS for tissue acquisition of suspected PDAC compared to conventional pain management. Patients were randomized only after cytopathological analysis of the aspirate confirmed malignancy and the patient being deemed inoperable following strict criteria. The authors demonstrated that early EUS-CPN in patients with inoperable PDAC led to lower pain scores at 1 and 3 months, and a non-significant trend towards lower consumption of morphine.

With a distinct lack of comparative studies, it is therefore unsurprising that the position of EUS CPN in the algorithm of pain management in patients with PDAC is not well defined. The NCCN has no specific recommendations regarding the timing or route of coeliac plexus interventions but has advocated its usage in patients with unsatisfactory pain control and a high burden of analgesia (particularly opioid) usage (104). Similarly, the European Society for Medical Oncology recommends the use of CPN (favoring an endoscopic route over the percutaneous route) in patients with refractory pain and in those who are not in a poor clinical condition (119).

2.3.6 Conclusion

Although EUS-CPN has been adopted in widespread practice for over a decade in patients with PDAC, there remains potential for ongoing research into the role of this in the treatment algorithm. There has not been direct comparison with other modalities such as percutaneous CPN, stereotactic radiotherapy or the plethora of analgesics that are available, including regimens that exclude opioid use. There is also variation in practice with at least three widely used approaches (CPN, CGN and BPN), and although all have been reported with similar efficacies in the literature, standardization of practice would require further comparator studies of all three techniques. Alternative neurolytic agents should also be studied to identify those that have the potential to provide a longer lasting analgesic effect.

2.4 EUS guided fiducial placement

Radiotherapy in PDAC is usually used for consolidation therapy for patients who have progressed despite first-line

chemotherapy after 2-6 months or did not tolerate chemotherapy either with gemcitabine/nab-paclitaxel or FOLFIRINOX (120). Image-guided radiation and stereotactic body radiation therapy is increasingly being offered due to the shorter treatment duration and acceptable toxicity risk with a higher dose of radiation (121).

Fiducials are inert, radio-opaque markers that are placed into or near a target lesion to allow real-time tracking of the lesion. They are made from platinum or gold, creating low CT and MR artefacts while maintaining good visibility (120). They facilitate the delivery of higher doses of radiation and limit exposure of surrounding healthy tissue by quantifying tumor extent. Due to the implantation into the target tissue, fiducial markers may improve the localization and targeting of the lesion in comparison to using adjacent bony anatomy alone (122).

Pancreatic fiducial markers have been traditionally placed percutaneously under radiological guidance; however, there are concerns about the adverse event rates, including bleeding. Traditional methods of placement also carry increased rates of fiducial migration (123).

EUS-guided placement may be a more precise method to facilitate closer placements in or adjacent to the target tissue. It has high technical success of up to 92% with low rates of migration (124, 125). The fiducials can be delivered through preloaded needles or hand-loaded devices via different sized needles (126). EUS-guided placement involves the placement of at least three markers in different EUS planes and into the tumor at the periphery (120, 124). There is a 5- 8% risk of adverse events, including acute pancreatitis, cholangitis, bleeding, fever, and biliary stent migration (120, 124, 127).

Although pancreatic tumors are radiation resistant, the organs that lie in relation to it have increased radiation sensitivity (120). In addition to placing the fiducials, endoscopic assessment for duodenal involvement of the tumor prior to treatment can also aid in guiding the dosage of radiation needed.

Patients with PDAC can undergo biliary stenting to relieve malignant obstruction. Metal stents have been proposed as an alternative to fiducial placement to guide therapy. Although they may present better anatomical markers than traditional bony alignment, they still have larger margins for targeting compared to fiducials (128).

Care should be taken to place fiducials after tissue acquisition has been performed and a diagnosis and management plan for the patient has been discussed in MDT. The role of the MDT is critical in defining the diagnostic and therapeutic path and weighing in on the timing of fiducial placement. Placement of fiducial markers after commencing chemotherapy can be challenging due to desmoplastic reaction making the borders less well defined and the tumour hard (120). At this point, there is still insufficient evidence that placement of fiducial markers leads to improved outcomes from radiotherapy compared to conventional methods of radiotherapy planning with cross sectional imaging or other methods of fiducial markers placement. Performing an EUS for the sole indication of fiducial placements has to take into account the aforementioned risk of adverse events, which may preclude subsequent oncological treatment. Further prospective comparator studies evaluating EUS- guided fiducial placement are required to evaluate its impact on relevant patient outcomes.

2.5 EUS guided intratumoral therapy

As with fiducial markers, EUS allows precisely delivered intratumoral therapies. There is a clear advantage in the real time capability of assessing the effect of the therapy on the lesion itself via its endosonographic appearances to ensure complete and adequate treatment via a minimally invasive route. It is also possible to achieve a high level of localized drug concentration when injected directly into the tumor, which may be of advantage if systemic administration of the drug is limited by its potential toxicities. However, despite the recognition of the capability of EUS in administering direct tumoral therapy with precision, there is a relative paucity of studies evaluating this technique.

2.5.1 Chemotherapy

In 2007, Matthes, et al. described EUS guided injection of paclitaxel into porcine pancreas with a demonstrable and sustained localized concentration of the drug up to 14 days post injection (129). Levy, et al. performed a study evaluating EUS guided injection of gemcitabine in 36 patients with locally advanced or metastatic PDAC (130). No adverse events relating to the EUS procedure were encountered. All patients then subsequently received either chemotherapy or chemoradiotherapy with a regime determined most appropriate by an oncologist. Interestingly, 4 out of 20 patients who were initially deemed unresectable were downstaged following treatment and each underwent an R0 resection. Whilst the nature of the study design precludes any specific impact intratumoral gemcitabine had on the subsequent resectability, at the very least, it demonstrates an avenue for further research.

2.5.2 Immunotherapy

Unlike in other solid organ malignancies, the administration of systemic or localized immunotherapy has yet to take hold as a widely accepted modality of treatment in the oncological armamentarium in patients with PDAC. In a phase I clinical trial, cytoimplant (allogeneic mixed lymphocyte culture) was injected in 8 patients with unresectable PDAC, with an aim to upregulate host anti-tumor mechanisms via a local cytokine release (131). Despite modest efficacy as measured by tumor response on imaging (3 patients displayed response), a subsequent randomized trial comparing cytoimplant with gemcitabine suggested a worse outcome in patients who had cytoimplant, leading to termination of the trial.

Other intratumoral immunotherapies such as dendritic cell vaccines and oncolytic viruses have been studied. Dendritic cells function as antigen presenting cells to stimulate the host primary T-cell response and induce tumor antigen specific T lymphocytes with cytotoxic properties (132). Oncolytic viruses are considered a form of virotherapy whereby selective genetic engineering is carried out to enhance their affinity to specific tumors to induce oncolysis

(133). These therapies have been the subject of small scale clinical studies and phase I/II trials. Herman, et al. reported a phase III RCT involving 304 patients with locally advanced PDAC evaluating TNFerade (an adenoviral vector capable of selective delivery of tumor necrosis factor-α) in combination with chemoradiation versus chemoradiation alone (134). There were no differences in survival between both groups.

2.6 EUS guided ablative therapies

Several modalities of ablative therapies have been demonstrated to be feasibly delivered via EUS with radiofrequency ablation (RFA) being the most prominent, although other forms such as photodynamic therapy, ethanol and laser ablation exist. The majority of the literature on EUS-RFA in pancreatic lesions lies within the study of this modality for pancreatic cystic lesions or pancreatic neuroendocrine tumors, but its utility in treating patients with PDAC is becoming increasingly studied.

The initial application of RFA in PDAC was via a peri-operative surgical approach during laparotomy as demonstrated in a prospective study of 50 patients with locally advanced PDAC by Girelli, et al. (135) In their study, there was a 24% rate of intra-abdominal adverse events that were attributable to RFA therapy. Crinò, et al. reported a feasibility study of EUS-RFA in 9 patients (8 of whom had PDAC), demonstrating that it was possible to achieve an ablation zone within the tumor margins and with no major adverse events (136). Similar conclusions were achieved by two separate studies involving only patients with PDAC; one with 6 patients by Song, et al. (137) and another with 10 patients by Scopelliti, et al. (138)

Overall, EUS-RFA appears to be fairly safe with a recent meta-analysis of 115 patients (with various pancreatic lesions being treated) demonstrating a pooled adverse event rate of 6.7% (95% CI: 3.4–11.7, I2 = 34.0%), the commonest being acute pancreatitis (3.3%) (139).

Photodynamic therapy (PDT) is a method of localized treatment of tumorous cells via administration of a photosensitizing agent which is activated by light leading to free oxygen radicals formation. Chan, et al. demonstrated in their pilot study involving porcine models that PDT could be feasibly delivered via EUS to induce a local ablation zone in the pancreas (140). Small studies of the use of EUS-PDT in humans with PDAC have demonstrated that a zone of necrosis can be safely achieved as detected on post procedural computed tomography scanning (141, 142).

There is yet to be standardization of the RFA or PDT technique with marked heterogeneity in reported studies, and how this may affect the fine balance between achieving efficacy and mitigating adverse events. Furthermore, all the studies on PDAC thus far have focused on technical feasibility of the procedure but other outcome measures such as symptom benefit, QOL and survival have yet to be studied. The functional outcome of 'successful' ablation as determined by endosonographic or radiological interpretation is difficult to quantify. Lastly, there has not been a uniformly acknowledged indication for EUS-RFA in patients with PDAC to determine who would best benefit from this intervention and how it fares against standard of care. Nevertheless, it appears to be a promising avenue of intervention and should be explored further with prospective studies.

3 Discussion

The field of interventional EUS has expanded rapidly over the past decade leading to substantial enthusiasm for its use in a variety of circumstances. Nonetheless, based on the review of the literature, we have the following observations.

Firstly, there is a lack of RCTs which is largely due to the relative novelty of interventional EUS as compared to other more widely accepted modalities of care. Although multiple meta-analyses on different aspects of interventional EUS have been published, there is general acknowledgement that the paucity of prospective data is a major limitation. This is likely to be amplified by the fact that interventional EUS continues to evolve and there is yet to be standardization of the plethora of techniques that have been described. There is also a general acceptance that a steep learning curve is associated with these procedures even amongst expert endoscopists (23, 78, 143). This is particularly pertinent in procedures such as EUS-BD and EUS-GJ, which consist of multiple steps with the potential for adverse event at each step, requiring technical and mental skill to rectify. It is only natural that innovation leads to collaborative working from which cumulative experiences across the endoscopy community worldwide have led to ongoing refinement of techniques and equipment.

Secondly, the majority of the studies have included patients with different aetiologies of MDBO or intraabdominal malignancies. Whilst PDAC tends to remain one of the majority patient groups, it is nonetheless a heterogenous study population. As each individual tumour biology and aggression differs, this is likely to affect the disease course and outcomes over the follow-up period.

Thirdly, the majority of studies have focused their primary outcomes on technical aspects such as procedural success and adverse event rates. Undoubtedly, these are relevant and important outcomes in the initial evaluation of an innovative technique. As experience and comfort with interventional EUS grows, there should be an impetus to evaluate more relevant outcomes such as survival, patient reported outcome measures, QOL, ability to receive anti-cancer treatment, and perhaps even composite endpoints.

Fourthly, there is heterogeneity of how key outcomes are defined and reported in the literature body of interventional EUS. These include parameters such as technical success, clinical success, adverse events, amongst others. The coming years are likely to see a multitude of prospective studies evaluating EUS-BD and it seems that the time is right for outcomes of interventional EUS to be formally defined.

In conclusion, interventional EUS has numerous applications in treating the multitude of clinical sequelae in patients with PDAC and should be considered where appropriate. Although interventional EUS has now established itself in the management algorithm of patients with PDAC (particularly EUS-BD and EUS-

GJ), there remain numerous avenues for prospective studies that should be undertaken.

Author contributions

WO conceptualized the idea, performed the literature review and drafted the manuscript. WA performed the literature review and drafted the manuscript. SE, MH and BP critically reviewed the manuscript. All authors contributed to the article and approved the submitted version.

Funding

The author(s) declare financial support was received for the research, authorship, and/or publication of this article. The authors would like to acknowledge Viatris Inc. for the financial support in the publication of this manuscript.

Conflict of interest

The authors declare that the research was conducted in the absence of any commercial or financial relationships that could be construed as a potential conflict of interest.

The reviewer YK declared a shared affiliation with the authors to the handling editor at the time of review.

Publisher's note

References

1. Allemani C, Matsuda T, Di Carlo V, Harewood R, Matz M, Nikšić M, et al. Global surveillance of trends in cancer survival 2000–14 (Concord-3): analysis of individual records for 37 513 025 patients diagnosed with one of 18 cancers from 322 population-based registries in 71 countries. *Lancet* (2018) 391(10125):1023–75. doi: 10.1016/S0140-6736(17)33326-3

2. Hall BR, Cannon A, Atri P, Wichman CS, Smith LM, Ganti AK, et al. Advanced pancreatic cancer: A meta-analysis of clinical trials over thirty years. *Oncotarget* (2018) 9(27):19396–405. doi: 10.18632/oncotarget.25036

3. Prades J, Arnold D, Brunner T, Cardone A, Carrato A, Coll-Ortega C, et al. Bratislava statement: consensus recommendations for improving pancreatic cancer care. *ESMO Open* (2020) 5(6):e001051. doi: 10.1136/esmoopen-2020-001051

4. Michl P, Löhr M, Neoptolemos JP, Capurso G, Rebours V, Malats N, et al. Ueg position paper on pancreatic cancer. Bringing pancreatic cancer to the 21st century: prevent, detect, and treat the disease earlier and better. *United Eur Gastroenterol J* (2021) 9(7):860–71. doi: 10.1002/ueg2.12123

5. Mizrahi JD, Surana R, Valle JW, Shroff RT. Pancreatic cancer. *Lancet* (2020) 395 (10242):2008–20. doi: 10.1016/S0140-6736(20)30974-0

6. Shrikhande SV, Barreto SG, Goel M, Arya S. Multimodality imaging of pancreatic ductal adenocarcinoma: A review of the literature. *HPB: Off J Int Hepato Pancreato Biliary Assoc* (2012) 14(10):658–68. doi: 10.1111/j.1477-2574.2012.00508.x

7. Zakaria A, Al-Share B, Klapman JB, Dam A. The role of endoscopic ultrasonography in the diagnosis and staging of pancreatic cancer. *Cancers* (2022) 14 (6). doi: 10.3390/cancers14061373

8. Vanella G, Bronswijk M, Arcidiacono PG, Larghi A, Wanrooij R, de Boer YS, et al. Current landscape of therapeutic eus: changing paradigms in gastroenterology practice. *Endoscopic Ultrasound* (2023) 12(1):16–28. doi: 10.4103/eus-d-21-00177

9. Giovannini M, Moutardier V, Pesenti C, Bories E, Lelong B, Delpero JR. Endoscopic Ultrasound-guided bilioduodenal anastomosis: A new technique for biliary drainage. *Endoscopy* (2001) 33(10):898–900. doi: 10.1055/s-2001-17324

10. Baars JE, Kaffes AJ, Saxena P. Eus-guided biliary drainage: A comprehensive review of the literature. *Endoscopic Ultrasound* (2018) 7(1):4–9. doi: 10.4103/eus.eus_105_17

11. Dietrich CF, Braden B, Burmeister S, Aabakken L, Arciadacono PG, Bhutani MS, et al. How to perform eus-guided biliary drainage. *Endoscopic Ultrasound* (2022) 11 (5):342–54. doi: 10.4103/eus-d-21-00188

12. van Wanrooij RLJ, Bronswijk M, Kunda R, Everett SM, Lakhtakia S, Rimbas M, et al. Therapeutic endoscopic Ultrasound: european society of gastrointestinal Endoscopy (Esge) technical review. *Endoscopy* (2022) 54(3):310–32. doi: 10.1055/a-1738-6780

13. Dumonceau J-M, Tringali A, Papanikolaou IS, Blero D, Mangiavillano B, Schmidt A, et al. Endoscopic biliary stenting: indications, choice of stents, and results: European society of gastrointestinal Endoscopy (Esge) clinical guideline – updated October 2017. *Endoscopy* (2018) 50(09):910–30. doi: 10.1055/a-0659-9864

14. Canakis A, Baron TH. Relief of biliary obstruction: choosing between endoscopic Ultrasound and endoscopic retrograde cholangiopancreatography. *BMJ Open Gastroenterol* (2020) 7(1). doi: 10.1136/bmjgast-2020-000428

15. Ekkelenkamp VE, de Man RA, Ter Borg F, Borg PC, Bruno MJ, Groenen MJ, et al. Prospective evaluation of ercp performance: results of a nationwide quality registry. *Endoscopy* (2015) 47(6):503–7. doi: 10.1055/s-0034-1391231

16. Castiglione D, Gozzo C, Mammino L, Failla G, Palmucci S, Basile A. Health-related quality of life evaluation in "Left" Versus "Right" Access for percutaneous transhepatic biliary drainage using eortc qlqbil-21 questionnaire: A randomized controlled trial. *Abdominal Radiol* (2020) 45(4):1162–73. doi: 10.1007/s00261-019-02136-7

17. Subramani VN, Avudaiappan M, Yadav TD, Kumar H, Sharma V, Mandavdhare H, et al. Outcome following percutaneous transhepatic biliary drainage (Ptbd) in carcinoma gallbladder: A prospective observational study. *J Gastrointest Cancer* (2022) 53(3):543–8. doi: 10.1007/s12029-021-00655-5

18. Nennstiel S, Weber A, Frick G, Haller B, Meining A, Schmid RM, et al. Drainage-related complications in percutaneous transhepatic biliary drainage: an analysis over 10 years. *J Clin Gastroenterol* (2015) 49(9):764–70. doi: 10.1097/mcg.0000000000000275

19. Facciorusso A, Mangiavillano B, Paduano D, Binda C, Crinò SF, Gkolfakis P, et al. Methods for drainage of distal malignant biliary obstruction after ercp failure: A systematic review and network meta-analysis. *Cancers* (2022) 14(13). doi: 10.3390/cancers14133291

20. Artifon ELA, Visconti TAC, Brunaldi VO. Choledochoduodenostomy: outcomes and limitations. *Endoscopic Ultrasound* (2019) 8(Suppl 1):S72–s8. doi: 10.4103/eus.eus_62_19

21. Artifon EL, Marson FP, Gaidhane M, Kahaleh M, Otoch JP. Hepaticogastrostomy or choledochoduodenostomy for distal malignant biliary obstruction after failed ercp: is there any difference? *Gastrointest Endoscopy* (2015) 81(4):950–9. doi: 10.1016/j.gie.2014.09.047

22. Paik WH, Park DH. Eus-guided versus ercp-guided biliary drainage for primary treatment of distal malignant biliary obstruction. *Curr Treat Options Gastroenterol* (2020) 18(2):188–99. doi: 10.1007/s11938-020-00282-2

23. Yamamoto Y, Ogura T, Nishioka N, Yamada T, Yamada M, Ueno S, et al. Risk factors for adverse events associated with bile leak during eus-guided hepaticogastrostomy. *Endoscopic Ultrasound* (2020) 9(2):110–5. doi: 10.4103/eus.eus_68_19

24. Mussetto A, Fugazza A, Fuccio L, Triossi O, Repici A, Anderloni A. Current uses and outcomes of lumen-apposing metal stents. *Ann Gastroenterol* (2018) 31(5):535–40. doi: 10.20524/aog.2018.0287

25. Anderloni A, Fugazza A, Troncone E, Auriemma F, Carrara S, Semeraro R, et al. Single-stage eus-guided choledochoduodenostomy using A lumen-apposing metal stent for malignant distal biliary obstruction. *Gastrointest Endoscopy* (2019) 89 (1):69–76. doi: 10.1016/j.gie.2018.08.047

26. Chin JY, Seleq S, Weilert F. Safety and outcomes of endoscopic Ultrasound-guided drainage for malignant biliary obstruction using cautery-enabled lumen-apposing metal stent. *Endoscopy Int Open* (2020) 8(11):E1633–e8. doi: 10.1055/a-1236-3217

27. Di Mitri R, Amata M, Mocciaro F, Conte E, Bonaccorso A, Scrivo B, et al. Eus-guided biliary drainage with lams for distal malignant biliary obstruction when ercp

fails: single-center retrospective study and maldeployment management. *Surg Endoscopy* (2022) 36(6):4553–69. doi: 10.1007/s00464-021-08808-0

28. El Chafic AH, Shah JN, Hamerski C, Binmoeller KF, Irani S, James TW, et al. Eus-guided choledochoduodenostomy for distal malignant biliary obstruction using electrocautery-enhanced lumen-apposing metal stents: first us, multicenter experience. *Digestive Dis Sci* (2019) 64(11):3321–7. doi: 10.1007/s10620-019-05688-2

29. Fugazza A, Fabbri C, Di Mitri R, Petrone MC, Colombo M, Cugia L, et al. Eus-guided choledochoduodenostomy for malignant distal biliary obstruction after failed ercp: A retrospective nationwide analysis. *Gastrointest Endoscopy* (2022) 95(5):896–904.e1. doi: 10.1016/j.gie.2021.12.032

30. Jacques J, Privat J, Pinard F, Fumex F, Valats JC, Chaoui A, et al. Endoscopic Ultrasound-guided choledochoduodenostomy with electrocautery-enhanced lumen-apposing stents: A retrospective analysis. *Endoscopy* (2019) 51(6):540–7. doi: 10.1055/a-0735-9137

31. Kunda R, Pérez-MIranda M, Will U, Ullrich S, Brenke D, Dollhopf M, et al. Eus-guided choledochoduodenostomy for malignant distal biliary obstruction using a lumen-apposing fully covered metal stent after failed ercp. *Surg Endoscopy* (2016) 30 (11):5002–8. doi: 10.1007/s00464-016-4845-6

32. On W, Paranandi B, Smith AM, Venkatachalapathy SV, James MW, Aithal GP, et al. Eus-guided choledochoduodenostomy with electrocautery-enhanced lumen-apposing metal stents in patients with malignant distal biliary obstruction: multicenter collaboration from the United Kingdom and Ireland. *Gastrointest Endoscopy* (2022) 95(3):432–42. doi: 10.1016/j.gie.2021.09.040

33. Tsuchiya T, Teoh AYB, Itoi T, Yamao K, Hara K, Nakai Y, et al. Long-term outcomes of eus-guided choledochoduodenostomy using a lumen-apposing metal stent for malignant distal biliary obstruction: A prospective multicenter study. *Gastrointest Endoscopy* (2018) 87(4):1138–46. doi: 10.1016/j.gie.2017.08.017

34. Binda C, Anderloni A, Fugazza A, Amato A, de Nucci G, Redaelli A, et al. Eus-guided gallbladder drainage using a lumen-apposing metal stent as rescue treatment for malignant distal biliary obstruction: A large multicenter experience. *Gastrointest Endoscopy* (2023). doi: 10.1016/j.gie.2023.06.054

35. Mangiavillano B, Moon JH, Facciorusso A, Vargas-Madrigal J, Di Matteo F, Rizzatti G, et al. Endoscopic Ultrasound-guided gallbladder drainage as a first approach for jaundice palliation in unresectable malignant distal biliary obstruction: prospective study. *Digestive Endoscopy* (2023). doi: 10.1111/den.14606

36. Wang K, Zhu J, Xing L, Wang Y, Jin Z, Li Z. Assessment of efficacy and safety of eus-guided biliary drainage: A systematic review. *Gastrointest Endoscopy* (2016) 83 (6):1218–27. doi: 10.1016/j.gie.2015.10.033

37. Krishnamoorthi R, Dasari CS, Thoguluva Chandrasekar V, Priyan H, Jayaraj M, Law J, et al. Effectiveness and safety of eus-guided choledochoduodenostomy using lumen-apposing metal stents (Lams): A systematic review and meta-analysis. *Surg Endoscopy* (2020) 34(7):2866–77. doi: 10.1007/s00464-020-07484-w

38. Bronswijk M, Vanella G, van Wanrooij RLJ, van der Merwe S. Eus-guided choledochoduodenostomy and duodenal stenosis: A marriage doomed to fail? *VideoGIE* (2022) 7(12):466–7. doi: 10.1016/j.vgie.2022.08.021

39. Vanella G, Bronswijk M, Dell'Anna G, Voermans RP, Laleman W, Petrone MC, et al. Classification, risk factors, and management of lumen apposing metal stent dysfunction during follow-up of endoscopic Ultrasound-guided choledochoduodenostomy: multicenter evaluation from the Leuven-Amsterdam-Milan study group. *Digestive Endoscopy* (2023) 35(3):377–88. doi: 10.1111/den.14445

40. Artifon EL, Aparicio D, Paione JB, Lo SK, Bordini A, Rabello C, et al. Biliary drainage in patients with unresectable, malignant obstruction where ercp fails: endoscopic ultrasonography-guided choledochoduodenostomy versus percutaneous drainage. *J Clin Gastroenterol* (2012) 46(9):768–74. doi: 10.1097/MCG.0b013e31825f264c

41. Lee TH, Choi J-H, Park DH, Song TJ, Kim DU, Paik WH, et al. Similar efficacies of endoscopic Ultrasound–guided transmural and percutaneous drainage for malignant distal biliary obstruction. *Clin Gastroenterol Hepatol* (2016) 14(7):1011–9.e3. doi: 10.1016/j.cgh.2015.12.032

42. Marx M, Caillol F, Autret A, Ratone JP, Zemmour C, Boher JM, et al. Eus-guided hepaticogastrostomy in patients with obstructive jaundice after failed or impossible endoscopic retrograde drainage: A multicenter, randomized phase ii study. *Endoscopic Ultrasound* (2022) 11(6):495–502. doi: 10.4103/eus-d-21-00108

43. Baniya R, Upadhaya S, Madala S, Subedi SC, Shaik Mohammed T, Bachuwa G. Endoscopic Ultrasound-guided biliary drainage versus percutaneous transhepatic biliary drainage after failed endoscopic retrograde cholangiopancreatography: A meta-analysis. *Clin Exp Gastroenterol* (2017) 10:67–74. doi: 10.2147/CEG.S132004

44. Sharaiha RZ, Khan MA, Kamal F, Tyberg A, Tombazzi CR, Ali B, et al. Efficacy and safety of eus-guided biliary drainage in comparison with percutaneous biliary drainage when ercp fails: A systematic review and meta-analysis. *Gastrointest Endoscopy* (2017) 85(5):904–14. doi: 10.1016/j.gie.2016.12.023

45. Moole H, Bechtold ML, Forcione D, Puli SR. A meta-analysis and systematic review: success of endoscopic Ultrasound guided biliary stenting in patients with inoperable malignant biliary strictures and a failed ercp. *Med (Baltimore)* (2017) 96(3): e5154. doi: 10.1097/md.0000000000005154

46. Schmitz D, Valiente CT, Dollhopf M, Perez-MIranda M, Küllmer A, Gornals J, et al. Percutaneous transhepatic or endoscopic Ultrasound-guided biliary drainage in malignant distal bile duct obstruction using a self-expanding metal stent: study protocol for a prospective European multicenter trial (Puma trial). *PloS One* (2022) 17(10):e0275029. doi: 10.1371/journal.pone.0275029

47. van der Merwe SW, van Wanrooij RLJ, Bronswijk M, Everett S, Lakhtakia S, Rimbas M, et al. Therapeutic endoscopic Ultrasound: european society of gastrointestinal Endoscopy (Esge) guideline. *Endoscopy* (2022) 54(2):185–205. doi: 10.1055/a-1717-1391

48. Akshintala VS, Kanthasamy K, Bhullar FA, Sperna Weiland CJ, Kamal A, Kochar B, et al. Incidence, severity and mortality of post ercp pancreatitis: an updated systematic review and meta-analysis of 145 randomized controlled trials. *Gastrointest Endoscopy* (2023) 98(1):1–6. doi: 10.1016/j.gie.2023.03.023

49. Bang JY, Navaneethan U, Hasan M, Hawes R, Varadarajulu S. Stent placement by eus or ercp for primary biliary decompression in pancreatic cancer: A randomized trial (With videos). *Gastrointest Endoscopy* (2018) 88(1):9–17. doi: 10.1016/j.gie.2018.03.012

50. Park JK, Woo YS, Noh DH, Yang JI, Bae SY, Yun HS, et al. Efficacy of eus-guided and ercp-guided biliary drainage for malignant biliary obstruction: prospective randomized controlled study. *Gastrointest Endoscopy* (2018) 88(2):277–82. doi: 10.1016/j.gie.2018.03.015

51. Paik WH, Lee TH, Park DH, Choi JH, Kim SO, Jang S, et al. Eus-guided biliary drainage versus ercp for the primary palliation of malignant biliary obstruction: A multicenter randomized clinical trial. *Am J Gastroenterol* (2018) 113(7):987–97. doi: 10.1038/s41395-018-0122-8

52. Jin Z, Wei Y, Lin H, Yang J, Jin H, Shen S, et al. Endoscopic Ultrasound-guided versus endoscopic retrograde cholangiopancreatography-guided biliary drainage for primary treatment of distal malignant biliary obstruction: A systematic review and meta-analysis. *Digestive Endoscopy* (2020) 32(1):16–26. doi: 10.1111/den.13456

53. Teoh AYB, Napoleon B, Kunda R, Arcidiacono PG, Kongkam P, Larghi A, et al. Eus-guided choledocho-duodenostomy using lumen apposing stent versus ercp with covered metallic stents in patients with unresectable malignant distal biliary obstruction: A multicenter randomized controlled trial (Dra-mbo trial). *Gastroenterology* (2023) 165(2):473–482 doi: 10.1053/j.gastro.2023.04.016

54. Vincent A, Herman J, Schulick R, Hruban RH, Goggins M. Pancreatic cancer. *Lancet (London England)* (2011) 378(9791):607–20. doi: 10.1016/s0140-6736(10) 62307-0

55. Riemann JF, Eickhoff A. Preoperative biliary drainage for pancreatic cancer. *Nat Rev Gastroenterol Hepatol* (2010) 7(6):308–9. doi: 10.1038/nrgastro.2010.65

56. Saxena P, Kumbhari V, Zein MEL, Khashab MA. Preoperative biliary drainage. *Digestive Endoscopy* (2015) 27(2):265–77. doi: 10.1111/den.12394

57. Lee PJ, Podugu A, Wu D, Lee AC, Stevens T, Windsor JA. Preoperative biliary drainage in resectable pancreatic cancer: A systematic review and network meta-analysis. *HPB: Off J Int Hepato Pancreato Biliary Assoc* (2018) 20(6):477–86. doi: 10.1016/j.hpb.2017.12.007

58. Nehme F, Lee JH. Preoperative biliary drainage for pancreatic cancer. *Digestive Endoscopy* (2022) 34(3):428–38. doi: 10.1111/den.14081

59. Lo W, Zureikat A. Neoadjuvant therapy in pancreatic cancer: A review and update on recent trials. *Curr Opin Gastroenterol* (2022) 38(5). doi: 10.1097/MOG.0000000000000874

60. Latenstein AEJ, Mackay TM, van Huijgevoort NCM, Bonsing BA, Bosscha K, Hol L, et al. Nationwide practice and outcomes of endoscopic biliary drainage in resectable pancreatic head and periampullary cancer. *HPB* (2021) 23(2):270–8. doi: 10.1016/j.hpb.2020.06.009

61. Dhindsa BS, Mashiana HS, Dhaliwal A, Mohan BP, Jayaraj M, Sayles H, et al. Eus-guided biliary drainage: A systematic review and meta-analysis. *Endoscopic Ultrasound* (2020) 9(2):101–9. doi: 10.4103/eus.eus_80_19

62. Fabbri C, Fugazza A, Binda C, Zerbi A, Jovine E, Cennamo V, et al. Beyond palliation: using eus-guided choledochoduodenostomy with a lumen-apposing metal stent as a bridge to surgery. A case series. *J Gastrointest Liver Diseases: JGLD* (2019) 28 (1):125–8. doi: 10.15403/jgld.2014.1121.281.eus

63. Janet J, Albouys J, Napoleon B, Jacques J, Mathonnet M, Magne J, et al. Pancreatoduodenectomy following preoperative biliary drainage using endoscopic Ultrasound-guided choledochoduodenostomy versus a transpapillary stent: A multicenter comparative cohort study of the achbt–french–sfed intergroup. *Ann Surg Oncol* (2023) 30(8):5036–46 doi: 10.1245/s10434-023-13466-8

64. Teoh AYB, Dhir V, Kida M, Yasuda I, Jin ZD, Seo DW, et al. Consensus guidelines on the optimal management in interventional eus procedures: results from the asian eus group rand/ucla expert panel. *Gut* (2018) 67(7):1209–28. doi: 10.1136/gutjnl-2017-314341

65. Binmoeller KF, Shah JN. Endoscopic Ultrasound-guided gastroenterostomy using novel tools designed for transluminal therapy: A porcine study. *Endoscopy* (2012) 44(5):499–503. doi: 10.1055/s-0032-1309382

66. Irani S, Itoi T, Baron TH, Khashab M. Eus-guided gastroenterostomy: techniques from east to west. *VideoGIE* (2020) 5(2):48–50. doi: 10.1016/j.vgie.2019.10.007

67. Mangiavillano B, Moon JH, Crinò SF, Larghi A, Pham KD, Teoh AYB, et al. Safety and efficacy of a novel electrocautery-enhanced lumen-apposing metal stent in interventional eus procedures (with video). *Gastrointest Endoscopy* (2022) 95(1):115–22. doi: 10.1016/j.gie.2021.07.021

68. Brimhall B, Adler DG. Enteral stents for malignant gastric outlet obstruction. *Gastrointest Endoscopy Clinics North America* (2011) 21(3):389–403. doi: 10.1016/j.giec.2011.04.002

69. Troncone E, Fugazza A, Cappello A, Del Vecchio Blanco G, Monteleone G, Repici A, et al. Malignant gastric outlet obstruction: which is the best therapeutic option? *World J Gastroenterol* (2020) 26(16):1847–60. doi: 10.3748/wjg.v26.i16.1847

70. Ly J, O'Grady G, Mittal A, Plank L, Windsor JA. A systematic review of methods to palliate malignant gastric outlet obstruction. *Surg Endoscopy* (2010) 24(2):290–7. doi: 10.1007/s00464-009-0577-1

71. Jeurnink SM, van Eijck CHJ, Steyerberg EW, Kuipers EJ, Siersema PD. Stent versus gastrojejunostomy for the palliation of gastric outlet obstruction: A systematic review. *BMC Gastroenterol* (2007) 7(1):18. doi: 10.1186/1471-230X-7-18

72. Fiori E, Lamazza A, Volpino P, Burza A, Paparelli C, Cavallaro G, et al. Palliative management of malignant antro-pyloric strictures. Gastroenterostomy vs. Endoscopic stenting. A randomized prospective trial. *Anticancer Res* (2004) 24(1):269–71.

73. Mehta S, Hindmarsh A, Cheong E, Cockburn J, Saada J, Tighe R, et al. Prospective randomized trial of laparoscopic gastrojejunostomy versus duodenal stenting for malignant gastric outflow obstruction. *Surg Endoscopy* (2006) 20(2):239–42. doi: 10.1007/s00464-005-0130-9

74. Jeurnink SM, Steyerberg EW, van Hooft JE, van Eijck CH, Schwartz MP, Vleggaar FP, et al. Surgical gastrojejunostomy or endoscopic stent placement for the palliation of malignant gastric outlet obstruction (Sustent study): A multicenter randomized trial. *Gastrointest Endoscopy* (2010) 71(3):490–9. doi: 10.1016/j.gie.2009.09.042

75. Khamar J, Lee Y, Sachdeva A, Anpalagan T, McKechnie T, Eskicioglu C, et al. Gastrojejunostomy versus endoscopic stenting for the palliation of malignant gastric outlet obstruction: A systematic review and meta-analysis. *Surg Endoscopy* (2022) 37 (6):4834–68. doi: 10.1007/s00464-022-09572-5

76. Adler DG. Should patients with malignant gastric outlet obstruction receive stents or surgery? *Clin Gastroenterol Hepatol* (2019) 17(7):1242–4. doi: 10.1016/j.cgh.2018.11.049

77. Cheung SLH, Teoh AYB. Optimal management of gastric outlet obstruction in unresectable malignancies. *Gut Liver* (2022) 16(2):190–7. doi: 10.5009/gnl210010

78. Jovani M, Ichkhanian Y, Parsa N, Singh S, Brewer Gutierrez OI, Keane MG, et al. Assessment of the learning curve for eus-guided gastroenterostomy for a single operator. *Gastrointest Endoscopy* (2021) 93(5):1088–93. doi: 10.1016/j.gie.2020.09.041

79. Iqbal U, Khara HS, Hu Y, Kumar V, Tufail K, Confer B, et al. Eus-guided gastroenterostomy for the management of gastric outlet obstruction: A systematic review and meta-analysis. *Endoscopic Ultrasound* (2020) 9(1):16–23. doi: 10.4103/eus.eus_70_19

80. McCarty TR, Garg R, Thompson CC, Rustagi T. Efficacy and safety of eus-guided gastroenterostomy for benign and malignant gastric outlet obstruction: A systematic review and meta-analysis. *Endoscopy Int Open* (2019) 07(11):E1474–E82. doi: 10.1055/a-0996-8178

81. Ghandour B, Bejjani M, Irani SS, Sharaiha RZ, Kowalski TE, Pleskow DK, et al. Classification, outcomes, and management of misdeployed stents during eus-guided gastroenterostomy. *Gastrointest Endoscopy* (2022) 95(1):80–9. doi: 10.1016/j.gie.2021.07.023

82. Chan SM, Dhir V, Chan YYY, Cheung CHN, Chow JCS, Wong IWM, et al. Endoscopic Ultrasound-guided balloon-occluded gastrojejunostomy bypass, duodenal stent or laparoscopic gastrojejunostomy for unresectable malignant gastric outlet obstruction. *Digestive Endoscopy* (2023) 35(4):512–9. doi: 10.1111/den.14472

83. Chen Y-I, Itoi T, Baron TH, Nieto J, Haito-Chavez Y, Grimm IS, et al. Eus-guided gastroenterostomy is comparable to enteral stenting with fewer re-interventions in malignant gastric outlet obstruction. *Surg Endoscopy* (2017) 31(7):2946–52. doi: 10.1007/s00464-016-5311-1

84. Ge PS, Young JY, Dong W, Thompson CC. Eus-guided gastroenterostomy versus enteral stent placement for palliation of malignant gastric outlet obstruction. *Surg Endoscopy* (2019) 33(10):3404–11. doi: 10.1007/s00464-018-06636-3

85. Jaruvongvanich V, Mahmoud T, Abu Dayyeh BK, Chandrasekhara V, Law R, Storm AC, et al. Endoscopic Ultrasound-guided gastroenterostomy for the management of gastric outlet obstruction: A large comparative study with long-term follow-up. *Endoscopy Int Open* (2023) 11(01):E60–E6. doi: 10.1055/a-1976-2279

86. Sánchez-Aldehuelo R, Subtil Iñigo JC, Martínez Moreno B, Gornals J, Guarner-Argente C, Repiso Ortega A, et al. Eus-guided gastroenterostomy versus duodenal self-expandable metal stent for malignant gastric outlet obstruction: results from a nationwide multicenter retrospective study (with video). *Gastrointest Endoscopy* (2022) 96(6):1012–20.e3. doi: 10.1016/j.gie.2022.07.018

87. van Wanrooij RLJ, Vanella G, Bronswijk M, de Gooyer P, Laleman W, van Malenstein H, et al. Endoscopic Ultrasound-guided gastroenterostomy versus duodenal stenting for malignant gastric outlet obstruction: an international, multicenter, propensity score-matched comparison. *Endoscopy* (2022) 54(11):1023–31. doi: 10.1055/a-1782-7568

88. Abbas A, Dolan RD, Bazarbashi AN, Thompson CC. Endoscopic Ultrasound-guided gastroenterostomy versus surgical gastrojejunostomy for the palliation of gastric outlet obstruction in patients with peritoneal carcinomatosis. *Endoscopy* (2022) 54 (07):671–9. doi: 10.1055/a-1708-0037

89. Bronswijk M, Vanella G, van Malenstein H, Laleman W, Jaekers J, Topal B, et al. Laparoscopic versus eus-guided gastroenterostomy for gastric outlet obstruction: an international multicenter propensity score-matched comparison (with video). *Gastrointest Endoscopy* (2021) 94(3):526–36.e2. doi: 10.1016/j.gie.2021.04.006

90. Khashab MA, Bukhari M, Baron TH, Nieto J, El Zein M, Chen Y-I, et al. International multicenter comparative trial of endoscopic ultrasonography-guided gastroenterostomy versus surgical gastrojejunostomy for the treatment of malignant gastric outlet obstruction. *Endoscopy Int Open* (2017) 05(04):E275–E81. doi: 10.1055/s-0043-101695

91. Kouanda A, Binmoeller K, Hamerski C, Nett A, Bernabe J, Watson R. Endoscopic Ultrasound-guided gastroenterostomy versus open surgical gastrojejunostomy: clinical outcomes and cost effectiveness analysis. *Surg Endoscopy* (2021) 35(12):7058–67. doi: 10.1007/s00464-020-08221-z

92. Perez-MIranda M, Tyberg A, Poletto D, Toscano E, Gaidhane M, Desai AP, et al. Eus-guided gastrojejunostomy versus laparoscopic gastrojejunostomy: an international collaborative study. *J Clin Gastroenterol* (2017) 51(10). doi: 10.1097/MCG.0000000000000887

93. Pawa R, Koutlas NJ, Russell G, Shen P, Pawa S. Endoscopic Ultrasound-guided gastrojejunostomy versus robotic gastrojejunostomy for unresectable malignant gastric outlet obstruction. *DEN Open* (2024) 4(1):e248. doi: 10.1002/deo2.248

94. Krishnamoorthi R, Bomman S, Benias P, Kozarek RA, Peetermans JA, McMullen E, et al. Efficacy and safety of endoscopic duodenal stent versus endoscopic or surgical gastrojejunostomy to treat malignant gastric outlet obstruction: systematic review and meta-analysis. *Endoscopy Int Open* (2022) 10(06): E874–E97. doi: 10.1055/a-1794-0635

95. Jue TL, Storm AC, Naveed M, Fishman DS, Qumseya BJ, McRee AJ, et al. Asge guideline on the role of Endoscopy in the management of benign and malignant gastroduodenal obstruction. *Gastrointest Endoscopy* (2021) 93(2):309–22.e4. doi: 10.1016/j.gie.2020.07.063

96. Freelove R, Walling AD. Pancreatic cancer: diagnosis and management. *Am Family physician* (2006) 73(3):485–92.

97. Moningi S, Walker AJ, Hsu CC, Reese JB, Wang JY, Fan KY, et al. Correlation of clinical stage and performance status with quality of life in patients seen in a pancreas multidisciplinary clinic. *J Oncol Pract* (2015) 11(2):e216–21. doi: 10.1200/jop.2014.000976

98. Ceyhan GO, Bergmann F, Kadihasanoglu M, Altintas B, Demir IE, Hinz U, et al. Pancreatic neuropathy and neuropathic pain–a comprehensive pathomorphological study of 546 cases. *Gastroenterology* (2009) 136(1):177–86.e1. doi: 10.1053/j.gastro.2008.09.029

99. Koulouris AI, Banim P, Hart AR. Pain in patients with pancreatic cancer: prevalence, mechanisms, management and future developments. *Digestive Dis Sci* (2017) 62(4):861–70. doi: 10.1007/s10620-017-4488-z

100. Barreto SG, Saccone GTP. Pancreatic nociception – revisiting the physiology and pathophysiology. *Pancreatology* (2012) 12(2):104–12. doi: 10.1016/j.pan.2012.02.010

101. Sharaiha RZ, Widmer J, Kahaleh M. Palliation of pancreatic ductal obstruction in pancreatic cancer. *Gastrointest Endoscopy Clinics North America* (2013) 23(4):917–23. doi: 10.1016/j.giec.2013.06.010

102. Demir IE, Schorn S, Schremmer-Danninger E, Wang K, Kehl T, Giese NA, et al. Perineural mast cells are specifically enriched in pancreatic neuritis and neuropathic pain in pancreatic cancer and chronic pancreatitis. *PloS One* (2013) 8(3):e60529. doi: 10.1371/journal.pone.0060529

103. di Mola FF, di Sebastiano P. Pain and pain generation in pancreatic cancer. *Langenbeck's Arch Surg* (2008) 393(6):919–22. doi: 10.1007/s00423-007-0277-z

104. Swarm RA, Paice JA, Anghelescu DL, Are M, Bruce JY, Buga S, et al. Adult cancer pain, version 3.2019, nccn clinical practice guidelines in oncology. *J Natl Compr Cancer Network: JNCCN* (2019) 17(8):977–1007. doi: 10.6004/jnccn.2019.0038

105. Kristensen A, Vagnildhaug O, Grønberg B, Kaasa S, Laird B, Solheim T. Does chemotherapy improve health-related quality of life in advanced pancreatic cancer? A systematic review. *Crit Rev Oncol Hematol* (2016) 99:286–98. doi: 10.1016/j.critrevonc.2016.01.006

106. Buwenge M, Arcelli A, Cellini F, Deodato F, Macchia G, Cilla S, et al. Pain relief after stereotactic radiotherapy of pancreatic adenocarcinoma: an updated systematic review. *Curr Oncol* (2022) 29(4):2616–29. doi: 10.3390/curroncol29040214

107. Yasuda I, Wang H-P. Endoscopic Ultrasound-guided celiac plexus block and neurolysis. *Digestive Endoscopy* (2017) 29(4):455–62. doi: 10.1111/den.12824

108. Wyse JM, Battat R, Sun S, Saftoiu A, Siddiqui AA, Leong AT, et al. Practice guidelines for endoscopic Ultrasound-guided celiac plexus neurolysis. *Endoscopic Ultrasound* (2017) 6(6):369–75. doi: 10.4103/eus.eus_97_17

109. Obstein KL, Martins FP, Fernández-Esparrach G, Thompson CC. Endoscopic Ultrasound-guided celiac plexus neurolysis using a reverse phase polymer. *World J Gastroenterol* (2010) 16(6):728–31. doi: 10.3748/wjg.v16.i6.728

110. Wiersema MJ, Wiersema LM. Endosonography-guided celiac plexus neurolysis. *Gastrointest Endoscopy* (1996) 44(6):656–62. doi: 10.1016/s0016-5107(96)70047-0

111. Koulouris AI, Alexandre L, Hart AR, Clark A. Endoscopic Ultrasound-guided celiac plexus neurolysis (Eus-cpn) technique and analgesic efficacy in patients with pancreatic cancer: A systematic review and meta-analysis. *Pancreatology* (2021) 21 (2):434–42. doi: 10.1016/j.pan.2020.12.016

112. Minaga K, Takenaka M, Kamata K, Yoshikawa T, Nakai A, Omoto S, et al. Alleviating pancreatic cancer-associated pain using endoscopic Ultrasound-guided neurolysis. *Cancers* (2018) 10(2):50. doi: 10.3390/cancers10020050

113. Puli SR, Reddy JBK, Bechtold ML, Antillon MR, Brugge WR. Eus-guided celiac plexus neurolysis for pain due to chronic pancreatitis or pancreatic cancer pain: A meta-analysis and systematic review. *Digestive Dis Sci* (2009) 54(11):2330–7. doi: 10.1007/s10620-008-0651-x

114. Kaufman M, Singh G, Das S, Concha-Parra R, Erber J, Micames C, et al. Efficacy of endoscopic Ultrasound-guided celiac plexus block and celiac plexus neurolysis for managing abdominal pain associated with chronic pancreatitis and pancreatic cancer. *J Clin Gastroenterol* (2010) 44(2):127–34. doi: 10.1097/MCG.0b013e3181bb854d

115. Asif AA, Walayat SK, Bechtold ML, Revanur V, Puli SR. Eus-guided celiac plexus neurolysis for pain in pancreatic cancer patients - a meta-analysis and systematic review. *J Community Hosp Intern Med Perspect* (2021) 11(4):536–42. doi: 10.1080/20009666.2021.1929049

116. Lu F, Dong J, Tang Y, Huang H, Liu H, Song L, et al. Bilateral vs. Unilateral endoscopic Ultrasound-guided celiac plexus neurolysis for abdominal pain management in patients with pancreatic malignancy: A systematic review and meta-analysis. *Support Care Cancer* (2018) 26(2):353–9. doi: 10.1007/s00520-017-3888-0

117. Alvarez-Sánchez MV, Jenssen C, Faiss S, Napoléon B. Interventional endoscopic ultrasonography: an overview of safety and complications. *Surg Endoscopy* (2014) 28(3):712–34. doi: 10.1007/s00464-013-3260-5

118. Wyse JM, Carone M, Paquin SC, Usatii M, Sahai AV. Randomized, double-blind, controlled trial of early endoscopic Ultrasound–guided celiac plexus neurolysis to prevent pain progression in patients with newly diagnosed, painful, inoperable pancreatic cancer. *J Clin Oncol* (2011) 29(26):3541–6. doi: 10.1200/JCO.2010.32.2750

119. Ducreux M, Cuhna AS, Caramella C, Hollebecque A, Burtin P, Goéré D, et al. Cancer of the pancreas: esmo clinical practice guidelines for diagnosis, treatment and follow-up. *Ann Oncol* (2015) 26:v56–68. doi: 10.1093/annonc/mdv295

120. Carrara S, Rimbas M, Larghi A, Di Leo M, Comito T, Jaoude JA, et al. Eus-guided placement of fiducial markers for image-guided radiotherapy in gastrointestinal tumors: A critical appraisal. *Endoscopic Ultrasound* (2021) 10(6):414–23. doi: 10.4103/eus-d-20-00116

121. Herman JM, Chang DT, Goodman KA, Dholakia AS, Raman SP, Hacker-Prietz A, et al. Phase 2 multi-institutional trial evaluating gemcitabine and stereotactic body radiotherapy for patients with locally advanced unresectable pancreatic adenocarcinoma. *Cancer* (2015) 121(7):1128–37. doi: 10.1002/cncr.29161

122. Packard M, Gayou O, Gurram K, Weiss B, Thakkar S, Kirichenko A. Use of implanted gold fiducial markers with mv-cbct image-guided imrt for pancreatic tumours. *J Med Imaging Radiat Oncol* (2015) 59(4):499–506. doi: 10.1111/1754-9485.12294

123. Kothary N, Heit JJ, Louie JD, Kuo WT, Loo BW Jr., Koong A, et al. Safety and efficacy of percutaneous fiducial marker implantation for image-guided radiation therapy. *J Vasc Interv Radiol* (2009) 20(2):235–9. doi: 10.1016/j.jvir.2008.09.026

124. Figueiredo M, Bouchart C, Moretti L, Mans L, Engelholm JL, Bali MA, et al. Eus-guided placement of fiducial markers for stereotactic body radiation therapy in pancreatic cancer: feasibility, security and a new quality score. *Endoscopy Int Open* (2021) 9(2):E253–e7. doi: 10.1055/a-1324-2892

125. Park WG, Yan BM, Schellenberg D, Kim J, Chang DT, Koong A, et al. Eus-guided gold fiducial insertion for image-guided radiation therapy of pancreatic cancer: 50 successful cases without fluoroscopy. *Gastrointest Endoscopy* (2010) 71(3):513–8. doi: 10.1016/j.gie.2009.10.030

126. Khashab MA, Kim KJ, Tryggestad EJ, Wild AT, Roland T, Singh VK, et al. Comparative analysis of traditional and coiled fiducials implanted during eus for pancreatic cancer patients receiving stereotactic body radiation therapy. *Gastrointest Endoscopy* (2012) 76(5):962–71. doi: 10.1016/j.gie.2012.07.006

127. Chandnani M, Faisal MF, Glissen-Brown J, Sawhney M, Pleskow D, Cohen J, et al. Eus-guided fiducial placement for pancreatobiliary Malignancies: safety, infection risk, and use of peri-procedural antibiotics. *Endoscopy Int Open* (2020) 8(2):E179–e85. doi: 10.1055/a-1068-9128

128. van der Horst A, Lens E, Wognum S, de Jong R, van Hooft JE, van Tienhoven G, et al. Limited role for biliary stent as surrogate fiducial marker in pancreatic cancer: stent and intratumoral fiducials compared. *Int J Radiat Oncol Biol Phys* (2014) 89(3):641–8. doi: 10.1016/j.ijrobp.2014.03.029

129. Matthes K, Mino-Kenudson M, Sahani DV, Holalkere N, Fowers KD, Rathi R, et al. Eus-guided injection of paclitaxel (Oncogel) provides therapeutic drug concentrations in the porcine pancreas (with video). *Gastrointest Endoscopy* (2007) 65(3):448–53. doi: 10.1016/j.gie.2006.06.030

130. Levy MJ, Alberts SR, Bamlet WR, Burch PA, Farnell MB, Gleeson FC, et al. Eus-guided fine-needle injection of gemcitabine for locally advanced and metastatic pancreatic cancer. *Gastrointest Endoscopy* (2017) 86(1):161–9. doi: 10.1016/j.gie.2016.11.014

131. Chang KJ, Nguyen PT, Thompson JA, Kurosaki TT, Casey LR, Leung EC, et al. Phase I clinical trial of allogeneic mixed lymphocyte culture (Cytoimplant) delivered by endoscopic Ultrasound–guided fine-needle injection in patients with advanced pancreatic carcinoma. *Cancer* (2000) 88(6):1325–35. doi: 10.1002/(SICI)1097-0142(20000315)88:6<1325::AID-CNCR8>3.0.CO;2-T

132. Hirooka Y, Kawashima H, Ohno E, Ishikawa T, Kamigaki T, Goto S, et al. Comprehensive immunotherapy combined with intratumoral injection of zoledronate-pulsed dendritic cells, intravenous adoptive activated T lymphocyte and gemcitabine in unresectable locally advanced pancreatic carcinoma: A phase I/ii trial. *Oncotarget* (2018) 9(2):2838–47. doi: 10.18632/oncotarget.22974

133. Zeyaullah M, Patro M, Ahmad I, Ibraheem K, Sultan P, Nehal M, et al. Oncolytic viruses in the treatment of cancer: A review of current strategies. *Pathol Oncol Res* (2012) 18(4):771–81. doi: 10.1007/s12253-012-9548-2

134. Herman JM, Wild AT, Wang H, Tran PT, Chang KJ, Taylor GE, et al. Randomized phase iii multi-institutional study of tnferade biologic with fluorouracil and radiotherapy for locally advanced pancreatic cancer: final results. *J Clin Oncol* (2013) 31(7):886–94. doi: 10.1200/jco.2012.44.7516

135. Girelli R, Frigerio I, Salvia R, Barbi E, Tinazzi Martini P, Bassi C. Feasibility and safety of radiofrequency ablation for locally advanced pancreatic cancer. *Br J Surg* (2010) 97(2):220–5. doi: 10.1002/bjs.6800

136. Crinò SF, D'Onofrio M, Bernardoni L, Frulloni L, Iannelli M, Malleo G, et al. Eus-guided radiofrequency ablation (Eus-rfa) of solid pancreatic neoplasm using an 18-gauge needle electrode: feasibility, safety, and technical success. *J gastrointest liver diseases: JGLD* (2018) 27(1):67–72. doi: 10.15403/jgld.2014.1121.271.eus

137. Song TJ, Seo DW, Lakhtakia S, Reddy N, Oh DW, Park DH, et al. Initial experience of eus-guided radiofrequency ablation of unresectable pancreatic cancer. *Gastrointest Endoscopy* (2016) 83(2):440–3. doi: 10.1016/j.gie.2015.08.048

138. Scopelliti F, Pea A, Conigliaro R, Butturini G, Frigerio I, Regi P, et al. Technique, safety, and feasibility of eus-guided radiofrequency ablation in unresectable pancreatic cancer. *Surg Endoscopy* (2018) 32(9):4022–8. doi: 10.1007/s00464-018-6217-x

139. Fahmawi Y, Mehta A, Abdalhadi H, Merritt L, Mizrahi M. Efficacy and safety of endoscopic Ultrasound-guided radiofrequency ablation for management of pancreatic lesions: A systematic review and meta-analysis. *Transl Gastroenterol Hepatol* (2022) 7:30. doi: 10.21037/tgh-20-84

140. Chan H-H, Nishioka NS, Mino M, Lauwers GY, Puricelli WP, Collier KN, et al. Eus-guided photodynamic therapy of the pancreas: A pilot study. *Gastrointest Endoscopy* (2004) 59(1):95–9. doi: 10.1016/S0016-5107(03)02361-7

141. Hanada Y, Pereira SP, Pogue B, Maytin EV, Hasan T, Linn B, et al. Eus-guided verteporfin photodynamic therapy for pancreatic cancer. *Gastrointest Endoscopy* (2021) 94(1):179–86. doi: 10.1016/j.gie.2021.02.027

142. DeWitt JM, Sandrasegaran K, O'Neil B, House MG, Zyromski NJ, Sehdev A, et al. Phase 1 study of eus-guided photodynamic therapy for locally advanced pancreatic cancer. *Gastrointest Endoscopy* (2019) 89(2):390–8. doi: 10.1016/j.gie.2018.09.007

143. Tyberg A, Mishra A, Cheung M, Kedia P, Gaidhane M, Craig C, et al. Learning curve for eus-guided biliary drainage: what have we learned? *Endoscopic Ultrasound* (2020) 9(6):392–6. doi: 10.4103/eus.eus_42_20

frontiers | Frontiers in Oncology

TYPE Original Research
PUBLISHED 15 January 2024
DOI 10.3389/fonc.2023.1336251

OPEN ACCESS

EDITED BY
Francisco Tustumi,
University of São Paulo, Brazil

REVIEWED BY
Wen-Quan Wang,
Fudan University, China
Abdullah Esmail,
Houston Methodist Hospital, United States

*CORRESPONDENCE
Yong Peng
13508081615@163.com

†These authors have contributed equally to this work and share first authorship

RECEIVED 10 November 2023
ACCEPTED 26 December 2023
PUBLISHED 15 January 2024

CITATION
Feng Y, Yang J, Duan W, Cai Y, Liu X and Peng Y (2024) LASSO-derived prognostic model predicts cancer-specific survival in advanced pancreatic ductal adenocarcinoma over 50 years of age: a retrospective study of SEER database research.
Front. Oncol. 13:1336251.
doi: 10.3389/fonc.2023.1336251

LASSO-derived prognostic model predicts cancer-specific survival in advanced pancreatic ductal adenocarcinoma over 50 years of age: a retrospective study of SEER database research

Yuan Feng†, Junjun Yang†, Wentao Duan, Yu Cai, Xiaohong Liu and Yong Peng*

Department of Hepatobiliary Pancreatic and Spleen Surgery, Nanchong Central Hospital, The Second Clinical Medical College, North Sichuan Medical College, Nanchong, China

Background: This study aimed to develop a prognostic model for patients with advanced ductal adenocarcinoma aged ≥50 years.

Methods: Patient information was extracted from the Surveillance, Epidemiology, and End Results (SEER) database. Least absolute shrinkage and selection operator (LASSO) Cox regression analysis was performed to screen the model variables. Cases from Nanchong Central Hospital were collected for external validation. The new nomogram and the American Joint Committee on Cancer (AJCC) criteria were evaluated using integrated discrimination improvement (IDI) and net reclassification index (NRI) indicators. Survival curves presented the prognosis of the new classification system and AJCC criteria.

Results: In total, 17,621 eligible patients were included. Lasso Cox regression selected 4 variables including age, chemotherapy, radiotherapy and AJCC stage. The C-index of the training cohort was 0.721. The C-index value of the validation cohort was 0.729. The AUCs for the training cohorts at 1, 2, and 3 years were 0.749, 0.729, and 0.715, respectively. The calibration curves showed that the predicted and actual probabilities at 1, 2, and 3 years matched. External validation confirmed the model's outstanding predictive power. Decision curve analysis indicated that the clinical benefit of the nomogram was higher than that of the AJCC staging system. The model evaluation indices preceded the AJCC staging with NRI (1-year: 0.88, 2-year: 0.94, 3-year: 0.72) and IDI (1-year: 0.24, 2-year: 0.23, 3-year: 0.22). The Kaplan–Meier curves implied that the new classification system was more capable of distinguishing between patients at different risks.

Conclusions: This study established a prognostic nomogram and risk classification system for advanced pancreatic cancer in patients aged ≥50 years to provide a practical tool for the clinical management of patients with pancreatic ductal adenocarcinoma.

KEYWORDS

advanced pancreatic ductal adenocarcinoma, nomogram, AJCC staging, risk stratification, cancer-specific survival

Background

Ductal adenocarcinoma of the pancreas is a fatal malignancy with the lowest five-year survival rate of all malignancies (1, 2). In the last decade, the mortality rate of pancreatic ductal adenocarcinoma has increased annually (3). The lack of obvious symptoms and lack of specific diagnostic techniques in the early stages of ductal adenocarcinoma of the pancreas has resulted in most patients not being detected until the advanced stages. Surgery is an effective treatment modality for pancreatic ductal adenocarcinoma; however, patients with advanced disease are deprived of surgical treatment (4–6). Induction therapy, chemotherapy, radiotherapy, and immunotherapy are the main modalities of treatment for advanced pancreatic ductal adenocarcinoma (7, 8).

Age is an influential factor in the incidence and mortality of pancreatic cancer. Recent studies have demonstrated that the incidence of pancreatic cancer is increasing every year worldwide. A population-based study found that only 10% of 10,298 patients included were younger than 50 years of age (9–11). Therefore, an age limit of >50 years was intended to identify our study population more accurately. AJCC staging is a common tool in the management of patients with pancreatic cancer. However, AJCC staging only considers neoplasm size and infiltration, and important factors affecting the prognosis of pancreatic ductal adenocarcinoma such as age and CA19-9, were not included (12). Ductal adenocarcinoma of the pancreas is a highly heterogeneous neoplasm, and survival prognosis varies widely among patients (13, 14). Therefore, there is a need to develop a personalized predictive tool to assist in the clinical management of patients with pancreatic ductal adenocarcinoma.

The nomogram has the advantage of being a visual tool and incorporating more clinical characteristics and are widely applied in oncology (15–17). In this study, information on advanced pancreatic ductal adenocarcinoma in patients aged ≥50 years was obtained from the SEER database. LASSO-based regression was performed to screen model variables and to develop a nomogram and risk classification system for patients with advanced pancreatic ductal adenocarcinoma aged ≥50 years.

Abbreviations: SEER, The Surveillance, Epidemiology and End Results; AJCC, The American Joint Committee on Cancer criteria; IDI, Integrated discrimination improvement; NRI, Net reclassification index; LASSO, Least absolute shrinkage and selection operator; ROC, Subject operating characteristic curve; CSS, Cancer-specific survival; C-index, Consistency index.

Methods

Patient population and study variables

Patient information was downloaded from the SEER database, which contains basic and treatment information for most oncology patients. The inclusion criteria were as follows: (a) pathological type of adenocarcinoma of the pancreatic duct, (b) detailed treatment information, (c) clear cause of death, and (d) age ≥50 years. Exclusion criteria were as follows (a) primary tumor not pancreatic, (b) incomplete treatment information, (c) unknown cause of death, (d) survival time of 0, and (e) unknown AJCC stage (Figure 1). C25.0–25.9 of the International Classification of Diseases for Oncology, 3rd Revision (ICD-O-3), was used to determine the site of pancreatic ductal adenocarcinoma. By examining the clinical data of patients recorded in the SEER database and referring to risk factors for pancreatic cancer patients in previous studies, age, sex, CA19-9, race, grade, site, number, AJCC stage, chemotherapy, and radiotherapy were selected as the appropriate variables to be investigated. The endpoint of the study is cancer-specific survival (CSS), which is the time between the diagnosis of pancreatic cancer and death due to pancreatic cancer.

Building the model

The least absolute shrinkage and selection operator (LASSO) Cox regression was applied to screen for model variables in advanced pancreatic ductal adenocarcinoma. Various methods have been employed to assess the predictive accuracy of the model, such as the C-index, receiver operating characteristic

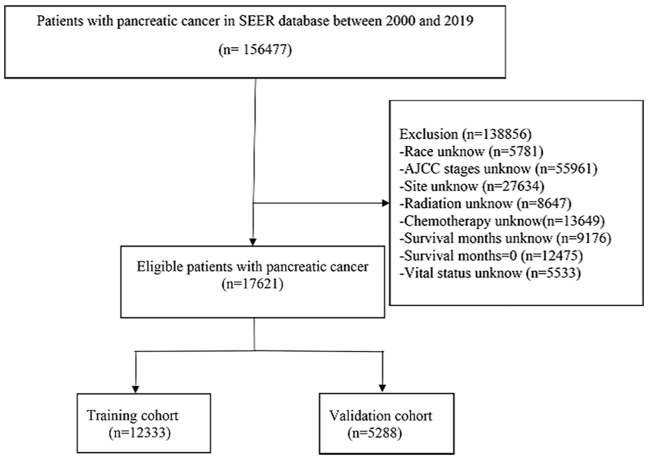

FIGURE 1
Screening process of the patients with advanced pancreatic ductal adenocarcinoma aged ≥50 years.

curves, and calibration curves. Decision curves were used to measure the clinical benefits of the nomograms.

External validation

A total of 149 patients with advanced pancreatic cancer aged ≥50 years were recruited from Nanchong Central Hospital. Written informed consent was obtained from all the patients participating in the study. The stability of the model was verified by calculating the C-index and ROC and calibration curves.

Comparison of the new model with the old model

The net reclassification index (NRI), integrated discrimination improvement (IDI), consistency index (C-index), and decision curve analysis (DCA) were used to estimate the practical applicability of the new model. The NRI and IDI indices were deployed to estimate the improved level of the new model compared with the AJCC. The C-index clearly demonstrated the high and low predictive power of the new model and AJCC staging.

The new classification system

Based on the scoring system of the nomogram, the total risk score of all patients was calculated. Based on the total score, all patients were divided into low-, middle-, and high-risk groups (X-tile software was applied to select the best cut-off value between groups).

Prognosis comparison

The AJCC staging system is the most accepted clinical tool for prognostic evaluation. Differences in the accuracy of the new risk classification system and AJCC staging in determining patient prognosis were compared by Kaplan–Meier curves.

Data analysis

Patient information was extracted using SEER*Stat software (https://seer.cancer.gov/seerstat/). All data analyses were performed using R software (version 3.6.1; http://www.r-project.org/) and related packages. The cut-off values for the risk classification were obtained with the X-tile software (version 3.6.1). A chi-square test was applied to compare the distribution of data between the training and validation groups for statistical differences. P-values were all two-sided statistical tests, and P-values less than 0.05 were considered statistically significant. This work was in line with the STROCSS criteria (18).

Results

Patient characteristics

A total of 17,621 screened and eligible cases of pancreatic ductal adenocarcinoma aged ≥50 years were included in the study. A 7:3 ratio of random allocation resulted in the training (12,333 patients) and validation cohorts (5,288 patients). Approximately 48.72% of patients were aged between 65 and 80 years. The percentage of patients who received chemotherapy was 61.20%. The median follow-up period was 4 (interquartile range [IQR]: 3–10) months in the whole population, 4 (IQR: 2–10) months in the training cohort, and 5 (IQR: 2–10) months in the validation cohort. Patient clinical data are presented in Table 1. A P-value of less than 0.05 for the chi-square test indicated no distributional differences between the training and validation cohorts.

Establishment of the nomogram

Ten variables were subjected to LASSO Cox regression, and four variables with non-zero coefficients were identified as significant

10.3389/fonc.2023.1336251

TABLE 1 Clinical information on patients aged ≥50 years with advanced pancreatic ductal adenocarcinoma.

Variable	Whole population		Training population		Validation population		P	Nanchong Central Hospital
	Number	%	Number	%	Number	%		149
	17,621		12,333		5,288			
Age								
50-65	6,262	35.54%	4,400	35.68%	1,862	35.21%	0.83	23
65-80	8,585	48.72%	5,983	48.51%	2,602	49.21%		84
≥80	2,774	15.74%	1,950	15.81%	824	15.58%		42
Race								
Black	2,072	11.76%	1,472	11.94%	600	11.35%	0.91	0
White	14,135	80.22%	9,861	79.96%	4,274	80.82%		0
Other	1,414	8.02%	1,000	8.11%	414	7.83%		149
Sex								
F	8,437	47.88%	5,919	47.99%	2,518	47.62%	0.56	64
M	9,184	52.12%	6,414	52.01%	2,770	52.38%		85
AJCC Stages								
III	3,087	17.52%	2,172	17.61%	915	17.30%	0.47	43
IV	14,534	82.48%	10,161	82.39%	4,373	82.70%		106
Site								
Head	8,045	45.66%	5,632	45.67%	2,413	45.63%		59
Body	3,542	20.10%	2,500	20.27%	1,042	19.70%	0.28	18
Tail	3,605	20.46%	2,512	20.37%	1,093	20.67%		32
Others	2,429	13.78%	1,689	13.69%	740	13.99%		40
Grade [a]								
Well	1,606	9.11%	1,136	9.21%	470	8.89%	0.15	17
Bad	1,805	10.24%	1,286	10.43%	519	9.81%		23
Unknow	14,210	80.64%	9,911	80.36%	4,299	81.30%		109
CA19-9								
Positive	5,371	30.48%	3,734	30.28%	1,637	30.96%	0.63	53
Negative	12,250	69.52%	8,599	69.72%	3,651	69.04%		96
Number							0.38	
1	14,333	81.34%	10,043	81.43%	4,290	81.13%		105
>1	3,288	18.66%	2,290	18.57%	998	18.87%		44
Radiation							0.29	
Yes	1,789	10.15%	1,285	10.42%	504	9.53%		34
No	15,832	89.85%	11,048	89.58%	4,784	90.47%		115
Chemotherapy								
Yes	10,784	61.20%	7,493	60.76%	3,291	62.24%	0.36	97
No	6,837	38.80%	4,840	39.24%	1,997	37.76%		52

[a]Well: Grades I and II; Bad: Grades III and IV.

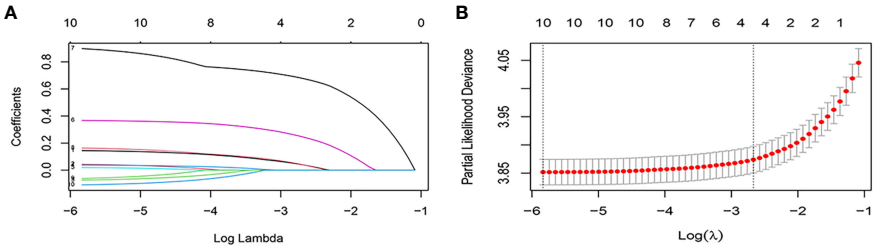

FIGURE 2
Feature selection using the LASSO Cox regression. **(A)** Profiles of lasso coefficient. **(B)** Selection of tuning parameter (lambda) in the LASSO regression using five-fold cross validation.

predictors of CSS in advanced pancreatic ductal adenocarcinoma, including age, chemotherapy, radiotherapy, and AJCC stage (Figure 2) (Table 2). Therefore, all these variables were included in the new model. To utilize the new model to forecast the probability of CSS in patients with advanced pancreatic ductal adenocarcinoma, a risk score for each variable was first derived from the patient's clinical information. Then, the sum of the scores for all variables was calculated, the location of the patient was found on the total score, and a plumb line was created through that point. The intersection of the plumb line and the three lines indicated the probability of CSS at 1, 2, and 3 years (Figure 3).

Validation model

The C-indices associated with the nomogram were 0.721 (95% CI: 0.715–0.735) and 0.729 (95% CI: 0.719–0.738) for the training and validation cohorts, respectively. The areas under the ROC curves for the training cohort at 1, 2, and 3 years were 0.749, 0.729, and 0.715, respectively. The areas under the ROC curves for the validation cohort at 1, 2, and 3 years were 0.749, 0.732, and 0.716, respectively (Figure 4). The calibration curves indicated that the predicted CSS probabilities and actual CSS probabilities for the nomogram were generally consistent (Figure 5). The results of the external validation showed that the model not only possessed outstanding predictive ability but also excellent stability (Figure 6).

Comparison of the new model and AJCC staging

In the results of the analysis, the C-index of the nomogram for both the training and validation cohorts was higher than the AJCC staging (Figure 7). The 1-, 2-, and 3-year NRIs for the training cohort were 0.88 (95% CI = 0.81–0.95), 0.94 (95% CI = 0.85–0.98), and 0.72 (0.60–0.86). Meanwhile, 0.91 (95% CI = 0.79–0.97), 0.95 (95% CI = 0.82–1.13), and 0.77 (0.51–1.02) were NRIs for the validation cohorts. The 1-, 2-, and 3-year IDIs values for the training were 0.24 (95% CI = 0.22–0.26), 0.23 (95% CI = 0.18–0.28), and 0.22 (95% CI = 0.16–0.29) (P <0.001). The IDI values were 0.24 (95% CI = 0.20–0.27), 0.46 (95% CI = 0.41–0.55), and 0.27 (95% CI = 0.20–0.34) (P <0.001) for the validation cohort (Table 3). The DCA curves implied that the clinical benefit of the nomogram was greater than that of AJCC staging in both cohorts (Figure 8).

TABLE 2 The results of non-zero coefficients.

Variable	Coefficients
Age	0.038
AJCC Stage	0.243
Chemotherapy	0.675
Radiation	0.038

Prognostic differences between the new classification system and AJCC staging

Based on the total score, patients with advanced pancreatic ductal adenocarcinoma aged ≥50 years were divided into three risk groups, low-risk (total points<50), medium-risk (50 ≤ total points <138) and high-risk (total points ≥138) (Figure 9) (Supplementary 1). The Kaplan–Meier survival curves demonstrated that the newly established classification system possesses excellent competence to differentiate patients at different risk levels compared with AJCC staging. This finding was validated in the validation cohort (Figure 10).

Discussion

Ductal adenocarcinoma of the pancreas has a five-year survival rate of less than 10% and is the second leading cause of cancer-related deaths worldwide by 2030 (1, 19–21). Ductal adenocarcinoma is the leading pathological type of pancreatic malignancy (22). Due to a lack of early screening and diagnostic techniques, 90% of patients are lost to surgery at diagnosis (4, 5, 23, 24). AJCC staging is widely adopted for treatment and survival prediction of most neoplasms. However, in addition to tumor stage, a variety of factors, such as age and chemotherapy, are also factors that significantly influence CSS. Therefore, new models are required to improve the accuracy of prognosis of patients with advanced pancreatic cancer. Various studies have shown that a nomogram incorporating more variables can guide the individual prediction of

10.3389/fonc.2023.1336251

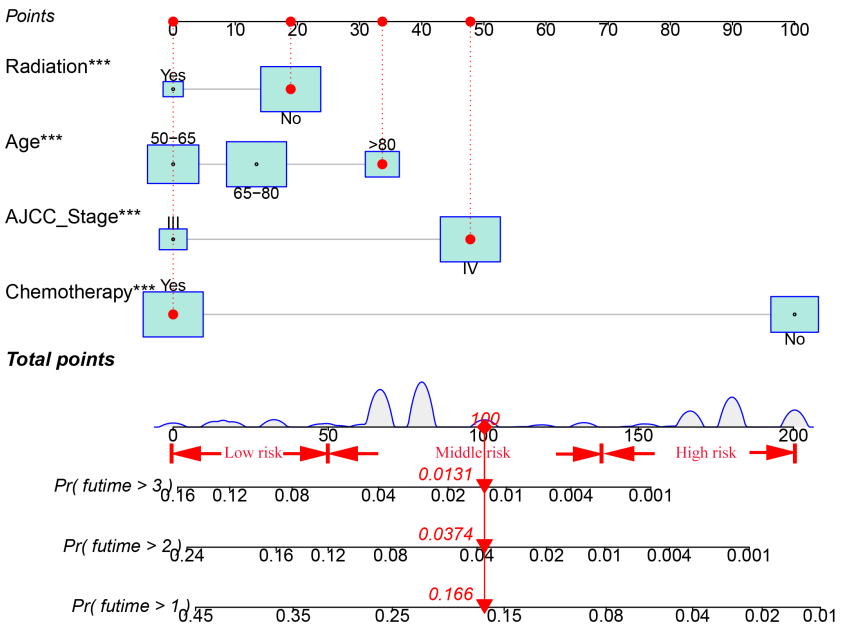

FIGURE 3
A nomogram for patients with advanced pancreatic ductal adenocarcinoma aged ≥50 years.

survival to help clinical patients (25, 26). This study applied information from the SEER database of 17,621 patients with advanced ductal adenocarcinoma aged ≥50 years to develop a new nomogram and risk stratification system to improve the accuracy of CSS prediction for patients with advanced ductal adenocarcinoma aged ≥50 years.

Although previous studies have reported prognostic models related to pancreatic cancer, they are quite different from the present study in terms of population and methodology (27, 28). A model with a large cohort would enhance its stability and credibility. However, the small number of cases in the existing studies on pancreatic cancer and the lack of scientific validation methods in some studies certainly reduce the credibility of the results (29, 30). Age has been shown to affect the incidence and prognosis of pancreatic cancer. The role of age in advanced pancreatic cancer has further increased in severity (31, 32). Therefore, studies on the prognosis of elderly patients with advanced pancreatic cancer are crucial. However, only a few studies have focused on this topic. This study selected 10 clinical data points from patients with advanced ductal adenocarcinoma aged ≥50 years from the SEER database. LASSO Cox regression analysis showed that four clinical variables, including age, AJCC stage, radiotherapy, and chemotherapy, were the preferred combination to construct a prognostic model for patients with advanced ductal adenocarcinoma aged ≥50 years. The incidence of pancreatic ductal adenocarcinoma is mostly in older patients, with the incidence of pancreatic ductal adenocarcinoma before the age of 50 years being less than 10% (33, 34). Studies have shown that the incidence of pancreatic ductal adenocarcinoma in whites increases by approximately 6% after the age of 50 years (35, 36). The increasing proportion of the global elderly population is increasing the disease burden of pancreatic ductal adenocarcinoma (24). Klein et al. (37) discovered that the incidence of pancreatic ductal adenocarcinoma will double in the next 30 years. Global aging is an irreversible trend, and early preventive measures for pancreatic ductal carcinoma are urgently required. Advanced ductal adenocarcinoma of the pancreas was lost during the surgery. Chemotherapy and radiotherapy are the mainstay of treatment for patients with advanced pancreatic ductal adenocarcinoma. However, the clinical management of advanced pancreatic ductal adenocarcinoma remains controversial. European Society for Medical Oncology (ESMO) guidelines recommend gemcitabine-based monotherapy and capecitabine-based radiotherapy as alternative options (38). The NCCN (National Comprehensive Cancer Network) recommends that patients with advanced pancreatic ductal adenocarcinoma should receive a combination of folic acid and albumin paclitaxel + gemcitabine for 4–6 months, followed by radiotherapy (39). While the benefit of radiotherapy in patients with advanced pancreatic ductal adenocarcinoma is unclear, both ESMO and NCCN highlight the necessity of radiotherapy combined with chemotherapy in the treatment process (40, 41). Primary treatment of some patients with advanced pancreatic ductal adenocarcinoma has been successful in reducing the neoplasm size and achieving the criteria for surgery-induction chemotherapy. Considering the treatment guidelines and differences in prognosis for patients with advanced pancreatic ductal adenocarcinoma, induction chemotherapy may be used as a management approach for some patients with advanced pancreatic ductal adenocarcinoma (42–44).

Age, AJCC stage, radiotherapy, and chemotherapy were included in the line plot by analyzing 10 clinical variables. The C-index were higher than 0.7 in both the training and validation cohorts, indicating the excellent application capabilities of the

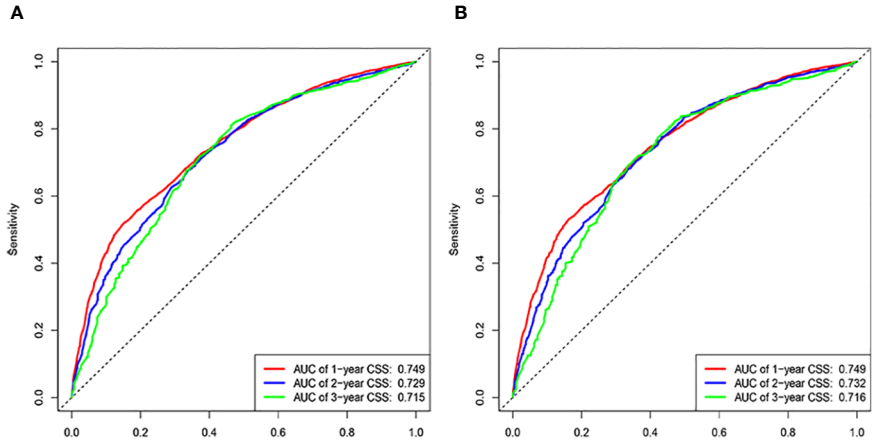

FIGURE 4
ROC curves of 1, 2, and 3 years. **(A)** Training cohorts. **(B)** Validation cohorts.

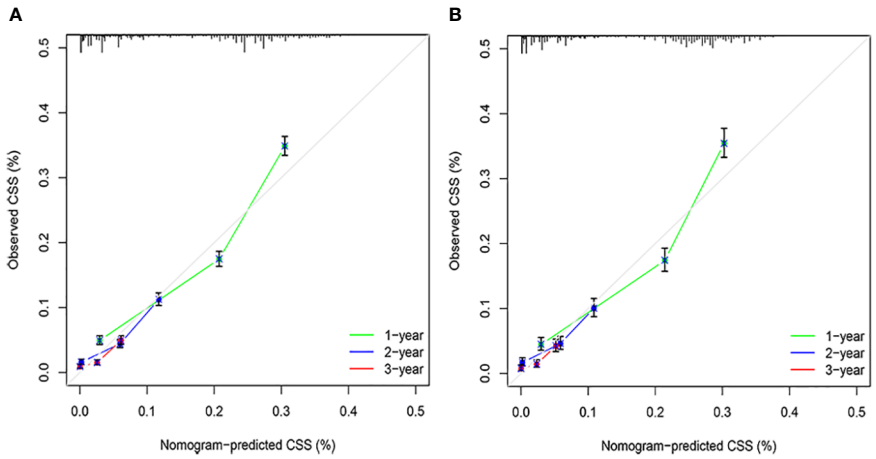

FIGURE 5
Calibration plots. **(A)** Training cohorts. **(B)** Validation cohorts.

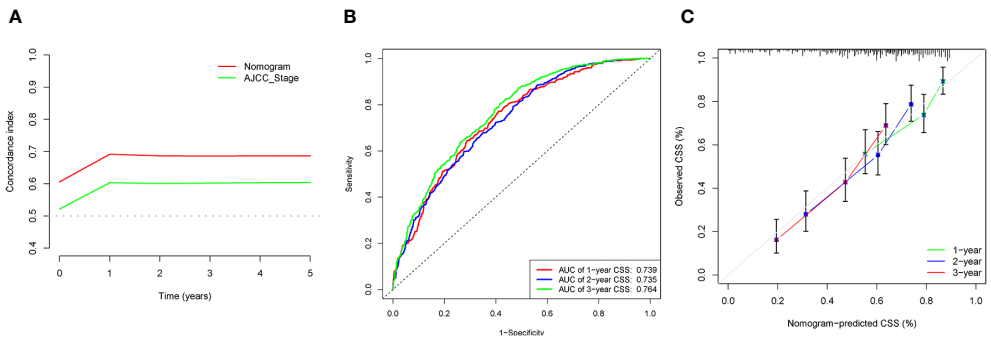

FIGURE 6
External validation of data analysis results. **(A)** C-index analysis. **(B)** Analysis of ROC curves. **(C)** Calibration curves analysis.

10.3389/fonc.2023.1336251

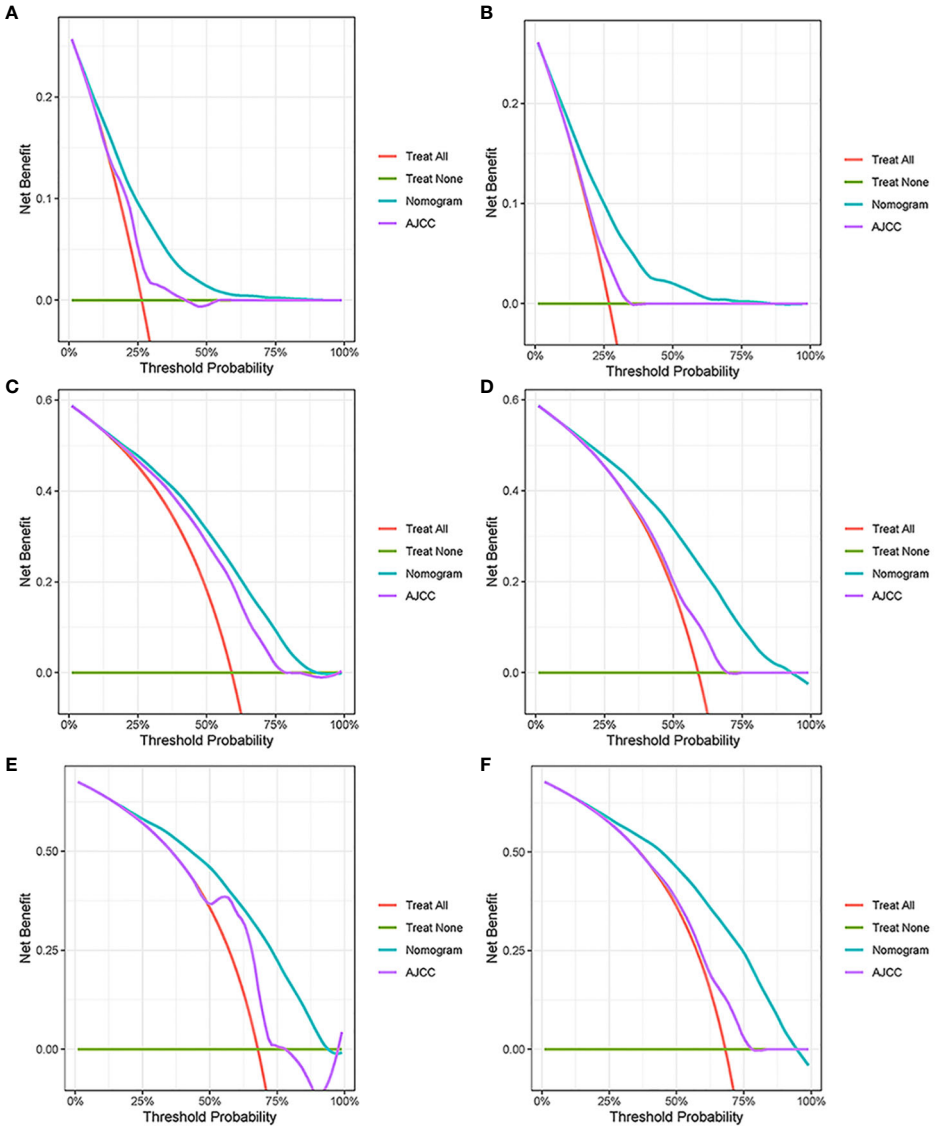

FIGURE 7
Decision curve analysis. **(A, C, E)** DCA curves in the training cohorts; **(B, D, F)** DCA curves in the validation cohorts.

TABLE 3 IDI and NRI analysis results.

Index		Training		*P* value	Validation		*P*
		Value	95%CI		Value	95%CI	
NRI	1 year	0.88	0.81–0.95	–	0.91	0.79–0.97	–
	2 years	0.94	0.85–0.98	–	0.95	0.82–1.13	–
	3 years	0.72	0.60–0.86	–	0.77	0.51–1.02	–
IDI	1 year	0.24	0.22–0.26	<0.05	0.24	0.20–0.27	<0.05
	2 years	0.23	0.18–0.28	<0.05	0.46	0.41–0.55	<0.05
	3 years	0.22	0.16–0.29	<0.05	0.27	0.20–0.34	<0.05

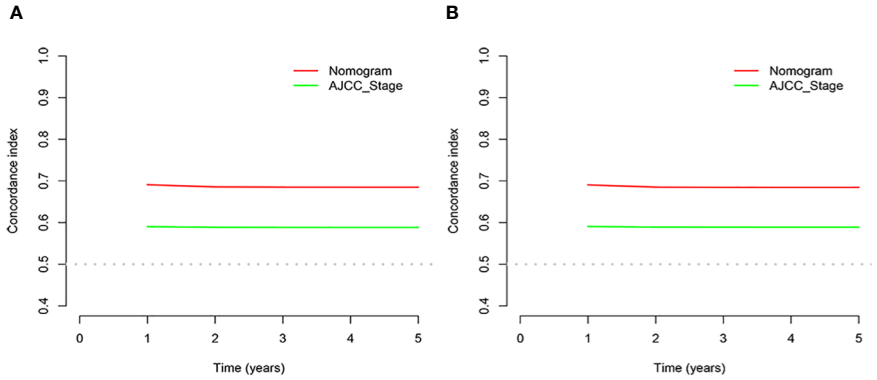

FIGURE 8
C-index plots. **(A)** Training cohorts. **(B)** Validation cohorts.

nomogram. The areas under the ROC curve were 0.749, 0.729, and 0.715 for the 1, 2, and 3 years in training cohorts, respectively. The area under the ROC curve was also greater than 0.7 in the validation cohorts, indicating that the nomogram had good predictive power. The predicted and actual CSS values largely overlapped between the two cohorts. The results of the NRIs, IDIs, and C-index associated with the nomogram showed that the nomogram had stable and excellent predictive ability compared to pure AJCC standard staging. DCA curves also showed excellent clinical benefits with the nomogram. In the nomogram, each variable value was a corresponding risk score, and the total score of the patient's risk score was calculated based on the nomogram. The X-tile software calculated the cutoff values for the risk groupings. Patients with advanced ductal adenocarcinoma aged ≥50 years were divided into a low-risk (points: 0–38), a medium-risk (points: 50–138), and a high-risk (points: 150–191) groups. KM survival curves suggested that the prognosis of patients with the new risk stratification system differed more significantly than those with AJCC staging. These results suggest that the new risk stratification system has a greater ability to identify patients with different risk factors than AJCC staging, providing a valuable instrument for the clinical treatment of patients with advanced ductal adenocarcinoma aged ≥50 years.

Although the model has strong practical applications, this study still has shortcomings. BMI and diabetes are an important factors in the prognosis of pancreatic cancer; however, there is no record of this in the SEER database. The SEER database contains

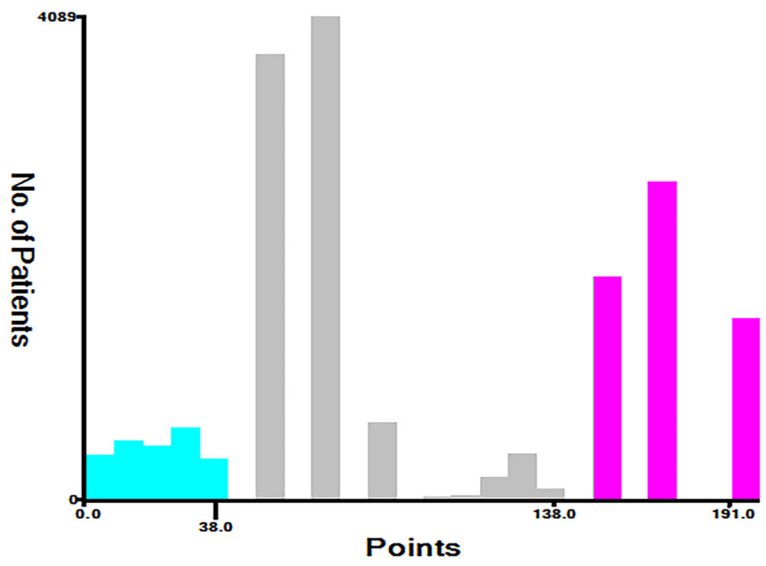

FIGURE 9
Cutoff point for risk stratifications selected using X-tile.

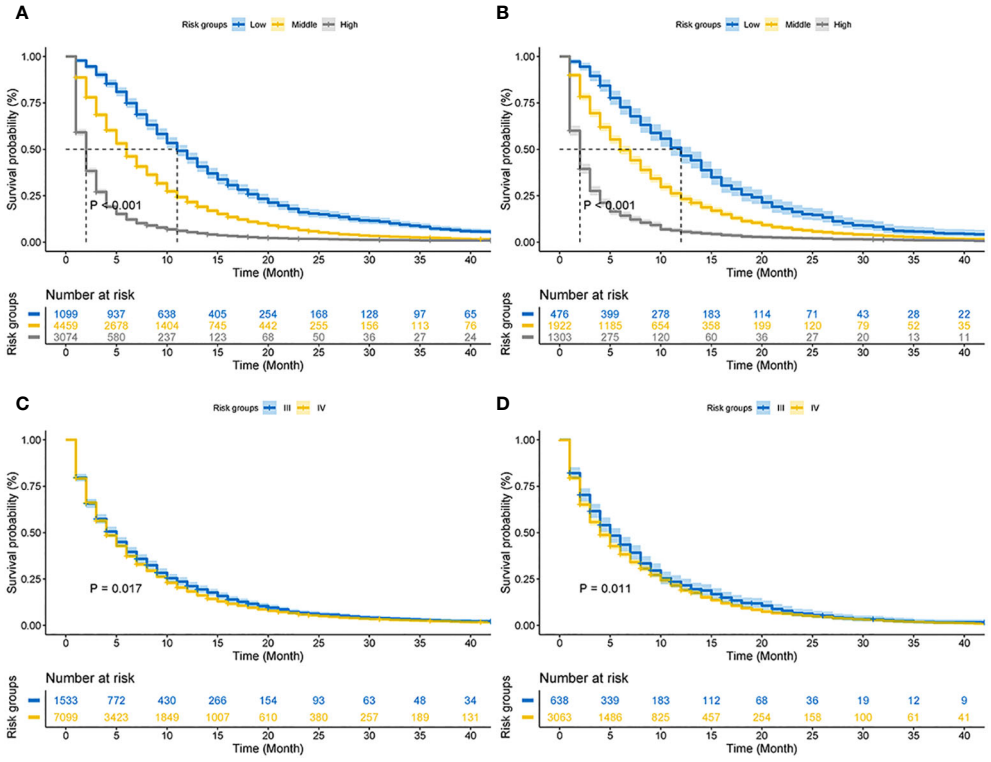

FIGURE 10
Kaplan–Meier CSS curves of advanced pancreatic ductal adenocarcinoma aged ≥50 years. **(A)** The new risk stratification system in the training cohorts. **(B)** The new risk stratification system in the validation cohorts. **(C)** AJCC staging in the training cohort. **(D)** AJCC staging in the validation cohort.

mostly patients from the Americas, and clinical data from European and Asian patients are needed to further validate the model results. Finally, the absence of patient-specific treatment options recorded in the SEER database limits the practical application of the model and risk classification system.

Conclusion

In conclusion, a prognostic nomogram for advanced pancreatic ductal adenocarcinoma aged ≥50 years was constructed using variables screened by LASSO regression. The new stratification system based on the nomogram possessed a stronger power to recognize patients with different risk groups than AJCC staging, which would give clinical decision-making an applicable tool.

Data availability statement

The original contributions presented in the study are included in the article/Supplementary Material. Further inquiries can be directed to the corresponding author.

Ethics statement

Ethical approval was not required for the study involving humans in accordance with the local legislation and institutional requirements. Written informed consent to participate in this study was not required from the participants or the participants' legal guardians/next of kin in accordance with the national legislation and the institutional requirements.

Author contributions

YP: Writing – review & editing. YF: Formal Analysis, Writing – original draft. JY: Conceptualization, Writing – original draft. WD: Data curation, Writing – original draft. YC: Formal Analysis, Writing – review & editing. XL: Data curation, Writing – review & editing.

Funding

The author(s) declare financial support was received for the research, authorship, and/or publication of this article. The study was financed by Project of Nanchong Science and Technology Bureau (22YYJCYO090).

Conflict of interest

The authors declare that the research was conducted in the absence of any commercial or financial relationships that could be construed as a potential conflict of interest.

Publisher's note

All claims expressed in this article are solely those of the authors and do not necessarily represent those of their affiliated organizations, or those of the publisher, the editors and the reviewers. Any product that may be evaluated in this article, or claim that may be made by its manufacturer, is not guaranteed or endorsed by the publisher.

Supplementary material

The Supplementary Material for this article can be found online at: https://www.frontiersin.org/articles/10.3389/fonc.2023.1336251/full#supplementary-material

References

1. Stoffel EM, Brand RE, Goggins M. Pancreatic Cancer: Changing Epidemiology and New Approaches to Risk Assessment, Early Detection, and Prevention. *Gastroenterology* (2023) 164(5):752–65. doi: 10.1016/j.jalz.2016.03.001

2. Zhao C, Gao F, Li Q, Liu Q, Lin X. The distributional characteristic and growing trend of pancreatic cancer in China. *Pancreas* (2019) 48(3):309–14. doi: 10.1097/MPA.0000000000001222

3. Ferlay J, Partensky C, Bray F. More deaths from pancreatic cancer than breast cancer in the EU by 2017. *Acta Oncol* (2016) 55(9-10):1158–60. doi: 10.1080/0284186X.2016.1197419

4. Gupta R, Amanam I, Chung V. Current and future therapies for advanced pancreatic cancer. *J Surg Oncol* (2017) 116(1):25–34. doi: 10.1002/jso.24623

5. Labori KJ, Katz MH, Tzeng CW, Bjørnbeth BA, Cvancarova M, Edwin B, et al. Impact of early disease progression and surgical complications on adjuvant chemotherapy completion rates and survival in patients undergoing the surgery first approach for resectable pancreatic ductal adenocarcinoma - A population-based cohort study. *Acta Oncol* (2016) 55(3):265–77. doi: 10.3109/0284186X.2015.1068445

6. Miksad RA, Calip GS. Early-onset pancreatic cancer research: Making sense of confounding and bias. *Cancer* (2021) 127(19):3505–7. doi: 10.1002/cncr.33663

7. Cai J, Chen H, Lu M, Zhang Y, Lu B, You L, et al. Advances in the epidemiology of pancreatic cancer: Trends, risk factors, screening, and prognosis. *Cancer Lett* (2021) 520:1–11. doi: 10.1016/j.canlet.2021.06.027

8. Heinrich S, Lang H. Neoadjuvant therapy of pancreatic cancer: definitions and benefits. *Int J Mol Sci* (2017) 18(8):1622–39. doi: 10.3390/ijms18081622

9. Higuera O, Ghanem I, Nasimi R, Prieto I, Koren L, Feliu J. Management of pancreatic cancer in the elderly. *World J gastroenterol* (2016) 22(2):764–75. doi: 10.3748/wjg.v22.i2.764

10. van Dongen JC, van der Geest LGM, de Meijer VE, van Santvoort HC, de Vos-Geelen J, Besselink MG, et al. Age and prognosis in patients with pancreatic cancer: a population-based study. *Acta Oncol (Stockholm Sweden)* (2022) 61(3):286–93. doi: 10.1080/0284186X.2021.2016949

11. Weble TC, Bjerregaard JK, Kissmeyer P, Vyberg M, Hansen CP, Holländer NH, et al. Incidence of pancreatic cancer in Denmark: 70 years of registration, 1943-2012. *Acta Oncol (Stockholm Sweden)* (2017) 56(12):1763–8. doi: 10.1080/0284186X.2017.1351036

12. Kaur S, Smith LM, Patel A, Menning M, Watley DC, Malik SS, et al. A combination of MUC5AC and CA19-9 improves the diagnosis of pancreatic cancer: A multicenter study. *Am J Gastroenterol* (2017) 112(1):172–83. doi: 10.1038/ajg.2016.482

13. Chawla A, Wo J, Castillo CF, Ferrone CR, Ryan DP, Hong TS, et al. Clinical staging in pancreatic adenocarcinoma underestimates extent of disease. *Pancreatology* (2020) 20(4):691–7. doi: 10.1016/j.pan.2020.03.011

14. Chun YS, Pawlik TM, Vauthey JN. 8th edition of the AJCC cancer staging manual: pancreas and hepatobiliary cancers. *Ann Surg Oncol* (2018) 25(4):845–7. doi: 10.1245/s10434-017-6025-x

15. Chen H, Huang C, Ge H, Chen Q, Chen J, Li Y, et al. A novel LASSO-derived prognostic model predicting survival for non-small cell lung cancer patients with M1a diseases. *Cancer Med* (2022) 11(6):1561–72. doi: 10.1002/cam4.4560

16. Gittleman H, Sloan AE, Barnholtz-Sloan JS. An independently validated survival nomogram for lower-grade glioma. *Neuro Oncol* (2020) 22(5):665–74. doi: 10.1093/neuonc/noz191

17. Iasonos A, Schrag D, Raj GV, Panageas KS. How to build and interpret a nomogram for cancer prognosis. *J Clin Oncol* (2008) 26(8):1364–70. doi: 10.1200/JCO.2007.12.9791

18. Agha R, Abdall-Razak A, Crossley E, Dowlut N, Iosifidis C, Mathew G. STROCSS 2019 Guideline: Strengthening the reporting of cohort studies in surgery. *Int J Surg* (2019) 72:156–65. doi: 10.1016/j.ijsu.2019.11.002

19. Eloranta S, Smedby KE, Dickman PW, Andersson TM. Cancer survival statistics for patients and healthcare professionals - a tutorial of real-world data analysis. *J Intern Med* (2021) 289(1):12–28. doi: 10.1111/joim.13139

20. Hu JX, Zhao CF, Chen WB, Liu QC, Li QW, Lin YY, et al. Pancreatic cancer: A review of epidemiology, trend, and risk factors. *World J Gastroenterol* (2021) 27(27):4298–321. doi: 10.3748/wjg.v27.i27.4298

21. Rahib L, Smith BD, Aizenberg R, Rosenzweig AB, Fleshman JM, Matrisian LM. Projecting cancer incidence and deaths to 2030: the unexpected burden of thyroid, liver, and pancreas cancers in the United States. *Cancer Res* (2014) 74(11):2913–21. doi: 10.1158/0008-5472.CAN-14-0155

22. Hidalgo M, Cascinu S, Kleeff J, Labianca R, Löhr JM, Neoptolemos J, et al. Addressing the challenges of pancreatic cancer: future directions for improving outcomes. *Pancreatology* (2015) 15(1):8–18. doi: 10.1016/j.pan.2014.10.001

23. Huang J, Lok V, Ngai CH, Zhang L, Yuan J, Lao XQ, et al. Worldwide Burden of, Risk Factors for, and Trends in Pancreatic Cancer. *Gastroenterology* (2021) 160(3):744–54. doi: 10.1053/j.gastro.2020.10.007

24. McGuigan A, Kelly P, Turkington RC, Jones C, Coleman HG, McCain RS. Pancreatic cancer: A review of clinical diagnosis, epidemiology, treatment and outcomes. *World J Gastroenterol* (2018) 24(43):4846–61. doi: 10.3748/wjg.v24.i43.4846

25. Balachandran VP, Gonen M, Smith JJ, DeMatteo RP. Nomograms in oncology: more than meets the eye. *Lancet Oncol* (2015) 16(4):e173–80. doi: 10.1016/S1470-2045(14)71116-7

26. Wu J, Zhang H, Li L, Hu M, Chen L, Xu B, et al. A nomogram for predicting overall survival in patients with low-grade endometrial stromal sarcoma: A population-based analysis. *Cancer Commun (Lond)* (2020) 40(7):301–12. doi: 10.1002/cac2.12067

27. Keyl J, Kasper S, Wiesweg M, Götze J, Schönrock M, Sinn M, et al. Multimodal survival prediction in advanced pancreatic cancer using machine learning. *ESMO Open* (2022) 7(5):100555. doi: 10.1016/j.esmoop.2022.100555

28. Tong Z, Liu Y, Ma H, Zhang J, Lin B, Bao X, et al. Development, validation and comparison of artificial neural network models and logistic regression models predicting survival of unresectable pancreatic cancer. *Front bioengineering Biotechnol* (2020) 8:196. doi: 10.3389/fbioe.2020.00196

29. Deng GC, Lv Y, Yan H, Sun DC, Qu TT, Pan YT, et al. Nomogram to predict survival of patients with advanced and metastatic pancreatic Cancer. *BMC cancer* (2021) 21(1):1227. doi: 10.1186/s12885-021-08943-w

30. Hamada T, Nakai Y, Yasunaga H, Isayama H, Matsui H, Takahara N, et al. Prognostic nomogram for nonresectable pancreatic cancer treated with gemcitabine-based chemotherapy. *Br J cancer* (2014) 110(8):1943–9. doi: 10.1038/bjc.2014.131

31. Fest J, Ruiter R, van Rooij FJ, van der Geest LG, Lemmens VE, Ikram MA, et al. Underestimation of pancreatic cancer in the national cancer registry - Reconsidering the incidence and survival rates. *Eur J Cancer (Oxford England: 1990)* (2017) 72:186–91. doi: 10.1016/j.ejca.2016.11.026

32. Kobayashi S, Ueno M, Ishii H, Furuse J. Management of elderly patients with unresectable pancreatic cancer. *Japanese J Clin Oncol* (2022) 52(9):959–65. doi: 10.1093/jjco/hyac101

33. Xie W, Yang T, Zuo J, Ma Z, Yu W, Hu Z, et al. Chinese and global burdens of gastrointestinal cancers from 1990 to 2019. *Front Public Health* (2022) 10:941284. doi: 10.3389/fpubh.2022.941284

34. Yang J, Xu R, Wang C, Qiu J, Ren B, You L. Early screening and diagnosis strategies of pancreatic cancer: a comprehensive review. *Cancer Commun (Lond)* (2021) 41(12):1257–74. doi: 10.1002/cac2.12204

35. Sharma A, Kandlakunta H, Nagpal SJS, Feng Z, Hoos W, Petersen GM, et al. Model to determine risk of pancreatic cancer in patients with new-onset diabetes. *Gastroenterology* (2018) 155(3):730–9.e3. doi: 10.1053/j.gastro.2018.05.023

36. Wood LD, Canto MI, Jaffee EM, Simeone DM. Pancreatic cancer: pathogenesis, screening, diagnosis, and treatment. *Gastroenterology* (2022) 163(2):386–402.e1. doi: 10.1053/j.gastro.2022.03.056

37. Klein AP. Pancreatic cancer epidemiology: understanding the role of lifestyle and inherited risk factors. *Nat Rev Gastroenterol Hepatol* (2021) 18(7):493–502. doi: 10.1038/s41575-021-00457-x

38. Ducreux M, Cuhna AS, Caramella C, Hollebecque A, Burtin P, Goéré D, et al. Cancer of the pancreas: ESMO Clinical Practice Guidelines for diagnosis, treatment and follow-up. *Ann Oncol* (2015) 26 Suppl 5:v56–68. doi: 10.1093/annonc/mdv295

39. Tempero MA, Malafa MP, Al-Hawary M, Asbun H, Bain A, Behrman SW, et al. Pancreatic adenocarcinoma, version 2.2017, NCCN clinical practice guidelines in oncology. *J Natl Compr Canc Netw* (2017) 15(8):1028–61. doi: 0.6004/jnccn.2017.0131

40. Hammel P, Huguet F, van Laethem JL, Goldstein D, Glimelius B, Artru P, et al. Effect of chemoradiotherapy vs chemotherapy on survival in patients with locally advanced pancreatic cancer controlled after 4 months of gemcitabine with or without erlotinib: the LAP07 randomized clinical trial. *Jama* (2016) 315(17):1844–53. doi: 10.1001/jama.2016.4324

41. Seufferlein T, Hammel P, Delpero JR, Macarulla T, Pfeiffer P, Prager GW, et al. Optimizing the management of locally advanced pancreatic cancer with a focus on induction chemotherapy: Expert opinion based on a review of current evidence. *Cancer Treat Rev* (2019) 77:1–10. doi: 10.1016/j.ctrv.2019.05.007

42. Balaban EP, Mangu PB, Khorana AA, Shah MA, Mukherjee S, Crane CH, et al. Locally advanced, unresectable pancreatic cancer: american society of clinical oncology clinical practice guideline. *J Clin Oncol* (2016) 34(22):2654–68. doi: 10.1200/JCO.2016.67.5561

43. Kaufmann B, Hartmann D, D'Haese JG, Stupakov P, Radenkovic D, Gloor B, et al. Neoadjuvant treatment for borderline resectable pancreatic ductal adenocarcinoma. *Dig Surg* (2019) 36(6):455–61. doi: 10.1159/000493466

44. Puleo F, Maréchal R, Demetter P, Bali MA, Calomme A, Closset J, et al. New challenges in perioperative management of pancreatic cancer. *World J Gastroenterol* (2015) 21(8):2281–93. doi: 10.3748/wjg.v21.i8.2281

frontiers | Frontiers in Oncology

TYPE Original Research
PUBLISHED 08 March 2024
DOI 10.3389/fonc.2024.1304187

OPEN ACCESS

EDITED BY
Francisco Tustumi,
University of São Paulo, Brazil

REVIEWED BY
Yong Chen,
Shanghai Jiao Tong University, China
Shuai Ren,
Affiliated Hospital of Nanjing University of Chinese Medicine, China

*CORRESPONDENCE
Seung Bae Yoon
sbyoon@catholic.ac.kr

RECEIVED 29 September 2023
ACCEPTED 16 February 2024
PUBLISHED 08 March 2024

CITATION
Choi MH, Yoon SB, Lee YJ, Jung ES, Pak S, Han D and Nickel D (2024) Rim enhancement of pancreatic ductal adenocarcinoma: investigating the relationship with DCE-MRI-based radiomics and next-generation sequencing. *Front. Oncol.* 14:1304187. doi: 10.3389/fonc.2024.1304187

Rim enhancement of pancreatic ductal adenocarcinoma: investigating the relationship with DCE-MRI-based radiomics and next-generation sequencing

Moon Hyung Choi[1], Seung Bae Yoon[2*], Young Joon Lee[1], Eun Sun Jung[3], Seongyong Pak[4], Dongyeob Han[4] and Dominik Nickel[5]

[1]Department of Radiology, Eunpyeong St. Mary's Hospital, College of Medicine, The Catholic University of Korea, Seoul, Republic of Korea, [2]Department of Internal Medicine, Eunpyeong St. Mary's Hospital, College of Medicine, The Catholic University of Korea, Seoul, Republic of Korea, [3]Department of Hospital Pathology, Eunpyeong St. Mary's Hospital, College of Medicine, The Catholic University of Korea, Seoul, Republic of Korea, [4]Research Collaboration, Siemens Healthineers Ltd., Seoul, Republic of Korea, [5]MR Applications Predevelopment, Siemens Healthcare GmbH, Erlangen, Germany

Purpose: To identify the clinical and genetic variables associated with rim enhancement of pancreatic ductal adenocarcinoma (PDAC) and to develop a dynamic contrast-enhanced (DCE) MRI-based radiomics model for predicting the genetic status from next-generation sequencing (NGS)

Materials and methods: Patients with PDAC, who underwent pretreatment pancreatic DCE-MRI between November 2019 and July 2021, were eligible in this prospective study. Two radiologists evaluated presence of rim enhancement in PDAC, a known radiological prognostic indicator, on DCE MRI. NGS was conducted for the tissue from the lesion. The Mann-Whitney U and Chi-square tests were employed to identify clinical and genetic variables associated with rim enhancement in PDAC. For continuous variables predicting rim enhancement, the cutoff value was set based on the Youden's index from the receiver operating characteristic (ROC) curve. Radiomics features were extracted from a volume-of-interest of PDAC on four DCE maps (K^{trans}, K_{ep}, V_e, and iAUC). A random forest (RF) model was constructed using 10 selected radiomics features from a pool of 392 original features. This model aimed to predict the status of significant NGS variables associated with rim enhancement. The performance of the model was validated using test set.

Results: A total of 55 patients (32 men; median age 71 years) were randomly assigned to the training (n = 41) and test (n = 14) sets. In the training set, KRAS, TP53, CDKN2A, and SMAD4 mutation rates were 92.3%, 61.8%, 14.5%, and 9.1%, respectively. Tumor size and KRAS variant allele frequency (VAF) differed between rim-enhancing (n = 12) and nonrim-enhancing (n = 29) PDACs with a cutoff of 17.22%. The RF model's average AUC from 10-fold cross-validation for predicting KRAS VAF status was 0.698. In the test set comprising 6 tumors with low KRAS VAF and 8 with high KRAS VAF, the RF model's AUC reached 1.000, achieving a sensitivity of 75.0%, specificity of 100% and accuracy of 87.5%.

Conclusion: Rim enhancement of PDAC is associated with KRAS VAF derived from NGS-based genetic information. For predicting the KRAS VAF status in PDAC, a radiomics model based on DCE maps showed promising results.

KEYWORDS

pancreatic cancer, radiomics, genetics, dynamic contrast-enhanced imaging, magnetic resonance imaging

Introduction

Pancreatic cancer is the fourth most common cancer with the lowest 5-year relative survival rate (11%) in the United States (1). MRI offers higher soft-tissue contrast, which is helpful for detecting and characterizing small lesions in the pancreas and liver (2, 3). A prior study attempted to find radiological findings that would predict clinical outcome, and rim enhancement of pancreatic ductal adenocarcinoma (PDAC) on MRI was an independent predictor of poor outcome in patients who received surgery (4). Lesions with rim enhancement showed more aggressive histologic tumor grades, fewer visible acini, and more necrosis inside the tumor than lesions without rim enhancement.

Although multiphase MRI is commonly utilized for pancreatic imaging, dynamic contrast-enhanced (DCE) MRI with short temporal resolution (< 10 seconds) has been investigated. Previous research found that DCE MRI findings differed significantly between pancreatic tumors and normal pancreas or benign disease (5–8). The tumor's characteristics are expected to be quantitatively analyzed using DCE MRI parameters which are correlated to pathological findings such as microvascular density or fibrosis (8–11). Additionally, DCE MRI parameters are different depending on the therapeutic response in PDAC patients (12, 13).

Radiomics is used to extract high-dimensional features and to quantitatively assess details on radiological images that cannot be seen visually (14, 15). In radiomics, features are selected based on predefined mathematical calculations that explain the relationships between signal intensities in pixels. A machine learning algorithm is used to choose several important features from hundreds of available ones and to construct a prediction model. Multiple studies have been performed to discover key radiomics features or to build radiomics models to predict pathologic characteristics or patient outcomes in oncology (16, 17). Radiomics in the pancreas has been used to differentiate pancreatic lesions from the normal pancreas, classify pancreatic masses, and predict therapeutic response or prognosis (18–20). Radiogenomics is a specialized application that connects radiomics to genetic data (21, 22). DCE MRI, however, has not been employed for radiomics or radiogenomics research in the pancreas. We anticipated that the quantitative analysis using radiomics in DCE MRI, which might reflect the histologic features of the tumor, could potentially have a correlation with qualitative MRI findings such as rim enhancement or genetic characteristics. If the quantitative analysis of MRI is related to genetic prognostic factors, it is expected that MRI variables could serve as potential prognostic factors. Therefore, the purpose of this study was to identify the clinical and genetic variables associated with rim enhancement of PDAC as well as to develop and test a radiomics model based on DCE MRI parametric maps for predicting the status of important genetic factors.

Materials and methods

Patients

Our hospital's institutional review board approved this prospective study, and informed consent was obtained from all participants.

Patients diagnosed with PDAC at our institution after July 2019, and had their diagnosis pathologically confirmed via biopsy or surgery, were eligible. From this group, we only included those who underwent a pre-treatment pancreas MRI that would be used for analysis. We set our target study participant count to 60 based on precedent. This decision was informed by previous DCE MRI studies on PDAC, where participant numbers ranged from 14 to 58, especially considering the unpredictability of correlating DCE MRI results with genetic information (8, 10, 11, 23–25). Exclusion criteria were as follows: (a) no pancreatic MRI prior to treatment; (b) pancreatic MRI that did not include DCE MRI; (c) pancreatic MRI at other institutions; and (d) refusal to participate in the study. Clinical data from electronic medical records were collected, including age, sex, initial carbohydrate antigen (CA) 19-9 level, and clinical staging. The patients were randomly assigned into two groups, i.e., training and test sets, in a 3:1 ratio.

MRI acquisition

A 3T MRI scanner (MAGNETOM Vida, Siemens Healthcare, Erlangen, Germany) with a 30-channel surface coil and a 32-channel or 72-channel spine coil was utilized for all MRI examinations. A power injector operating used to deliver 0.1 mmol/kg gadoterate meglumine (Dotarem, Guerbet, Paris, France) followed by a 20-mL saline flush for DCE MRI. The

temporal resolution of DCE MRI was 13.5 seconds for the first two images, 8.4 seconds for 180 seconds, and 13.5 seconds for the remaining 121 seconds. The MRI sequences and parameters are summarized in Supplementary Table E1. Pharmacokinetic maps were generated from DCE MRI after automatic motion correction and registration using a commercially available program (MR Tissue4D in Syngo.via VB40B, Siemens Healthcare): volume transfer constant (K^{trans}), reverse reflux constant (K_{ep}), extravascular extracellular volume fraction (V_e). The initial area under the curve (iAUC) was measured for the first 60 seconds. The arterial input function was chosen by having the smallest chi2 value as supplied by the program.

Image analysis

MR examinations were reviewed independently by two abdominal radiologists. They measured tumor size based on DCE MRI referring to all other sequences. They also evaluated whether the tumor had rim enhancement on DCE MRI images, as defined in a previous study: irregular ring-like enhancement with a relatively hypo-enhancing central area (4). The discordant results were solved by consensus, and the final decision was regarded as the gold standard of tumor size and rim enhancement.

Next generation sequencing (NGS)

An expert pathologist reviewed the hematoxylin-eosin-stained slides to determine the cancer area and normal pancreas tissue as well as the existence of an adequate amount of tissue for NGS. The Oncomine Comprehensive Assay Plus panel (Thermo Fisher Scientific, USA) was used for NGS, which targeted 411 genes of solid tumors. Tier I or II genetic alterations were detected using standards and guidelines for the assessment and reporting of sequence variants in cancer (26). The thresholds of variant allele frequency for hotspot variants, single nucleotide variants (SNVs), and insertions and deletions (indels) were ≥ 4%, ≥ 5% and ≥ 5%, respectively. Copy number variation ≥ 4 was considered a gain (amplification), and a variation < 0.7 was considered a loss (deletion).

Tumor segmentation

One radiologist with 10 years of experience in abdominal imaging performed 3D tumor segmentation on the pancreatic phase of DCE MRI by referring to all available MR images. Volume of interest (VOI) segmentation was performed manually on all axial images of the tumor, using open source software ITK-SNAP, version 3.8.0 (http://www.itksnap.org/) (27). If a patient had multiple cancer lesions, tumor segmentation was performed on the largest tumor. To assess intraobserver agreement, the radiologist performed tumor segmentation again for each patient more than a month after completing the first segmentation.

Radiomics feature extraction

Software for radiomics analysis (Syngo. Via Frontier, Version 1.2.2; Siemens Healthineers) was used (28). This software package was developed based on the PyRadiomics library, version 3.0.1 (https://github.com/Radiomics/pyradiomics) and scikit-learn machine learning library (https://scikit-learn.org/stable/modules/generated/sklearn.ensemble.RandomForestClassifier.html). Four DCE parametric maps were simultaneously loaded into the software with a segmentation mask. MR images were resampled using B-Spline interpolation at a spatial resolution of 1 × 1 × 1 mm3. The bin width was set as 25 to make a histogram of discretization of the image gray levels. On each DCE parametric map, 110 original features were extracted from a VOI. They included 18 first-order features, 17 shape features and 75 texture features (gray level dependence matrix [GLDM], gray level co-occurrence matrix [GLCM], gray level run length matrix [GLRLM], gray level size zone matrix [GLSZM], and neighboring gray tone difference matrix (NGTDM) features). The software generated a cluster map to show associations between the identified clusters of patients and features using the Ward variance minimization algorithm to calculate the cluster distances (Supplementary Figure E1).

Feature selection, radiomics model development and testing

Radiomics features from four DCE parametric maps were integrated. In the training set, features having an intraclass correlation coefficient (ICC) of less than 0.75 between two VOIs were removed (29). Radiomics features were reduced to a maximum of 10 features using the classic minimum redundancy maximum relevance (mRMR) method based on the R^2 difference. The algorithm selects the most relevant features for target classification while minimizing feature redundancy. Using the selected features, a random forest (RF) model for predicting the significant genetic factor was built. The model was optimized using tenfold cross-validation, and the average area under the receiver operating characteristic curve (AUC), sensitivity, specificity and accuracy were calculated. The model was optimized using tenfold cross-validation and validated with a test set.

Statistical analysis

The Kolmogorov-Smirnov test was performed to evaluate the normality of the continuous clinical variables, including age, tumor size and CA19-9 level, and variant allele frequency (VAF) of four most common mutations identified by NGS. Cohen's kappa value and ICC were used to assess interobserver agreement for rim enhancement and tumor size measurement. The Dice similarity coefficient was employed to assess spatial agreement between two sets of VOIs of PDAC. Mann-Whitney U and Chi-square tests were used to compare clinical and genetic factors between training and test sets as well as between tumors with and without rim

enhancement. The correlations among the significant factors were evaluated using the Spearman correlation coefficient. Receiver operating characteristic (ROC) curve analysis was assessed the discriminative ability of continuous variables from NGS in predicting the presence of rim enhancement. Youden's index, applied to the training set, determined the cutoff values for significant factors linked to rim enhancement.

A radiomics model was built utilizing radiomics features from DCE parametric maps to predict the status of the significant genetic factor. The sensitivity, specificity, accuracy, and AUC of the radiomics model were calculated in the test set and training set. Statistical analyses were performed using SPSS software version 23.0 (IBM, Armonk, NY, USA) and GraphPad Prism version 8.0 (GraphPad Software, Inc., La Jolla, CA, USA). P <.05 was considered statistically significant.

Results

Patients

From November 2019 to July 2021, 60 patients consented to participate in this study. Five patients were excluded due to unavailable NGS results because of insufficient amounts of tissue (Figure 1). A total of 55 patients (32 men, median age 71 years, interquartile range [IQR], 66–77]) were included. The median CA19-9 level was 470.2 U/mL (IQR, 49.3–2972.0 U/mL). Although two patients had two pancreatic cancer lesions, only the largest lesion was included in the analysis. Resectable, borderline resectable, locally advanced, and metastatic PDAC were diagnosed in 16 (29.1%), 3 (5.5%), 7 (12.7%) and 29 (52.7%) patients, respectively. Histological tumor grading was available for 29 patients: 8 had well-differentiated tumors, 18 had moderately differentiated tumors, and 3 had poorly differentiated tumors. Surgery was performed in 14 patients. In the training and test sets, 41 and 14 patients were randomly assigned. Table 1 summarizes the baseline characteristics of the patients. There were no statistically significant differences in any clinical factor between the training and test sets.

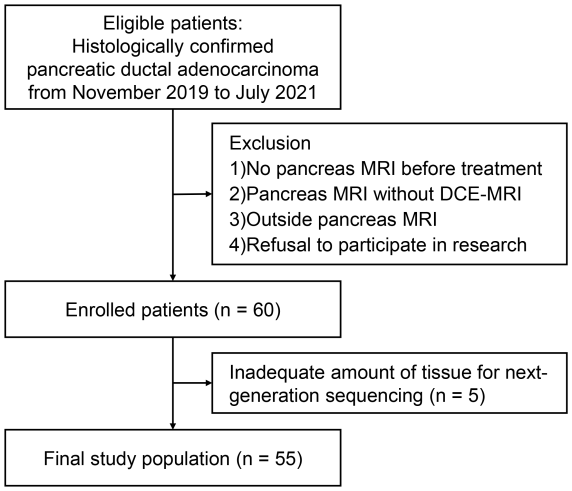

FIGURE 1
Flow diagram of study participants.

Image analysis and segmentation

The median tumor size in all patients was 3.5 cm (IQR, 2.3–5.0 cm). The ICC for the size measurement between two readers was 0.900. The two radiologists classified 19 and 17 tumors as positive rim enhancement, respectively ($\kappa = 0.670$). Following the resolution of the disagreement, 18 patients (32.7%) were categorized as having tumors with rim enhancement, including 12 patients in the training set and 6 patients in the test set. In all cases, the Dice similarity coefficient between the two sets of VOIs in all patients was 0.760.

Clinical and genetic factors between tumors according to rim enhancement

In the training set, tumors with rim enhancement were significantly larger than tumors without rim enhancement (P = 0.021) (Table 2). Other clinical factors were not different according to rim enhancement. As a result of NGS, a wide variety of genetic mutations were discovered (Supplementary Figure E2). We evaluated the four most common mutations in PDAC. KRAS, TP53, CDKN2A, and SMAD4 mutation rates were 92.3%, 61.8%, 14.5%, and 9.1%, respectively. The presence or absence of these mutations was not different according to tumor rim enhancement. The VAF of KRAS mutation was significantly higher in tumors with rim

TABLE 1 Clinical characteristics in the training and test sets.

Characteristics	Training set (n = 41)	Test set (n = 14)	P value
Age (years)	72.0 (66.0–77.5)	69.0 (66.0–77.3)	0.756
Male patient	23 (56.1%)	9 (64.3%)	0.416
Body weight (kg)	60.0 (50.0–68.5)	61.5 (52.3–68.5)	0.977
CA 19-9 (U/mL)	421.1 (60.5–3184.5)	664.2 (20.9–2797.5)	0.885
Tumor size (cm)	3.6 (2.4–5.0)	2.8 (2.3–4.2)	0.422
Tumor location			
Head	20 (48.8%)	6 (42.9%)	0.704
Body to tail	21 (51.2%0)	8 (57.1%)	
Clinical staging			
Resectable PDAC	10 (24.4%)	6 (42.9%)	0.291
Borderline resectable PDAC	2 (4.9%)	1 (7.1%)	
Locally advanced PDAC	7 (17.1%)	0 (0%)	
Metastatic PDAC	22 (53.7%)	7 (50.0%)	

Data are presented as median (interquartile range) or number (%).
CA, Carbohydrate antigen.

enhancement than in others. The VAFs of other mutations did not differ between the two groups. Spearman correlation test showed that tumor size and KRAS VAF were not correlated (ρ = 0.275, P = 0.082).

The cutoff value for positive rim enhancement

Two factors (tumor size and KRAS VAF) that exhibited significant differences between tumors with and without rim enhancement were further evaluated with ROC curves. In the training set, the cutoff values of tumor size and KRAS VAF for predicting positive rim enhancement were > 3.9 cm and > 17.22%; they had AUCs of 0.728 and 0.762, respectively. Based on the established cutoff of KRAS VAF, 10 out of the 12 rim-enhancing PDAC cases and 8 out of the 29 nonrim-enhancing PDAC cases were classified with high KRAS VAF. In the test set, the AUCs for the tumor size and KRAS VAF were 0.510 and 0.750, respectively (Supplementary Figure E3). According to the KRAS VAF cutoff, patients in the test set were divided into two groups, namely, low KRAS VAF [n = 6] and high KRAS VAF [n = 8].

Development and testing of the radiomics model

A radiomics model utilizing DCE parameters was developed to predict KRAS VAF status. After excluding 17 features with low ICC from each parametric map, 93 features were selected from each DCE map. Consequently, a total of 372 features were extracted from the four DCE maps. From the training set, the ten most important characteristics for predicting low and high KRAS VAF were chosen (Supplementary Figure E4). The average AUC of the radiomics model with 10-fold cross validation was 0.698. The model's sensitivity, specificity, and accuracy were 66.7%, 82.6% and 75.6%, respectively. In the test set, the AUC of the model was 1.000 (Figure 2). The sensitivity, specificity and accuracy of the model were 75.0%, 100% and 87.5%, respectively. The example cases are depicted in Figures 3, 4.

TABLE 2 Differences in clinical characteristics and genetic information according to rim enhancement in the training set.

Parameters	Rim enhancement (n = 12)	No rim enhancement (n = 29)	*P* value
Clinical characteristics			
Age (years)	71.0 (64.3–79.3)	72.0 (66.0–77.5)	0.767
Male patient	7 (58.3%)	16 (55.2%)	0.853
Body weight (kg)	71.0 (64.3–67.3)	60.0 (50.0–70.0)	0.372
CA 19-9 (U/mL)	1993.6 (99.9–16911.5)	261.8 (43.3–1265.9)	0.176
Tumor size (cm)	4.8 (4.2–6.0)	3.3 (2.2–4.9)	0.021
Clinical stage			
Resectable PDAC	1 (8.3%)	9 (31.0%)	0.221
Borderline resectable PDAC	1 (8.3%)	1 (3.4%)	
Locally advanced PDAC	1 (8.3%)	6 (20.7%)	
Metastatic PDAC	9 (75.0%)	13 (44.8%)	
Mutation profile			
KRAS mutant	12 (100%)	25 (86.2%)	0.235
KRAS VAF (%)	27.3 (20.8–35.7)	13.2 (6.3–25.4)	0.008
TP53 mutant	9 (75.0%)	16 (55.2%)	0.236
TP53 VAF (%)	13.0 (0–40.1)	10.5 (0–21.8)	0.488
CDKN2A mutant	2 (16.7%)	4 (13.8%)	0.813
CDKN2A VAF (%)	0 (0–0)	0 (0–0)	0.956
SMAD4 mutant	1 (8.3%)	3 (10.3%)	0.843
SMAD4 VAF (%)	0 (0–0)	0 (0–0)	0.944

Data are presented as median (interquartile range) or number (%).
PDAC, pancreatic ductal adenocarcinoma; CA, Carbohydrate antigen; VAF, variant allele frequency.

Discussion

Our study evaluated the clinical and genetic factors that are associated with rim enhancement of PDAC, which has been identified as a predictive imaging feature for postsurgical prognosis (4). Only tumor size and VAF of KRAS mutation were associated with rim enhancement; the presence of any common mutation in PDAC was not associated. We used a machine learning model based on radiomics of DCE MRI to predict low and high KRAS VAFs (cutoff 17.22%). A machine learning model incorporating DCE parametric maps (K^{trans}, K_{ep}, V_e, iAUC) produced excellent results with an AUC of 1.000 in the test set that was randomly selected from the entire patient cohort. In this study, we discovered genetic differences in PDAC based on rim enhancement and used DCE MRI radiomics to predict genetic information.

KRAS, TP53, CDKN2A, and SMAD4 are well-known driver mutations in PDAC. Recent advances in NGS technology enable accurate genetic mutation profiling of PDAC even with a small biopsy sample (30). The mutation rates of KRAS/TP53/CDKN2A/SMAD in the entire patient group in our study were consistent with previous results (31, 32). Because PDAC involves a very intricate molecular process, single major genetic alterations have seldom demonstrated therapeutic or prognostic implications in clinical settings. Beyond the presence of mutations, quantitative genetic variant analysis may be necessary to properly assess clinical genomic information in PDAC.

In the current study, KRAS VAF levels were linked to PDAC rim enhancement in MRI. VAF is defined as the percentage of sequence reads in a particular sample that have a certain deoxyribonucleic acid (DNA) variant. According to recent research, patients with higher KRAS VAF exhibited greater tumor

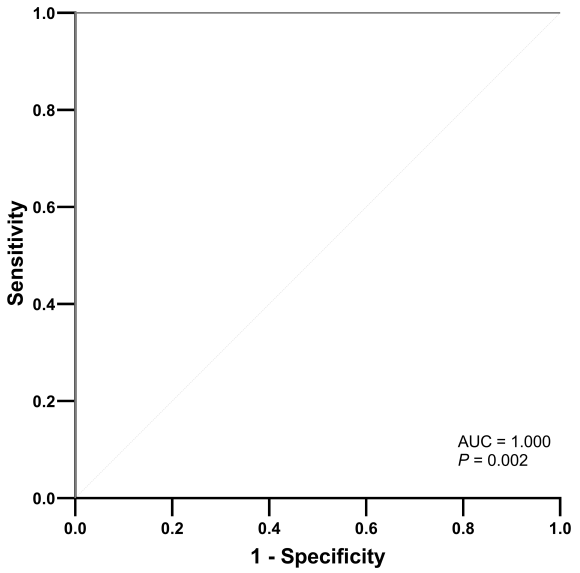

FIGURE 2
ROC curve of the radiomics model for predicting high KRAS variant allele frequency in the test set.

cellularity and worse survival outcomes (33, 34). There was no significant relationship between the positivity of KRAS mutation and survival outcome in a recent study on KRAS mutation in resected pancreatic cancer specimens. Rather, inverse relationships of KRAS VAF with survival outcomes were consistently reported across strata of tumor cellularity levels (35). The same study reported that a higher KRAS VAF was associated with a higher frequency of neural/lymphatic invasion, increased tumor cellularity, and decreased inflammatory cellularity. Mechanical evidence from animal models supports our findings, which suggest that a higher rate of KRAS mutation contributes to rapid cancer progression and metastasis (36, 37).

Rim-enhancing PDAC exhibited significantly greater intratumoral necrosis and a higher aggressive grade as well as a significantly worse survival result than nonrim-enhancing PDAC (4). MRI-based intratumoral necrosis, defined as a region with fluid signal intensity and poor contrast enhancement, was correlated with more pathological intratumoral necrosis, higher tumor cellularity and worse clinical outcome in another study (38). As a result, the enhancement pattern may represent the histological features of PDAC as well as the clinical outcome.

In our study, rim-enhancing PDAC exhibited significantly higher levels of KRAS VAF than nonrim-enhancing PDAC. While we did not investigate the direct association between patient survival and high KRAS VAF, our results indicate that the radiologically unfavorable prognostic finding is related to high KRADS VAF, which has been associated with a worse prognosis in prior research (35). However, no relationship was found between the existence of major genetic mutations and the rim enhancement of PDAC. The particular mutation in PDAC may not alter the phenotype on radiological imaging, similar to earlier clinical research in which KRAS mutation was not associated with the patient's prognosis (35).

Because the enhancement pattern is connected to NGS-based genetic information, quantitative analysis for contrast enhancement utilizing DCE MRI was applied in this study. As rim enhancement indicates varying degrees of enhancement in the peripheral and central areas of the tumor, the mean values of DCE parameters in the entire tumor may not accurately reflect tumor enhancement. Therefore, we used radiomics analysis of DCE parametric maps to predict KRAS VAF status in PDAC. In a prior study, radiomics models based on arterial and portal phase contrast-enhanced MRI were developed to predict Mucin 4 expression levels (39). However,

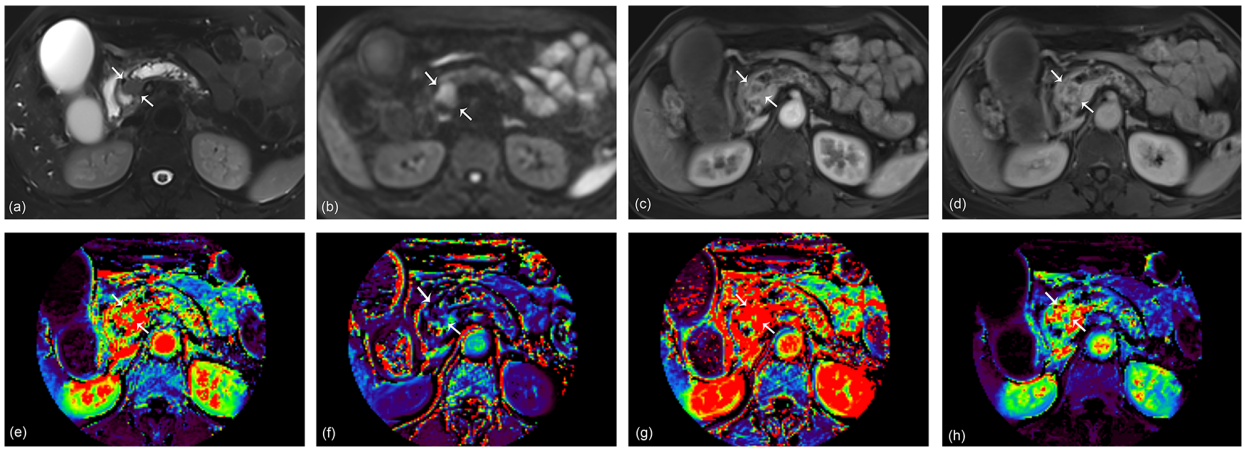

FIGURE 3
A 68-year-old woman with pancreatic ductal adenocarcinoma in the pancreas head. A 2.3 cm tumor shows high signal intensity on axial T2-weighted image **(A)** and diffusion-weighted image **(B)**. Arterial **(C)** and portal **(D)** phase images of dynamic contrast-enhanced (DCE) MRI show rim enhancement of the tumor. K^{trans} **(E)**, K_{ep} **(F)**, V_e **(G)**, and iAUC **(H)** maps are displayed at the level of the tumor. The KRAS variant allele frequency (VAF) of this lesion was 20.6%, and the patient was classified as having a high VAF level. The radiomics model based on DCE parameters predicted the lesion as a high VAF tumor with a probability of 0.59.

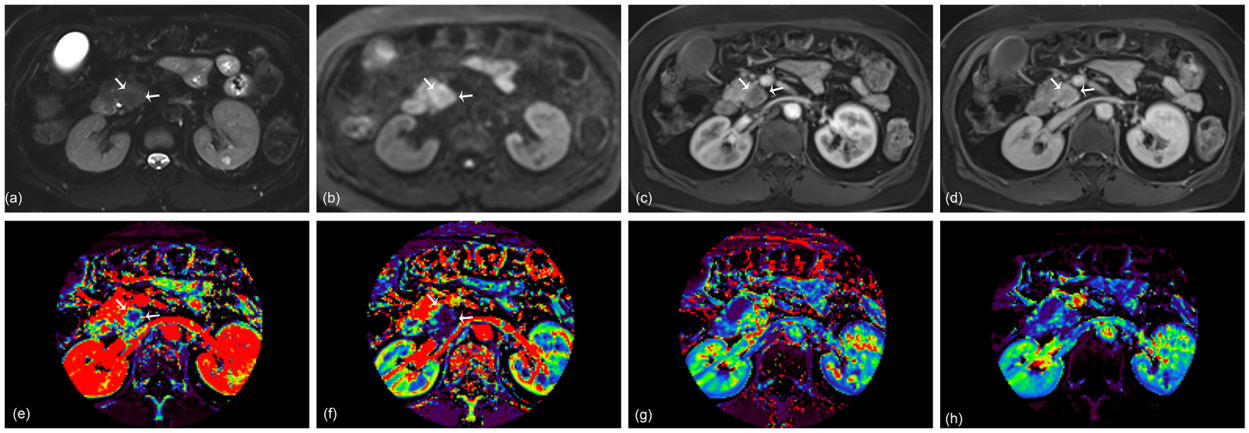

FIGURE 4
A 67-year-old woman with pancreatic ductal adenocarcinoma in the pancreas head. A 2.4 cm tumor shows high signal intensity on axial T2-weighted image **(A)** and diffusion-weighted image **(B)**. Arterial **(C)** and portal **(D)** phase images of dynamic contrast-enhanced (DCE) MRI show no rim enhancement of the tumor. K^{trans} **(E)**, K_{ep} **(F)**, V_e **(G)**, and iAUC **(H)** maps are displayed at the level of the tumor. The KRAS variant allele frequency (VAF) of this lesion was 13.5%, and the patient was classified as having a low VAF level. The probability score of the radiomics model based on DCE parameters was 0.12 and predicted the lesion as a low VAF tumor.

no radiomics study of DCE parametric maps has been performed in PDAC. To build a radiomics model, we combined three DCE parametric maps (K^{trans}, K_{ep}, and V_e maps) and an iAUC map. Furthermore, to simplify the radiomics model, we used only the original features, excluding filtered features from processes like wavelet and Laplacian of Gaussian filtering. The radiomics model with 10 features selected from four different maps showed excellent results in predicting high and low KRAS VAF tumors in the test set with an AUC of 1.000. Although radiomics features may not be directly interpreted as classical image findings, we can infer their implications. Among the 10 selected features, tumors with high KRAS VAF exhibited lower 10th percentile values on the V_e map, indicating a tendency towards decreased signal intensity of the tumor. Additionally, a higher value of size zone nonuniformity normalized (SNZZ) on the K_{ep} map suggested the presence of heterogeneous zone size volumes in high KRAS VAF tumors. These findings imply that the DCE-parameter-based radiomics model has the potential to capture genetic or radiologic characteristics of tumors.

There are several limitations to be noted regarding this study. First, the number of patients in the cohort was small. This prospective study explored genetic information and DCE MRI, which are not routinely obtained during the management of PDAC patients. Therefore, having a small number of participants was inevitable. Second, we could not perform external validation using public or outside data. It was difficult to find publicly available data on patients, including DCE MRIs of the pancreas and genetic information. Further prospective studies in other hospitals may be necessary to generalize the results of this study. Third, we could not evaluate the impact of KRAS VAF on patient survival. As some research has shown that a high KRAS VAF is associated with poor patient outcomes, it would be better to evaluate the impact of the KRAS VAF or DCE radiomics model on survival outcomes in our cohort. However, this was impossible because variable treatment methods were applied to the patients in this study. This issue should be solved with a further study involving patients who undergo homogeneous treatment. Fourth, the interobserver agreement for rim enhancement was good, albeit relatively low ($\kappa = 0.670$). In MRI research, it has been reported as 0.85, whereas in CT research it was 0.64 and 0.766 (4, 40, 41). We speculate that differences in imaging modality can cause the differences in interobserver agreement. Even though we used to consensus results to reduce the variability between radiologists, further studies with more readers with different imaging modality would be helpful to generalize the current results.

In conclusion, rim enhancement of PDAC is associated with KRAS VAF among NGS-based genetic information. For predicting the KRAS VAF status in PDAC, a radiomics model based on DCE maps showed promising results.

Data availability statement

The original contributions presented in the study are included in the article/Supplementary Material, further inquiries can be directed to the corresponding authors.

Ethics statement

The studies involving humans were approved by The institutional review board of Eunpyeong St. Mary's hospital. The studies were conducted in accordance with the local legislation and

institutional requirements. The participants provided their written informed consent to participate in this study.

Author contributions

MC: Writing – review & editing, Writing – original draft, Visualization, Investigation, Funding acquisition, Formal analysis, Data curation, Conceptualization. SY: Writing – review & editing, Writing – original draft, Supervision, Methodology, Investigation, Formal analysis, Data curation, Conceptualization. YL: Writing – review & editing, Formal analysis, Conceptualization. EJ: Writing – review & editing, Formal analysis, Data curation. SP: Writing – review & editing, Software, Resources. DH: Writing – review & editing, Software, Resources. DN: Writing – review & editing, Software, Resources.

Funding

The author(s) declare financial support was received for the research, authorship, and/or publication of this article. This work was supported by a Research Fund from Guerbet Korea Ltd. L.102. The funder was not involved in the study design, collection, analysis, interpretation of data, the writing of this article or the decision to submit it for publication.

Conflict of interest

SP, DH, and DN were employed by the company Siemens Healthineers/Healthcare. MC is currently receiving a research grant from Siemens Healthineers, but the research is not related to this topic.

The remaining authors declare that the research was conducted in the absence of any commercial or financial relationships that could be construed as a potential conflict of interest.

Publisher's note

Supplementary material

The Supplementary Material for this article can be found online at: https://www.frontiersin.org/articles/10.3389/fonc.2024.1304187/full#supplementary-material

References

1. Siegel RL, Miller KD, Fuchs HE, Jemal A. Cancer statistics, 2022. *CA Cancer J Clin*. (2022) 72:7–33. doi: 10.3322/caac.21708

2. Jeon SK, Lee JM, Joo I, Lee DH, Ahn SJ, Woo H, et al. Magnetic resonance with diffusion-weighted imaging improves assessment of focal liver lesions in patients with potentially resectable pancreatic cancer on CT. *Eur Radiol*. (2018) 28:3484–93. doi: 10.1007/s00330-017-5258-1

3. Choi SY, Kim YK, Min JH, Cha DI, Jeong WK, Lee WJ. The value of gadoxetic acid-enhanced MRI for differentiation between hepatic microabscesses and metastases in patients with periampullary cancer. *Eur Radiol*. (2017) 27:4383–93. doi: 10.1007/s00330-017-4782-3

4. Lee S, Kim SH, Park HK, Jang KT, Hwang JA, Kim S. Pancreatic Ductal Adenocarcinoma: Rim Enhancement at MR Imaging Predicts Prognosis after Curative Resection. *Radiology*. (2018) 288:456–66. doi: 10.1148/radiol.2018172331

5. Zhang TT, Wang L, Liu HH, Zhang CY, Li XM, Lu JP, et al. Differentiation of pancreatic carcinoma and mass-forming focal pancreatitis: qualitative and quantitative assessment by dynamic contrast-enhanced MRI combined with diffusion-weighted imaging. *Oncotarget*. (2017) 8:1744–59. doi: 10.18632/oncotarget.12120

6. Kim JH, Lee JM, Park JH, Kim SC, Joo I, Han JK, et al. Solid pancreatic lesions: characterization by using timing bolus dynamic contrast-enhanced MR imaging assessment–a preliminary study. *Radiology*. (2013) 266:185–96. doi: 10.1148/radiol.12120111

7. Donati F, Boraschi P, Cervelli R, Pacciardi F, Lombardo C, Boggi U, et al. 3 T MR perfusion of solid pancreatic lesions using dynamic contrast-enhanced DISCO sequence: Usefulness of qualitative and quantitative analyses in a pilot study. *Magn Reson Imaging*. (2019) 59:105–13. doi: 10.1016/j.mri.2019.03.001

8. Bali MA, Metens T, Denolin V, Delhaye M, Demetter P, Closset J, et al. Tumoral and nontumoral pancreas: correlation between quantitative dynamic contrast-enhanced MR imaging and histopathologic parameters. *Radiology*. (2011) 261:456–66. doi: 10.1148/radiol.11103515

9. Wu L, Lv P, Zhang H, Fu C, Yao X, Wang C, et al. Dynamic contrast-enhanced (DCE) MRI assessment of microvascular characteristics in the murine orthotopic pancreatic cancer model. *Magn Reson Imaging*. (2015) 33:737–60. doi: 10.1016/j.mri.2014.08.014

10. Ma W, Li N, Zhao W, Ren J, Wei M, Yang Y, et al. Apparent diffusion coefficient and dynamic contrast-enhanced magnetic resonance imaging in pancreatic cancer: characteristics and correlation with histopathologic parameters. *J Comput Assist Tomogr*. (2016) 40:709–16. doi: 10.1097/RCT.0000000000000434

11. Klaassen R, Steins A, Gurney-Champion OJ, Bijlsma MF, van Tienhoven G, Engelbrecht MRW, et al. Pathological validation and prognostic potential of quantitative MRI in the characterization of pancreas cancer: preliminary experience. *Mol Oncol*. (2020) 14:2176–89. doi: 10.1002/1878-0261.12688

12. Tang W, Liu W, Li HM, Wang QF, Fu CX, Wang XH, et al. Quantitative dynamic contrast-enhanced MR imaging for the preliminary prediction of the response to gemcitabine-based chemotherapy in advanced pancreatic ductal carcinoma. *Eur J Radiol*. (2019) 121:108734. doi: 10.1016/j.ejrad.2019.108734

13. Akisik MF, Sandrasegaran K, Bu G, Lin C, Hutchins GD, Chiorean EG. Pancreatic cancer: utility of dynamic contrast-enhanced MR imaging in assessment of antiangiogenic therapy. *Radiology*. (2010) 256:441–9. doi: 10.1148/radiol.10091733

14. Gillies RJ, Kinahan PE, Hricak H. Radiomics: images are more than pictures, they are data. *Radiology*. (2016) 278:563–77. doi: 10.1148/radiol.2015151169

15. Rogers W, Thulasi Seetha S, Refaee TAG, Lieverse RIY, Granzier RWY, Ibrahim A, et al. Radiomics: from qualitative to quantitative imaging. *Br J Radiol*. (2020) 93:20190948. doi: 10.1259/bjr.20190948

16. Lambin P, Leijenaar RTH, Deist TM, Peerlings J, de Jong EEC, van Timmeren J, et al. Radiomics: the bridge between medical imaging and personalized medicine. *Nat Rev Clin Oncol*. (2017) 14:749–62. doi: 10.1038/nrclinonc.2017.141

17. Boon IS, Yap MH, Au Yong TPT, Boon CS. Radiomics: quantitative radiology transforming oncology care. *Br J Radiol*. (2020) 93:20200333. doi: 10.1259/bjr.20200333

18. Abunahel BM, Pontre B, Kumar H, Petrov MS. Pancreas image mining: a systematic review of radiomics. *Eur Radiol*. (2021) 31:3447–67. doi: 10.1007/s00330-020-07376-6

19. Virarkar M, Wong VK, Morani AC, Tamm EP, Bhosale P. Update on quantitative radiomics of pancreatic tumors. *Abdom Radiol (NY)*. (2022) 47:3118–60. doi: 10.1007/s00261-021-03216-3

20. Bartoli M, Barat M, Dohan A, Gaujoux S, Coriat R, Hoeffel C, et al. CT and MRI of pancreatic tumors: an update in the era of radiomics. *Jpn J Radiol*. (2020) 38:1111–24. doi: 10.1007/s11604-020-01057-6

21. Bodalal Z, Trebeschi S, Nguyen-Kim TDL, Schats W, Beets-Tan R. Radiogenomics: bridging imaging and genomics. *Abdom Radiol (NY)*. (2019) 44:1960–84. doi: 10.1007/s00261-019-02028-w

22. Kuo MD, Jamshidi N. Behind the numbers: Decoding molecular phenotypes with radiogenomics–guiding principles and technical considerations. *Radiology*. (2014) 270:320–5. doi: 10.1148/radiol.13132195

23. Yao X, Zeng M, Wang H, Sun F, Rao S, Ji Y. Evaluation of pancreatic cancer by multiple breath-hold dynamic contrast-enhanced magnetic resonance imaging at 3.0T. *Eur J Radiol*. (2012) 81:e917–922. doi: 10.1016/j.ejrad.2012.05.011

24. Kim H, Arnoletti PJ, Christein J, Heslin MJ, Posey JA 3rd, Pednekar A, et al. Pancreatic adenocarcinoma: a pilot study of quantitative perfusion and diffusion-weighted breath-hold magnetic resonance imaging. *Abdom Imaging*. (2014) 39:744–52. doi: 10.1007/s00261-014-0107-z

25. Fukukura Y, Kumagae Y, Fujisaki Y, Nakamura S, Dominik Nickel M, Imai H, et al. Extracellular volume fraction with MRI: As an alternative predictive biomarker to dynamic contrast-enhanced MRI for chemotherapy response of pancreatic ductal adenocarcinoma. *Eur J Radiol*. (2021) 145:110036. doi: 10.1016/j.ejrad.2021.110036

26. Li MM, Datto M, Duncavage EJ, Kulkarni S, Lindeman NI, Roy S, et al. Standards and guidelines for the interpretation and reporting of sequence variants in cancer: A joint consensus recommendation of the association for molecular pathology, American society of clinical oncology, and college of American pathologists. *J Mol Diagn*. (2017) 19:4–23. doi: 10.1016/j.jmoldx.2016.10.002

27. Yushkevich PA, Piven J, Hazlett HC, Smith RG, Ho S, Gee JC, et al. User-guided 3D active contour segmentation of anatomical structures: significantly improved efficiency and reliability. *Neuroimage*. (2006) 31:1116–28. doi: 10.1016/j.neuroimage.2006.01.015

28. Wels M, Lades F, Muehlberg A, Suehling M. General purpose radiomics for multi-modal clinical research. Proceedings of SPIE: medical Imaging 2019 - computer-aided diagnosis. Vol 10950. Bellingham, Wash: International Society for Optics and Photonics (2019) 095046. doi: 10.1117/12.2511856

29. Park JE, Park SY, Kim HJ, Kim HS. Reproducibility and generalizability in radiomics modeling: possible strategies in radiologic and statistical perspectives. *Korean J Radiol*. (2019) 20:1124–37. doi: 10.3348/kjr.2018.0070

30. Nikas IP, Mountzios G, Sydney GI, Ioakim KJ, Won JK, Papageorgis P. Evaluating pancreatic and biliary neoplasms with small biopsy-based next generation sequencing (NGS): doing more with less. *Cancers (Basel)*. (2022) 14:397. doi: 10.3390/cancers14020397

31. Hu HF, Ye Z, Qin Y, Xu XW, Yu XJ, Zhuo QF, et al. Mutations in key driver genes of pancreatic cancer: molecularly targeted therapies and other clinical implications. *Acta Pharmacol Sin*. (2021) 42:1725–41. doi: 10.1038/s41401-020-00584-2

32. McIntyre CA, Lawrence SA, Richards AL, Chou JF, Wong W, Capanu M, et al. Alterations in driver genes are predictive of survival in patients with resected pancreatic ductal adenocarcinoma. *Cancer*. (2020) 126:3939–49. doi: 10.1002/cncr.33038

33. Heid I, Steiger K, Trajkovic-Arsic M, Settles M, Esswein MR, Erkan M, et al. Co-clinical assessment of tumor cellularity in pancreatic cancer. *Clin Cancer Res*. (2017) 23:1461–70. doi: 10.1158/1078-0432.CCR-15-2432

34. Nauheim D, Moskal D, Renslo B, Chadwick M, Jiang W, Yeo CJ, et al. KRAS mutation allele frequency threshold alters prognosis in right-sided resected pancreatic cancer. *J Surg Oncol*. (2022) 126:314–21. doi: 10.1002/jso.26860

35. Suzuki T, Masugi Y, Inoue Y, Hamada T, Tanaka M, Takamatsu M, et al. KRAS variant allele frequency, but not mutation positivity, associates with survival of patients with pancreatic cancer. *Cancer Sci*. (2022) 113:3097–109. doi: 10.1111/cas.15398

36. Mueller S, Engleitner T, Maresch R, Zukowska M, Lange S, Kaltenbacher T, et al. Evolutionary routes and KRAS dosage define pancreatic cancer phenotypes. *Nature*. (2018) 554:62–8. doi: 10.1038/nature25459

37. Chan-Seng-Yue M, Kim JC, Wilson GW, Ng K, Figueroa EF, O'Kane GM, et al. Transcription phenotypes of pancreatic cancer are driven by genomic events during tumor evolution. *Nat Genet*. (2020) 52:231–40. doi: 10.1038/s41588-019-0566-9

38. Kim H, Kim DH, Song IH, Kim B, Oh SN, Choi JI, et al. Survival prediction after curative resection of pancreatic ductal adenocarcinoma by imaging-based intratumoral necrosis. *Cancers (Basel)*. (2022) 14:5671. doi: 10.3390/cancers14225671

39. Deng Y, Li Y, Wu JL, Zhou T, Tang MY, Chen Y, et al. Radiomics models based on multi-sequence MRI for preoperative evaluation of MUC4 status in pancreatic ductal adenocarcinoma: a preliminary study. *Quant Imaging Med Surg*. (2022) 12:5129–39. doi: 10.21037/qims-22-112

40. Bai X, Wu L, Dai J, Wang K, Shi H, Lu Z, et al. Rim enhancement and peripancreatic fat stranding in preoperative MDCT as predictors for occult metastasis in PDAC patients. *Acad Radiol*. (2023) 30:2954–61. doi: 10.1016/j.acra.2023.03.007

41. Takaji R, Yamada Y, Matsumoto S, Kiyonaga M, Hongo N, Mori H, et al. Small pancreatic ductal carcinomas on triple-phase contrast-enhanced computed tomography: enhanced rims and the pathologic correlation. *Abdom Radiol (NY)*. (2018) 43:3374–80. doi: 10.1007/s00261-018-1645-6

frontiers | Frontiers in Oncology

TYPE Systematic Review
PUBLISHED 08 April 2024
DOI 10.3389/fonc.2024.1197424

OPEN ACCESS

EDITED BY
Samir Pathak,
Bristol Royal Infirmary, United Kingdom

REVIEWED BY
Satvinder Singh Mudan,
The London Clinic, United Kingdom
Rafael Davalos,
Virginia Tech, United States

*CORRESPONDENCE
Dedong Yu
985379736@qq.com
Wei Zhu
ekinbao@126.com

RECEIVED 31 March 2023
ACCEPTED 11 March 2024
PUBLISHED 08 April 2024

CITATION
Cao Y, Yu D, Wu Y and Zhu W (2024) Regional intra-arterial vs. systemic chemotherapy for the treatment of advanced pancreatic cancer: a systematic review and meta-analysis. *Front. Oncol.* 14:1197424. doi: 10.3389/fonc.2024.1197424

Regional intra-arterial vs. systemic chemotherapy for the treatment of advanced pancreatic cancer: a systematic review and meta-analysis

Yanjie Cao, Dedong Yu*, Yun Wu and Wei Zhu*

Department of Oncology, Baotou Central Hospital, Baotou, China

Introduction: Pancreatic cancer is a highly aggressive malignancy with limited response to chemotherapy. This research aims to compare the effectiveness and safety of regional intra-arterial chemotherapy (RIAC) with conventional systemic chemotherapy in treating advanced stages of pancreatic cancer.

Methods: A comprehensive literature review was conducted using databases such as PubMed, Embase, Web of Science, and the Cochrane Library. Studies assessing the comparative outcomes of RIAC and systemic chemotherapy were included. Data extraction and quality evaluation were performed independently by two researchers. Statistical analysis was conducted using STATA16 software, calculating odds ratios (OR), risk differences (RD), and 95% confidence intervals (CI).

Results: Eleven studies, comprising a total of 627 patients, were included in the meta-analysis. The findings showed that patients undergoing RIAC had significantly higher rates of partial remission (PR) compared to those receiving systemic chemotherapy (OR = 2.23, 95% CI: 1.57, 3.15, I2= 0%). Additionally, the rate of complications was lower in the RIAC group (OR = 0.45, 95% CI: 0.33, 0.63, I2= 0%). Moreover, patients treated with RIAC had notably longer median survival times.

Discussion: The results of this research indicate that RIAC is associated with a higher rate of partial remission, improved clinical benefits, and fewer complications compared to systemic chemotherapy in the management of advanced pancreatic cancer. These findings suggest that RIAC may be a more effective and safer treatment option for patients with advanced stages of pancreatic cancer.

Systematic review registration: https://www.crd.york.ac.uk/prospero/, identifier CRD42023404637.

KEYWORDS

systemic chemotherapy, pancreatic cancer, partial remission, meta-analysis, regional intra-arterial chemotherapy

Introduction

Pancreatic cancer is a malignant digestive tract tumor with an extremely high degree of malignancy and rapid progression. Pancreatic cancer patients usually have poor prognosis (1), and the 5-year overall survival rate is approximately 10% in the USA (2). Also, in recent years, the incidence rate of pancreatic cancer has been on the rise (3). Radical surgery remains the most effective approach, and the 5-year survival rate after surgery is about 20% (4, 5). However, considering that 85-90% of patients present with advanced tumors at the time of diagnosis, other treatment methods must be selected. Adjuvant chemotherapy has been recommended for patients with advanced pancreatic cancer. For example, gemcitabine (GEM), which is given systemically, is effective as postoperative adjuvant chemotherapy in patients with stage IV pancreatic cancer, with a response rate of only 5-15% (6). GEM does not significantly improve survival when combined with other anti-cancer drugs (7, 8). Still, some studies have shown that certain patients do not respond well to conventional systemic intravenous chemotherapy (9). On the other hand, conventional radiotherapy and chemotherapy for pancreatic cancer have limited effects, with an average survival time of 6 months (10).

In recent years, RAIC has been clinically used as a new chemotherapy regimen for advanced pancreatic cancer (9, 11). Pancreatic cancer is a retroperitoneal tumor lacking blood supply. RAIC delivers antineoplastic drugs to the tumor site through the ductus arteriosus, producing locally high drug concentrations while maintaining low systemic drug levels. Compared with conventional systemic intravenous chemotherapy, RAIC can improve the effect of the drug and reduce the appearance of adverse events in patients with colorectal cancer and liver metastases (12). Fang et al. (13) reported a clinical benefit of RIAC of 78.06% for patients with advanced pancreatic cancer, compared to 29.37% for those who received systemic chemotherapy. Also, the one-year survival rate for RIAC (28.6%) was higher than for systemic chemotherapy (0%) (13). Thus, it is believed that RIAC can improve the clinical benefit and survival rates in patients with advanced pancreatic cancer (14–16).

To the best of our knowledge, an increasing number of investigations have explored the efficacy of RIAC in advanced pancreatic cancer over the last few years (9, 17, 18). Nevertheless, the value of RIAC in treating advanced pancreatic has not been conclusively demonstrated. In addition, most of these studies remain in the phase II clinical trial stage, lacking comprehensive subgroup analysis of clinical research subjects. Considering the small number of patients included in the published studies and that most of the studies were retrospective, a systematic review and meta-analysis are necessary to provide a more reliable conclusion to guide clinical practice.

Herein, we used systematic review and meta-analysis to clarify the value of RIAC in treating advanced pancreatic cancer by comparing the safety and efficacy of RIAC with systemic chemotherapy.

Materials and methods

This systematic review was conducted in accordance with the standards of the Preferred Reporting Items for Systematic Reviews and Meta-Analyses (PRISMA) (19). No ethical approval or informed consent was required for this article because all data were retrieved from published literature.

Search strategy

Four electronic databases, i.e., PubMed, Embase, Web of Science, and Cochrane Library, were searched on May 30, 2023, and no time limitation was applied. Two investigators performed searching, identification of eligibility, data extraction, and quality assessment; disagreements were resolved through discussion. Vocabulary and syntax were specifically adapted according to the database. The specific search terms were: ((pancreatic or pancreas), (cancer or neoplasms or carcinoma or malignant tumor)), ((arteries or arterial) and (infusion or perfusion or chemotherapy)). Only studies published in the English language were included. Reference lists of relevant articles were also manually screened for additional possible records.

Inclusion criteria

Studies were selected based on the following inclusion criteria (1): study design: randomized controlled trials (RCTs) (2); population: adult patients who were histologically and/or clinically diagnosed with pancreatic cancer (3); intervention: RIAC (given via cancer feeding artery, hepatic artery, celiac artery, gastroduodenal artery, superior mesenteric artery, common hepatic artery, splenic artery, or other regional arteries, with or without regional embolization), or systemic intravenous chemotherapy (given via central or peripheral veins) (4); outcomes: provided 1 of the following outcome of interest: complete remission (CR), partial remission (PR), or complications (5); sufficient data could be extracted. If more than one study provided overlapping data, only the latest study or a study with the most comprehensive data was included. Case reports, commentaries, expert opinions, and narrative reviews were excluded.

Data extraction

Requisite data extracted and recorded to standardized Excel files included the first author's surname, publication year, study inclusion interval, country, study design, demographic information of participants, number of patients in the RIAC and systemic treatment groups, gender, and route of drug administration. The primary endpoints were: complete response (CR), partial response (PR), and complication rate where CR indicated a disappearance of all target lesions [any pathological lymph nodes (whether target or non-target) must have reduction in short axis to <10 mm] and PR indicated at least a 30% decrease in the sum of diameters of target lesions, taking as reference the baseline sum diameters, with no evidence of new or progressive lesions. Side effects of interest mainly involved hematology (leukopenia, thrombocytopenia, or anemia) and gastrointestinal system complications (nausea, vomiting, or duodenal ulcers); other complications were embolism, thrombophlebitis, and catheter displacement.

Quality assessment

The quality of the included non-RCTs was assessed by using the risk of bias in non-randomized studies of interventions (ROBINS-I). The RCTs were evaluated using the Cochrane risk bias tool 2.0.

Statistical analyses

The heterogeneity between studies was assessed using Chi-square statistics and qualified by the size of I^2. Heterogeneity among included studies was assessed using the I^2 statistic. An I^2 value of 0% implied no observed heterogeneity, and values of > 50% indicated substantial heterogeneity. All meta-analyses used a fixed-effects model: I^2 < 25% for all accessed outcomes. The analyzed parameters included the number of patients, major endpoints (CR, PR, and complication rate), and side effects. The value of a two-sided P< 0.05 was considered statistically significant. Stata version 16 (StataCorp, College Station, TX, USA) was used to analyze data from RCTs meeting inclusion criteria. The potential publication bias was examined using Egger's tests and funnel plot. Finally, sensitivity analyses were performed to identify individual study effects on pooled results and test the reliability of the results.

Results

Search results and study selection

A total of 969 relevant papers were obtained from the preliminary search. There were 833 potentially relevant studies after excluding duplicates. After performing an initial screening of the title and abstract, 54 articles with strong correlations were obtained. Eleven articles (20–30) were finally included in the meta-analysis after assessing the full-text content and analyzing the data integrity according to the exclusion criteria. Figure 1 shows the selection process of the included studies.

Study characteristics

Eleven studies involved 627 patients, 322 of whom received regional intra-arterial chemotherapy, and 305 received systemic chemotherapy. The mean ages of included patients ranged from 55.0 to 62.4 years, and the proportion of males ranged from 52.9% to 57.1%. The chemotherapy regimen included FAM [adriamycin 40 mg/m^2, mitomycin (MMC) 6 mg/m^2, and 5-fluorouracil (5-FU) 375 mg/m^2], GEM (1000 mg/m^2), MF [MMC 2 mg, 5-FU 750 mg], MmMC [mitomycin C at a total dose of 18 mg/m^2, mitoxantrone 6 mg/m^2, and cisplatin 30 mg/m^2]. GP (gemcitabine 1000 mg/m^2, cisplatin 50 mg/m^2), and GF (GEM+5-FU)[GEM 1000 mg/m^2; 5-Fu, 600 mg/m^2]. The drug delivery routes included celiac artery splenicartery, tumor-feeding arteries, splenic artery, gastroduodenal artery, common hepatic artery, and superior mesenteric artery (Table 1). Of note, the study by Wang et al. did not report the information on survival time (so the survival time in Table 1 for this study is empty); yet, this study was included ins the meta-analysis because it met the inclusion criteria and reported the necessary data for meta-analysis.

Results of quality assessment

We assessed the methodological quality of each non-RCT by using the ROBINS-I and each RCT using ROB 2. The risks of bias and corresponding ratios are summarized in Figure 2.

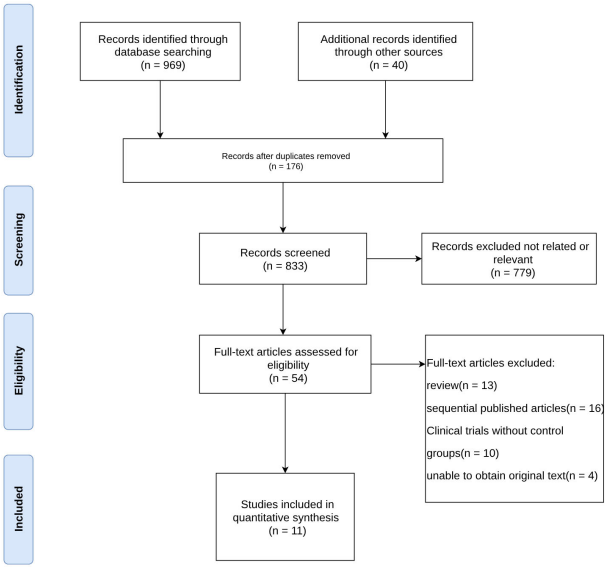

FIGURE 1
Selection process of included studies.

TABLE 1 Characteristics of studies included in the meta-analysis.

Author	Country	Sample size	Diagnosis	Mean age	Drugs	Drug delivery routes	Side effects	Survival time (median or mean, interval)	Survival time (median or mean, interval)	Follow-up time (months)
		RIAC/SC						RIAC	SC	
Ji et al., 2003 (28)	China	18\11	pathological/CT/CA199/MRI	62.4	MF	splenic artery, gastroduodenal artery, common hepatic artery	cytopenia (mild), nausea and anorexia (mild), abscess around the pump (mild)	12.5	4.8	>1
Shamseddine et al., 2005 (29)	America	7\4	Biopsy proven	NR	GEM	tumor-feeding arteries	pain and fever (mild)	5	5.6	>28
Han et al., 2006 (27)	China	70\70	Biopsy proven	60.2	FAM	celiac artery splenic artery	nausea and vomiting (48.6% in RIAC/41.3% in SC); three severe myelosuppression and one death in SC	13.5 (3–34 months)	6.2 (1–13 months)	1-34
Hong et al., 2007 (30)	China	25\26	pathological/CT/MRI	NR	GF	tumor-feeding arteries	leukopenia, thrombocytopenia, anemia, nausea/vomiting, arrhythmia, aminotransferase (mild to moderate)	10	7.3	1-12
Liu et al., 2007 (24)	China	32\33	pathological/CT/MRI	55	GF	tumor-feeding arteries	leukopenia, thrombocytopenia, renal hypoplasia (mild)	11	8	0-140
Hong et al., 2008	China	25\26	pathological/CT/MRI	NR	GF	superior mesenteric artery	leukopenia, thrombocytopenia, anemia, nausea and vomiting(mild to moderate), arrhythmia, aminotransferase(mild)	12	6	0-30
Liu et al., 2008 (23)	China	26\27	pathological/CT/MRI	61	GP	superior mesenteric artery	leukopenia (severe, 2 in RIAC, 3 in SC), thrombocytopenia, nausea and vomiting, hepatic and renal hypoplasia (mild)	21(10.5–28 months)	14(5–20.5 months)	>28
Jia et al., 2009 (22)	China	21\22	pathological/CT/MRI	60	GF	superior mesenteric artery	leukopenia, thrombocytopenia, nausea and vomiting, constipation, hepatic and renal hypoplasia (mild to moderate), oral mucosal reactions (mild)	13.5	6.2	NR
Qi et al., 2011 (25)	China	36\32	pathological/CT/CA199/MRI	62	GP	splenic artery, gastroduodenal artery, common hepatic artery	leukopenia, thrombocytopenia, nausea and vomiting, hepatic and renal hypoplasia (mild)	12	8	24
Wang et al., 2012 (26)	China	38\30	pathological/CT/CA199/MRI	58.7	GF	gastroduodenal artery, common hepatic artery	nausea and vomiting(mild to moderate, two severe in SC), leukopenia, thrombocytopenia(four severe in RIAC, one in SC)	NR	–	NR

(Continued)

10.3389/fonc.2024.1197424

TABLE 1 Continued

Author	Country	Sample size	Diagnosis	Mean age	Drugs	Drug delivery routes	Side effects	Survival time (median or mean, interval)		Survival time (median or mean, interval)		Follow-up time (months)
		RIAC/SC						RIAC		SC		
Hong et al., 2012 (20)	China	24\24	pathological	59.5	GF	abdominal cavity artery and upper mesentery artery	leukopenia, thrombocytopenia, nausea and vomiting, arrhythmia, aminotransferase (mild to moderate), hepatic hypoplasia (mild)	16.3		8.6		1-6

RIAC, Regional intra-arterial chemotherapy; SC, systemic chemotherapy.
FAM, adriamycin 40 mg/m2, mitomycin (MMC) 6 mg/m2, d1; 5-fluorouracil (5-FU), 375 mg/m2, d2-6.
GEM, gemcitabine, 1000 mg/m2, day 1, 8.
MF, MMC, 2 mg, d2, 4,6; 5-FU, 750 mg, day 1, 3, 5.
MmMC, Mitomycin C at a total dose of 18 mg/m2, day 1–5; mitoxanthrone, 6 mg/m2, day 6; cisplatin, 30 mg/m2, day 7–8.
GP, Gemcitabine 1000 mg/m2, day 1; cisplatin, 50 mg/m2, day 1. GF (GEM+5-FU):
GEM 1000 mg/m2, day 1; 5-Fu, 600 mg/m2, day 1–5.
NR, not reported

Complete remission, partial remission, and objective response rate

Among eleven initially selected studies (627 patients), ten were finally included in this meta-analysis of CR. Figure 3 shows that the RIAC and systemic groups did not differ significantly for CR (RD = 0.03, 95% CI: -0.01, 0.06, I^2 = 0%) (Figure 3A). However, Figure 3B also shows that patients treated with RIAC had better PR than those treated with systemic chemotherapy (OR = 2.23, 95% CI: 1.57, 3.15, I^2 = 0%). In addition, according to CR and PR, the pooled ORR of RIAC patients was (OR = 0.09, 95% CI: 0.05, 0.16, I2 = 56.5%) (Figure 4A), while the pooled ORR of the systemic chemotherapy patients was (OR = 0.13, 95% CI: 0.05, 0.29, I2 = 30.7%) (Figure 4B).

Median survival times

Ten studies (21–25, 27–29) reported that RIAC median survival times (10–21 months) were longer than for systemic chemotherapy (4.8–14 months). One study (30) reported that systemic chemotherapy median survival times (5.6 months) were longer than for RIAC (5 months). One study (26) did not report the median survival times. We tried contacting the authors but could not obtain further information. The median survival times were longer in patients receiving RIAC than those receiving systemic chemotherapy.

Side effects

The results in Figure 5 show that the overall complication rate was lower in patients with RIAC than in patients receiving systemic chemotherapy (OR = 0.45, 95% CI: 0.33, 0.63, I^2 = 0%). Common side effects included myelosuppression (leukopenia, thrombocytopenia, gastrointestinal reactions (nausea, vomiting, and diarrhea), and hepatic and renal impairment. Two studies reported severe myelosuppression in both RIAC and SC (systemic chemotherapy) groups (23, 27). One study reported severe myelosuppression and one death in the SC group (26). No deaths due to drug toxicity were reported in the RIAC group.

Subgroup analysis

We performed subgroup analysis on each outcome by diagnostic criteria, drug, and route of administration. RIAC patients showed higher CR than the SC patients in the biopsy-proven group (RD = 0.08, 95% CI: 0.01, 0.15, I2 = 0%) and FAM group (RD = 0.07, 95% CI: 0.01, 0.14, I^2 = 0%) (Supplementary Figure S1). Also, RIAC patients showed higher PR than the SC group when patients were stratified into those receiving drugs through the celiac artery (OR = 2.93, 95% CI: 1.81, 4.74, I^2 = 4.2%), MF group (OR = 7.07, 95% CI: 1.17, 42.85, I^2 = 0%), FAM group (OR = 2.08, 95% CI: 0.07, 63.42, I^2 = 0%), proven group (OR = 1.81, 95% CI: 1.20, 2.71, I^2 = 0%), and biopsy-proven group (OR = 4.07, 95% CI: 2.03, 8.14, I^2 = 0%) (Supplementary Figure S2).

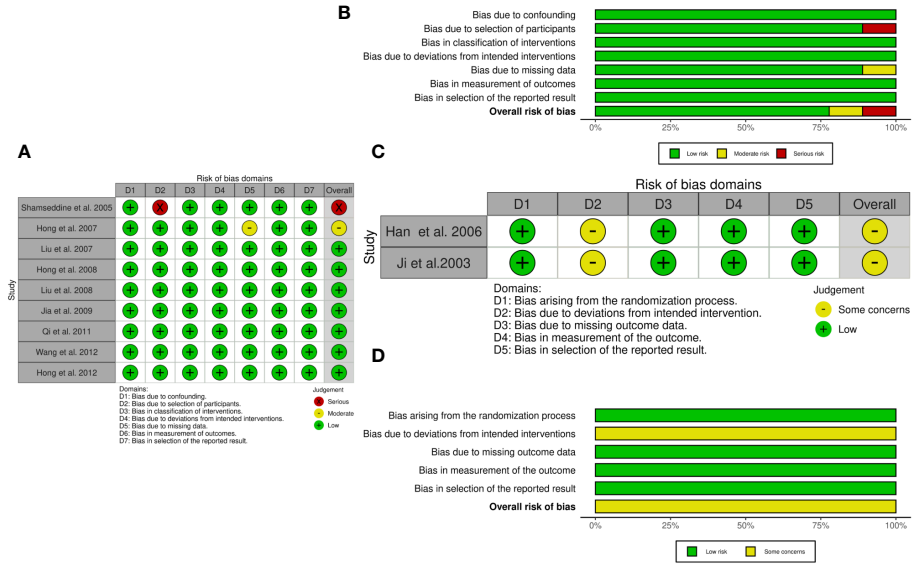

FIGURE 2
The quality assessment according to ROBINS-I and ROB 2 of each non-RCTs and RCTs. **(A)** Risk of bias ROBINS-I per study; **(B)** Risk of bias ROBINS-I per domain; **(C)** Risk of bias ROB-2 per study; **(D)** Risk of bias ROB-2 per domain.

Also, the RIAC group showed fewer side effects than the SC group when patients were stratified in the pathologically proven group (OR = 0.48, 95% CI: 0.33, 0.70, I^2 = 0%), biopsy-proven group (OR = 0.39, 95% CI: 0.19, 0.78, I^2 = 71.8%), FAM group (OR = 0.30, 95% CI: 0.14, 0.63, I^2 = 0%), GF group (OR = 0.48, 95% CI: 0.30, 0.75, I^2 = 0%), GP group (OR = 0.44, 95% CI: 0.21, 0.96, I^2 = 0%), drugs administered through abdominal cavity artery group (OR = 0.40, 95% CI: 0.25, 0.62, I^2 = 0%) and drugs administered through superior mesenteric artery group (OR = 0.45, 95% CI: 0.23, 0.90, I^2 = 0%) (Supplementary Figure S3).

Sensitivity analysis

Sensitivity analysis was performed to estimate the effect of each study on pooled OR by consecutive deletion of each study. The results showed no eligible study significantly influenced the pooled estimate (Figure 6).

Publication bias

Funnel plot and Egger's test were performed to assess publication bias among the studies. As shown in Figure 7, there was no evidence of publication bias for PR (Egger's test P = 0.469) (Figure 7A) and CR (Egger's test P = 0.330) (Figure 7B). However, side effects may be subject to publication bias (Egger's test P = 0.002) (Figure 7C).

Discussion

Our data revealed that patients who received RIAC treatment had better outcomes than those who received systemic chemotherapy, regardless of whether the treatment resulted in complete or partial remission or extended median survival time. Additionally, the incidence of side effects for patients who received RIAC was lower.

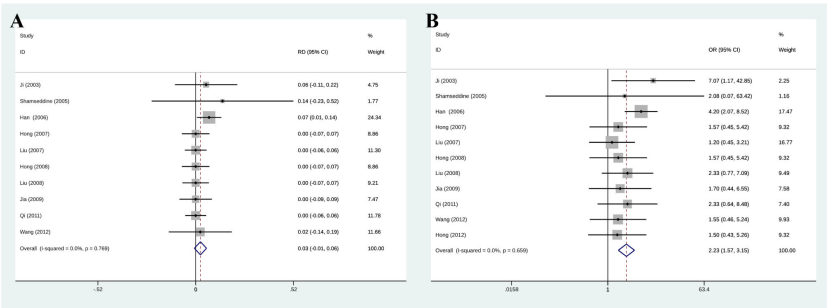

FIGURE 3
(A) Meta-analysis of CR. Diamonds represent pooled effects. CR, complete remission; **(B)** Meta-analysis of PR. Diamonds represent pooled effects. PR, partial remission.

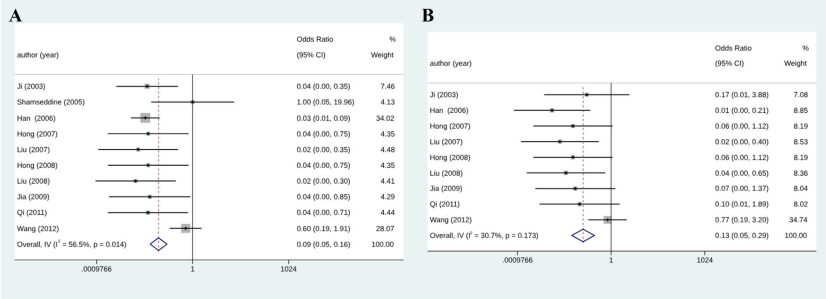

FIGURE 4
(A) Meta-analysis of ORR for RIAC patients; **(B)** Meta-analysis of ORR for systemic chemotherapeutics patients.

Conventional systemic chemotherapy for advanced pancreatic cancer can improve symptoms and prolong survival to a certain extent, but the overall efficacy is not ideal. Due to the drug resistance and poor sensitivity to chemotherapy, the therapeutic effect of chemotherapy on pancreatic cancer is limited (31, 32). Also, considering that pancreatic cancer has a poor blood supply and its tumor surface is often covered by a dense fibrous envelope, the effect of chemotherapeutics is limited (17). Moreover, pancreatic cancer often expresses medium to high levels of multi-drug resistance gene, which influences the chemotherapeutics effect (9, 16, 33). Therefore, increasing the concentration of tumor local drugs is necessary. Thus, changing the route of administration is often considered for these patients.

Pancreatic cancer has a dose-dependent sensitivity to local chemotherapy (34). The application of targeted arterial perfusion therapy can effectively increase the tissue drug concentration, increasing the sensitivity of tumor cells to chemotherapeutic drugs and contributing to overcoming tumor cell resistance induced by P-170 glycoprotein (9). Therefore, this method has often been applied for treating pancreatic cancer (35). Regional chemotherapy is a comprehensive treatment for pancreatic cancer.

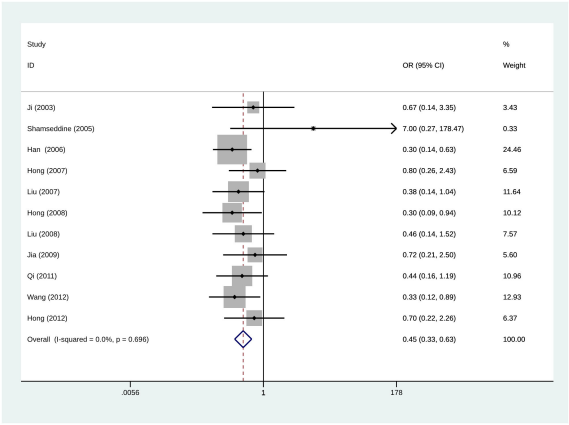

FIGURE 5
Meta-analysis of the incidence of total complications using Regional Intra-Arterial Chemotherapy or systemic administration of chemotherapeutics. Diamonds represent pooled effects.

The main arterial blood supply to the pancreas comes from the trunk celiac artery and the superior mesenteric artery, so anti-cancer drugs injected through the trunk celiac artery and the superior mesenteric artery can cover the entire pancreas (17). Regional arterial perfusion chemotherapy of the pancreas can significantly increase the concentration of drugs in the pancreas, duodenum, and peripancreatic lymph nodes, enhance drug action, reduce systemic toxic and side effects, and improve the effect of chemotherapy (35, 36).

Based on the results of the present meta-analysis, we concluded that RIAC has fewer complications than systemic chemotherapy. In particular, the drug dose used for each treatment regimen was the same across studies, and RIAC had fewer severe myelosuppression events and GI reactions than systemic chemotherapy. (37) Local perfusion chemotherapy increases the blood concentration of tumor tissue, while the influence of chemotherapy drugs on other tissues, such as bone marrow tissue, liver, kidney, and gastrointestinal tract, is reduced, alleviating the toxic and side effects of systemic chemotherapy (10). Although the value of RIAC has been demonstrated, several disadvantages have limited the expansion of its clinical use. The studies included in this paper did not describe the exact length of the procedure; other studies have shown that RIAC is often more challenging to perform than systemic chemotherapy. It is also less frequently used than regular intravenous chemotherapy as the surgeon who performs it requires special training. Moreover, it is an invasive procedure that increases hospitalization time, costs, and local complications (9). However, RIAC has superior clinical benefits and fewer complications, which makes it a good strategy for advanced pancreatic cancer treatment and a good option for palliative or neoadjuvant therapy, especially in patients who do not respond to standard therapy. Generally, regional arterial chemotherapy may be more expensive than other cancer treatments, such as systemic chemotherapy or radiation therapy. However, the cost of regional arterial chemotherapy may be justified due to its potential benefits, such as higher response rates and fewer side effects compared to other treatment methods. Also, when considering the economic impact of regional intra-arterial versus systemic chemotherapy, several factors should be considered; these may include the cost of the drugs themselves, the cost of administering the treatment, the cost of any necessary hospital stays or follow-up appointments, and the potential for lost income due to time off work. Additionally, it's important to

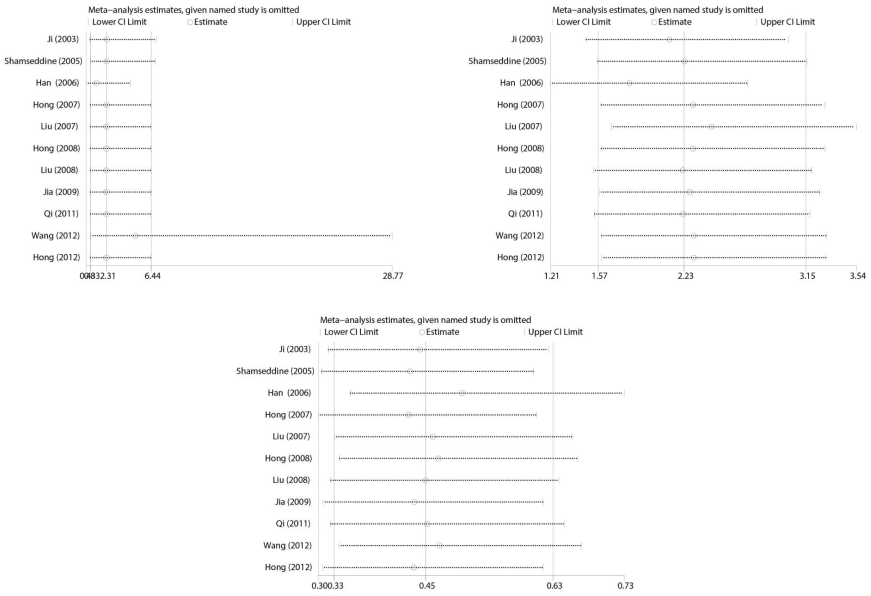

FIGURE 6
Meta-analysis of Sensitivity analysis.

consider the potential benefits of each treatment option in terms of overall survival, quality of life, and potential side effects. By carefully weighing these factors, healthcare providers can make informed decisions about which treatment option is most appropriate for each individual patient.

Our study has several major strengths compared with the former meta-analysis conducted in 2012 (13). First, we included 11 studies with 627 participants, while the previous study, conducted by Liu et al., was based on 5 RCTs, which included 298 participants. Also, we included four articles that were identical to Liu et al.; one article was excluded for not meeting the inclusion criteria, and 7 new articles after 2012 were included. Therefore, the result of our study may be more reliable. Second, compared with the previous meta-analysis, we used Stata software for meta-analysis; the results are more intuitive and straightforward for clinicians to understand. In the meta-analysis of the complication incidence in regional and systemic chemotherapeutics, our study yielded 0% in the heterogeneity index I^2 (24% in the previous study); the lower I^2

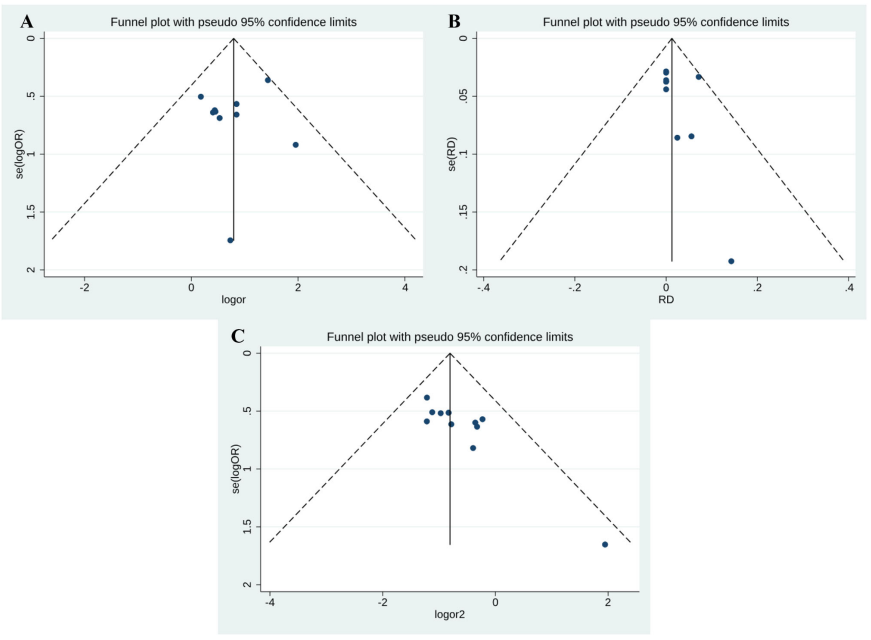

FIGURE 7
Meta-analysis of Publication bias. **(A)** CR; **(B)** PR; **(C)** ORR.

indicated a less heterogeneous population and more robust results than the former meta-analysis. Finally, the pooled CR of regional intra-arterial vs. systemic chemotherapy for treating advanced pancreatic cancer was higher than that reported by the previous meta-analysis. The different results suggested that the latest research has added new evidence to the current understanding, and RIAC is still the more effective option.

Potential limitations of this meta-analysis should also be considered. First, due to the small amount of literature in this study, the original literature is not detailed enough, and the reliability of each literature differed. Only a few studies gave a definite length of follow-up, and although the length of follow-up was consistent between the RIAC and SC groups, data on long-term prognosis are still insufficient. In addition, unpublished studies were not included in this meta-analysis, and the sample size in this study was small. Furthermore, our original literature was not randomized, and there has been an evident lack of research in recent years. Therefore, more rigorous RCTs are needed to enhance our understanding of this issue further.

Conclusions and future directions

Based on the results of the current meta-analysis, we concluded that compared with systemic chemotherapy, RIAC has a higher PR, greater clinical benefit, and fewer complications in the treatment of advanced pancreatic cancer.

Data availability statement

The original contributions presented in the study are included in the article/Supplementary Material. Further inquiries can be directed to the corresponding authors.

Author contributions

Conception and design: YC. Administrative support: YW. Provision of study materials or patients: DY. Collection and assembly of data: YC. Data analysis and interpretation: YC. Manuscript writing: WZ. Final approval of manuscript: YC. All authors contributed to the article and approved the submitted version.

Funding

The author(s) declare that no financial support was received for the research, authorship, and/or publication of this article.

Conflict of interest

The authors declare that the research was conducted in the absence of any commercial or financial relationships that could be construed as a potential conflict of interest.

Publisher's note

Supplementary material

The Supplementary Material for this article can be found online at: https://www.frontiersin.org/articles/10.3389/fonc.2024.1197424/full#supplementary-material

SUPPLEMENTARY FIGURE 1
Subgroup analysis of CR: **(A)** diagnostic criteria; **(B)** drug; **(C)** route of administration.

SUPPLEMENTARY FIGURE 2
Subgroup analysis of PR: **(A)** diagnostic criteria; **(B)** drug; **(C)** route of administration.

SUPPLEMENTARY FIGURE 3
Subgroup analysis of side effects: **(A)** diagnostic criteria; **(B)** drug; **(C)** route of administration.

References

1. Klein AP. Pancreatic cancer epidemiology: understanding the role of lifestyle and inherited risk factors. *Nat Rev Gastroenterol Hepatol*. (2021) 18:493–502. doi: 10.1038/s41575-021-00457-x

2. Mizrahi JD, Surana R, Valle JW, Shroff RT. Pancreatic cancer. *Lancet*. (2020) 395:2008–20. doi: 10.1016/s0140-6736(20)30974-0

3. Cao D, Song Q, Li J, Jiang Y, Wang Z, Lu S. Opportunities and challenges in targeted therapy and immunotherapy for pancreatic cancer. *Expert Rev Mol Med*. (2021) 23:e21. doi: 10.1017/erm.2021.26

4. Ilic M, Ilic I. Epidemiology of pancreatic cancer. *World J Gastroenterol*. (2016) 22:9694–705. doi: 10.3748/wjg.v22.i44.9694

5. Ansari D, Tingstedt B, Andersson B, Holmquist F, Sturesson C, Williamsson C, et al. Pancreatic cancer: yesterday, today and tomorrow. *Future Oncol*. (2016) 12:1929–46. doi: 10.2217/fon-2016-0010

6. Chin V, Nagrial A, Sjoquist K, O'Connor CA, Chantrill L, Biankin AV, et al. Chemotherapy and radiotherapy for advanced pancreatic cancer. *Cochrane Database Syst Rev*. (2018) 3:Cd011044. doi: 10.1002/14651858.CD011044.pub2

7. Zhao Z, Liu W. Pancreatic cancer: A review of risk factors, diagnosis, and treatment. *Technol Cancer Res Treat*. (2020) 19:1533033820962117. doi: 10.1177/1533033820962117

8. Chawla A. Contemporary trials evaluating neoadjuvant therapy for resectable pancreatic cancer. *J Surg Oncol*. (2021) 123:1423–31. doi: 10.1002/jso.26393

9. Laface C, Laforgia M, Molinari P, Foti C, Ambrogio F, Gadaleta CD, et al. Intra-arterial infusion chemotherapy in advanced pancreatic cancer: A comprehensive review. *Cancers (Basel)*. (2022) 14. doi: 10.3390/cancers14020450

10. Park W, Chawla A, O'Reilly EM. Pancreatic cancer: A review. *Jama*. (2021) 326:851–62. doi: 10.1001/jama.2021.13027

11. Ishikawa T. Is it relevant that intra-arterial chemotherapy may be effective for advanced pancreatic cancer? *World J Gastroenterol*. (2007) 13:4306–9. doi: 10.3748/wjg.v13.i32.4306

12. Kow AWC. Hepatic metastasis from colorectal cancer. *J Gastrointest Oncol*. (2019) 10:1274–98. doi: 10.21037/jgo.2019.08.06

13. Liu F, Tang Y, Sun J, Yuan Z, Li S, Sheng J, et al. Regional intra-arterial vs. systemic chemotherapy for advanced pancreatic cancer: a systematic review and meta-analysis of randomized controlled trials. *PloS One*. (2012) 7:e40847.

14. Ma N, Wang Z, Zhao J, Long J, Xu J, Ren Z, et al. Improved survival in patients with resected pancreatic carcinoma using postoperative intensity-modulated radiotherapy and regional intra-arterial infusion chemotherapy. *Med Sci Monit*. (2017) 23:2315–23. doi: 10.12659/msm.904393

15. Liu X, Yang X, Zhou G, Chen Y, Li C, Wang X. Gemcitabine-based regional intra-arterial infusion chemotherapy in patients with advanced pancreatic adenocarcinoma. *Med (Baltimore)*. (2016) 95:e3098. doi: 10.1097/md.0000000000003098

16. Gupta R, Amanam I, Chung V. Current and future therapies for advanced pancreatic cancer. *J Surg Oncol*. (2017) 116:25–34. doi: 10.1002/jso.24623

17. Aigner KR, Gailhofer S, Selak E, Aigner K. Intra-arterial infusion chemotherapy versus isolated upper abdominal perfusion for advanced pancreatic cancer: a retrospective cohort study on 454 patients. *J Cancer Res Clin Oncol*. (2019) 145:2855–62. doi: 10.1007/s00432-019-03019-6

18. Qiu B, Zhang X, Tsauo J, Zhao H, Gong T, Li J, et al. Transcatheter arterial infusion for pancreatic cancer: a 10-year National Cancer Center experience in 115 patients and literature review. *Abdom Radiol (NY)*. (2019) 44:2801–8. doi: 10.1007/s00261-019-02022-2

19. McInnes MDF, Moher D, Thombs BD, McGrath TA, Bossuyt PM, Clifford T, et al. Preferred reporting items for a systematic review and meta-analysis of diagnostic test accuracy studies: the PRISMA-DTA statement. *Jama*. (2018) 319:388–96. doi: 10.1001/jama.2017.19163

20. Hong GB, Zhou JX, Sun HB, Li CY, Song LQ. Continuous transarterial infusion chemotherapy with gemcitabine and 5-Fluorouracil for advanced pancreatic carcinoma. *Asian Pac J Cancer Prev*. (2012) 13:2669–73. doi: 10.7314/apjcp.2012.13.6.2669

21. Hong G, Zhou J, Liang B. Clinical analysis of continuous arterial infusion chemotherapy for advanced pancreatic cancer. *Cancer Prev Treat Res*. (2007) 34:54–6. doi: 10.3971/j.issn.1000-8578.2007.01.017

22. Jia L, Zheng J, Zhang S, Xie D. A comparative study of gemcitabine arterial infusion chemotherapy and peripheral intravenous chemotherapy in the treatment of advanced pancreatic cancer. *Chin J Pancreatic Dis*. (2009), 15–7.

23. Liu H, Li Y, Huang R, Huang X. Clinical observation of regional arterial perfusion of pancreas with GP scheme for advanced pancreatic cancer. *Basic Clin Oncol*. (2008) 21:479–81.

24. Liu L, Wang J, Wang X, Yan Z, Liu R, Chen Y, et al. Effect analysis of arterial gemcitabine chemotherapy for advanced pancreatic cancer. *Chin J Med Comput Imaging*. (2007), 202–7. doi: 10.19627/j.cnki.cn31-1700/th.2007.03.016

25. Qi X, Liu D, Jiang Y. A comparative study of regional chemotherapy and intravenous chemotherapy with GP protocol in the treatment of advanced pancreatic cancer. *Chin J Cancer Prev*. (2011) 18:1556–1558+1562. doi: 10.16073/j.cnki.cjcpt.2011.19.016

26. Wang W, Peng Z, Lei X, Lin Y. Comparison of the efficacy of arterial infusion chemotherapy and systemic chemotherapy in the treatment of advanced pancreatic cancer. *Med J West China*. (2012) 24:1730–2.

27. Han GH, Yin ZX, Meng XJ, He CY, Zhang HB, Sun AH, et al. Prospective randomized clinical trial of two drug delivery pathway in the treatment of inoperable advanced pancreatic carcinoma. *Chin J Dig Dis*. (2006) 7:45–8. doi: 10.1111/j.1443-9573.2006.00243.x

28. Ji Z, Wang Y, Chen X, Wu T. Peripancreatic artery ligation and artery infusion chemotherapy for advanced pancreatic carcinoma. *Chin Med J (Engl)*. (2003) 116:89–92.

29. Shamseddine AI, Khalifeh MJ, Mourad FH, Chehal AA, Al-Kutoubi A, Abbas J, et al. Comparative pharmacokinetics and metabolic pathway of gemcitabine during intravenous and intra-arterial delivery in unresectable pancreatic cancer patients. *Clin Pharmacokinet*. (2005) 44:957–67. doi: 10.2165/00003088-200544090-00005

30. Hong G, Zhou J, Luo J, Xu L, Chen Y, Jiang R. A clinical study on continuous transarterial infusion chemotherapy and systemic venous chemotherapy with gemcitabine and 5-fluorouracil in treating patients with advanced pancreatic carcinoma. *Chinese-German J Clin Oncol*. (2007) 6:457–60. doi: 10.1007/s10330-007-0086-4

31. Grasso C, Jansen G, Giovannetti E. Drug resistance in pancreatic cancer: Impact of altered energy metabolism. *Crit Rev Oncol Hematol*. (2017) 114:139–52. doi: 10.1016/j.critrevonc.2017.03.026

32. Li J, Wientjes MG, Au JL. Pancreatic cancer: pathobiology, treatment options, and drug delivery. *AAPS J*. (2010) 12:223–32. doi: 10.1208/s12248-010-9181-5

33. Furuse J, Shibahara J, Sugiyama M. Development of chemotherapy and significance of conversion surgery after chemotherapy in unresectable pancreatic cancer. *J Hepatobiliary Pancreat Sci*. (2018) 25:261–8. doi: 10.1002/jhbp.547

34. de Sousa Cavalcante L, Monteiro G. Gemcitabine: metabolism and molecular mechanisms of action, sensitivity and chemoresistance in pancreatic cancer. *Eur J Pharmacol*. (2014) 741:8–16. doi: 10.1016/j.ejphar.2014.07.041

35. Okusaka T, Furuse J. Recent advances in chemotherapy for pancreatic cancer: evidence from Japan and recommendations in guidelines. *J Gastroenterol*. (2020) 55:369–82. doi: 10.1007/s00535-020-01666-y

36. Liu GF, Li GJ, Zhao H. Efficacy and toxicity of different chemotherapy regimens in the treatment of advanced or metastatic pancreatic cancer: A network meta-analysis. *J Cell Biochem*. (2018) 119:511–23. doi: 10.1002/jcb.26210

37. Jain A, Bhardwaj V. Therapeutic resistance in pancreatic ductal adenocarcinoma: Current challenges and future opportunities. *World J Gastroenterol*. (2021) 27:6527–50. doi: 10.3748/wjg.v27.i39.6527

frontiers | Frontiers in Oncology

TYPE Original Research
PUBLISHED 16 April 2024
DOI 10.3389/fonc.2024.1347752

OPEN ACCESS

EDITED BY
Liang Qiao,
The University of Sydney, Australia

REVIEWED BY
Ying-Tai Chen,
Chinese Academy of Medical Sciences and Peking Union Medical College, China
Shun-Xian Zhang,
Chinese Center For Disease Control and Prevention, China
Jinxin Zheng,
Ruijin Hospital North, China
Xinyu Feng,
Chinese Center For Disease Control and Prevention, China

*CORRESPONDENCE
Wen-Ce Zhou
zhouwc129@163.com

RECEIVED 01 December 2023
ACCEPTED 03 April 2024
PUBLISHED 16 April 2024

CITATION
Wang Z-F, Zhang B, Xu H and Zhou W-C (2024) Efficacy of the 'Five-Needle' method for pancreatojejunostomy in laparoscopic pancreaticoduodenectomy: an observational study.
Front. Oncol. 14:1347752.
doi: 10.3389/fonc.2024.1347752

Efficacy of the 'Five-Needle' method for pancreatojejunostomy in laparoscopic pancreaticoduodenectomy: an observational study

Zheng-Feng Wang[1], Bo Zhang[1], Hao Xu[1] and Wen-Ce Zhou[2]*

[1]The Fourth Ward of General Surgery, The First Hospital of Lanzhou University, Lanzhou, China, [2]The Second Hospital of Lanzhou University, Lanzhou, China

Objective: The five-needle pancreato-intestinal anastomosis method is used in laparoscopic pancreaticoduodenectomy (LPD). The aim of this study was to explore the clinical efficacy and adverse reactions of this new surgical method and to provide a scientific reference for promoting this new surgical method in the future.

Methods: A single-centre observational study was conducted to evaluate the safety and practicality of the five-needle method for pancreatojejunostomy in LPD surgeries. The clinical data of 78 patients who were diagnosed with periampullary malignancies and underwent LPD were collected from the 1st of August 2020 to the 31st of June 2023 at Lanzhou University First Hospital. Forty-three patients were treated with the 'Five-Needle' method (test groups), and 35 patients were treated with the 'Duct-to-Mucosa' method (control group) for pancreatojejunostomy. These two methods are the most commonly used and highly preferred pancreatointestinal anastomosis methods worldwide. The primary outcome was pancreatic fistula, and the incidence of which was compared between the two groups.

Results: The incidence of pancreatic fistula in the five-needle method group and the duct-to-mucosa method group was not significantly different (25.6% vs. 28.6%, p=0.767). Additionally, there were no significant differences between the two groups in terms of intraoperative blood loss (Z=-1.330, p=0.183), postoperative haemorrhage rates (p=0.998), length of postoperative hospital stay (Z=-0.714, p=0.475), bile leakage rate (p=0.745), or perioperative mortality rate (p=0.999). However, the operative time in the 'Five-Needle' method group was significantly shorter than that in the 'Duct-to-Mucosa' method group (270 ± 170 mins vs. 300 ± 210 mins, Z=-2.336, p=0.019). Further analysis revealed that in patients with pancreatic ducts smaller than 3 mm, the incidence of pancreatic fistula was lower for the 'Five-Needle' method than for the 'Duct-to-Mucosa' method (12.5% vs. 53.8%, p=0.007).

Conclusion: The five-needle method is safe and efficient for pancreatojejunostomy in LPD, and is particularly suitable for anastomosis in nondilated pancreatic ducts. It is a promising, valuable, and recommendable surgical method worthy of wider adoption.

KEYWORDS

laparoscopic pancreaticoduodenectomy (LPD), Five-Needle method, duct-to-mucosa method, pancreatic fistula, operative time

1 Introduction

Laparoscopic pancreaticoduodenectomy (LPD), as one of the more complex general surgical procedures, remains the primary surgical method for treating periampullary malignancies. The procedure, involving concomitant organ resection and the establishment of gastroenteric, hepaticojejunostomy, and pancreatojejunostomy anastomoses, is associated with postoperative complications such as pancreatic fistula, bile leakage, intra-abdominal haemorrhage, and infection, posing significant postoperative risks to patients (1–3). Clinical studies indicate that the incidence of postoperative pancreatic fistula ranges from 21.4% to 28.0%, with severe fistulas (grades B and C) occurring in approximately 8% and 12.2%, respectively, of patients experiencing postoperative haemorrhage. The surgery-related mortality rate is reported to be between 3% and 6% (1–3). Inadequate healing of the pancreatojejunostomy is a primary contributor to these complications. Clinical manifestations include not only pancreatic fistulas but also leakage of pancreatic fluid rich in amylase, lipase, and protease, increasing the risk of secondary complications such as intra-abdominal haemorrhage and infection (4, 5).

Since the first LPD reported by Gagner et al. in 1994 (6), minimally invasive methods have been applied to pancreaticoduodenectomy, especially with recent advancements in laparoscopic and robotic-assisted technologies. Various LPD methods have been proposed, somewhat simplifying the anastomosis process (7, 8). However, the rate of postoperative complications has not significantly decreased, remaining a major hindrance to the successful execution of laparoscopic pancreatic surgery (9–11). Therefore, an LPD method that is not only straightforward in terms of execution but is also effective in reducing the incidence of pancreatic fistula and bleeding is urgently needed.

Open and LPD surgeries were first introduced 20 years ago, and due to an improved understanding of tissue healing physiology and the specifics of laparoscopic surgical methods, we have developed an innovative, straightforward, safe, and effective method for LPD, termed the five-needle method. The aim of this study was to preliminarily evaluate the clinical effectiveness and application value of the five-needle method for pancreatojejunostomy in LPD.

2 Materials and methods

2.1 Patients

This single-centre retrospective study was conducted to evaluate the safety and practicality of the five-needle method for pancreatojejunostomy in LPD. The clinical data of 116 patients who were diagnosed with periampullary malignancies and underwent LPD were collected from the 1st of August 2020 to the 31st of June 2023 at Lanzhou University First Hospital. After excluding 38 patients (18 with benign pathology diagnosed postoperatively without regional lymph node dissection, 14 who required conversion to open surgery, and 6 with incomplete observational data), 78 patients were enrolled in the study. Forty-three patients were treated with the 'Five-Needle' method (test groups), and 35 patients were treated with the 'Duct-to-Mucosa' method (control group) for pancreatojejunostomy. These two methods are the most commonly used and most highly preferred pancreatointestinal anastomosis methods worldwide.

2.2 Intervention measures

2.2.1 'Five-Needle' method

a. A silicone tube matching the internal diameter of the main pancreatic duct is inserted through the cut end of the duct, leaving approximately 3-4 cm of the tube extending beyond the pancreatic remnant.
b. Three 4-0 Prolene 'U'-shaped interrupted sutures are stitched through the end of the pancreas. These sutures close the branch pancreatic ducts, ensure haemostasis, and firmly fix the stent tube to the main pancreatic duct to prevent dislodgement. The upper and lower sutures are tied, leaving approximately 4 cm of suture tail for later use (Figures 1A–C).
c. The jejunum is brought up adjacent to the pancreatic remnant. A small opening is created on the antimesenteric border of the jejunum at an appropriate location. The fourth 4-0 Prolene vascular suture is used for a "U"-shaped

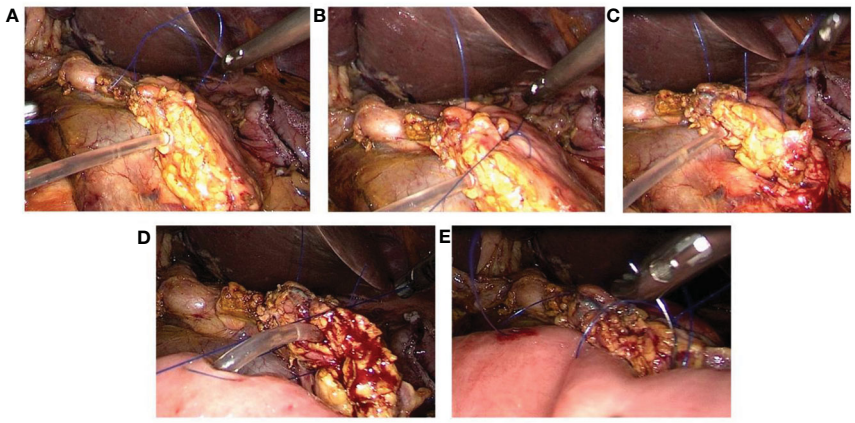

FIGURE 1
Laparoscopic 'Five-Needle' method for Pancreatojejunostomy. **(A)** A silicone tube is inserted into the main pancreatic duct, followed by a 'U'-shaped suture through the upper margin of the pancreatic stump using 4-0 Prolene (the first needle). **(B)** A 4-0 Prolene suture is passed through the upper and lower edges of the pancreatic duct and used for a 'U'-shaped suture through the middle of the pancreatic stump (the second needle). **(C)** A 'U'-shaped suture through the lower margin of the pancreatic stump is executed with 4-0 Prolene (the third needle). **(D)** A small opening is made on the opposite side of the jejunal mesentery, and a 4-0 Prolene suture is used for a 'U'-shaped pancreatojejunostomy. The pancreatic stent tube is inserted into the jejunum without tying the suture immediately (the fourth needle). **(E)** A continuous suture through the full thickness of the pancreatic stump and the seromuscular layer of the jejunum is performed with 4-0 Prolene, from the upper to the lower margin of the pancreas. The ends of this suture are tied to the reserved ends of the first and third sutures (the fifth needle).

pancreatojejunostomy. Both ends of the suture pass through the front of the pancreas, entering and exiting. The pancreatic stent tube is inserted into the jejunum, which is closed but not tied, to facilitate the fifth suture (Figure 1D).

d. The fifth 4-0 Prolene vascular suture creates a continuous full-thickness anastomosis from the upper to the lower edge of the pancreatic stump and the seromuscular layer of the jejunum. The fourth suture is then tightened and tied, followed by tightening the fifth suture. The ends of this suture are tied to the residual ends of the first and third sutures (Figure 1E).

2.2.2 'Duct-to-Mucosa' method

a. The neck of the pancreas is adequately mobilized to expose the cut end of the pancreatic duct. Continuous suturing of the posterior wall of the pancreatic stump to the seromuscular layer of the intestine is performed using 4-0 Prolene sutures from the upper to the lower margin of the pancreatic stump, followed by tightening the suture (Figures 2A, B).

b. A small opening corresponding to the diameter of the pancreatic duct is created on the antimesenteric border of

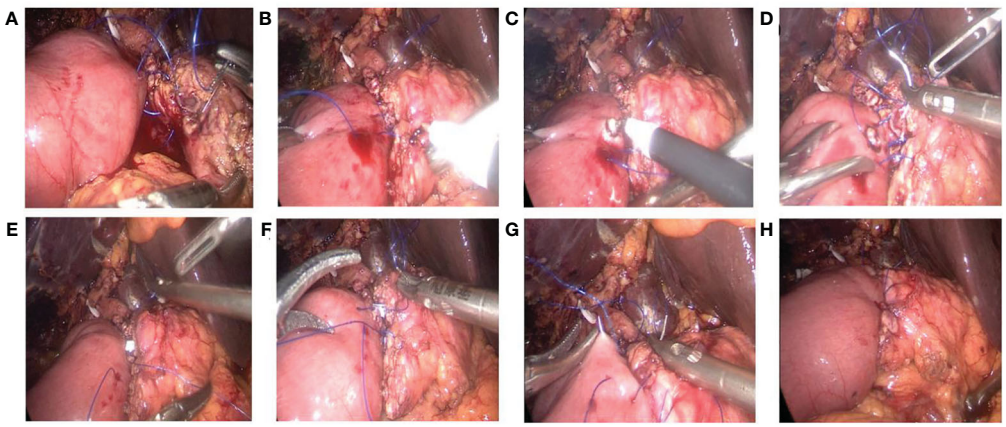

FIGURE 2
Laparoscopic 'Duct-to-Mucosa' pancreatojejunostomy. **(A)** Continuous suture of the posterior wall of the pancreatic stump to the jejunum using 4-0 Prolene. **(B)** The suture line is tightened upon completion of the posterior wall suturing. **(C)** A small opening is created in the jejunum with an electrocautery hook. **(D)** Continuous suturing of the posterior wall of the pancreatic duct to the jejunal opening using 5-0 Prolene. **(E, F)** After the insertion of the pancreatic duct stent tube, the anterior wall of the pancreatic duct and the jejunal opening are sutured together using 5-0 Prolene. **(G, H)** The anterior wall of the pancreatic stump is continuously sutured to the jejunum using 4-0 Prolene.

the jejunum (near the cut end of the pancreatic duct) using an electrocautery hook (Figure 2C).

c. The posterior wall of the pancreatic duct and the posterior wall of the jejunal opening are continuously sutured together using 5-0 Prolene sutures. A pancreatic duct stent tube, matching the diameter of the pancreatic duct, is inserted, with one end of the stent placed into the jejunal lumen. The anterior wall of the pancreatic duct and the anterior wall of the jejunal opening are then continuously sutured together with the same 5-0 Prolene sutures, completing the continuous 'Duct-to-Mucosa anastomosis' (Figures 2D–F).

d. The anterior wall of the pancreatic stump is continuously sutured to the seromuscular layer of the intestine using the original 4-0 Prolene sutures from the lower to the upper margin of the pancreatic stump, followed by tightening the suture to complete the pancreatojejunostomy (Figures 2G, H).

2.3 Outcome measures

2.3.1 Primary outcome indicators

Pancreatic Fistula: Postoperative pancreatic fistulas are characterized the presence of an amylase concentration in the abdominal cavity drainage fluid that is more than three times the upper limit of normal serum amylase levels, coupled with relevant clinical symptoms necessitating active intervention. Based on the 2016 classification scheme of the International Study Group on Pancreatic Fistula (ISGPF) (12), fistulas are classified as Grade A (biochemical leak), Grade B, or Grade C (Table 1). Grade B or C fistulas are categorized as severe pancreatic fistulas.

2.3.2 Secondary outcome indicators

Operative time: The duration from the completion of anaesthesia and related preparations to the establishment of pneumoperitoneum until the closure of the abdomen.

Intraoperative blood loss Amount of blood loss recorded in the surgical records.

Postoperative hospital stay The time from the end of the surgery to the patient's discharge (if the patient underwent a second surgery due to postoperative complications, the duration was considered the end of the first surgery).

Bile leak: A bile concentration in the abdominal drainage fluid or ascites more than three times the upper limit of normal serum bilirubin levels, persisting for more than 3 days postoperatively, or requiring interventional treatment or reoperation due to bile accumulation or biliary peritonitis.

Postoperative haemorrhage: Postoperative bleeding manifested through abdominal drainage tubes and/or gastrointestinal decompression tubes, possibly presenting as rectal bleeding, accompanied by symptoms of haemorrhagic shock such as hypotension and tachycardia and a decrease in haemoglobin concentration.

Perioperative mortality: Death of a patient during surgery or during the postoperative hospital stay due to surgery-related complications or cardiovascular incidents induced by the surgery.

TABLE 1 Classification of pancreatic fistula.

Grade	Grade A	Grade B	Grade C
The concentration of amylase in drainage fluid was 3 times higher than the upper limit of amylase in serum	Yes	Yes	Yes
Continuous peripancreatic drainage ≥ 3 weeks	No	Yes	Yes
Changes in clinical decision-making related to pancreatic fistula	No	Yes	Yes
The effusion needs to be resolved by puncture drainage	No	Yes	Yes
Pancreatic fistula-associated haemorrhage was studied by angiography	No	Yes	Yes
Signs of pancreatic fistula associated infection	No	Yes (not associated with organ failure)	Yes (not associated with organ failure)
Reoperation	No	No	Yes
Pancreatic fistula-related organ failure	No	No	Yes
Pancreatic fistula-related death	No	No	Yes

2.4 Inclusion and exclusion criteria

The study included a postoperative pathological diagnosis of periampullary malignancies (cholangiocarcinoma, pancreatic head cancer, duodenal papillary cancer) and complete surgical data. The exclusion criteria were as follows: 1) a postoperative pathological diagnosis of benign periampullary disease; and 2) Incomplete laparoscopic surgery.

2.5 Data collection and handling

A standardized protocol was implemented to maintain consistency in interviewer training and quality control supervision across all instances of data collection. Trained interviewers utilized a standardized questionnaire to gather the following information: age, sex, body mass index (BMI), pancreatic duct diameter, and pathological results. This information was primarily extracted from the electronic medical records.

2.6 Statistical analysis

Missing data were imputed using multiple imputation (MI, R package MICE, R Foundation for Statistical Computing, Vienna, Austria, https://cran.r-project.org/, with 20 imputed datasets). This method incorporates randomness in the imputation process to account for the uncertainty of generated values.

Based on expert knowledge, this study primarily investigated the impact of surgical methods on clinical outcomes. The covariates

included sex, age, BMI, diabetes status, hypertension status, pancreatic duct diameter, diagnosis (pathological type), and coronary stent placement. The dependent variables included primary and secondary outcomes, with the primary outcome being pancreatic fistula. The secondary outcomes included operative time, postoperative hospital stay, intraoperative blood loss, pancreatic fistula grades A, B, and C rate, severe pancreatic fistula (grades B and C) rate, bile leakage rate, postoperative haemorrhage rate, and perioperative mortality rate.

Quantitative data (age, BMI, pancreatic duct diameter, operative time, intraoperative blood loss, postoperative hospital stay) were compared between the experimental and control groups. Initially, a Kolmogorov-Smirnov (KS) test was used for normality assessment, and an F test was used for homogeneity of variance. For normally distributed data, the mean ± SD was used for description. If variance homogeneity was present, a t test was used for group comparisons; otherwise, a rank-sum test was employed. For nonnormally distributed data in at least one group, the median ± range was calculated, and comparisons were made using a rank-sum test for two completely independent samples. Categorical variables are presented as counts and percentages, with comparisons between test and control groups made using the chi-square test or Fisher's exact test. The odds ratio (OR) and 95% confidence interval (*CI*) of categorical variables were calculated using two-tailed tests.

For subgroup analysis, pancreatic duct diameter was used for stratification to assess the impact of surgical method on pancreatic fistula in populations with duct diameters <= 3 mm and > 3 mm. Additional assessments were made across different age groups (<60 years, >=60 years), BMI categories (<18.5, 18.5-24.0, >24 kg/m^2), sex, hypertension status, diabetes status, and stent placement, as well as among different pathological types.

Multiple models have been developed to assess the impact of surgical methods on pancreatic fistula development via sensitivity analysis. The base model (Model 1) included only the surgical method. Model 2 was adjusted for sex, age, and BMI, while Model 3 was further adjusted for diabetes status, hypertension status, pathological type, coronary stent placement, and pancreatic duct diameter. All models were constructed using multivariate logistic regression with all variables included.

All the statistical analyses were performed using R software (version 4.2.3, R Foundation for Statistical Computing, Vienna, Austria, https://cran.r-project.org/). All tests were two-tailed, with a significance level set at $P<0.05$.

3 Results

3.1 Patient clinical baseline characteristics

Initially, quantitative indicators (age, BMI, pancreatic duct diameter, operative time, postoperative hospital stay, and intraoperative blood loss) of patients in both groups were subjected to normality testing. Age and BMI were found to follow a normal distribution and were thus described using the mean ± standard deviation. In contrast, indicators such as pancreatic duct diameter, operative time, postoperative hospital stay, and intraoperative blood loss did not conform to a normal distribution and were therefore described using the median ± range (Supplementary Table S1 in Supplementary 1).

The study included a total of 78 patients; 43 patients were treated with the five-needle method (test group), and 35 patients were treated with the duct-to-mucosa method (control group). The average age was 63 ± 9 years, with no significant difference in age between the test group and control group (Z=0.116, p=0.908). There were 44 male patients (56.4%). The average BMI for all subjects was 24.7 ± 4.0 kg/m^2, and the average pancreatic duct diameter was 4 ± 5 mm. Among all the subjects, 28 (35.9%) had pancreatic head cancer, 32 (41.0%) had cholangiocarcinoma, and 18 (23.1%) had duodenal papillary cancer. A total of 33 patients (42.3%) had hypertension, 18 (23.1%) had diabetes, and 7 (9.0%) had undergone coronary stent placement. There were no significant differences in clinical baseline data, such as age, sex, BMI, pancreatic duct diameter, diagnosis, or underlying disease status, between the test group and control group (Table 2).

3.2 Evaluation of clinical outcome indicators

3.2.1 Primary outcome indicators

Twenty-one out of the 78 patients experienced a pancreatic fistula, representing 26.9% of all patients, including 15 with Grade A fistulas (19.2%) and 6 with severe fistulas (grades B and C), 7.7%). In the test group of 43 patients who were treated with the five-needle method, 11 (25.6%) developed a pancreatic fistula (9 Grade A fistulas, 20.9%; 2 severe fistulas, 4.7%), whereas in the control group of 35 patients who were treated with the Duct-to-Mucosa method, 10 (28.6%) developed a pancreatic fistula (6 Grade A fistulas, 17.1%). 4 severe fistulas, 11.4%). There was no significant difference in the occurrence rate of pancreatic fistulas between the test and control groups (25.6% vs. 28.6%, p=0.767). Table 3). However, there was a trend towards a lower incidence of pancreatic fistulas in the test group than in the control group (rate difference of 2.99%, 95% CI: -17.75%, 24.32%). Similarly, the percentage of patients with severe pancreatic fistulas tended to be lower in the test group than in the control group (4.7% vs. 11.4%, p=0.400; difference of 6.78%, 95% CI: -6.04, 21.69).

3.2.2 Secondary outcome indicators

There were no significant differences in the Grade A, Grade B or Grade C pancreatic fistula rate, postoperative hospital stay, intraoperative blood loss, postoperative haemorrhage rate, or postoperative death rate between the test group and the control group (Table 3). However, the test group had a significantly shorter operative time (270 ± 170 mins vs. 300 ± 210 mins, p=0.019).

3.3 Subgroup analysis

All patients were stratified into groups based on age, BMI, sex, hypertension status, coronary heart disease status, diabetes status, or whether the pancreatic duct diameter exceeded 3 mm. The study revealed that in patients with a pancreatic duct diameter of 3 mm or

TABLE 2 Comparison of baseline characteristics between the 'Five-Needle' method group and the 'Duct-to-Mucosa' method group.

Variables	Total n=78	'Duct-to-Mucosa' method group n=35	'Five-Needle' method Group n=43	t/ z/χ^2	*P*
Age (years, mean ± SD)	63 (9)	63 (9)	63 (10)	-0.116	0.908
<60 years (n(%))	26(33.3)	11(31.4)	15(34.9)	0.104	0.747
>= 60 years(n(%))	52(66.7)	24(68.6)	28(65.1)		
BMI (kg/m^2, mean ± SD)	24.7(4.0)	24.8 (4)	24.7(4.1)	-0.17	0.865
18.5-24.0(normal, n(%))	25(32.1)	10(28.6)	15(34.9)	0.676	0.713
<18.5 (underweight, n(%))	7(9.0)	4(11.4)	3(7.0)		
>24(overweight, n(%))	46(59.0)	21(60.1)	25(58.1)		
Pancreatic duct diameter (mm, median ± range)	4 (5)	4 (4)	3 (3)	-2.059	0.039
Sex					
Male(n(%))	44(56.4)	20(57.1)	24(55.9)	0.014	0.906
Female(n(%))	34(43.6)	15(42.9)	19(44.2)		
Hypertension					
No(n(%))	45(57.7)	21(60.0)	24(55.8)	0.139	0.71
Yes(n(%))	33(42.3)	14(40.0)	19(44.2)		
Diabetes					
No(n(%))	60(76.9)	27(77.1)	33(76.7)	0.002	0.967
Yes(n(%))	18(23.1)	8(22.9)	10(23.3)		
Coronary stent placement					
No(n(%))	71(91.0)	32(91.4)	39(90.7)	–	0.998
Yes(n(%))	7(9.0)	3(8.6)	4(9.3)		
Pathological type					
Cholangiocarcinoma (n(%))	32(41.0)	16(45.7)	16(37.2)	2.861	0.329
Duodenal papillary cancer (n(%))	18(23.1)	5(14.3)	13(30.2)		
Pancreatic head cancer (n(%))	28(35.9)	14(40.0)	14(32.5)		

less (including 3 mm), the incidence of pancreatic fistula in the test group was lower than that in the control group (12.5% vs. 53.8%, p=0.007). Conversely, in patients with a duct diameter greater than 3 mm, the incidence of pancreatic fistula in the test group was higher than that in the control group (41.2% vs. 13.6%, p=0.041). Finally, there were no significant differences in the incidence of pancreatic fistula between the test and control groups across different age groups, sexes, or patients with or without various basic diseases (Table 4).

3.4 Sensitivity analysis

Multivariate logistic regression analysis was used to develop several models. Model 1 included the surgical method as the sole independent variable. Models 2 and 3 incorporated adjustments for various covariates. In all three models, the incidence of pancreatic fistula did not significantly differ between the test and control groups, as indicated by the 95% CI of the OR encompassing 1. However, the regression coefficients were negative regarding the intervention measures and presence of pancreatic fistula. This suggests that the absolute number of pancreatic fistulas was lower in the test group than in the control group, as detailed in Supplementary Table S2 of Supplementary 1.

4 Discussion

The pancreas secretes approximately 1-2 litres of pancreatic juice daily in a healthy adult, containing a plethora of digestive

10.3389/fonc.2024.1347752

TABLE 3 Comparison of primary and secondary outcome variables between the five-needle method group and the Duct-to-Mucosa method group.

Outcomes	Variable	Total n=78	'Duct-to-Mucosa' method group n=35	'Five-Needle' method Group n=43	z/χ^2	P	OR(95% CI)
Primary Outcome	PF						
	No(n(%))	57(73.1)	25(71.4)	32(74.4)	0.088	0.767	0.921 (0.539, 1.574)
	Yes(n(%))	21(26.9)	10(28.6)	11(25.6)			
Secondary Outcomes	PF-A						
	No(n(%))	63(80.8)	29(82.9)	34(79.1)	0.178	0.673	1.151 (0.586, 2.260)
	Yes(n(%))	15(19.2)	6(17.1)	9(20.9)			
	PF-B						
	No(n(%))	74(94.9)	32(91.4)	42(97.1)	–	0.321	0.577 (0.309, 1.075)
	Yes(n(%))	4(5.1)	3(8.6)	1(2.3)			
	PF-C						
	No(n(%))	76(97.4)	34(97.1)	42(97.7)	–	0.998	0.895 (0.219, 3.658)
	Yes(n(%))	2(2.6)	1(2.9)	1(2.3)			
	PF(B+C)						
	No(n(%))	72(92.3)	31(88.6)	41(95.3)	–	0.401	0.646 (0.346, 1.207)
	Yes(n(%))	6(7.7)	4(11.4)	2(4.7)			
	OT (minutes, median ± range)	280 (270)	300 (210)	270 (170)	-2.336	0.019	–
	PHS (days, median ± range)	11 (16)	11 (16)	11 (11)	-0.714	0.475	
	IB (millilitre, median ± range)	150 (300)	150 (250)	150 (250)	-1.331	0.183	
	BL						
	No(n(%))	68(87.2)	30(85.7)	38(88.4)			
	Yes(n(%))	10(12.8)	5(14.3)	5(11.6)	–	0.745	0.882 (0.449, 1.733)
	PH						
	No(n(%))	71(91.0)	32(91.4)	39(90.7)	–	0.998	1.052 (0.431, 2.569)
	Yes (n(%))	7(9.0)	3(8.6)	4(9.3)			
	PD						
	No (n(%))	75(96.2)	33(94.3)	42(97.7)	–	0.999	0.661 (0.285, 1.529)
	Yes(n(%))	3(3.8)	2(5.7)	1(2.3)			

PF, pancreatic fistula; OT, operative time; PHS, postoperative hospital stay; IBL, intraoperative blood loss; BL, bile leak; PH, postoperative haemorrhage; PD, postoperative death.

enzymes (pancreatic lipase, protease, and amylase) essential for the digestion and absorption of food in the intestine. Postpartial pancreatectomy for benign or malignant pancreatic tumours, or even pancreatic trauma, is often necessary to re-establish an anastomosis between the remaining pancreatic duct and the jejunum to ensure the smooth entry of pancreatic juice into the intestine. However, due to the unique physicochemical properties of pancreatic juice, the activation of its digestive enzymes can degrade sugars, proteins, and fats. In the context of pancreatic surgery, leakage of pancreatic fluid into the peritoneal cavity can lead to severe complications such as infection, haemorrhage, and enteric fistulas, posing a significant risk to the patient's postoperative survival. Consequently, surgeons continually explore various methods to prevent pancreatic leakage, including improvements

10.3389/fonc.2024.1347752

TABLE 4 Subgroup analysis to explore the impact of the characteristics of the 'Five-Needle' method group and the 'Duct-to-Mucosa' method group.

Variable	Total	'Duct-to-Mucosa' method group	'Five-Needle' method group	$\chi 2$	P	OR (95% CI)
Sex						
male(n,(%))	9(20.5)	4(20.0)	5(20.8)	0.051	0.946	1.029 (0.455,2.323)
female(n,(%))	12 (34.3)	6(40.0)	6(31.6)	0.261	0.611	0.818 (0.384,1.743)
Age						
< 60 years	7(26.9)	3(27.3)	4(26.7)	0.001	0.973	0.982 (0.360,2.684)
>= 60 years	38 (26.9)	7(29.2)	7(25.0)	0.114	0.763	0.895 (0.476,1.683)
BMI						
18.5-24.0 kg/m^2 (normal, n(%))	5(20.0)	3(30.0)	2(13.2)	1.041	0.307	0.583 (0.230,1.482)
<18.5 kg/m^2 (underweight, n(%))	0(0.0)	0(0.0)	0(0.0)	–	–	–
>24 kg/m^2 (overweight, n(%))	16 (34.8)	7(33.3)	9(36.0)	0.036	0.849	1.067 (0.543, 2.094)
Hypertension						
No(n(%))	9(20.0)	5(23.8)	4(16.7)	0.357	0.551	0.800 (0.402, 1.594)
Yes(n(%))	12 (36.4)	5(35.7)	7(36.8)	0.004	0.971	1.029 (0.448,2.363)
Type 2 diabetes						
No(n(%))	16 (26.7)	7(25.9)	9(27.3)	0.014	0.907	1.039 (0.546,1.976)
Yes(n(%))	5(27.8)	3(37.5)	2(20.0)	0.678	0.411	0.641 (0.238,1.729)
Pathology						
cholangiocarcinoma(n(%))	10 (31.3)	5(31.3)	5(31.3)	0.001	0.998	1.000 (0.474,2.112)
Carcinoma of duodenal papilla (n(%))	3(16.7)	2(40.0)	1(7.7)	2.714	0.099	0.300 (0.083,1.090)
pancreatic cancer(n(%))	8(28.6)	3(21.4)	5(35.7)	0.701	0.403	1.467 (0.551,3.902)
Pancreatic duct diameter						
<=3 mm	10 (27.0)	7(53.8)	3(12.5)	7.039	0.007	0.317 (0.141,0.716)
> 3 mm	11 (26.8)	3(13.6)	8(41.2)	4.209	0.041	2.322 (0.852,6.329)
Coronary stent implantation						
No(n(%))	17 (23.9)	8(25.0)	9(23.1)	0.036	0.851	0.944 (0.526,1.697)
Yes(n(%))	4(57.1)	2(66.7)	2(50.0)	0.194	0.659	0.667 (0.102,4.354)

in surgical methods, intraoperative protective measures, and perioperative pharmacological prevention. Over the years, the methods for pancreatojejunostomy have evolved from initial pancreatic stump-jejunum invagination and pancreatic stump-gastric invagination to the more commonly used 'Duct-to-Mucosa' anastomosis (11, 13), which is widely applied in both laparoscopic and open pancreaticoduodenectomy. Despite these advances, the incidence of postoperative pancreatic fistula and related complications has not significantly decreased, and the occurrence of pancreatic fistula after pancreatojejunostomy is still a major challenge impeding the advancement of pancreatic surgery (14–16).

With the advancement of minimally invasive methods, laparoscopic pancreatic surgery has become increasingly prevalent. However, the flexibility of laparoscopic operations is somewhat limited, and certain anatomical angles are less than ideal, especially during pancreatojejunostomy. The small angle between the needle and the needle holder makes the procedure awkward. Furthermore, in cases where the pancreatic texture is soft and the pancreatic duct diameter is small, traditional anastomosis methods are time-consuming and imprecise, potentially exacerbating serious postoperative complications such as pancreatic fistula. This is particularly true for patients with narrow pancreatic ducts, where suturing is difficult, and the incidence of postoperative pancreatic fistula is relatively high (17, 18). Additionally, the difficulty of performing pancreatojejunostomy is a major reason for a prolonged operation and conversion to open surgery, adversely affecting patient safety during the perioperative period and postoperative recovery, as well as undermining the surgeon's confidence. In recent years, to adapt to LPD, domestic scholars have made various improvements and proposed more straightforward methods, such as Hong Defei's "Hong's One-Needle" method and Liu Rong's "301" method (7, 8, 19, 20). These methods achieve biological healing through precise apposition of the cut pancreatic surface to the jejunal serosal layer, while pancreatic juice is drained into the jejunal cavity through a stent tube, thereby preventing pancreatic fistula (19). In summary, with the development of minimally invasive methods and surgeons gaining a deeper understanding of the importance of physiological healing at anastomotic sites, simplified and safe pancreatojejunostomy methods are gradually gaining acceptance over previous, more complex methods.

Drawing inspiration and learning from the methods and experiences of several domestic predecessors in laparoscopic and robot-assisted pancreatojejunostomy, the new five-needle method was proposed for laparoscopic pancreatojejunal mucosal anastomosis (as detailed in the surgical methods section). Compared to other anastomosis methods, this method has the following main characteristics. The pancreatic stump is completely sutured using a through-and-through method, eliminating the need for interrupted or continuous suturing from the pancreatic duct to the jejunum. As such, it is not limited by the diameter of the pancreatic duct and is even more suitable for patients with a narrow pancreatic duct, a soft pancreatic texture, and a small pancreatic neck. None of the five sutures are passed through the full thickness of the pancreas and intestine, reducing the impact on the blood supply of the pancreatojejunostomy site and preventing the penetrating injury of sutures to the pancreatic duct and intestinal tube, which could lead to the leakage of pancreatic fluid through the suture holes, forming a fistula. For pancreatojejunostomy, we adhere to the principles of 'tight, loose, sparse' (tight apposition between the pancreatic cut surface and the intestinal wall, leaving no dead space; natural stacking of the intestine on the cut surface after being brought up to the wound, ensuring no tension postanastomosis; and sparse suturing to minimize tissue cutting injury and ischaemia). This method aligns well with these principles and robustly ensures the safety of the anastomosis site.

In our study, the clinical data of 78 patients were collected to investigate the efficacy of the five-needle method for pancreaticojejunostomy during laparoscopic pancreaticoduodenectomy. The findings revealed that the method did not significantly differ from the traditional 'Duct-to-Mucosa' method, particularly in terms of the incidence of pancreatic fistula, the incidence of biliary leakage, the rate of postoperative haemorrhage, the rate of perioperative mortality, the duration of hospital stay, or the intraoperative blood loss volume. Further analysis through multivariable logistic regression revealed negative regression coefficients across the three models, indicating a lower absolute incidence of pancreatic fistula in the experimental group than in the control group. The consistency of the results across different models underscores their robustness. This signifies that the 'Five-Needle' method for pancreaticojejunostomy is not only safe and effective but also has a significantly lower incidence of clinical fistula than the control group, making it a promising method worthy of broader clinical application.

According to the secondary observational indices, the test group had significant advantages over the control group in certain aspects. First, statistically, the overall operative time for the conventional anastomosis method was significantly longer than that for the five-needle method. Since this was a retrospective study, we did not have data on the duration of pancreato-enterostomy. However, as an important surgical step, it was believed that the reduction was attributable to the decrease in pancreaticojejunostomy time. The primary aim of the five-needle method was to simplify the anastomosis process, thereby reducing the operative time, minimizing the need for conversion to open surgery, and enhancing confidence among novice surgeons. Second, as previously mentioned, the diameter of the pancreatic duct is a crucial objective factor influencing pancreaticojejunostomy, especially in cases of narrower ducts where anastomosis is relatively challenging. In our study, there was no statistically significant difference in the incidence of pancreatic fistula between the two surgical methods. However, through subgroup analysis of pancreatic duct diameter, it was found that in patients with a duct diameter of 3 mm or less, the incidence of pancreatic fistula in the five-needle method group was lower than that in the duct-to-mucosa group. This further confirms the suitability of the 'Five-Needle' method for patients with narrower pancreatic ducts, as it has high practical value in clinical practice. The advantage arises from our focus on ensuring closer alignment between the support tube and the pancreatic duct during suturing, without the need to ensure that the stitches precisely penetrate the pancreatic duct.

There are still many shortcomings in the study. First, although there was no significant difference between the two groups in the statistical analysis of baseline data in this study, the selection of surgical methods is susceptible to interference by patients' objective conditions because this was a retrospective study. Second, the collection of observation indicators, such as the amount of abdominal drainage fluid and the drainage time of pancreatic fistula patients, was not detailed enough, and the duration of pancreatoenteroanastomosis was also not available. Third, the study was an exploratory study, with a small sample size that does not allow for definitive conclusions. Fourth, in the realm of clinical predictive modelling research, nonlinear analysis has progressively become a focal method, and multitemporal data hold greater value (21, 22). Therefore, in future predictive studies, the incorporation of multidimensional and multitemporal models, as well as nonlinear models, should be duly integrated into the endeavours undertaken at our research centre. In addition, there is a need for larger scale, multicentre randomized, and open studies to establish more robust findings in the future.

5 Conclusion

In summary, the five-needle method can significantly reduce the incidence of pancreatic fistula and shorten the operative time without increasing the incidence of other surgery-related complications in patients with narrower pancreatic ducts and is a safe and effective laparoscopic method for LPD. Therefore, the application of this new method can further promote the widespread adoption of LPD, warranting its broader clinical implementation.

Data availability statement

The raw data supporting the conclusions of this article will be made available by the authors, without undue reservation.

Author contributions

ZW: Conceptualization, Methodology, Writing – original draft. BZ: Investigation, Project administration, Resources, Validation, Writing – review & editing. HX: Data curation, Formal analysis, Supervision, Visualization, Writing – original draft, Writing – review & editing. WZ: Conceptualization, Investigation, Methodology, Project administration, Resources, Writing – review & editing.

Funding

The author(s) declare financial support was received for the research, authorship, and/or publication of this article. This study was supported by the Natural Science Foundation of Gansu Province Project (22JR5RA901), the Three-year Action Plan for Promoting Clinical Skills and Innovation Ability of Municipal Hospitals (SHDC2022CRS039), the Talent Fund of Longhua Hospital affiliated to Shanghai University of Traditional Chinese Medicine (LH001.007), Research Ward Construction Project of Shanghai Hospital Development Center (SHDC2022CRW006).

Acknowledgments

This is a short text to acknowledge the contributions of specific colleagues, institutions, or agencies that aided the efforts of the authors.

Conflict of interest

The authors declare that the research was conducted in the absence of any commercial or financial relationships that could be construed as a potential conflict of interest.

Publisher's note

Supplementary material

The Supplementary Material for this article can be found online at: https://www.frontiersin.org/articles/10.3389/fonc.2024.1347752/full#supplementary-material

References

1. Wang M, Cai H, Meng L, Cai Y, Wang X, Li Y, et al. Minimally invasive pancreaticoduodenectomy: A comprehensive review. *Int J Surg*. (2016) 35:139–46. doi: 10.1016/j.ijsu.2016.09.016

2. Karim SAM, Abdulla KS, Abdulkarim QH, Rahim FH. The outcomes and complications of pancreaticoduodenectomy (Whipple procedure): Cross sectional study. *Int J Surg*. (2018) 52:383–7. doi: 10.1016/j.ijsu.2018.01.041

3. Dong Z, Xu J, Wang Z, Petrov MS. Stents for the prevention of pancreatic fistula following pancreaticoduodenectomy. *Cochrane Database Syst Rev*. (2016) 2016: CD008914. doi: 10.1002/14651858.CD008914.pub3

4. Schuh F, Mihaljevic AL, Probst P, Trudeau MT, Müller PC, Marchegiani G, et al. A simple classification of pancreatic duct size and texture predicts postoperative pancreatic fistula: A classification of the international study group of pancreatic surgery. *Ann Surg*. (2023) 277:e597–608. doi: 10.1097/SLA.0000000000004855

5. Kawaida H, Kono H, Hosomura N, Amemiya H, Itakura J, Fujii H, et al. Surgical techniques and postoperative management to prevent postoperative pancreatic fistula after pancreatic surgery. *World J Gastroenterol*. (2019) 25:3722–37. doi: 10.3748/wjg.v25.i28.3722

6. Gagner M, Pomp A. Laparoscopic pylorus-preserving pan-creatoduodenectomy. *Surg Endosc*. (1994) 8:408–10. doi: 10.1007/BF00642443

7. Wang M, Peng B, Liu J, Yin X, Tan Z, Liu R, et al. Practice patterns and perioperative outcomes of laparoscopic pancreaticoduodenectomy in China: A retrospective multicenter analysis of 1029 patients. *Ann Surg*. (2021) 273:145–53. doi: 10.1097/SLA.0000000000003190

8. Qin R, Kendrick ML, Wolfgang CL, Edil BH, Palanivelu C, Parks RW, et al. International expert consensus on laparoscopic pancreaticoduodenectomy. *Hepatobil Surg Nutr*. (2020) 9:464–83. doi: 10.21037/hbsn

9. Peng L, Lin S, Li Y, Xiao W. Systematic review and meta-analysis of robotic versus open pancreaticoduodenectomy. *Surg Endosc*. (2017) 31:3085–97. doi: 10.1007/s00464-016-5371-2

10. Lyu Y, Cheng Y, Wang B, Xu Y, Du W. Minimally invasive versus open pancreaticoduodenectomy: an up-to-date meta-analysis of comparative cohort studies. *J Laparoendosc Adv Surg Tech A*. (2019) 29:449–57. doi: 10.1089/lap.2018.0460

11. Hua J, He Z, Qian D, Meng H, Zhou B, Song Z. Duct-to-mucosa versus invagination pancreaticojejunostomy following pancreaticoduodenectomy: A systematic review and meta-analysis. *J Gastrointest Surg*. (2015) 19(10):1900–9. doi: 10.1007/s11605-015-2913-1

12. Bassi C, Marchegiani G, Dervenis C, Sarr M, Abu Hilal M, Adham M, et al. The 2016 update of the International Study Group (ISGPS) definition and grading ofpostoperative pancreatic fistula: 11 Years After. *Surgery*. (2017) 161:584–91. doi: 10.1016/j.surg.2016.11.014

13. Bai X, Zhang Q, Gao S, Lou J, Li G, Zhang Y. Duct-to-Mucosa vs Invagination for Pancreaticojejunostomy after Pancreaticoduodenectomy: A Pro-spective, Randomized Controlled Trial from a Single Surgeon. *J Am Coll Surg*. (2016) 222:10–8. doi: 10.1016/j.jamcollsurg.2015.10.003

14. Zhang B, Xu Z, Gu W, Zhou J, Tang N, Zhang S, et al. Postoperative complications and short-term prognosis of laparoscopic pancreaticoduodenectomy vs. open pancreaticoduodenectomy for treating pancreatic ductal adenocarcinoma: a retrospective cohort study. *World J Surg Oncol*. (2023) 21:26. doi: 10.1186/s12957-023-02909-x

15. Lee B, Yoon YS, Kang CM, Choi M, Lee JS, Hwang HK, et al. Fistula risk score-adjusted comparison of postoperative pancreatic fistula following laparoscopic vs open pancreatoduodenectomy. *J Hepatobil Pancreat Sci*. (2021) 28:1089–97. doi: 10.1002/jhbp.866

16. Boggi U, Amorese G, Vistoli F, Caniglia F, De Lio N, Perrone V, et al. Laparoscopic pancreaticoduodenectomy: a systematic literature review. *Surg Endosc*. (2015) 29:9–23. doi: 10.1007/s00464-014-3670-z

17. Hosotani R, Doi R, Imamura M. Duct-to-mucosa pancreaticojejunostomy reduces the risk of pancreatic leakage after pancreatoduo-denectomy. *World J Surg*. (2002) 26:99–104. doi: 10.1007/s00268-001-0188-z

18. Wang M, Xu S, Zhang H, Peng S, Zhu F, Qin R. Imbedding pancreaticojejunostomy used in pure laparoscopic pancreaticoduodenectomy for nondilated pancreatic duct. *Surg Endosc*. (2017) 31:1986–92. doi: 10.1007/s00464-016-4805-1

19. Hong D, Li H, Liu X, Jiang P, Yu G, Liu X, et al. Incidence of postoperative pancreatic fistula after using a defined pancreaticojejunostomy technique for laparoscopic pancreaticoduodenectomy: A prospective multicenter study on 1033 patients. *Int J Surg*. (2022) 101:106620. doi: 10.1016/j.ijsu.2022.106620

20. Chao YJ, Lu WH, Liao TK, Su PJ, Wang CJ, Lai CH, et al. Feasibility of simultaneous development of laparoscopic and robotic pancreaticoduodenectomy. *Sci Rep*. (2023) 13:6190. doi: 10.1038/s41598-023-33269-x

21. Zhang SX, Wang JC, Li ZW, Zheng JX, Zhou WT, Yang GB. Impact factors of Blastocystis hominis infection in persons living with human immunodeficiency virus: a large-scale, multi-center observational study from China. *Infect Dis Poverty*. (2023) 12:82. doi: 10.1186/s40249-023-01137-5

22. Lu Z, Yang M, Pan C, et al. Multi-modal deep learning based on multi-dimensional and multi-level temporal data can enhance the prognostic prediction for multi-drug resistant pulmonary tuberculosis patients. *Sci One Health*. (2022) 1:100004. doi: 10.1016/j.soh.2022.100004

frontiers | Frontiers in Oncology

TYPE Methods
PUBLISHED 05 July 2024
DOI 10.3389/fonc.2024.1346237

OPEN ACCESS

EDITED BY
Sharon R. Pine,
University of Colorado Anschutz Medical Campus, United States

REVIEWED BY
Antonella Argentiero,
National Cancer Institute Foundation (IRCCS), Italy
Stefano Marletta,
University of Verona, Italy

*CORRESPONDENCE
Sungmoon Jeong
jeongsm00@gmail.com

†These authors have contributed equally to this work and share first authorship

RECEIVED 29 November 2023
ACCEPTED 31 May 2024
PUBLISHED 05 July 2024

CITATION
Kim J, Bae S, Yoon S-M and Jeong S (2024) Roadmap for providing and leveraging annotated data by cytologists in the PDAC domain as open data: support for AI-based pathology image analysis development and data utilization strategies.
Front. Oncol. 14:1346237.
doi: 10.3389/fonc.2024.1346237

Roadmap for providing and leveraging annotated data by cytologists in the PDAC domain as open data: support for AI-based pathology image analysis development and data utilization strategies

Jongkwang Kim[1†], Sumok Bae[1†], Seong-Mi Yoon[2] and Sungmoon Jeong[1*]

[1]Department of Medical Informatics, School of Medicine, Kyungpook National University, Daegu, Republic of Korea, [2]Department of Pathology at the Medical Center, Medical Research Institute, ORTHOTECH, Daegu, Republic of Korea

Pancreatic cancer is one of the most lethal cancers worldwide, with a 5-year survival rate of less than 5%, the lowest of all cancer types. Pancreatic ductal adenocarcinoma (PDAC) is the most common and aggressive pancreatic cancer and has been classified as a health emergency in the past few decades. The histopathological diagnosis and prognosis evaluation of PDAC is time-consuming, laborious, and challenging in current clinical practice conditions. Pathological artificial intelligence (AI) research has been actively conducted lately. However, accessing medical data is challenging; the amount of open pathology data is small, and the absence of open-annotation data drawn by medical staff makes it difficult to conduct pathology AI research. Here, we provide easily accessible high-quality annotation data to address the abovementioned obstacles. Data evaluation is performed by supervised learning using a deep convolutional neural network structure to segment 11 annotated PDAC histopathological whole slide images (WSIs) drawn by medical staff directly from an open WSI dataset. We visualized the segmentation results of the histopathological images with a Dice score of 73% on the WSIs, including PDAC areas, thus identifying areas important for PDAC diagnosis and demonstrating high data quality. Additionally, pathologists assisted by AI can significantly increase their work efficiency. The pathological AI guidelines we propose are effective in developing histopathological AI for PDAC and are significant in the clinical field.

KEYWORDS

pancreatic ductal adenocarcinoma, deep convolutional neural network, whole slide image, histopathology, supervised learning, dice score, high quality

1 Introduction

Pancreatic cancer is one of the most lethal malignancies, with a five-year survival rate of approximately 5%–9%, which has remained virtually unchanged since the 1960s (1, 2). More than 85% of pancreatic cancers are adenocarcinomas (PDACs), which arise from the pancreatic duct epithelium in the head, body, and tail of the pancreas (2). The head of the pancreas is the most common site of PDAC. PDAC is not effectively preventable or screened for and is associated with 98% of expected lifetime loss and 30% of disability-adjusted life years (3, 4). In addition, recent studies have suggested that a molecular subgroup of PDAC characterized by bone metastases may have an unfavorable outcome, suggesting that this subgroup of patients may have distinctive prognostic features and may be potential candidates for specific targeted therapies (5). Further molecular-level research is needed to explore this, which could contribute to better PDAC treatments and AI development. Nevertheless, research funding for PDAC remains markedly lower than for other cancer types; the European Commission and the United States Congress designated it as a neglected cancer (3). The rapid progression and high frequency of pancreatic cancer distant metastases pose a challenge in pathology, where the misdiagnosis consequences can be severe (6–8). Multidetector computed tomography, magnetic resonance imaging, and endoscopic ultrasound are recommended initial imaging modalities for timely PDAC diagnosis (9). The gold standard for clinical diagnosis is the histopathologic imaging assessment by a pathologist (10); however, during the diagnostic process, pathologists must repeatedly zoom in and out of the field of view, determine areas critical for diagnosis, and classify them according to features because of the large slide sizes. Thus, the manual analysis of pathological slides is extremely time-consuming and labor-intensive and may miss important diagnostic information (11). In modern medicine, artificial intelligence (AI) is emerging as a revolutionary technology that can help make faster and more accurate decisions in the medical field. This has led to its application in a wide range of medical fields, including radiology, pathology, pharmacology, infectious diseases, and personalized decision-making, and it has shown the potential to improve current standards of care (12).

Digital pathology has become a rapid and convenient standard of practice in pathology, as it allows for the management and analysis of data from digitized specimen slides using high-resolution digital imaging (13). With the significant advances in artificial intelligence (AI) algorithms and data management capabilities, combining digital pathology and AI has emerged as a front-runner in modern clinical practice (13, 14). The number of publications on AI for clinical decision-making in oncology has increased exponentially in recent years (15).

In surgical pathology, AI can be used to evaluate lymph nodes (LNs) for the presence of metastatic disease by automatically identifying metastatic cancer cells in whole slide images (WSI), which can help in the staging of cancer patients and the prediction of prognosis (16). Other examples include the use of pathology AI for microbial identification to supplement manual microscopy, which is a time-consuming process for the efficient identification of many microbes (17). Digital pathology has shown promising results with regard to the digital evaluation of cytological samples, with the development of portable mobile devices such as smartphones that allow pathologists to examine both surgical and cytological samples (18). The development of digital pathology and AI in various pathology fields has the potential to improve the quality of healthcare in resource-limited settings, where there is a shortage of specialized healthcare professionals. Digital pathology systems can enable remote patient samples to be easily sent to experts, and AI-based automated analysis can be used. Whole slide imaging (WSI) is a major innovation in pathology, which digitizes glass slides to improve pathology workflow, reproducibility, availability of educational materials, outreach to underserved populations, and inter-institutional collaboration (19). However, due to the limited computing resources available currently, performing image analysis using whole slide images (WSIs) as input to convolutional neural network (CNN) classification models (20), which are currently widely used in image-based AI, remains challenging. Here, we adopted a novel scheme to realize whole slide analysis while preserving the high resolution and accuracy of pathological slide analysis. Deep learning approaches to WSI analysis have major limitations: labeled data for histopathology images are particularly scarce; WSIs are large; experienced pathologists must invest significant time and cost to annotate them using specialized labeling tools; and pathological images have rich background regions (e.g., vessels or lymphocytes) that can affect the analysis (21). Here, we provide high-quality data hand-drawn by Hepatobiliary-pancreatic pathologists in an open-access manner—so that anyone can easily use it—to address the abovementioned issues. We applied basic supervised learning (SL), already open to the public, as a data quality assessment and application method. SL algorithms rely on a training dataset that depends on ground truth labels provided by human annotations for input variables (i.e., features) to predict the corresponding output, allowing SL models to mimic expert annotators in predicting features of unknown inputs (22). This study suggests an effective application method for the quality assessment of open-annotation data provided by Hepatobiliary-pancreatic pathologists and the development of pathology AI (Figure 1).

2 Materials and methods

2.1 Data collection

2.1.1 Dataset

The primary data set comprises pathology images of Clinical Proteomic Tumor Analysis Consortium (CPTAC) patients collected and publicly released by The Cancer Imaging Archive to enable researchers to investigate cancer phenotypes that may be correlated with the corresponding proteomic, genomic, and clinical data. Pathology images are collected as part of the CPTAC qualification workflow (23, 24). The data collection includes hospitals from three institutions (Beaumont Health System, Royal Oak, MI; Boston Medical Center, Boston, MA; St. Joseph's Hospital and Medical Center, Phoenix, AZ) and medical research institutes from three institutions (International Institute

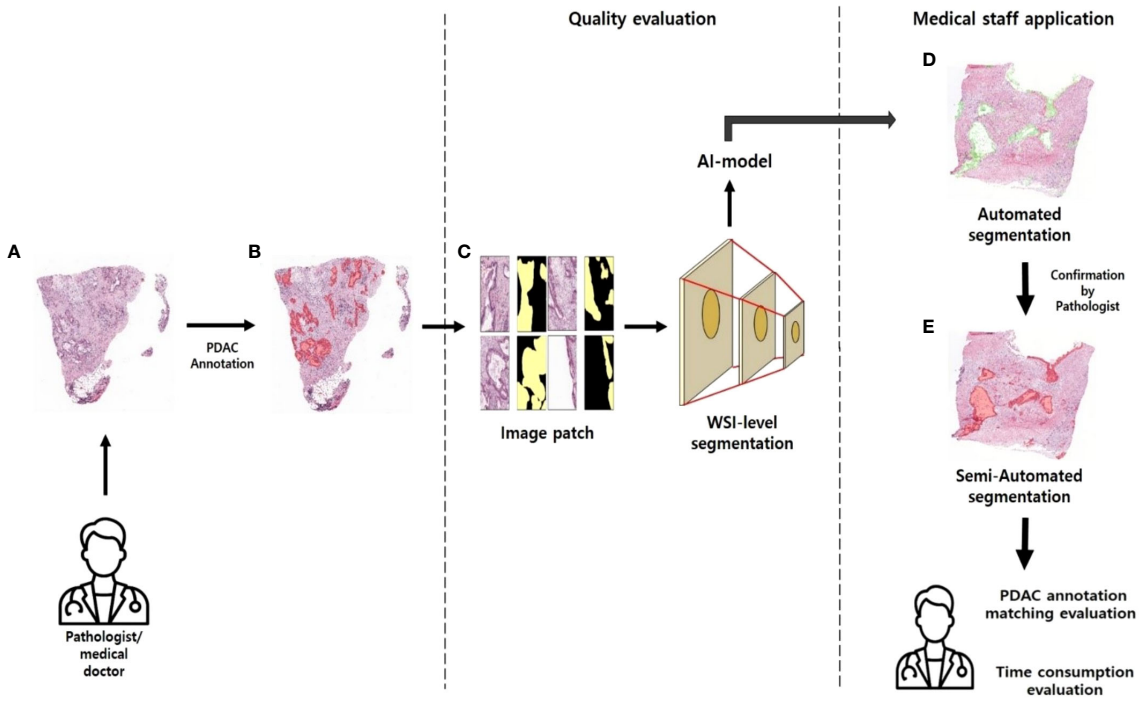

FIGURE 1
Approaches to pathology research **(A)** WSI images of PDAC patients without labels. **(B)** WSI images annotated in PDAC regions. **(C)** Patch images with masked annotated PDAC regions. **(D)** PDAC region predicted by AI model. **(E)** Pathologists review the areas predicted as PDAC by the AI model and annotate them.

for Molecular Oncology, Poznań, Poland; University of Calgary, Alberta, Canada; Cureline, Inc. team and clinical network, Brisbane, CA) and includes subjects from the National Cancer Institute's CPTAC Pancreatic Adenocarcinoma (CPTAC-PDA) cohort. All CPTAC cohorts are released as single-cohort data sets or, where appropriate, are split into discovery and validation. For this study, we selected 11 high-resolution WSIs of cancerous pancreatic tissue samples as the dataset. Each sample was collected via surgical resection and stained with hematoxylin and eosin (H&E) and stored as high-resolution WSIs (Figure 2A). The inclusion criteria for patient samples were as follows: organ: pancreas; tumor site: head, body, tail; disease: PDAC; patient age: 40–80 years old; and staining type: H&E. WSIs are typically about 100 MB, with a resolution of about 10,000 × 10,000 pixels, but the size can vary between WSIs. The data utilization method we present leverages our provided labeled data to generate tiles to train segmentation models.

2.1.2 Data annotation

In this study, model training is conducted using an SL approach. Training, test, and validation sets were prepared to train and validate the PDAC detection algorithm on labeled WSIs. All annotations for the annotation dataset were validated by a common golden standard of at least two double board-certified cytopathologists & Hepatobiliary-pancreatic pathologists who agreed on the annotation placement (Figure 3). The WSI information for all annotation datasets is listed in Table 1. To generate ground truth SL labels, human encoders hand-drew annotations using the open-source pathology and bioimage analysis software QuPath (v0.1.3.5). For each WSI, the PDAC regions were annotated by Hepatobiliary-pancreatic pathologists with a red line (Figure 2B).

2.2 Data preprocessing

2.2.1 WSIs to patch images

In pathology diagnosis, high-resolution images are necessary for accurate diagnosis. Most WSIs are 10,000 × 10,000 pixels or larger and are typically stored as SVS files. However, directly using such high-resolution images in a deep learning model is not feasible due to the GPU memory limitations, which prevents implementing WSI convolutional operations. Therefore, it is necessary to reduce the images' size. However, directly downsizing high-resolution images to low-resolution ones can result in losing important features. To address this problem, a patch-based approach was adopted, allowing us to maintain the original resolution while dividing the image into smaller patches. The patch dataset comprised three types. First, each image was divided into partially overlapping patches for the training dataset to enhance the model's learning capability. Second, the validation and test datasets used in the model's quantitative evaluation did not require overlapping patch images; each image was divided into non-overlapping patches. These patch data types required the original and mask images to be divided into patches in the same manner, which was achieved using the scripting function provided by QuPath also used for

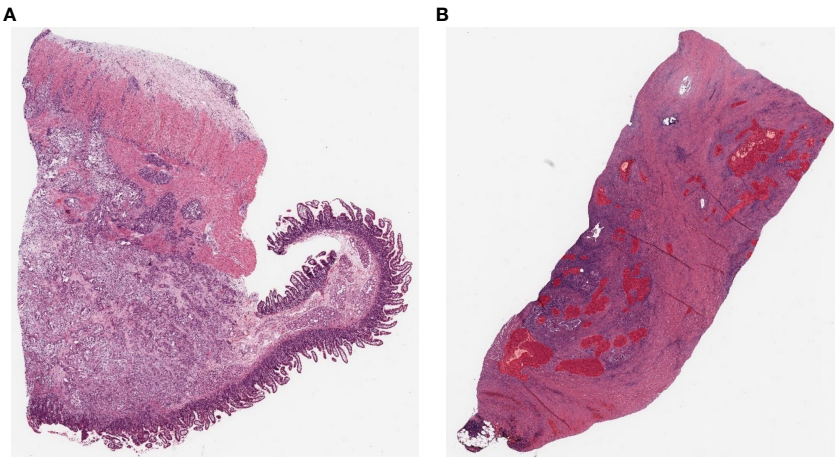

FIGURE 2
Example pathology slide images of PDAC patients **(A)** Open H&E-stained WSI image. **(B)** WSI image after hand-drawn annotation.

annotation. Last, the test dataset used in clinical evaluation required merging the patch images back into a single large image during the postprocessing stage when the WSI was divided into patch images. The PyHIST library was utilized, which outputs the x and y coordinates of each patch image during the patch division process (25), allowing tracking of each patch's spatial information and reconstructing the original image by aligning the patches based on their respective coordinates. These patches were saved as PNG files of 512 × 512 pixels and maintained the highest resolution of the WSI, which is 20X [0.5 microns per pixel (MPP)], to prevent resolution degradation. The MPP value was calculated as shown in Equation 1.

$$MPP = \frac{1\ \mu m}{pixel} \quad (1)$$

2.2.2 Augmentation

Data augmentation techniques are essential in data preprocessing to prevent overfitting and improve the AI models' performance during training. Various data augmentation methods

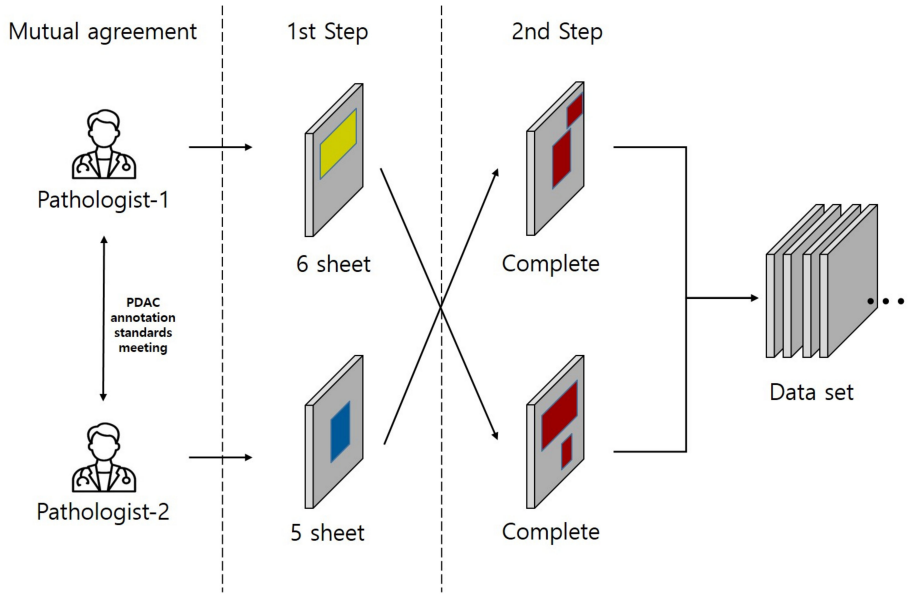

FIGURE 3
This study was conducted on a total of 11 Whole Slide Images (WSIs) where two pathologists agreed on a common annotation range for Pancreatic Ductal Adenocarcinoma (PDAC), also referred to as the gold standard, from each of 6 and 5 WSIs respectively. The annotation for PDAC was carried out in two steps. In the first step, the two pathologists individually annotated the images. In the second step, the pathologist who annotated in the first step had their work reviewed by the other pathologist. This second pathologist added any missed PDAC areas to the annotation, thus completing the annotation process. Yellow region: Annotation by Pathologist 1, Blue region: Annotation by Pathologist 2, Red region: Final completed annotation.

TABLE 1 Clinical information and characteristics of patients with pathology slides.

Slide ID	Tumor	Topographic Site	Tumor Site	THT	PTN	PTC	PN	Gender	Age
C3L-00017–22	PDA	Pancreas	Head	Ductal adenocarcinoma	20	100	0	Male	60–70
C3L-00017–23	PDA	Pancreas	Head	Ductal adenocarcinoma	20	100	0	Male	60–70
C3L-00102–21	PDA	Pancreas	Head	Ductal adenocarcinoma	20	98	0	Male	40–50
C3L-00102–22	PDA	Pancreas	Head	Ductal adenocarcinoma	10	100	0	Male	40–50
C3L-01637–21	PDA	Pancreas	Body	Ductal adenocarcinoma	20	90	5	Female	70–80
C3L-00277–21	PDA	Pancreas	Tail	Ductal adenocarcinoma	70	90	10	Male	60–70
C3L-00277–22	PDA	Pancreas	Tail	Ductal adenocarcinoma	70	90	0	Male	60–70
C3L-00277–23	PDA	Pancreas	Tail	Ductal adenocarcinoma	70	90	0	Male	60–70
C3L-01453–22	PDA	Pancreas	Tail	Ductal adenocarcinoma	60	90	0	Male	60–70
C3L-01662–23	PDA	Pancreas	Head	Ductal adenocarcinoma	70	100	0	Female	60–70
C3L-00819–22	PDA	Pancreas	Head	Ductal adenocarcinoma	60	100	0	Male	70–80

THT, Tumor Histological Type; PTN, Percent Tumor Nuclei; PTC, Percent Total Cellularity; PN, Percent Necrosis.

are available, and using appropriate augmentation techniques for each task is essential. For our task, which involved segmentation, applying the same augmentation techniques to the original and mask images was crucial as they were matched. Therefore, we implemented effective image transformations using the Albumentations library, which provides most of the commonly used augmentation techniques in deep learning while simultaneously transforming the original and mask images (26). We normalized the images for image transformations and then added noise through ColorJitter. Additionally, we applied various data augmentation techniques by randomly choosing one of three methods: HorizontalFlip, RandomRotate, and VerticalFlip. This approach allowed us to augment the data diversely. By implementing these image transformations, we created a training environment for the AI model to effectively learn the features of the target region, even in extreme conditions.

2.3 AI model architecture

Accurate segmentation of histopathological images is increasingly recognized as a key challenge in diagnosis and treatment. An appropriate deep learning model is essential for accurately segmenting histopathological features with various sizes and characteristics. Therefore, we adopted the DeepLabV3+ model and used ResNet18 as its backbone. Additionally, we employed transfer learning by applying pretrained weights from ImageNet to ResNet18, enabling the model to learn the general features of the images. Subsequently, we trained the model using histopathological images relevant to the main task and performed fine-tuning for the histopathological features. ResNet18 is a well-known model for image feature extraction and effectively overcomes the gradient vanishing problem when training deep neural networks through residual connections (27). This characteristic contributes to effectively extracting histopathological features with various sizes and complexities. Moreover, in DeepLabV3+, the features extracted from ResNet18 are utilized using the Atrous Spatial Pyramid Pooling (ASPP) method. ASPP employs parallel convolution layers with different dilate rates to capture receptive fields of various sizes (28), allowing accurate target classification at different scales without losing spatial information. In particular, for model training using histopathological images where features of various sizes are important, ASPP can comprehensively recognize features of various sizes, enabling more accurate training of the model. Therefore, we adopted DeepLabV3+ with ASPP as the base model and upsampled the features through the decoder part of DeepLabV3+. This process involved restoring the low-resolution feature maps to their original input size, thus obtaining the segmentation results as the final step of the model.

2.4 Data postprocessing

Unlike typical deep learning segmentation tasks, deep learning on WSIs requires a data preprocessing step to convert WSIs into

patch images. Additionally, during model training, unnecessary background images need to be removed. As a result, the mask images predicted from the model are output as patch images without including background images, similar to the input images. In typical quantitative AI model evaluation processes, the generated patch images and the corresponding label patch images can be compared using evaluation metrics to evaluate the model's performance. However, in our study, we conducted quantitative and qualitative evaluations to assess the effectiveness of AI assistance in histopathological diagnosis scenarios. Therefore, visualizing the mask patch images generated by the model to assist pathologists is essential. It requires a postprocessing step that comprises two main processes. First, the binary mask patch images obtained from the model's predictions are overlayed onto the original image patches. Second, the overlayed patch images are combined into a single large-sized image. The 1-channel grayscale mask images are converted into 3-channel RGB images while using distinctive colors to make them visually stand out. Then, utilizing the x and y coordinates, which represent the location information of each patch obtained during the image segmentation, the mask patch images are accurately overlayed onto the corresponding positions of the original WSIs. By merging the patch images into an image of the same size as the original image, we prevent a decrease in resolution. The images obtained through the postprocessing step are used for clinical evaluation.

3 Experiments and results

3.1 Dataset description

The patch dataset comprised three types. For the training dataset used in model training, each patch image had partial overlap and was generated by dividing 23,239 images from 8 WSIs. The mask patch images, corresponding to the patch images, were also created, resulting in 23,239 mask patch images. The validation and test datasets used in the model's quantitative evaluation were generated using the same method as the training dataset but without overlapping patch images. Therefore, they were composed of fewer patch images. The validation dataset comprised 630 patch images (with corresponding mask patch images) generated from 1 WSI, and the test dataset included 1,202 patch images (with corresponding mask patch images) generated from 2 WSIs. In total, the validation and test datasets were composed of 25,071 patch images (with corresponding mask patch images) generated from 11 WSIs. The detailed distribution of this dataset is listed in Table 2.

Additionally, the test dataset used in the model's qualitative evaluation was generated from the same WSIs as the test dataset used in the quantitative evaluation. It comprised 1,214 patch images, and a data table containing coordinate information for each patch image was also created for postprocessing purposes. All patch datasets comprised 512 × 512-pixel images with the background removed.

TABLE 2 Dataset used for model training and quantitative evaluation.

	WSIs	Image patches	Mask patches
Train	8	23,239	23,239
Validation	1	630	630
test	2	1,202	1,202

3.2 Training and evaluation metrics

In this study, we conducted experiments using two GPUs, namely NVIDIA QUADRO RTX 6000 and NVIDIA TITAN RTX, in parallel, with CUDA 11.6 and cuDNN 8. A total of 48GB of GPU memory, with each GPU having 24GB, was utilized for the experiments. The deep learning framework used was PyTorch 1.13.1. During the AI model training process, small batch training iterations were used with a batch size set to 128, and the total number of training epochs was set to 50. The training was configured to terminate early if the validation Dice score did not improve for 30 consecutive epochs. The training time took about 3 hours. We utilized the Adam optimization algorithm with a learning rate set to $1e^{-4}$ and used the Dice score as an evaluation metric. Dice score is one of the most common methods for evaluating image segmentation performance in medical imaging (29); it measures the similarity between the predicted mask by the model and the ground truth label mask. The Dice score value was calculated as shown in Equation 2. Dice loss was employed, commonly used as a loss function in image segmentation tasks, was used for the loss function, aiming to train the model to maximize the Dice score. The Dice loss value was calculated as shown in Equation 3.

$$Dice = \frac{2 \times Area\ of\ Overlap}{Total\ Sum\ of\ Pixels\ in\ All\ Areas} \quad (2)$$

$$Dice\ Loss = 1 - \frac{2 \times Area\ of\ Overlap}{Total\ Sum\ of\ Pixels\ in\ All\ Areas} \quad (3)$$

3.3 AI model results

In a quantitative evaluation of the AI model based on DeepLabV3+, we achieved a specificity of 96.37%, an accuracy of 93.77%, and a Dice score of 73% (Table 3). For qualitative evaluation, we visualized the predicted segmentation for each patch image in the test dataset (Figure 4). The AI model has achieved high performance and demonstrated the ability to predict and segment the lesion areas (Figure 5A). Compared to

TABLE 3 Metrics for the DeepLabV3+ model's various scores for PDAC on WSIs.

Metrics	Score (%)
DICE	73.20
Specificity	96.37
Accuracy	93.77
Sensitivity	75.22
Precision	73.04

the ground truth, it excelled in representing PDAC regions of various shapes, especially in the main pancreatic and interlobular ducts. However, the accuracy was lower due to the false positive rate, as the predicted region recognized an area larger than the actual PDAC annotation or recognized some non-PDAC areas. Visualizing the whole image through postprocessing, converting patch images to WSIs, confirmed the consistency with the Hepatobiliary-pancreatic pathologist's annotation (Figure 5B) level. In addition, our test results were confirmed at low and high magnifications (Figure 5). The AI model trained with the annotated WSIs data we provided displayed high sensitivity to PDAC, the cancerous area of the pancreas.

3.4 Technical application

3.4.1 Progress assessment

To compare the annotation rates of PDAC regions in WSIs, a pathologist hand-annotated PDAC regions in two different WSIs under two experimental conditions. We performed repeated experiments in which the pathologist annotated two WSI images in four consecutive cycles, one for each image, in the absence and presence of AI model assistance. Each cycle lasted 15 min, with a 3-min break, timed using the iPhone 13 stopwatch. We used an evaluation metric called the sensitivity to evaluate the area annotated by the pathologist within a limited time compared to the ground truth area in each cycle. The sensitivity value is calculated as shown in Equation 4). When the pathologist annotated the PDAC regions in WSIs without AI assistance, the rate of the overall annotation achieved a relatively low sensitivity

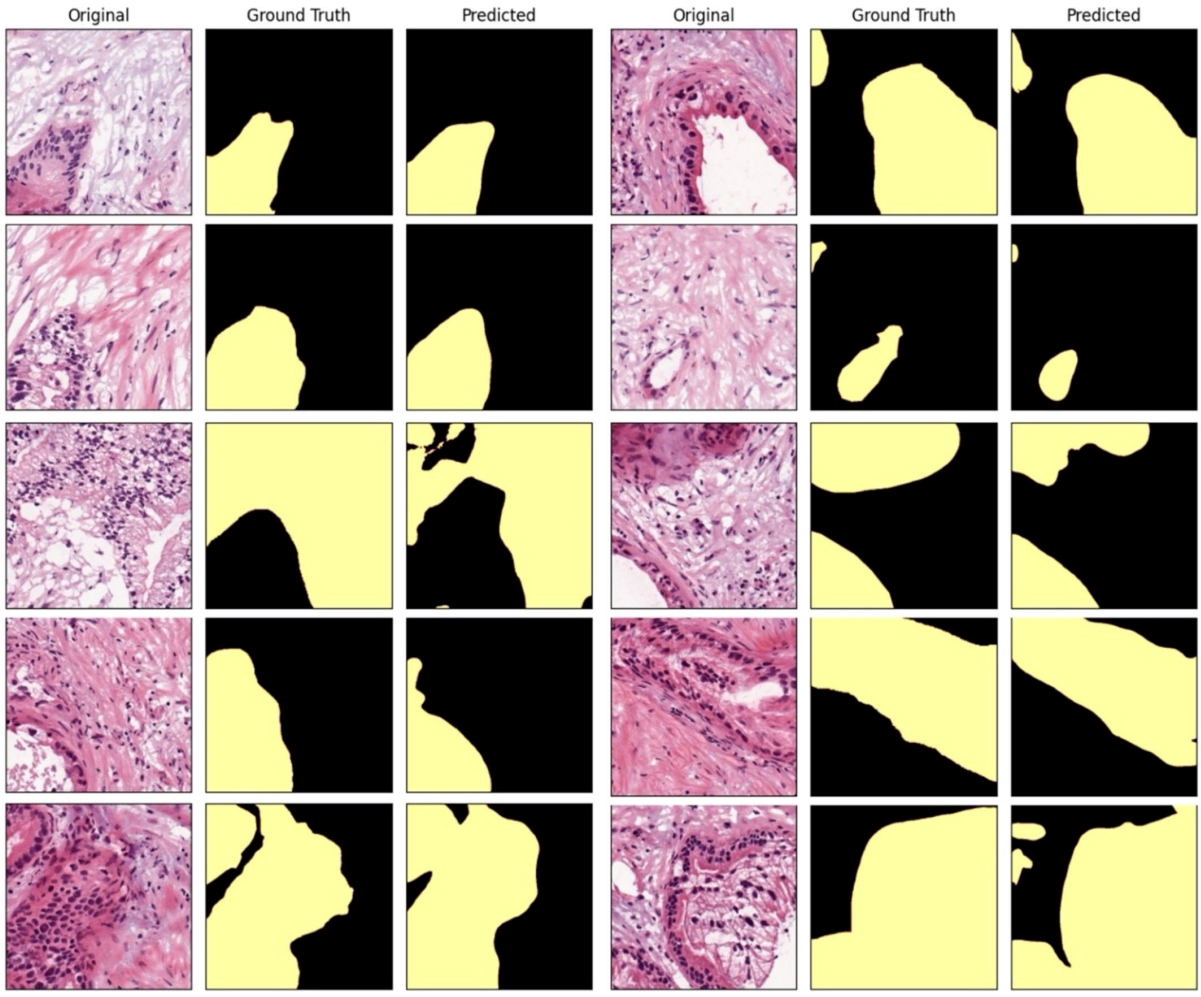

FIGURE 4
Comparison between the AI-predicted segmented patch images in the test dataset and the ground truth.

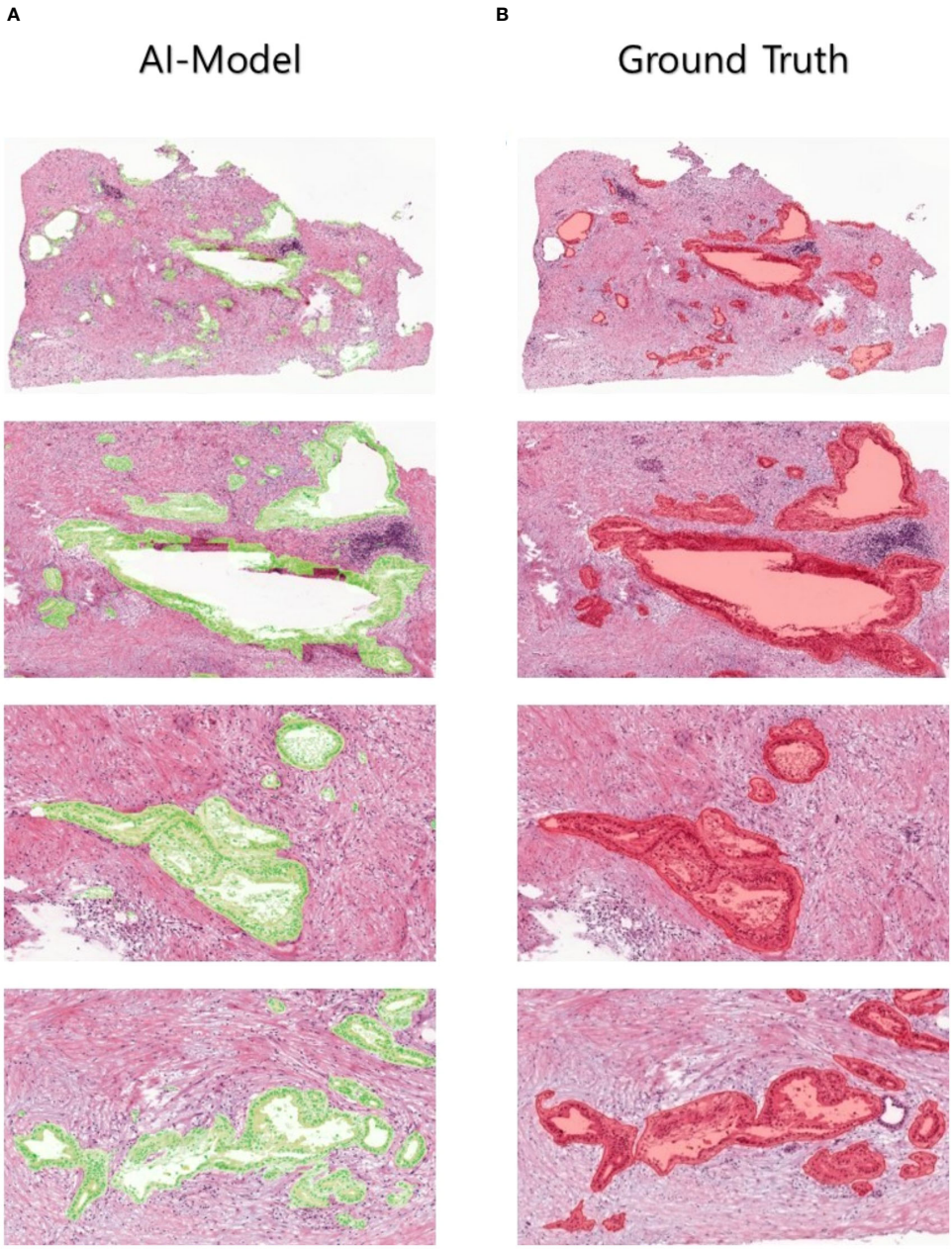

FIGURE 5
Human-annotated and AI-predicted PDAC regions. The WSIs of ground truth and AI predictions are displayed at different magnifications, from low to high, allowing for the inspection of PDAC regions at different scales.

average of 44.64% in the final four cycles (Table 4). In contrast, when the pathologist confirmed and annotated the PDAC regions identified by the AI model using WSI-level segmentation, the annotation rate was overwhelmingly higher than without AI model assistance from the first cycle, and the overall PDAC annotation rate also achieved a significantly high sensitivity average of 85.54% (Table 4). As a result, AI assistance helped achieve a significantly higher annotation rate than the human without AI assistance. We can also expect the annotation accuracy to be significantly higher when the human is assisted by the AI model. We also visualized the images to increase the understanding of these clinical trial results (Figure 6).

$$Sensitivity = \frac{2 \times Area\ of\ Overlap}{Total\ Sum\ of\ Pixels\ in\ Ground\ Truth\ Area} \quad (4)$$

4 Discussion

In this study, we demonstrated the AI potential to aid the diagnosis and prognostic assessment of PDAC, a deadly cancer classified as a public health emergency. Although the majority of PDACs occur in the head of the pancreas, the WSI dataset used in this study contains WSIs with patterns of various PDAC regions that

TABLE 4 Clinical trial: Sensitivity for PDAC annotation rate in WSIs of humans using humans and AI.

Sensitivity (%)	Test1		Test2	
	AI (O)	AI (X)	AI (O)	AI (X)
1 Cycle	**67.26**	10.54	**80.29**	8.16
2 Cycle	**81.31**	30.97	**83.25**	23.32
3 Cycle	**84.60**	35.49	**86.07**	24.12
4 Cycle	**84.65**	43.70	**86.43**	45.59

The bold values are highlighted to emphasize that the Sensitivity performance was significantly higher with AI assistance than without it as cycles progressed.

occur in the body and tail, which are less common than PDACs in the head (30), to explore PDAC in depth. The results represent a significant step forward in AI application to the tissue pathological diagnosis and prognostic assessment of PDAC. The research findings suggest that AI, especially CNN deep learning models, can be effectively used to segment and analyze PDAC tissue pathological WSIs, thereby simplifying and improving the accuracy of PDAC diagnosis. One key aspect highlighted in the study is the challenge posed by the limited access to medical data, especially public pathology data (31). This issue has been a persistent obstacle in pathology AI research. For this study, two pathologists collaboratively annotated PDAC regions in WSIs (Figure 3), and the WSI data used in the study is publicly available for anyone to use, including high-quality annotations. This approach increases the amount of high-quality data available for training AI models and ensures that these models are trained with reliable and accurate information. SL using a deep CNN architecture to segment 11 annotated PDAC WSIs presented promising results. It displayed high Dice scores on the whole tissue image, including PDAC regions, indicating accurate segmentation, and identified areas important for PDAC diagnosis through image visualization. It also showed high specificity and accuracy with a specificity of 96.37% and an accuracy of 93.77% through a precise analysis. These observations demonstrate our high-quality dataset and suggest that AI can play an essential role as an auxiliary tool to improve the efficiency and accuracy of histopathological analysis. In addition, when the whole image was visualized and patch images were converted to WSIs through post-processing, the performance was not significantly different from the pathologist's annotations, but some parts of the small pancreatic ducts, intercalated ducts, and intralobular ducts showed false positives. This is an impressive achievement considering the complexity of pancreatic cancer in interpreting tissue pathological images, but it is expected that increasing the number of pathologists and adding training data will minimize false positives while improving the reliability of the data. Visualization techniques, such

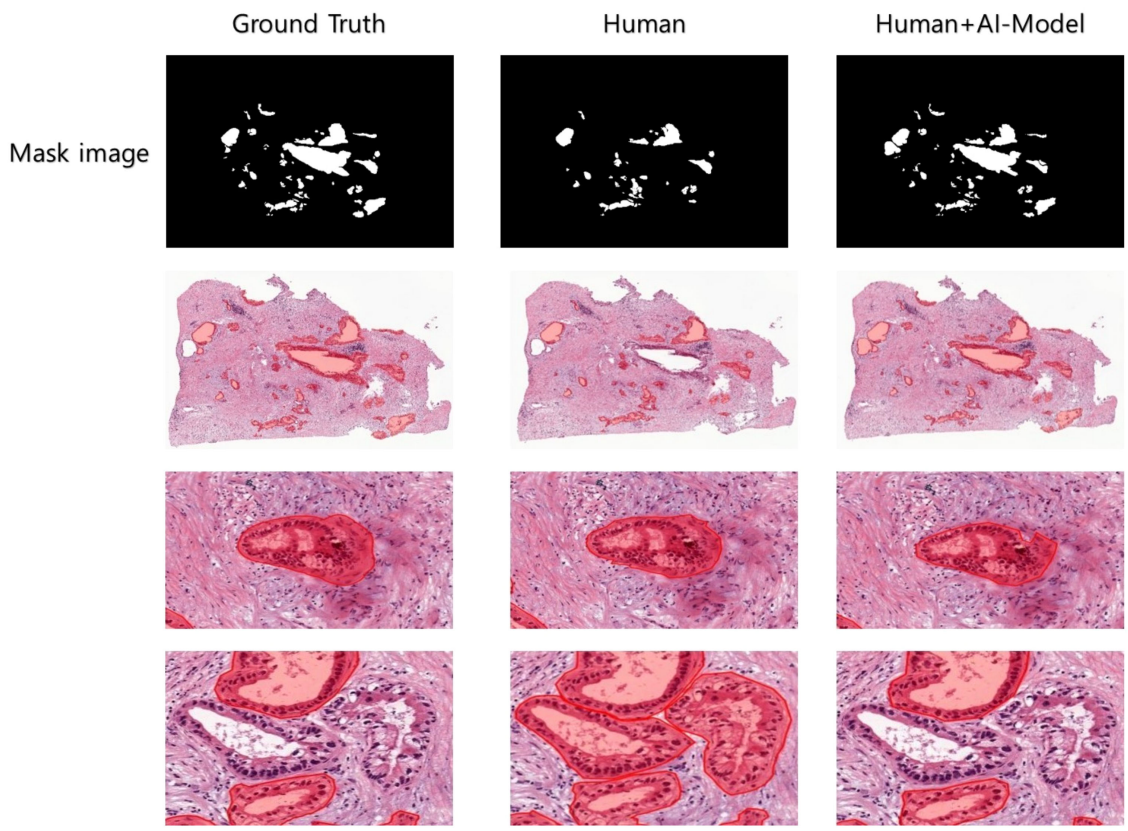

FIGURE 6
Clinical experiments were conducted to visualize the PDAC areas predicted by Human and Human+AI Model in WSI after cycle 4. Human and Human+AI Model drew similar shapes to the correct values, but the Human part made errors in recognizing TIS (carcinoma *in situ*) as PDAC, probably due to decreased concentration and increased fatigue.

as postprocessing techniques that convert patch images back to WSIs, were crucial in validating model performance against expert annotations. In some cases, the AI models achieved high performance, but when visualized and compared with the pathologist's annotations, the AI model recognized areas other than the annotated lesion area. This observation reinforces how essential visualization tools are in evaluating the interpretability of AI models in medical imaging tasks. Our study results indicated that SL deep learning models trained on hand-drawn annotated WSIs displayed high sensitivity for malignant pancreatic areas (i.e., PDAC areas), One important aspect of this study was to confirm the significant improvement in the efficiency of annotation work by pathologists assisted by AI, as AI provides a user-friendly, intuitive interface that minimizes complex technical content and allows pathologists to focus on pathological findings. When pathologists were assisted by the SL model in annotating PDAC in WSIs, the annotation accuracy of pathologists increased while the area of PDAC regions did not differ significantly from the ground truth, and the average annotation progress rate increased by about 2 times compared to the same time spent, which indicates that the annotation time was significantly reduced. Therefore, AI-assisted pathology interpretation of PDAC can diagnose a large number of clinical specimens quickly and accurately, and a cohort study on the prognosis of patients after diagnosis is needed to consider the survival of patients. In addition, if pathological image data for Acinar Cell Carcinoma and Pancreatic Neuroendocrine Tumors (PNETs), which are very rare pancreatic cancers in addition to PDAC, are collected together and used for pathological AI research, the performance of the model can be evaluated in a more comprehensive range for pancreatic cancer, and the applicability of pathological research is expected to increase significantly. Moreover, previous pathological image AI studies mainly used classification models, but due to the reduced image resolution, it is difficult for pathologists to accurately identify the lesion area predicted by AI, so there are limitations in using AI as an auxiliary tool for diagnosis in the clinical pathology field. However, there are few studies that can compensate for this using segmentation, and in the case of PDAC, which has fewer patient cases than other diseases, the application of segmentation is limited to patch-level segmentation rather than whole-slide images, which limits its use (32). To address these issues, this study provides a clear analysis result that identifies PDAC regions with high resolution at low and high magnifications through segmentation in the whole pathological slide images of PDAC patients, and proves that pathologists in the actual pathological clinical field are assisted by AI models. It has significant value in annotation and diagnosis. In addition, it can contribute to the development of pathology AI for pancreatic cancer by providing high-quality pathology annotation data for free. We used open tissue pathology data from six hospitals and medical research institutions to ensure data diversity. As well as, by continuously uploading public data with PDAC annotations to the https://github.com/moksu27/PDAC_pathological_image_segmentation, we can resolve the data imbalance for data with a small number of cases. Also, with the increase in data, data diversity can be achieved through external validation using data from various hospitals, preventing overfitting of AI models and reducing bias to improve the generalization performance of AI models and give objectivity. This will increase the reliability of AI performance for pathologists who will receive direct assistance in the clinical setting, and AI will play the role of an auxiliary tool, or co-pilot, in the pathologist's diagnostic process. Direct diagnosis will still be made after review by a pathologist, so patients will be free from anxiety and prejudice about AI. This is expected to contribute significantly to cost-effectiveness and improved patient outcomes. If our annotated data and AI model manual are used in pathology AI research, AI will be able to assist in the diagnosis of the WHO classification screening reading and 8th-edition AJCC pTNM staging (33) defined by the American Joint Committee on Cancer (AJCC) for PDAC patient slides in clinical practice, and pathologists will be able to quickly and accurately diagnose many clinical specimens through digital pathology. However, several obstacles must be overcome before the results of this study can be applied to actual clinical practice. First, the need for data standardization between hospitals. It is difficult to ensure the compatibility of AI tools because the data format or structure used by each hospital is different, making it difficult to apply AI tools to the clinical field. It is necessary to ensure technical compatibility through standardization of data between hospitals, and systematic integration between medical institutions is required for this. Second, there is the problem of increasing the understanding of medical personnel about AI technology. For medical personnel with a low understanding of AI technology, the use of AI tools may be difficult. To solve this, it is important to support additional promotion and education to enable medical personnel to effectively use AI tools. This will encourage the use of AI tools in multiple institutions and provide a safer and more standardized medical environment. Finally, I would like to emphasize that in order to effectively use AI in pathology interpretation, not only technical development but also institutional structure and education system that support it must develop together. This will be the future research direction of this study, and will play an important role in further expanding the use of AI in the field of pathology.

5 Conclusion

This study provides essential insights to develop effective AI solutions for the specific diagnosis of PDAC and significantly contributes to the pathological AI guidelines, which may have broader implications, even within oncology. Making high-quality annotated datasets publicly accessible and applying advanced machine learning techniques, such as SL, can revolutionize our approach to annotating and diagnosing complex diseases, like pancreatic cancer. We also reiterate the importance of public access to high-quality datasets for AI research while encouraging active research in pathology AI to develop more sophisticated models with improved diagnostic capabilities.

Data availability statement

The datasets presented in this study can be found in online repositories. The names of the repository/repositories and accession number(s) can be found in the article/supplementary material.

Ethics statement

Ethical approval was not required for the studies involving humans because using open data. The dataset is collected and publicly released by The Cancer Imaging Archive. The studies were conducted in accordance with the local legislation and institutional requirements. Written informed consent for participation was not required from the participants or the participants' legal guardians/next of kin in accordance with the national legislation and institutional requirements.

Author contributions

JK: Writing – review & editing, Writing – original draft, Project administration, Methodology, Data curation. SB: Validation, Software, Writing – review & editing, Writing – original draft, Data curation. SY: Writing – review & editing, Investigation, Data curation. SJ: Writing – review & editing, Project administration, Investigation, Funding acquisition, Conceptualization.

Funding

The author(s) declare financial support was received for the research, authorship, and/or publication of this article. This research was supported by the MSIT(Ministry of Science and ICT), Korea, under the ITRC(Information Technology Research Center) support program(IITP-2023-2020-0-01808) supervised by the IITP(Institute of Information & Communications Technology Planning & Evaluation) And This research was supported by a grant of the Korea Health Technology R&D Project through the Korea Health Industry Development Institute (KHIDI), funded by the Ministry of Health & Welfare, Republic of Korea (grant number: HR22C1832).

Acknowledgments

The authors would like to express their sincere gratitude to the National Cancer Institute Clinical Proteomic Tumor Analysis Consortium (CPTAC) for providing the data necessary for this study.

Conflict of interest

Author SY was employed by company ORTHOTECH.

The remaining authors declare that the research was conducted in the absence of any commercial or financial relationships that could be construed as a potential conflict of interest.

Publisher's note

References

1. Hidalgo M. Pancreatic cancer. *N Engl J Med*. (2010) 362:1605–17. doi: 10.1056/NEJMra0901557

2. Rawla P, Sunkara T, Gaduputi V. Epidemiology of pancreatic cancer: global trends, etiol-ogy and risk factors. *World J Oncol*. (2019) 10:10. doi: 10.14740/wjon1166

3. Michl P, Löhr M, Neoptolemos JP, Capurso G, Rebours V, Malats N, et al. UEG position paper on pancreatic cancer. Bringing pancre-atic cancer to the 21st century: pre-vent, detect, and treat the disease earlier and better. *United Eur Gastroenterol J*. (2021) 9:860–71. doi: 10.1002/ueg2.12123

4. Löhr JM. Pancreatic cancer should be treated as a medical emer-gency. *BMJ*. (2014) 349:g5261. doi: 10.1136/bmj.g5261

5. Argentiero A, Calabrese A, Solimando AG, Notaristefano A, Panarelli MG, Brunetti O. Bone metastasis as primary presentation of pancreatic ductal adenocarcinoma: A case report and literature review. *Clin Case Rep*. (2019) 7:1972–6. doi: 10.1002/ccr3.2412

6. Dal Molin M, Zhang M, De Wilde RF, Ottenhof N, Rezaee L, Wolfgang C, et al. Very long-term survival following resection for pancreatic cancer is not explained by commonly mutated genes: results of whole-exome sequencing analysis. *Clin Cancer Res*. (2015) 21:1944–50. doi: 10.1158/1078–0432

7. Strobel O, Neoptolemos J, Jager D, Buchler MW. Optimizing the outcomes of pancreatic cancer surgery. *Nat Rev Clin Oncol*. (2019) 16:11–26. doi: 10.1038/s41571–018-0112–1

8. Yamamoto T, Yagi S, Kinoshita H, Sakamoto Y, Okada K, Uryuhara K, et al. Long-term survival after resection of pancreatic cancer: a single-center retrospective analysis. *World J Gastroenterol*. (2015) 21:262. doi: 10.3748/wjg.v21.i1.262

9. McGuigan A, Kelly P, Turkington RC, Jones C, Coleman HG, McCain RS. Pancreatic cancer: A review of clinical diagnosis, epidemiology, treatment and outcomes. *World J Gastroenterol*. (2018) 24:4846–61. doi: 10.3748/wjg.v24.i43.4846

10. Xu Y, Jia Z, Wang L-B, Ai Y, Zhang F, Lai M, et al. Large scale tissue histopathology image classification, segmentation, and visualization via deep convolutional activation features. *BMC Bioinf*. (2017) 18:1–17. doi: 10.1186/s12859–017-1685-x

11. De Matos J, Ataky STM, de Souza Britto A, Soares de Oliveira LE, Lameiras Koerich A. Machine learning methods for histopathological image analysis: A review. *Electronics*. (2021) 10:562. doi: 10.3390/electronics10050562

12. Koteluk O, Wartecki A, Mazurek S, Kołodziejczak I, Mackiewicz A. How do machines learn? Artificial intelligence as a new era in medicine. *J Personalized Med*. (2021) 11:32. doi: 10.3390/jpm11010032

13. Niazi MKK, Parwani AV, Gurcan MN. Digital pathology and artificial intelligence. *Lancet Oncol*. (2019) 20:e253–61. doi: 10.1016/S1470–2045(19)30154–8

14. Tizhoosh HR, Pantanowitz L. Artificial intelligence and digital pathology: challenges and opportunities. *J Pathol Inform*. (2018) 9:38. doi: 10.4103/jpi.jpi_53_18

15. Krizhevsky A, Sutskever I, Hinton GE. ImageNet classification with deep convolutional neural networks. *Commun ACM*. (2017) 60:84–90. doi: 10.1145/3065386

16. Caldonazzi Nicolò, Rizzo PC, Eccher A, Girolami I, Fanelli GNicolò, Naccarato AG, et al. Value of artificial intelligence in evaluating lymph node metastases. *Cancers*. (2023) 15:2491. doi: 10.3390/cancers15092491

17. Marletta S, L'Imperio V, Eccher A, Antonini P, Santonicco N, Girolami I, et al. Artificial intelligence-based tools applied to pathological diagnosis of microbiological diseases. *Pathol - Res Pract*. (2023) 243:154362. doi: 10.1016/j.prp.2023.154362

18. Santonicco N, Marletta S, Pantanowitz L, Fadda G, Troncone G, Brunelli M, et al. Impact of mobile devices on cancer diagnosis in cytology. *Diagn cytopathology*. (2022) 50:34–45. doi: 10.1002/dc.24890

19. Zarella MD, Bowman D, Aeffner F, Farahani N, Xthona A, Absar SF, et al. A practical guide to whole slide imaging: A white paper from the digital pathology association. *Arch Pathol Lab Med*. (2019) 143:222–34. doi: 10.5858/arpa.2018–0343-RA

20. Simonyan K, Zisserman A. Very deep convolutional networks for large-scale image recognition. ICLR (2015) Conference Track Proceedings, May 7-9, 2015. San Diego, CA, USA.

21. Jiang Y, Sui X, Ding Y, Xiao W, Zheng Y, Zhang Y. A semi-supervised learning approach with consistency regularization for tumor histopathological images analysis. *Front Oncol*. (2023) 12:1044026. doi: 10.3389/fonc.2022.1044026

22. Rashidi HH, Tran NK, Betts EV, Howell LP, Green R. Artificial intelligence and machine learning in pathology: the present landscape of supervised methods. *Acad Pathol*. (2019) 6:2374289519873088. doi: 10.1177/2374289519873088

23. National Cancer Institute Clinical Proteomic Tumor Analysis Consortium (CPTAC). The clinical proteomic tumor analysis consortium pancreatic ductal adenocarcinoma collection (CPTAC-PDA) (Version 14) [Data set]. *Cancer Imaging Arch*. (2018). doi: 10.7937/K9/TCIA.2018.SC20FO18

24. Clark K, Vendt B, Smith K, Freymann J, Kirby J, Koppel P, et al. The cancer imaging archive (TCIA): maintaining and operating a public information repository. *In J Digital Imaging*. (2013) 26:1045–1057). doi: 10.1007/s10278–013-9622–7

25. Muñoz-Aguirre M, Ntasis VF, Rojas S, Guigó R. PyHIST: a histological image segmentation tool. *PloS Comput Biol*. (2020) 16:e1008349. doi: 10.1371/journal.pcbi.1008349

26. Buslaev A, Iglovikov VI, Khvedchenya E, Parinov A, Druzhinin M, Kalinin AA. Albumentations: fast and flexible image augmentations. *Information*. (2020) 11:125. doi: 10.3390/info11020125

27. He K, Zhang X, Ren S, Sun J. Deep residual learning for image recognition. *IEEE Xplore (2016) Conference Track Proceedings*, June 27-30, 2016. Las Vegas, NV, USA.

28. Liu M, Fu B, Xie S, He H, Lan F, Li Y, et al. …Comparison of multi-source satellite images for classifying marsh vegetation using DeepLabV3 Plus deep learning algorithm. *Ecol Indic*. (2021) 125:107562. doi: 10.1016/j.ecolind.2021.107562

29. Crum WR, Camara O, Hill DL. Generalized overlap measures for evaluation and validation in medical image analysis. *IEEE Trans Med Imaging*. (2006) 25:1451–61. doi: 10.1109/TMI.2006.880587

30. Tomasello G, Ghidini M, Costanzo A, Ghidini A, Russo A, Barni S, et al. Outcome of head compared to body and tail pancreatic cancer: a systematic review and meta-analysis of 93 studies. *J Gastrointest Oncol*. (2019) 10:259–69. doi: 10.21037/jgo.2018.12.08

31. Schuurmans M, Alves N, Vendittelli P, Huisman H, Hermans JPANCAIM Consortium. Artificial intelligence in pancreatic ductal adenocarcinoma imaging: A commentary on potential future applications. *Gastroenterology*. (2023) 165:309–16. doi: 10.1053/j.gastro.2023.04.003

32. Janssen BV, Theijse R, Roessel SV, Ruiter RD, Berkel A, Huiskens J, et al. Artificial intelligence-based segmentation of residual tumor in histopathology of pancreatic cancer after neoadjuvant treatment. *Cancers*. (2021) 13:5089. doi: 10.3390/cancers13205089

33. Roessel S, Gyulnara G, Verheij J, Najarian R, Maggino L, Pastena M, et al. International validation of the eighth edition of the american joint committee on cancer (AJCC) TNM staging system in patients with resected pancreatic cancer. *JAMA Surg*. (2018) 153:e183617. doi: 10.1001/jamasurg.2018.3617

Frontiers in Oncology

Advances knowledge of carcinogenesis and tumor progression for better treatment and management

The third most-cited oncology journal, which highlights research in carcinogenesis and tumor progression, bridging the gap between basic research and applications to imrpove diagnosis, therapeutics and management strategies.

Discover the latest Research Topics

See more →

Frontiers

Avenue du Tribunal-Fédéral 34
1005 Lausanne, Switzerland
frontiersin.org

Contact us

+41 (0)21 510 17 00
frontiersin.org/about/contact